NHSH-CR-1 /2, 446 -VOl. 1

NASA Contractor Report 172446-1

Sources, Paths, and Concepts for Reduction of Noise in the Test Section of the NASA Langley 4 x 7m Wind Tunnel

R.E. Hayden, J.F. Wilby

**Bolt Beranek and Newman Inc.
Cambridge, MA 02238**

FOR REFERENCE

NOT TO BE TAKEN FROM THIS ROOM

NASA
National Aeronautics and
Space Administration

Langley Research Center
Hampton, Virginia 23665
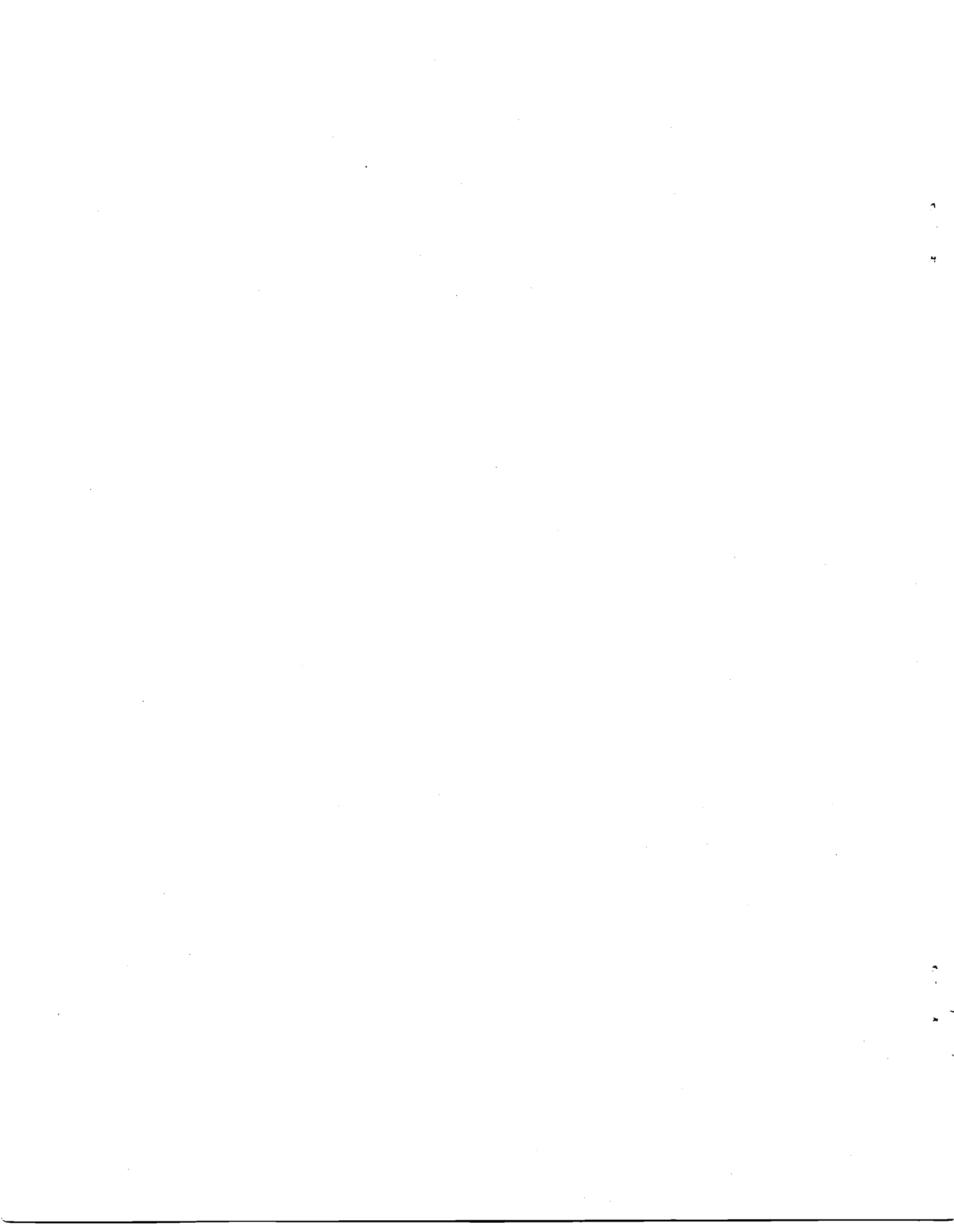
ENTER:
```
 15      1       1 RN/NASA-CR-172446-VOL-1
          DISPLAY 15/2/1
        85N14666*#   ISSUE 5    PAGE 726    CATEGORY 71   RPT#: NASA-CR-172446-VOL-1
        NAS 1.26:172446-VOL-1 BBN-5416   CNT#: NAS1-16521    84/09/00   2 VOLS   325
        PAGES   UNCLASSIFIED DOCUMENT
```
UTTL: Sources, paths, and concepts for reduction of noise in the test section of
      the NASA Langley 4x7m wind tunnel   TLSP: Final Report, Jul. 1983 - Mar.
      1984
AUTH: A/HAYDEN, R. E.; B/WILBY, J. F.
CORP: Bolt, Beranek, and Newman, Inc., Cambridge, Mass.   AVAIL.NTIS   SAP: HC
   A14/MF A01
MAJS: /*ACOUSTIC PROPERTIES/*BACKGROUND NOISE/*FANS/*NOISE REDUCTION/*WIND
      TUNNELS
MINS: / AEROACOUSTICS/ DATA BASES/ HELICOPTERS/ MICROPHONES/ NOISE SPECTRA/
      ROTARY WINGS/ TRANSFER FUNCTIONS/ VANES/ WIND TUNNEL DRIVES
ABA: R.S.F.
ABS: NASA is investigating the feasibility of modifying the 4x7m Wind Tunnel at
      the Langley Research Center to make it suitable for a variety of
      aeroacoustic testing applications, most notably model helicopter rotors.
      The amount of noise reduction required to meet NASA's goal for test
      section background noise was determined, the predominant sources and paths
      causing the background noise were quantified, and trade-off studies
      between schemes to reduce fan noise at the source and those to attenuate
      the sound generated in the circuit between the sources and the test

ENTER:
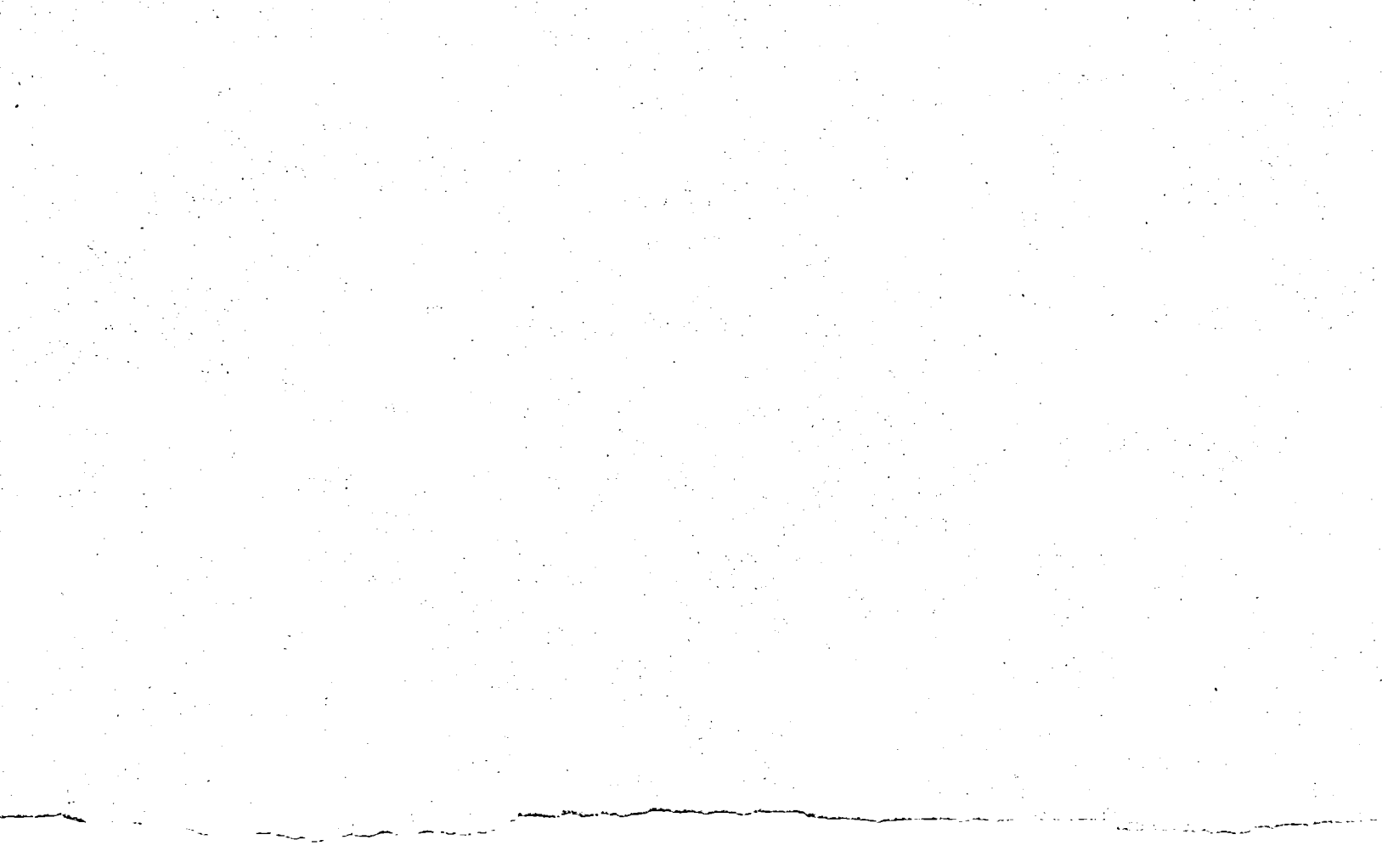
FOREWORD

This report describes tests and analyses aimed at devising
methods for reducing background noise levels and improving the
acoustic environment in the test section of the NASA Langley
4x7 m wind tunnel. The 4x7 m wind tunnel is a low speed facility
which can be operated in either the open-jet or closed-jet mode;
the tunnel is envisioned as a possible aeroacoustic test facility
for helicopter noise research.

The emphasis of this work has been on (1) obtaining as clear
a definition as possible of the predominant noise sources and the
paths by which the noise reaches the test section of the 4x7 m
wind tunnel, and (2) exploration of alternatives for achieving
the necessary noise reduction in the test section. Candidate
noise control approaches are outlined and several promising
approaches are highlighted; however, since the final selection of
noise control treatment must necessarily include further consid-
eration of aerodynamic penalties, structural and operational
implications, and cost, a preferred treatment concept cannot be
recommended until such evaluations are completed.

i

N85 - 14666#

TABLE OF CONTENTS

TABLE OF CONTENTS (cont.)

LIST OF FIGURES

LIST OF FIGURES (cont.)

x

xiv

LIST OF TABLES

SOURCES, PATHS, AND CONCEPTS FOR REDUCTION OF NOISE IN THE TEST SECTION OF THE NASA LANGLEY 4x7M WIND TUNNEL

1. INTRODUCTION AND SUMMARY

1.1 Description of Wind Tunnel and Envisioned Uses

The NASA Langley 4x7 m wind tunnel (formerly known as the V/STOL Transition Wind Tunnel), is a closed circuit wind tunnel which can be operated either in the open-jet or closed-jet mode. The open-jet mode is accomplished by removing test section walls, raising a moveable ceiling element, and introducing a bell-mouth collector (note that NASA has recently completed a design study to develop an improved collector configuration for the facility). The wind tunnel is powered by an 8000 HP variable-speed electric drive system, which is connected to a nine-bladed fan approximately 12.5 m (41 feet) in diameter. Seven stator vanes are located behind the fan to remove swirl from the flow. The layout of the facility and some pertinent dimensions are shown in Figure 1(a). Microphone locations used in the test program are shown in Figures 1.(b) and 1.(c). The range of speeds which are of interest here in the test section is 6 mps to 90 mps.

The envisioned uses of the 4x7 m wind tunnel for acoustic measurements include testing of complete scale model helicopters, as well as component studies of propellers and isolated rotors (See Ref. 1). It will typically be of interest to measure and map out the radiated sound field from these models over all angles corresponding to sound radiation into a hemisphere below the plane of the rotor. Both discrete frequency and broadband noise sources are of interest. The facility may be used to develop or to validate concepts for future low noise helicopters. Therefore, it must be quieted to a background noise level which provides an adequate margin (signal-to-noise ratio) for convenient direct measurement of noise from all these source

PLAN VIEW

ELEVATION
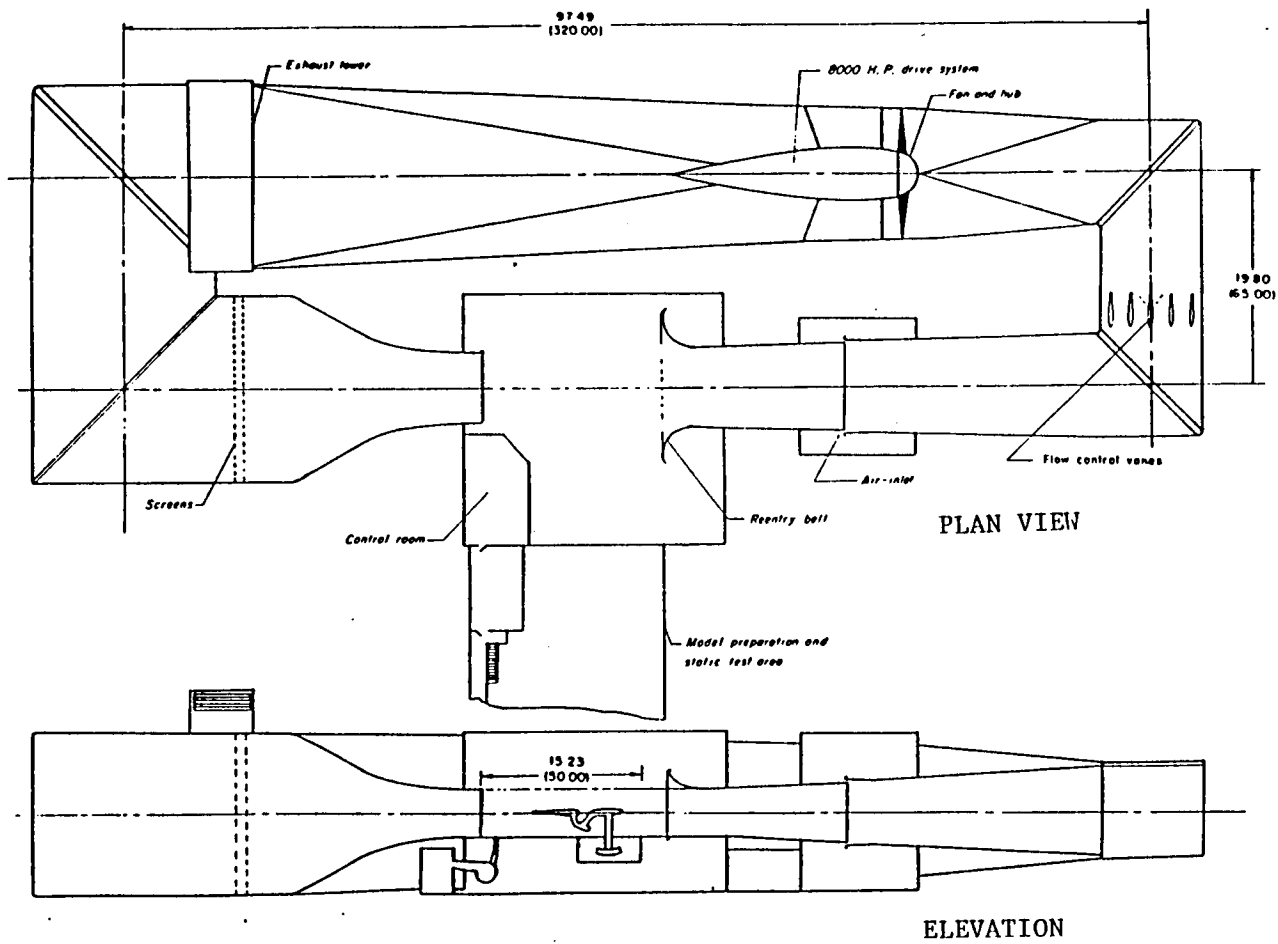
FIGURE 1(a)   CONFIGURATION OF NASA 4 x 7m WIND TUNNEL.

2
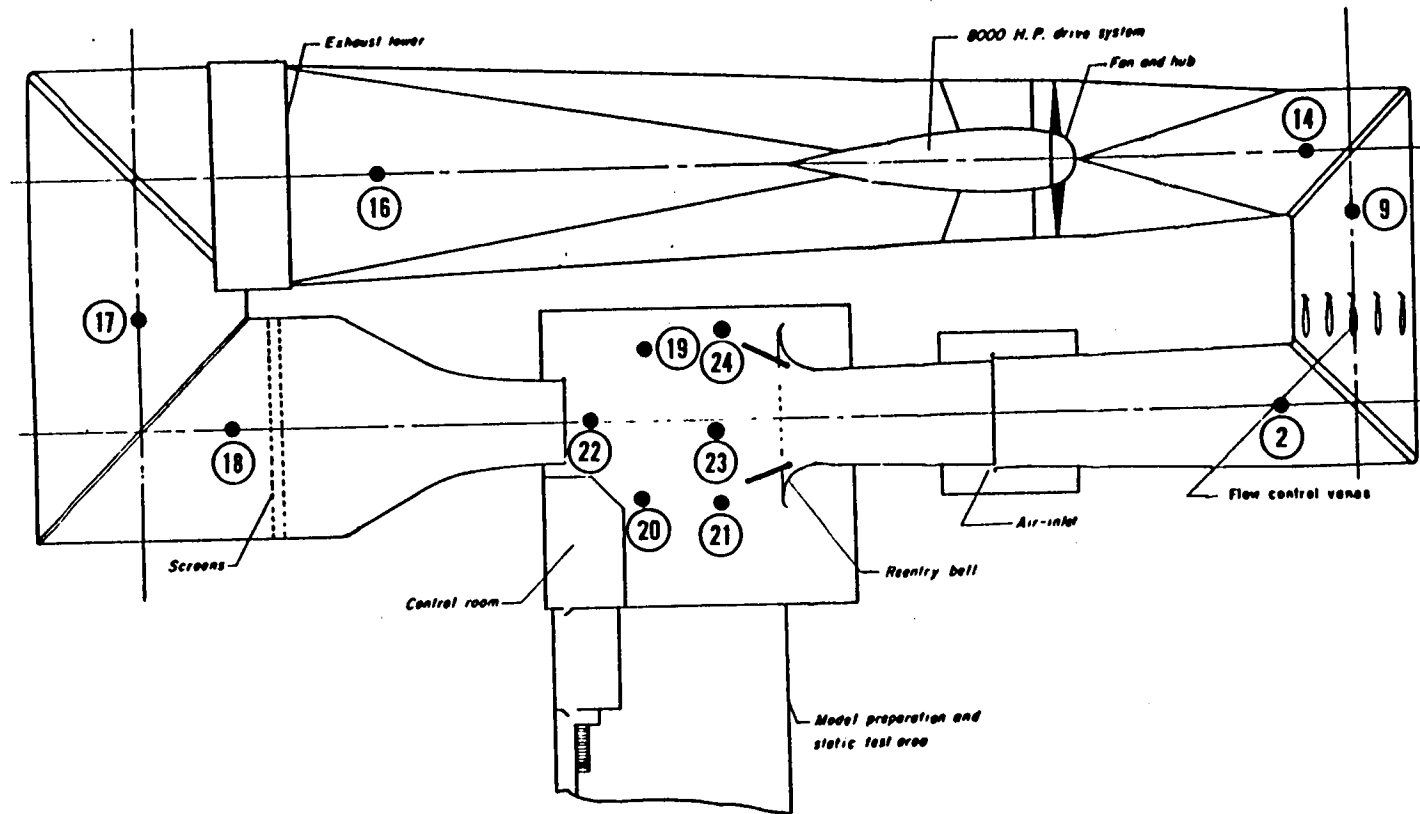
FIGURE 1(b)   MICROPHONE LOCATIONS FOR STEADY-STATE NOISE PROPAGATION
               TESTS (TEST 2).

3
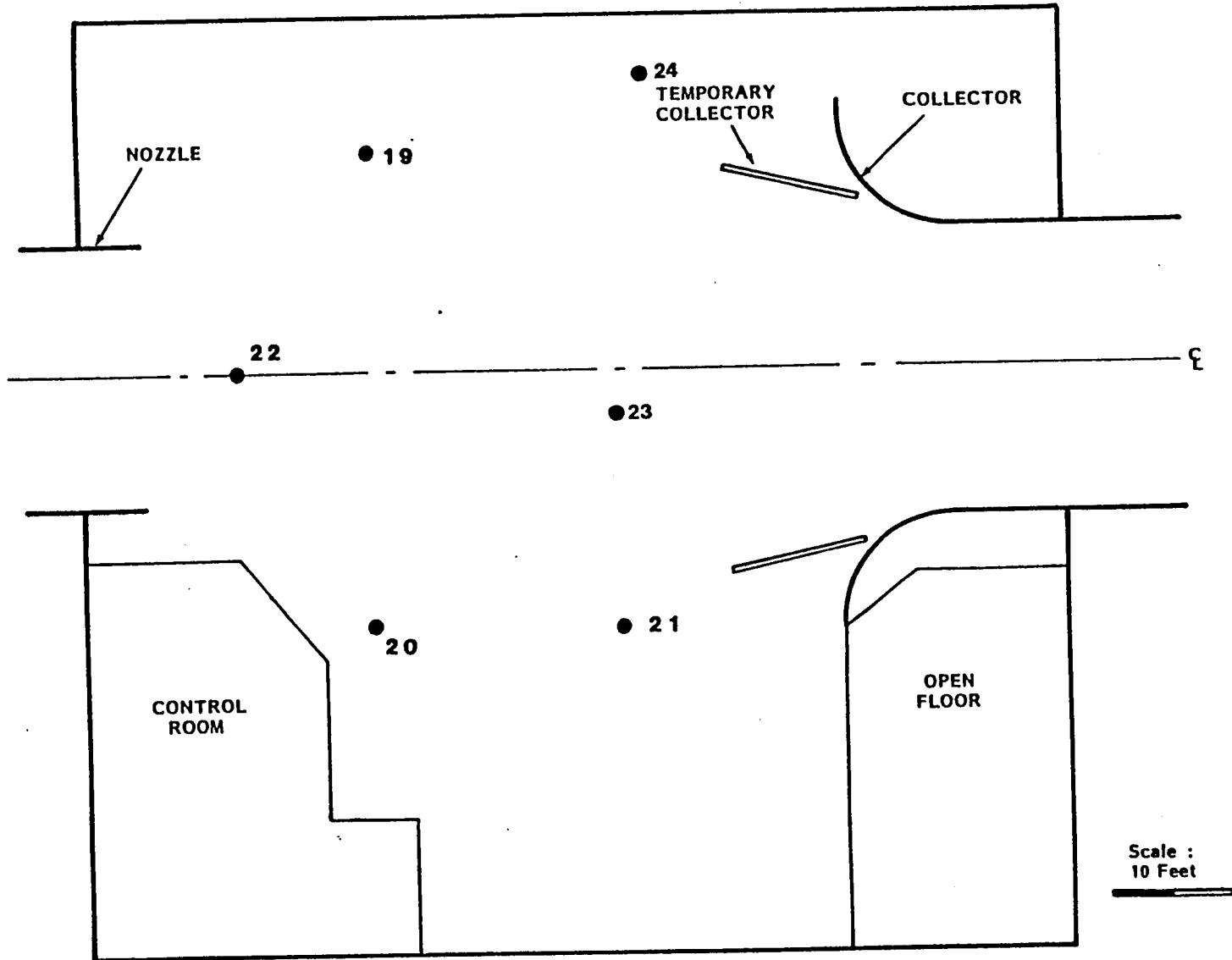
FIGURE 1(c)   CONFIGURATION OF NASA 4 x 7m WIND TUNNEL SHOWING
MAJOR MICROPHONE LOCATIONS.

mechanisms, and it must provide an acoustic environment in the test section which is sufficiently free from reflections and standing waves to allow straightforward interpretation of the measured noise. Such requirements imposed on an existing facility of the scale of the 4x7m wind tunnel may result in the necessity for substantial modifications to the facility in order to achieve the low background noise levels required and an adequate freefield environment in the test section itself. The goal of this study is to investigate the feasibility of modifying the tunnel to satisfy the requirements of present and future scale model helicopter testing.

1.2 Background Noise Environment

Criteria: Straightforward acoustic measurements require that background noise levels be at least 6 dB below the level of the lowest radiated noise level of interest. Modern signal processing techniques allow this criterion to be relaxed somewhat, at the expense of increased experimental complexity (and thus cost) and lower confidence in measured data. Therefore, estimates of radiated noise from scale model helicopters (both present and future designs) will establish the background noise requirement for the test section. Such predictions have been made by a NASA Langley study committee [1]. The resulting criterion is summarized in Fig. 2 along with a measured background spectrum from the DNW tunnel (out-of-flow; open jet mode) [2]. Note that the NASA criterion applies to both in-flow and out-of-flow locations. It will be shown later that for frequencies below the 2 kHz-4 kHz range, the levels proposed in the criterion are substantially below the minimum achievable flow-induced pressure fluctuation levels in current microphones with streamlined nose cones. Thus the criterion is either irrelevant for in-flow measurements or a concerted effort will be needed to develop microphones which are less sensitive to flow-induced
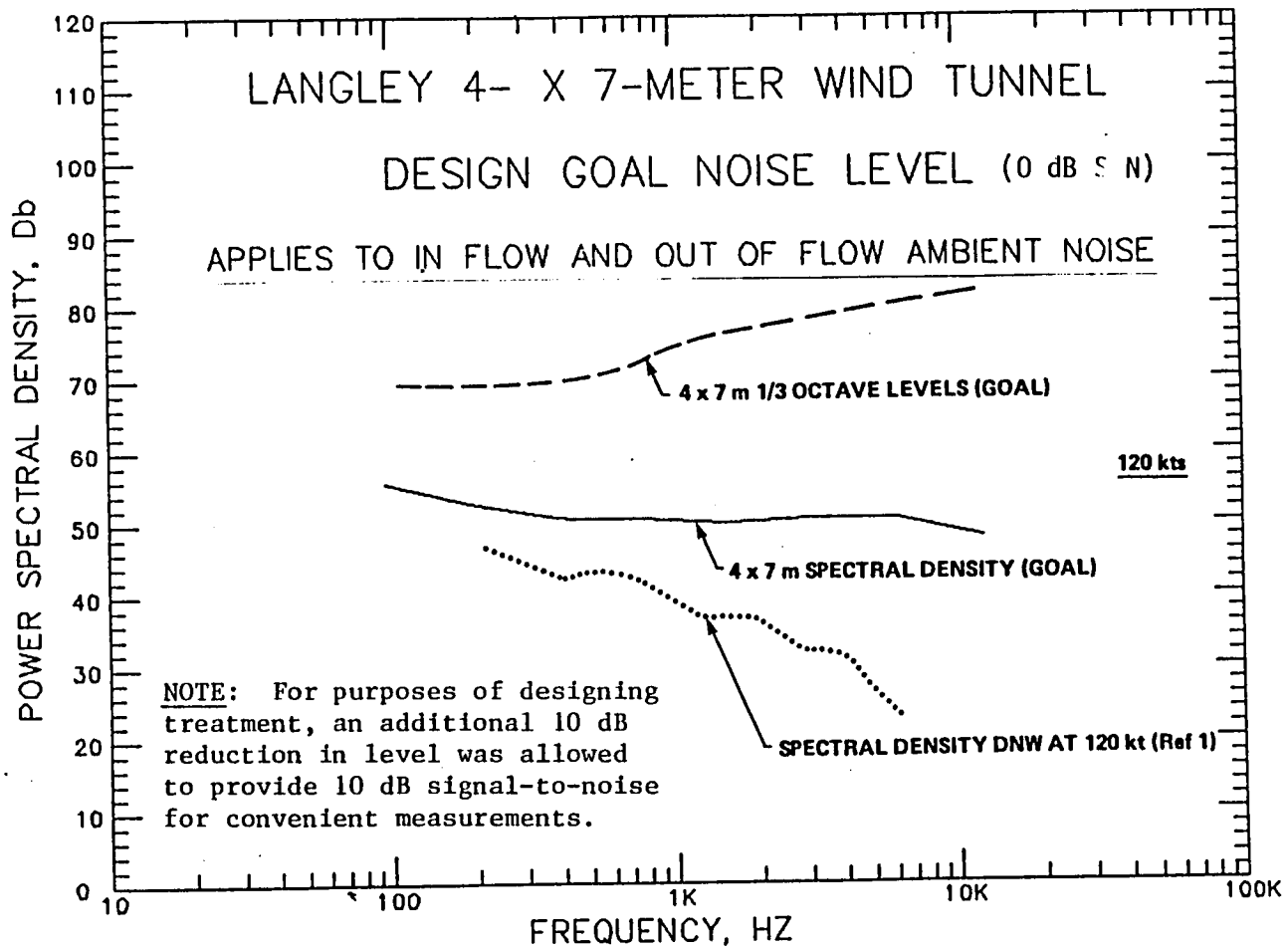
FIGURE 2.   BACKGROUND NOISE GOAL FOR 4 x 7m TUNNEL AT 120 kt
            (FROM REF. 1.)

pressure fluctuations. For the purposes of deriving noise control requirements, NASA instructed the authors to reduce the criterion levels in figures by 10 dB to provide that amount of signal-to-noise ratio for typical measurements.

Existing background noise environment: Figures 3 and 4 show the measured background noise environment in the 4x7 m wind tunnel at five representative measurement locations inside the facility (note that extraneous noise caused by microphone stands has been removed). Figure 5 compares the existing noise levels in the 4x7m with the NASA criterion (reduced by 10 dB for signal-to-noise allowance), out-of-flow levels in the DNW tunnel, and microphone self-noise. It is clear from these data that significant background noise reduction is required in the 4x7 m wind tunnel to meet the criterion and/or to match the DNW tunnel performance. (Note that in-flow data reported by DNW [2] are clearly microphone self-noise and not acoustic; therefore, the in-flow levels are not presented for comparision). The previously-mentioned microphone self-noise problem is also illustrated by these comparisons.

1.3 Overview of Tests and Analyses Performed

An extensive test program was conducted during the week of August 15-20, 1983, to diagnose the sources of background noise in the 4x7 m wind tunnel test section, and the paths by which those background noise sources reach the test section. A set of tests was also carried out to assist in locating and quantifying those reflecting surfaces in the test section which may lead to difficulties in making freefield measurements from model helicopters.

The tests carried out consisted of:

- straightforward noise surveys at various locations around the tunnel circuit, in the test section, and outside the wind tunnel;

7
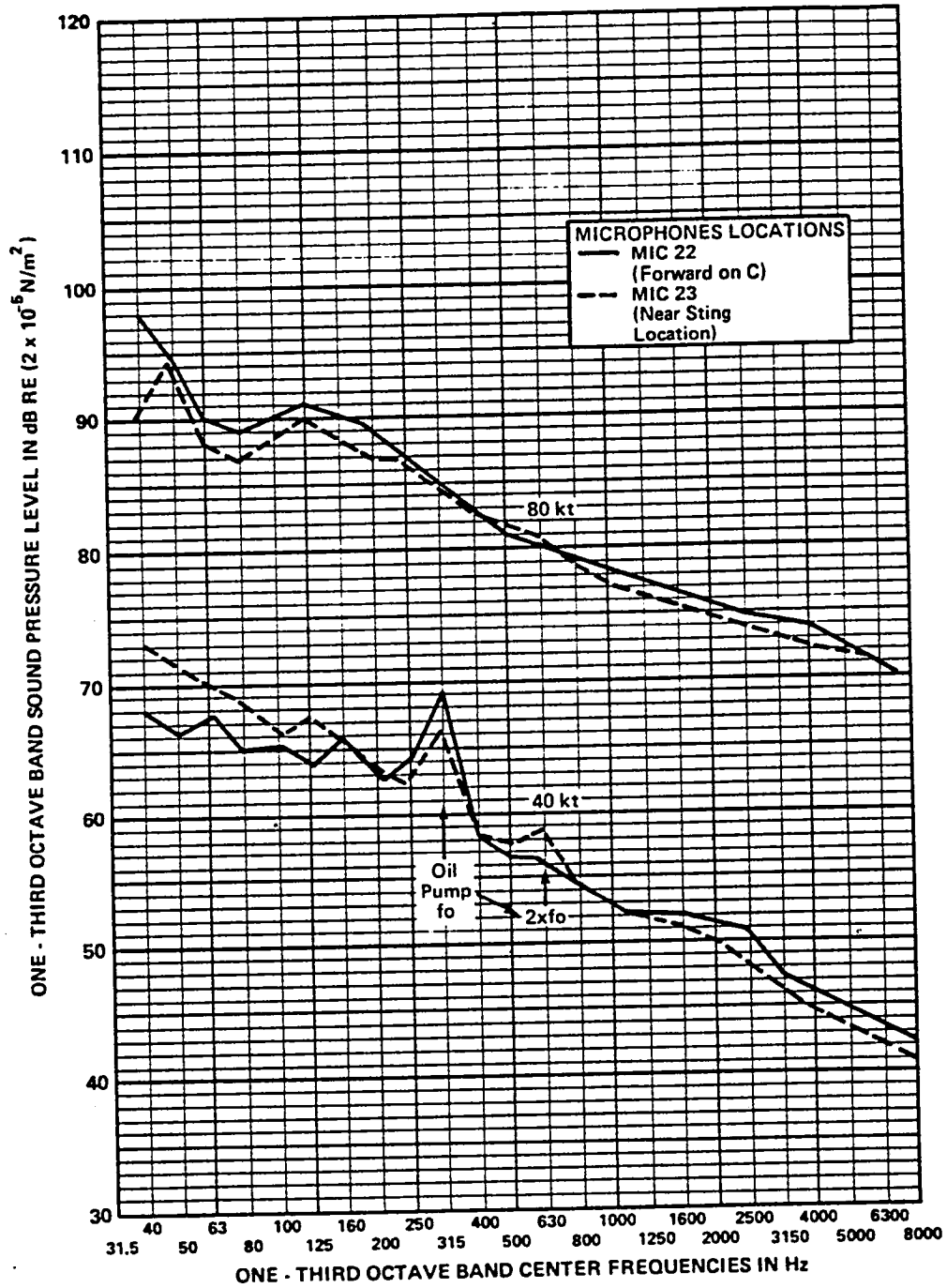
FIGURE 3. MEASURED TEST SECTION BACKGROUND NOISE LEVELS IN 4 x 7m TUNNEL IN FLOW PATH.

8
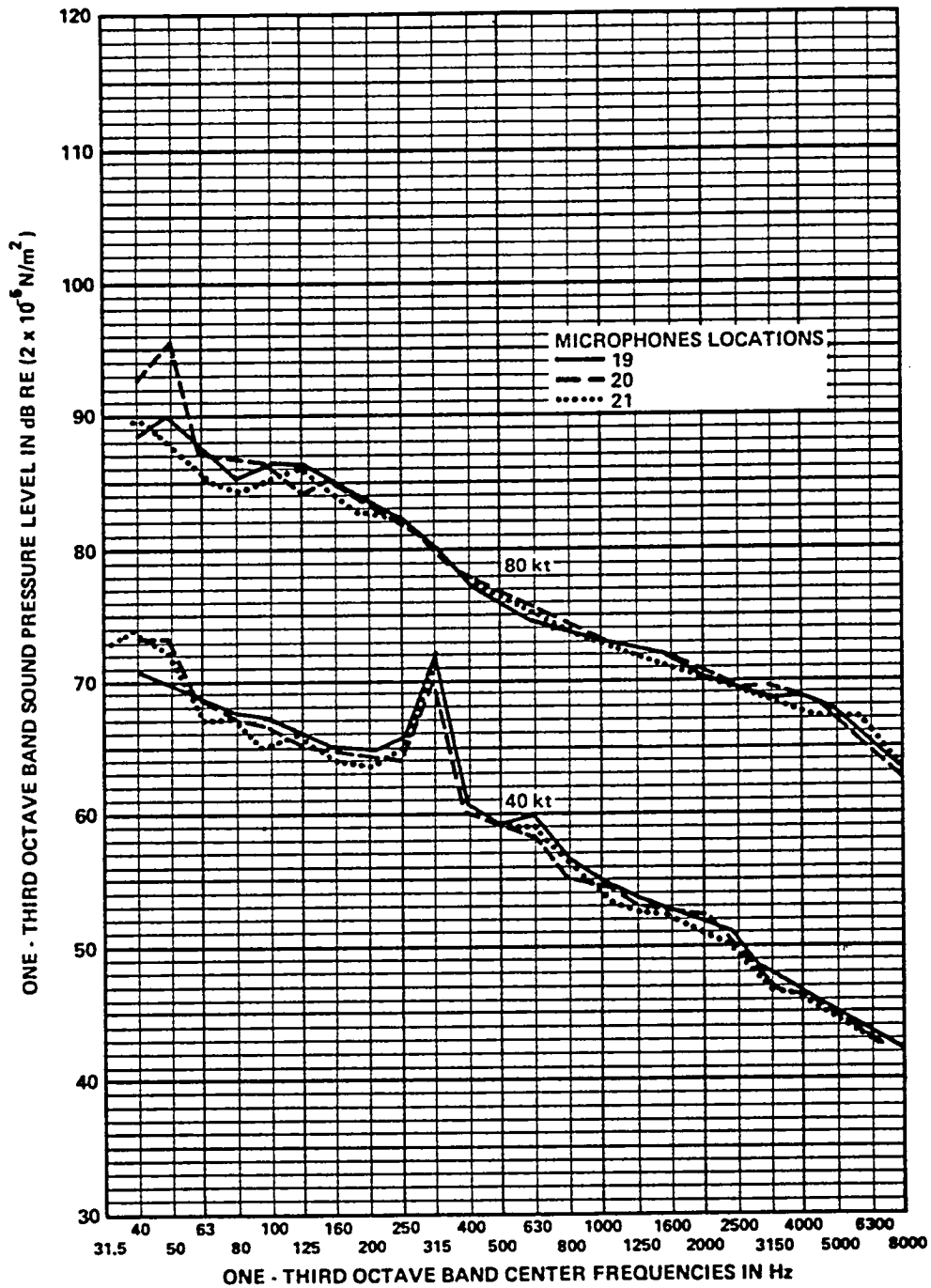
FIGURE 4. MEASURED TEST SECTION BACKGROUND NOISE LEVELS IN
4 x 7m TUNNEL OUTSIDE FLOW PATH.
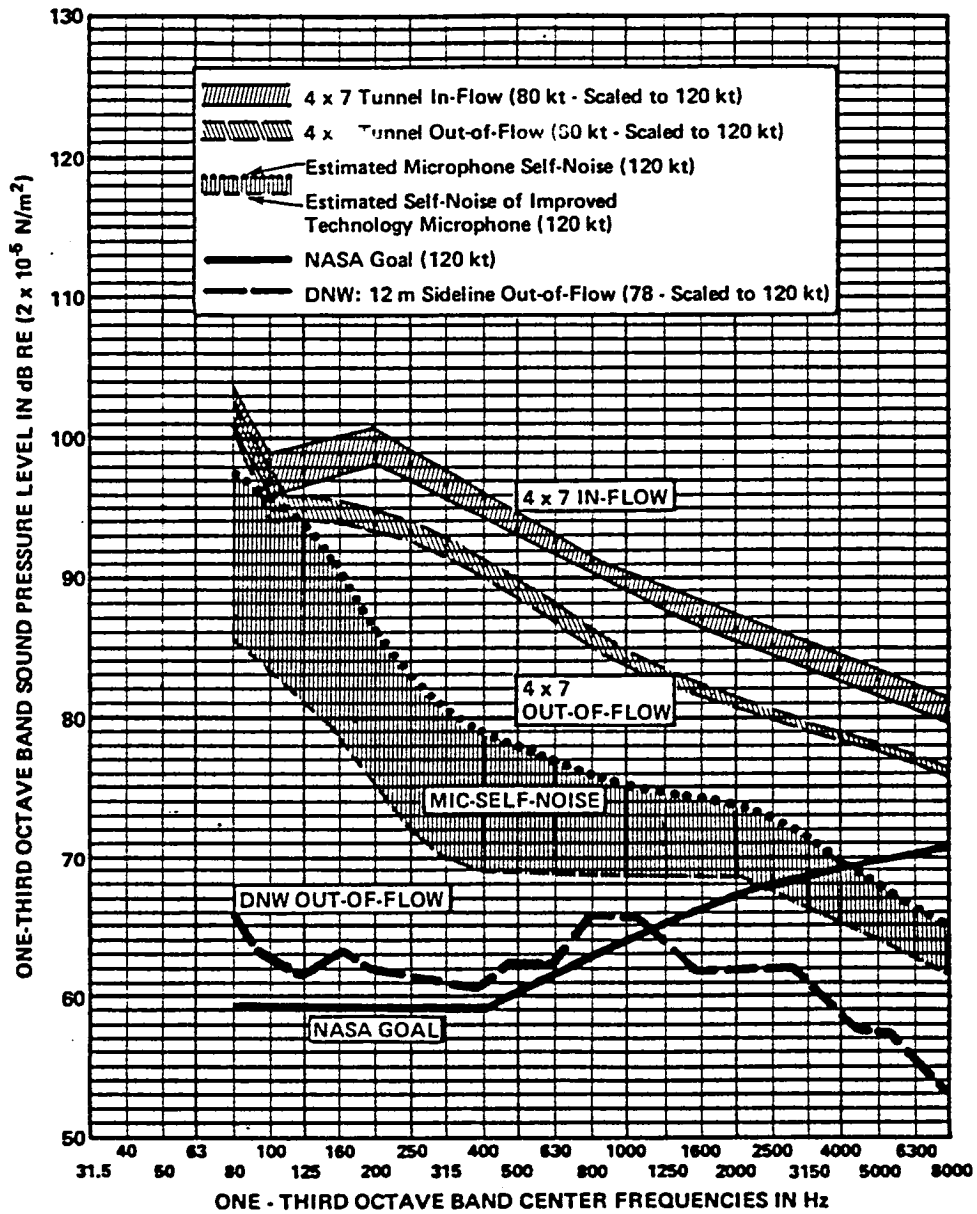
FIGURE 5.   NASA NOISE GOAL; DNW AND 4 x 7m TUNNEL BACKGROUND
LEVELS, AND MICROPHONE SELF-NOISE

10

- controlled tests using known sound sources (with no tunnel flow);

- phased microphone array measurements to assist in (a) isolation of predominant propagation of sound around the circuit for different frequencies, (b) determination of the approximate propagation angle at different stations around the circuit, from which the performance of candidate wall treatments can be more easily assessed, (c) causality correlations for turning vane and flap noise sources, (d) investigation of sound transmission through turning vanes;

- impulse response tests to measure existing absorption in the tunnel circuit and isolation of predominant paths in the circuit;

- a series of measurements in the test section to quantify standing wave problems and to provide data to isolate contributions of various reflecting surfaces to the disorder in the room acoustics.

The analysis performed on this data consisted of the following:

- speed and frequency scaling of 1/3 octave spectra at each location to identify overall trends and to eliminate data artifacts

- prediction of test section contributions of each component source using assumed source spectra and no-flow transfer functions

- separation of predominant propagation paths and modes using coherence function spectra and phase plots from cross spectra of closely-spaced microphones

- correlation of trailing edge pressures on first corner turning vanes and flow-control vanes with nearby microphones.

Also used were published and unpublished data from similar facilities in which background noise diagnosis had been carried out.

At the conclusion of the data analysis and evaluation, several noise control concepts were proposed and analyzed to determine their acoustic effectiveness, aerodynamic and operational impacts, and rough relative initial cost.

Most of the data analysis, comparisons, and noise control design analyses are reported for a test section speed of 80 kt, since that speed was the highest speed achievable during the test program as a result of the temporary nature of a prototype collector which was installed in the test section. In order to derive the noise reduction requirement for the 120 kt case for which NASA has estimated the background noise required for typical tests, the 80 kt data from the test section were scaled to 120 kt and the noise reduction was determined to be the difference between the scaled levels and the criterion. This procedure may introduce some possible detailed inaccuracies in the noise reduction requirements in some frequency bands, but there is no evidence to suggest that the overall conclusions or recommendations are substantially impacted. It should, however, be noted that since the background noise requirement at 80 kt is virtually the same as that at 120 kt, the noise reduction required at that speed would be considerably less than that estimated for the 120 kt speed.
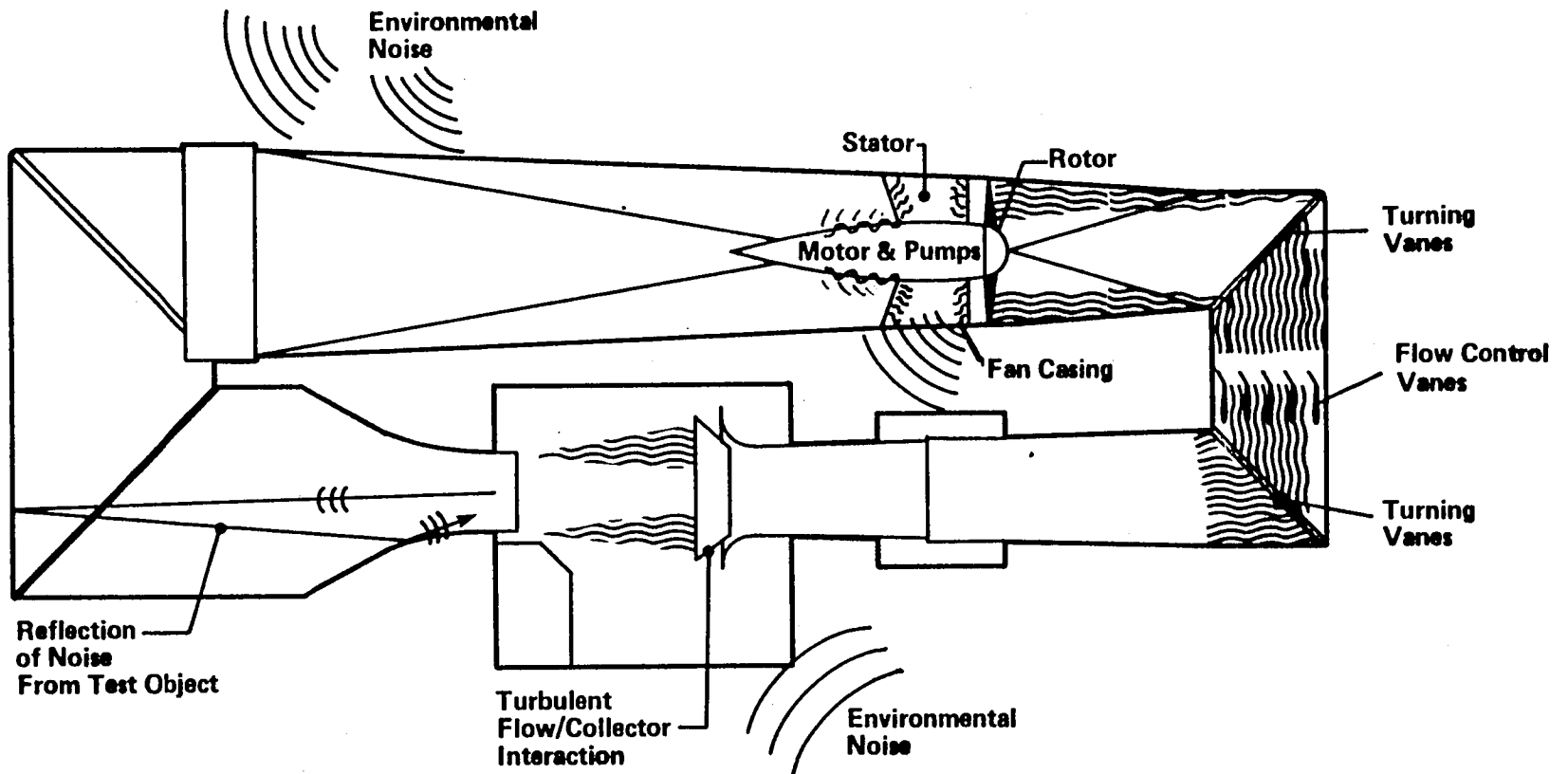
FIGURE 6. SCHEMATIC OF NOISE SOURCES IN 4 x 7m TUNNEL.

1.4 Summary of Key Findings

1.4.1 Sources

Predominant sources producing unwanted sound in the test section depend upon the speed regime in which the tunnel is operating and the frequency range of interest. The possible sources are shown schematically in Figure 6, and include the tunnel drive fan (which contributes primarily broadband noise in the frequency range of interest), flow impingement on the turning vanes - particularly those on the first corner, flow impingement on the collector inside the tunnel test section, noise generated by auxiliary equipment such as pumps and compressors, intrusive noise from adjacent facilities, aircraft flyovers, vehicular traffic. Potential test section sources not illustrated include "lip noise" from the nozzle, flow interaction with the tunnel floor, and flow interaction with the model support. The paths of the sound reaching the test section from each of these sources are relatively straightforward to visualize. Fan noise propagates via three potential paths: (1) upstream around the second corner, through the second diffuser, around the first corner and through the first diffuser; (2) downstream through the remainder of the fourth diffuser, around the third corner and fourth corner, and through the nozzle in the test section; (3) along flanking paths in the tunnel structure and/or as a result of radiation into the outdoor spaces around the tunnel, reentering through test section walls and air exchange ports. The turning vane sources radiate in both the upstream and downstream directions, as do any sources associated with the flow control vanes in the second diffuser. The sources in the test section radiate directly into the measurement space, and therefore may ultimately present the most difficult challenge in limiting the background noise levels in the tunnel.

14

The estimated acoustic power levels of the various sources are shown in Fig. 7, for reference test section speeds of 40, 80, and 160 kt. (Note that the maximum speed tested was 90 kt, due to temporary limitations on the facility and thus the 160 kt data have been estimated by extrapolation.) The fan is clearly the dominant source at high speeds. Analysis of flowfield data indicates that the fan is partially stalled and is thus unnecessarily noisy. However, the evaluation of the significance of each of these sources in creating background noise test section must take into account propagation losses between each source and the test section.

1.4.2 Propagation path characteristics

The tunnel circuit is highly reverberant; thus the paths between each source and the test section are complex. Section 2 discusses the path characteristics in detail. Figure 8 summarizes the range of estimates of the reduction in acoustic intensity between a source at the fan or the first corner and the test section via both upstream and downstream propagation paths. These estimates were derived from no-flow tests and by scaling data from other facilities. The range of losses presented for each propagation path is wide because of certain ambiguities which result from limitations on the ability to separately study each path during full-scale diagnostic measurements. Note that for these "transfer functions," there will be differences between microphones located in the flow and those outside the flow caused by directivity effects of the nozzle and collector openings. Further differences will arise at high speeds as a result of refraction through the shear layer and possible changes in the in-duct propagation characteristics. Such effects are not taken into account in Figure 8.

The predominant propagation path for sound generated by the fan and second corner turning vane noise appears to be through the
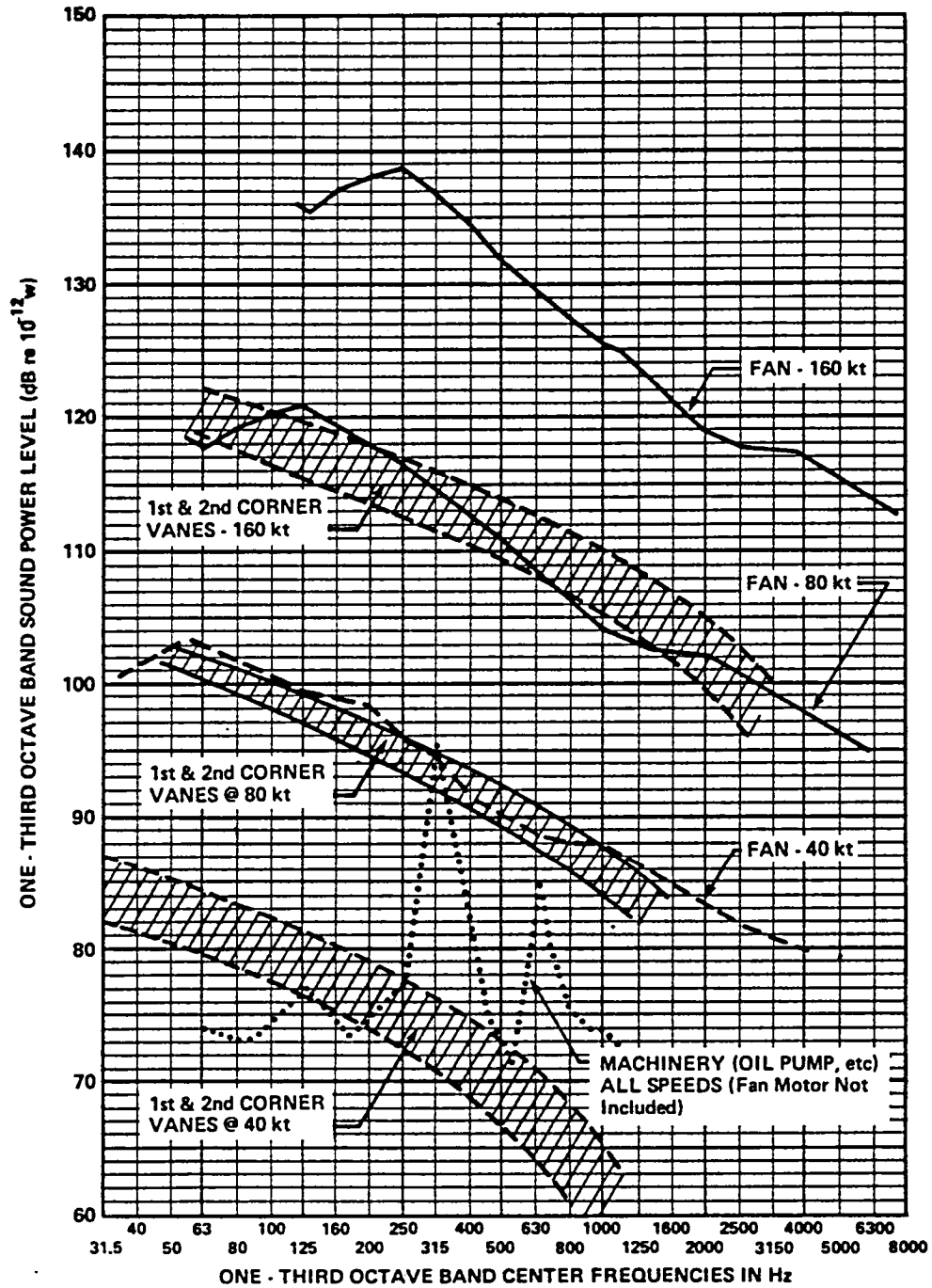
FIGURE 7. ESTIMATED SOURCE POWER LEVEL OF FAN AND TURNING VANES.
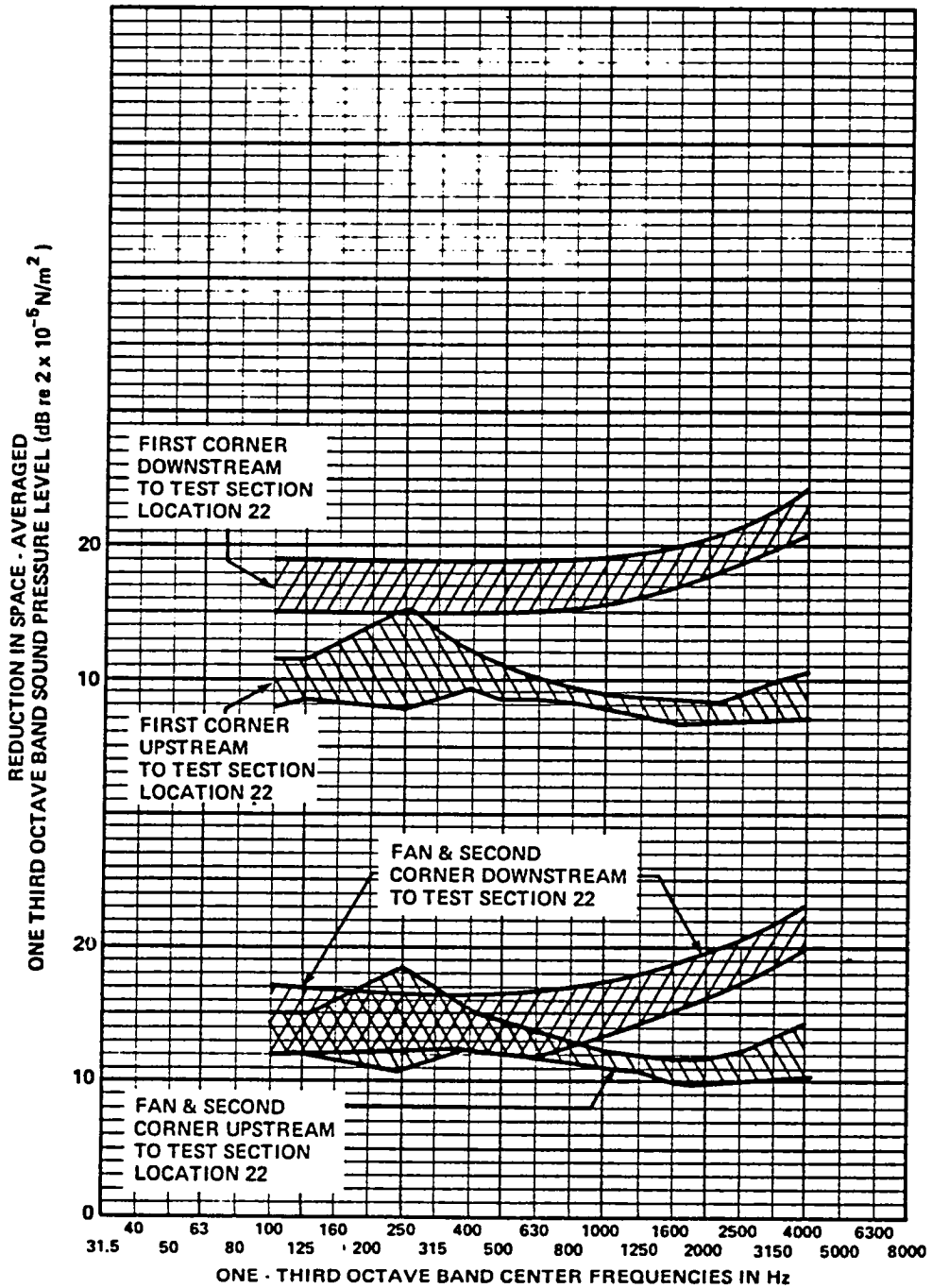
FIGURE 8. ESTIMATED REDUCTION IN ACOUSTIC INTENSITY BETWEEN VARIOUS SOURCES AND TEST SECTION.

17

second and first diffusers (i.e., upstream) except perhaps at frequencies below 500 Hz, where the losses in the downstream direction are in the same range as those in the upstream direction. The first corner turning vane noise propagates primarily through the first diffuser, although the propagation loss of the downstream path is not much greater at low frequencies.

Flanking paths were not explicitly evaluated in this study.

1.4.3 Composite noise spectra in test section

The relative contribution of each of the dominant sources was calculated using the source and path characteristics. In the computation procedure, estimated the power levels were first converted to sound pressure levels through use of experimentally-derived absorption coefficients and standard room acoustics formulas. The location selected for the comparison is microphone 22, on the tunnel centerline in the forward part of the test section, since it is representative of a frequently-used measurement location. Figure 9 presents the predicted spectra at the test section reference microphone for each of the source/path combinations, for the 80 kt speed used for most tests.

The fan noise propagation via the upstream leg is predicted to be dominant, with nearly equal contributions at low frequencies from fan noise propagating via the downstream leg. Turning vane noise is seen to be less important, but will need to be controlled if the goals set forward above are to be achieved. (note that the turning vane noise calculation is subject to substantial error - possibly ±10 dB - due to lack of necessary detailed information regarding the flow field incident upon the vanes). (Note also that the machinery noise associated with the drive motor oil pump exceeds the interim criterion at several frequencies, especially in the 315 Hz band; this data is contained in Figures A.4 and A.5.) The collector noise does not
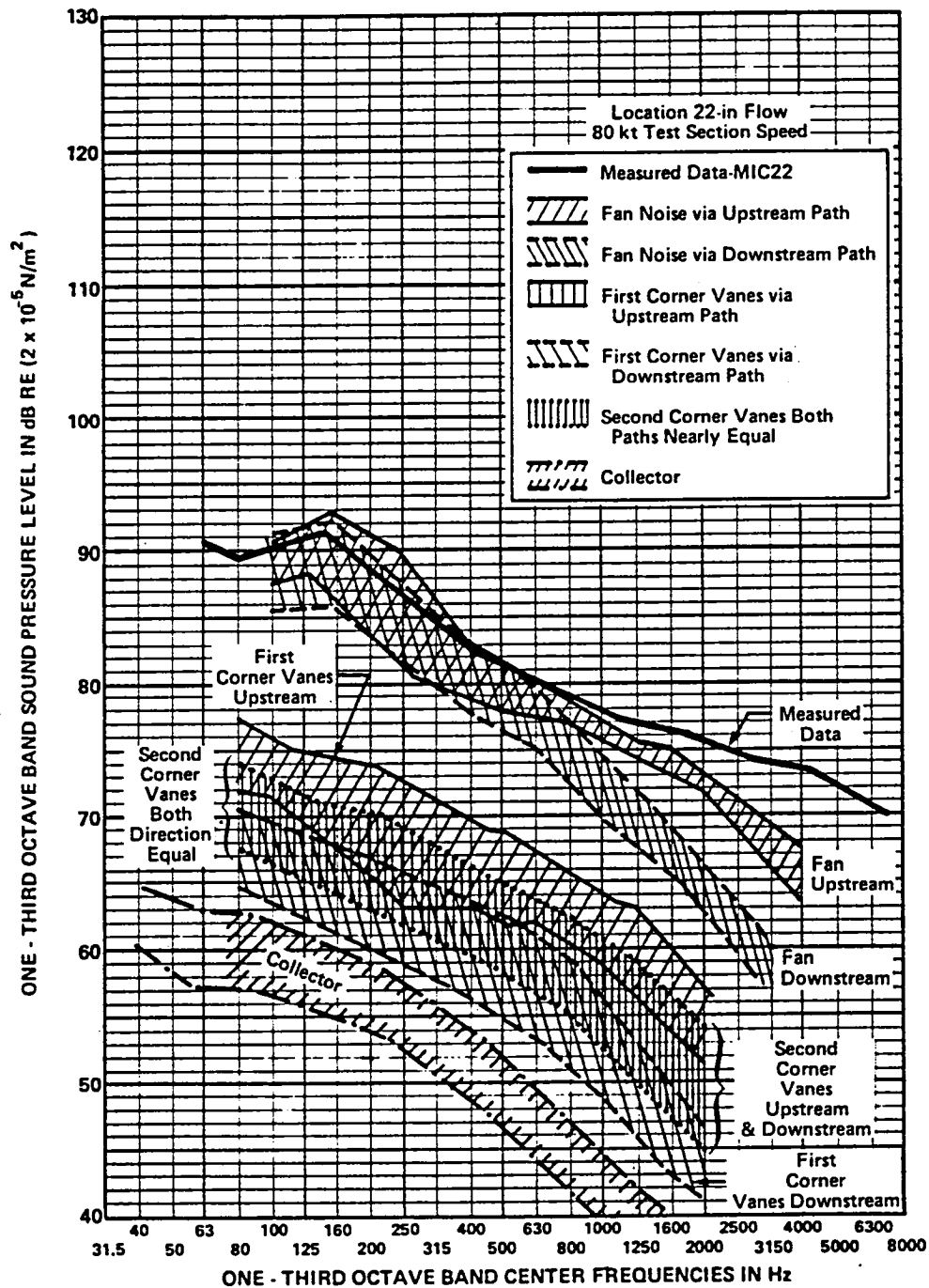
FIGURE 9. PREDICTED SOURCE/PATH COMBINATIONS AT 80 kt
(SAME RELATIVE LEVELS EXPECTED AT 120 kt)

19

appear to be a problem, except at low frequencies. Intrusive noise from other facilities has not been estimated, nor has the noise from flow past the nozzle lip , the floor, or model supports. However, it is noteworthy that the DNW aeroacoustics staff believe that the primary residual source of mid- to high-frequency noise in the DNW tunnel is the nozzle's turbulent boundary layer interaction with the lip; it is unlikely that the "lip noise" levels in the 4 x 7 m tunnel are substantially greater than those in the DNW facility, in which case the lip noise would not account for the "underprediction" shown in Figure 9.

The composite noise prediction agrees reasonably well with the test section measurements; however, the high frequency levels are underestimated by a substantial amount. The explanation for this underestimate may lie in the differences in propagation characteristics with flow-on as compared with the no-flow situation from which the acoustic transfer functions were derived (such as refraction of propagating waves away from the tunnel walls by the velocity profile). It is also possible that the microphone self-noise is higher than estimated in App. G, due to differences in the microphone mounting techniques between the referenced self-noise study and the 4 x 7 tests, higher than assumed turbulence levels in the 4 x 7, or near-field radiation from the microphone stand itself. This discrepancy should be resolved, or at least accounted for prior to finalizing treatment specifications. Further testing may be required to resolve this point.

1.4.4 Noise reduction required to achieve background noise goals

The frequency spectrum of noise reduction required to achieve the goal for the background noise environment is shown in Figure 10. Figure 11 shows the predicted noise reduction of the
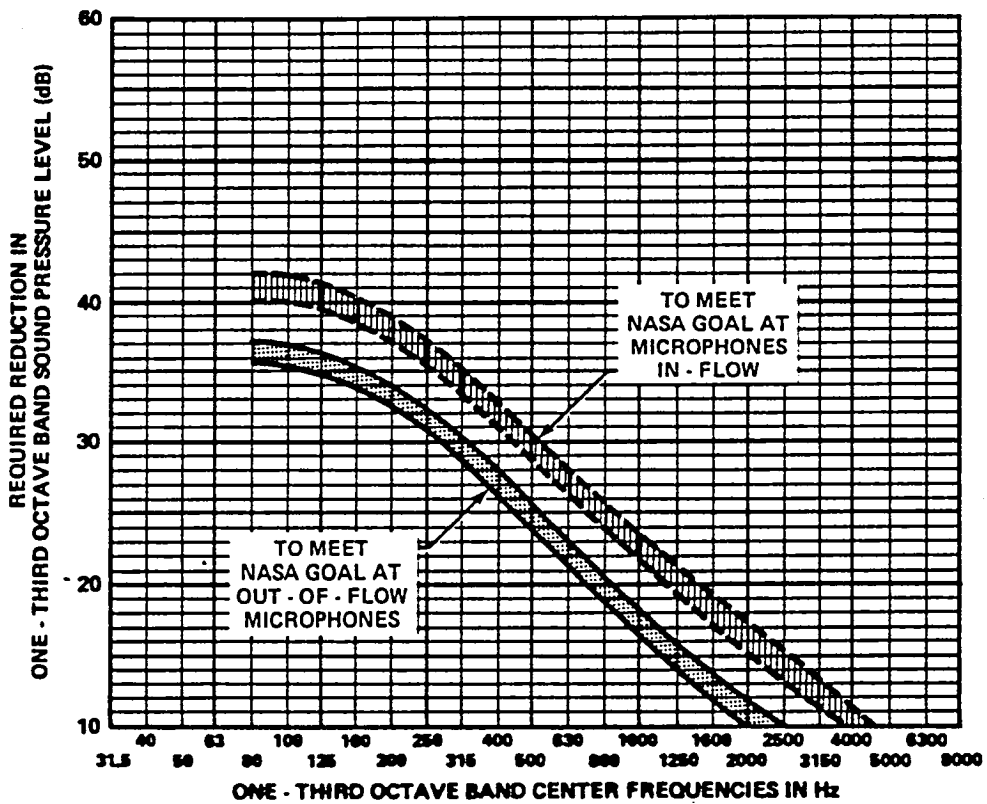
FIGURE 10. TYPICAL REQUIRED REDUCTIONS OF TEST SECTION LEVEL TO MEET 120 kt BACKGROUND NOISE GOAL WITH 10 dB SIGNAL-TO- NOISE MARGIN.

21

Y-axis: REDUCTION IN ONE - THIRD OCTAVE BAND SOUND PRESSURE LEVEL (dB)

Top chart labels:
- Fan and First Corner Turning Vane Noise Reduction Required
- FAN
- Upstream Path
- 1st Corner Vanes
- Via Upstream Path
- Downstream Path
- Downstream Path

(Note: If all "n" Sources are Brought Down to Equal Contributions, then Additional Attenuation of 10 Log n will be Required of each Source)

Bottom chart labels:
- Second Corner Turning Vane Noise Reduction Required
- Upstream Path
- Downstream Path

X-axis: ONE - THIRD OCTAVE BAND CENTER FREQUENCIES IN Hz

FIGURE 11. REDUCTIONS REQUIRED TO BRING EACH SOURCE/PATH CONTRIBUTION TO NASA CRITERION (SEE NOTE).

22

various sources and paths required to achieve the noise reduc-
tions shown. In this figure it can been seen that the reduction
of fan-generated noise requires treatment of both low frequency
and high frequency regimes; the low frequency regime must be
treated for propagation in both the upstream and downstream
direction.   It is likely that the first-corner vane noise will
prevent reduction of test section levels to the interim goal. In
such a case, treatment must be applied to the first diffuser in
order to attenuate all possible sources of high frequency noise.
The oil pump noise must be controlled for low speed (< 60 kt)
operations; however, if treatment is applied to the circuit to
reduce fan noise, the oil pump noise will also be treated. Noise
reaching the tunnel from external sources (other facilities,
traffic, aircraft) may be a problem in certain situations; at the
time of this report we did not have a controlled set of measure-
ments documenting the background noise levels caused by some of
the heavily-used facilities in the vicinity of the 4x7m wind
tunnel. However, low frequency sound transmitted through the
east and north walls of the tunnel into the settling chamber
upstream of the nozzle, and via the air exchange port in the
first diffuser appears to be a potential problem for the cases
involving low speed operation of the wind tunnel, low source
levels from the test object, and high background noise from
adjacent facilities.

1.4.5 Overall results of noise reduction study

This study has shown that the 4 x 7m tunnel requires two
major improvements in order to meet the objectives set forth by
NASA:

1)   the test chamber must be made anechoic for all frequen-
      cies of interest by use of high quality acoustic wedges
      wherever possible, and flat or conformal sound absorbing

23

coverings on all other surfaces, including the tunnel floor;

2) Source levels of the fan, turning vanes, and ancillary machinery must be reduced and/or substantial amounts of treatment must be placed at several locations in the circuit.

The test chamber anechoic treatment is straightforward and can be largely designed by and procured from commercial suppliers of anechoic rooms and acoustic treatment. Therefore, the room treatment will not be discussed further here.

The noise reduction effort is more complex because of the large reduction needed - which exposes a multiplicity of sources and paths, and because the noise reduction must be achieved without substantial performance penalties, thereby eliminating several acoustically-effective sound suppression concepts.

This study has concluded that fan noise could be reduced at the source by two means:

1) elimination of the stall which presently exists, either through modifying the inflow with upstream devices such as a large nose cone or reworked turning vanes, or through repitching or replacing the blades;

2) reduction of tip speed through increased blade chord and radial redistribution of the aerodynamic loads.

We estimate that at least 15-25 dB of broadband noise reduction could be obtained if both these steps were taken, an improvement which does not reach the goal but which could minimize the amount of absorptive treatment required elsewhere in the circuit, and which would reduce the power requirements for all

testing in the tunnel. At the very least, the stall problem should be eliminated (8 dB improvement).

The sound absorption concepts applicable to the 4x7m wind tunnel circuit can be broadly classified as:

A. Non-Intrusive Liners: absorbing surfaces which do not modify the contours of the flow path and therefore do not represent sources of potentially-significant aerodynamic losses.

B. Splitters: large-chord streamlined surfaces which effectively cut the ducts in half, but which represent relatively little blockage and thus relatively small aerodynamic penalties.

C. Baffles: traditional industrial-type closely-spaced acoustically-absorbing "splitters" which are acoustically effective but aerodynamically inefficient.

D. Treated Turning Vanes: long-chord airfoil-shaped turning vanes which contain acoustic treatment; such vanes have inherently low aerodynamic losses if designed according to good aerodynamic practice.

Many variations of these general concepts were studies to attempt to rank order the concepts in terms of noise reduction effectiveness, potential performance impact, initial cost, and operational impact. A figure-of-merit was devised which basically compared the insertion loss in the bands of interest from 125 Hz to 1 kHz on the basis of the total surface area treated since, to the first order, the applicable noise control hardware costs approximately the same per unit area or unit volume. Several concepts emerged as being most promising for upstream-propagating noise:

1) The combination of a duct liner with a treated nose cone and a single annular splitter on the upstream side of the

fan was approximately twice as effective as a number of other treatments. Since this treatment could also be used to reshape the inflow to the fan, it should be studied further to clarify those additional benefits. Losses predicted for this concept were relatively small;

2) Treatments which were approximately equal in their effectiveness included:

- long-chord treated turning vanes (little aero penalty);

- simple wall liners in the first and second diffusers (non-intrusive, therefore little aero penalty);

- parallel baffle silencers (25% blockage).

The simple splitters used in conjuction with wall treatments were the least effective on the basis of performance per unit surface area.

For downstream-propagating sound (from the fan), the most effective concepts were:

1) treated turning vanes (with elongated chords);

2) a lined fan duct and tail cone with a streamlined treated splitter (similar to the fan inlet duct).

Less effective were the parallel baffles in the fourth diffuser, and least effective were the fully-lined walls with or without single splitters.

However, the above rank-ordering does not fully account for all potential impacts and benefits which must be considered.

The estimated cost of implementing various treatments is $5-5.5M.

1.4.6 Summary of impacts from different noise control strategies

Table 1 summarizes the relative benefits and impacts of the three basic approaches to quieting the 4 x 7m wind tunnel test section.

Option 1: Simply treating the existing circuit can result in a test section acoustic spectrum which meets the goal, but at considerable expense and a measurable performance impact.

Option 2: Redesign of the fan, rotor and stators will reduce the noise levels, improve performance, and minimize the amount of additional treatment, but will not alone be adequate to reach the goal.

Option 3: Redesign of the fan and partial treatment of the circuit offers the opportunity to reach or exceed the noise goal with minimum performance impact (perhaps improvements due to fan redesign and flow tailoring). This option could have the highest initial cost, if it becomes necessary to replace major mechanical parts of the fan motor system; however, if only fan blade and hub re-work is necessary, this option could have the lowest initial cost.

IMPACT ON FACILITY CAPABILITIES AND OPERATIONS

APPROACH*	BACKGROUND NOISE GOAL	FLOW QUALITY / PLANNED FLOW QUALITY	MAXIMUM q_0 / CURRENT MAXIMUM q_0	RELATIVE INTIAL COST	RELATIVE OPERATING COSTS	MAINTENANCE REQUIRED	DOWNTIME FOR CONVERSION	ADDITIONAL STEPS NEEDED
① Maintain Current Fan; Add Acoustic Treatment to Circuit	Can Meet or Exceed	Possible Minor Degradation (or Minor Improvement	May Reduce by 8–10%	High	Increase $\propto \Delta q/q_0$	Periodic Cleaning of Certain Treatment	Substantial (to Be Determined)	● Model Tests ● Design ● Procurement
② Rebuild Fan	Probably Can't Meet Without Some Treatment in Circuit	Could Improve	Could Increase	Low	Below Current Costs	Probably Below Current Levels	Substantial (to Be Determined)	● Model Tests ● Full Scale Flow Measurements ● Design ● Model Test ● Procurement
③ Rebuild Fan and Add Acoustic Treatment to Circuit	Could Exceed Goals by Large Margin	Could Improve	Could Increase	High to Highest	Below Current Costs	FAN: Less Than Current TREATMENT: Periodic Cleaning	Substantial	① + ②

* All choices assume that suitable anechoic treatment will be installed in test section.

TABLE 1. SUMMARY OF RELATIVE BENEFITS AND IMPACTS OF PRINCIPAL APPROACHES TO REDUCING BACKGROUND NOISE IN TEST SECTION.

2. ACOUSTIC CHARACTERISTICS OF THE TUNNEL CIRCUIT

2.1 Objectives and Methods

The acoustic characteristics of the wind tunnel are of importance to the noise control effort because they provide information regarding the manner in which acoustic energy is transmitted around the circuit and into the test section. The information can then be used to determine the locations and spatial extent of the required acoustic treatments. Several tests were performed with the objective of describing the acoustic characteristics. These tests included:

(a) acoustic reverberation measurements at several locations in the tunnel;

(b) acoustic propagation around the tunnel circuit with a steady-state sound source;

(c) sound pressure cross-correlation measurements across first and second corner turning vanes;

(d) sound pressure coherence and phase measurements between closely-spaced microphones, with a sound source in the tunnel;

(e) sound pressure coherence and phase measurements between closely-spaced microphones in the presence of flow.

The first two tests provide data on the dissipation of acoustical energy in the tunnel and the distribution of sound levels around the circuit when sound sources are placed in different locations. The third test determines the role played by the turning vanes in reflecting sound around the corners of the tunnel. Finally the fourth and fifth tests provide information regarding the sound propagation paths in the presence of flow and the contributions of local aerodynamic noise sources

29

to the total acoustic power in the tunnel. Data acquired from the steady-state sound source tests, the cross-correlation measurements, and the coherence and phase measurements are presented in Appendices B, E and D, respectively. The results are summarized in this section and general conclusions drawn regarding the acoustic characteristics of the tunnel circuit.

2.2 Reverberation and Acoustic Absorption

The acoustic reverberation tests were performed using a small cannon as the impulsive sound source; the cannon was placed separately at five locations in the tunnel circuit. The decay of the sound field was measured by a series of microphones placed at a number of locations in the diffuser, settling chamber and test sections. Source and microphone locations are shown in Figure 12. The acoustic signals from the microphones were recorded on magnetic tape and replayed through octave band filters to obtain reverberation decay rates. Typical decay signatures are plotted in Figure 13.

2.3 Propagation of Sound from Steady-State Source

The results of the steady-state sound source tests (Test 2) are presented in Appendix B. Sound pressures at several locations are shown in terms of one-third octave band levels. In addition, the sound pressure levels are normalized with respect to the local cross-sectional area in the tunnel circuit. If the acoustic environment consisted of a propagating sound field without dissipation, the acoustic power would be constant around the tunnel circuit and the normalized spectra should collapse onto a single curve. The actual acoustic field consists of propagating and reverberant components with some, albeit small, dissipation. Furthermore, the acoustic power entering the test section/chamber is dispersed over a large area and is dissipated at the chamber walls. Thus, it is difficult to determine the

30
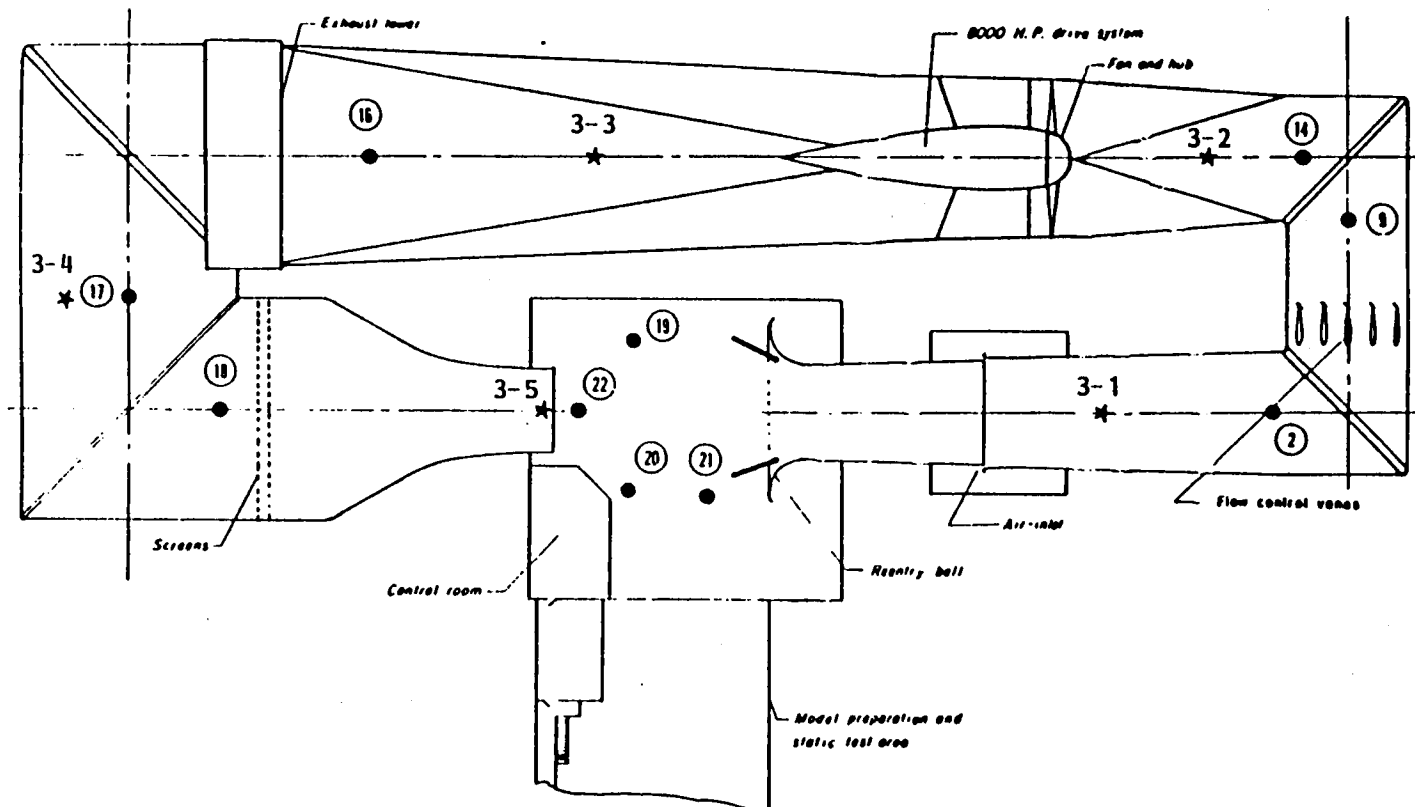
FIGURE 12. MICROPHONE AND SOURCE LOCATIONS FOR IMPULSIVE SOUND
TESTS (TEST 3).

(a) OVERALL SIGNAL IN
TEST SECTION

10 dB

$10 \log (p^2/p^2_{ref})$

1 sec

1 sec/in

← TIME INCREASING

(b) 4.0 kHz OCTAVE BAND
IN 1st DIFFUSER

10 dB

1.0 sec

← TIME INCREASING
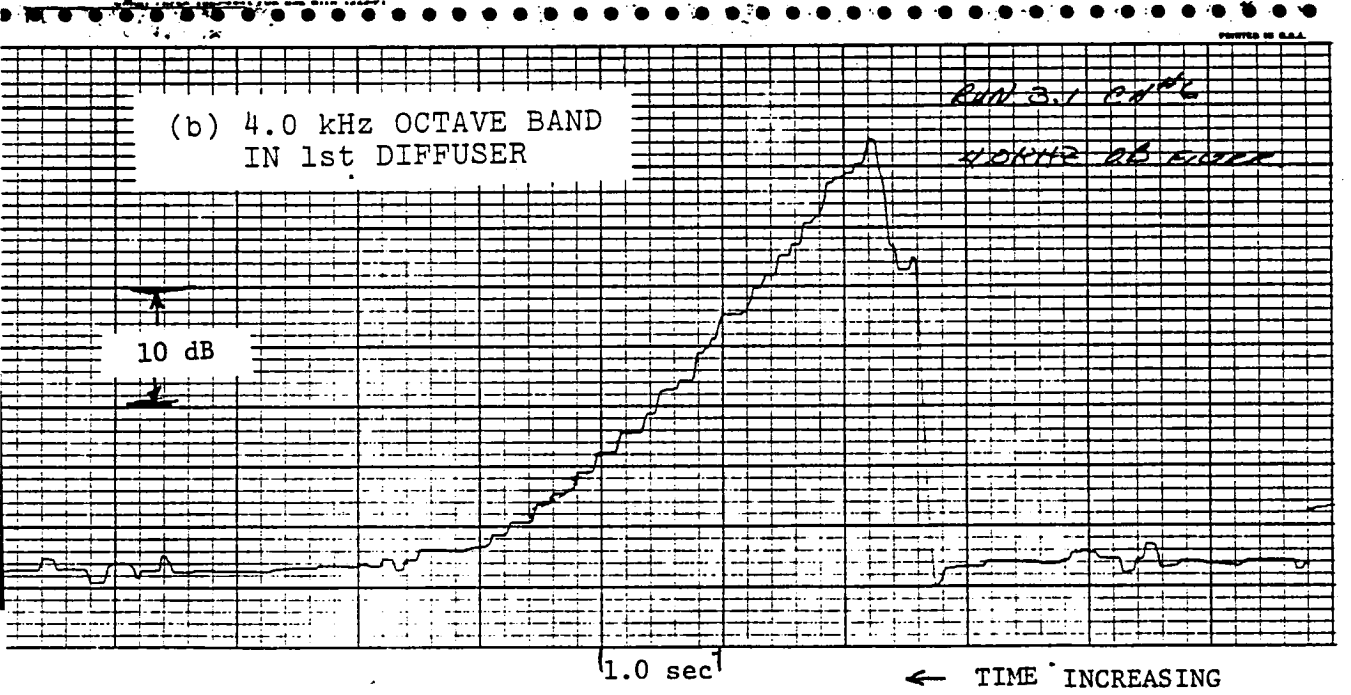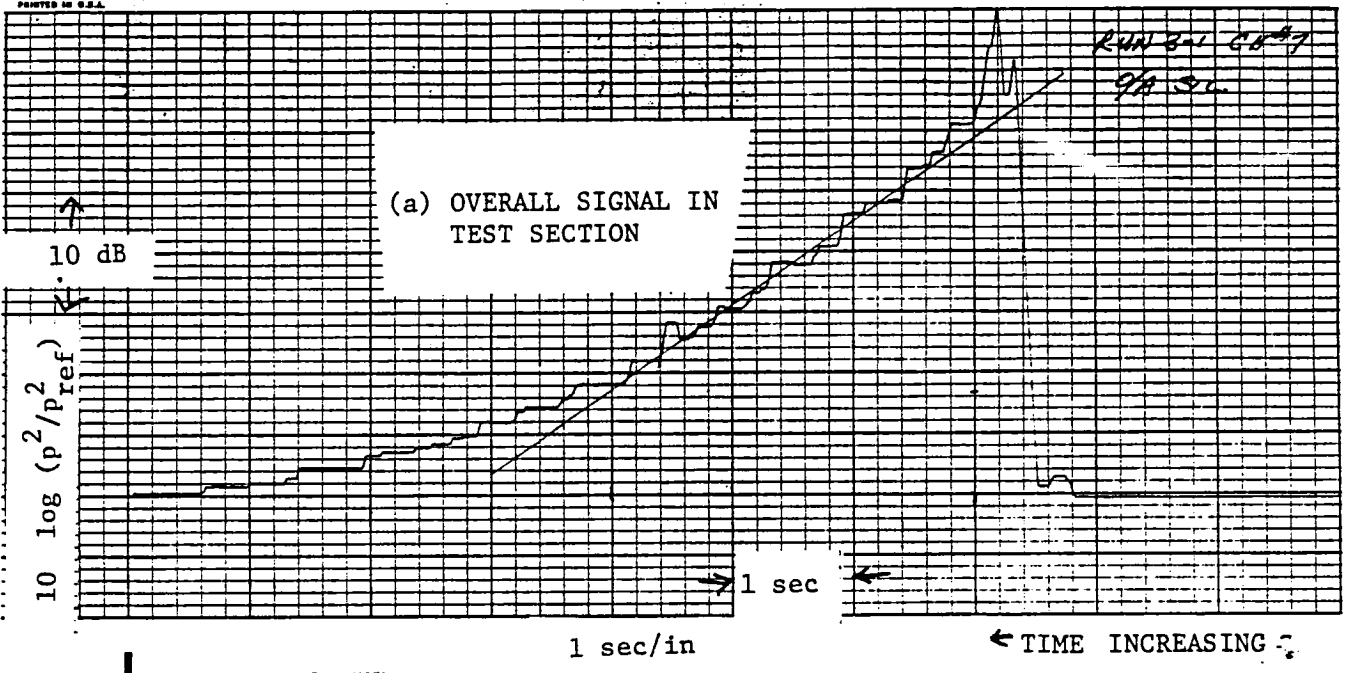
FIGURE 13. TYPICAL SPL DECAY TIME HISTORIES

appropriate value of the normalizing area for the test section microphones. The data show a much better collapse (Figure 14) when the cross-sectional area of the test chamber is used instead of the value for the test section (or nozzle) (see Figs. B.6 through B.8) except when the sound source is in the nozzle. This uncertainly regarding the precise value of the normalizing area makes it difficult to assess the dissipation losses in the tunnel circuit.

When the sound source is in the tunnel circuit, source directivity has little effect on the sound distribution around the tunnel, presumably because of the highly-reverberant conditions present in the tunnel. However, when the source is in the test section, directivity is important since off-axis radiation is not necessarily reflected by the test chamber walls back into the diffuser or nozzle without loss energy. This is true particularly at high frequencies where source directivity and acoustic absorption at chamber surfaces can be significant.

Measurements of the sound levels at several locations in the test section/chamber showed that the highest sound levels occurred on the tunnel centerline. One possible interpretation of the results is that sound radiating from the diffuser entry is influenced by the directivity characteristics of the diffuser collector. However, the sound pressure levels change more rapidly with angle than would be predicted for an unbaffled opening as large as the diffuser entry. Thus, the sound levels are probably being influenced by several factors including radiation from the nozzle and reflections from the surfaces in the chamber. In Appendix B, through the use of data from other facilities, the actual directivity patterns of the 4 x 7m tunnel nozzle and collector openings were estimated, and the result is shown in Fig. 15.
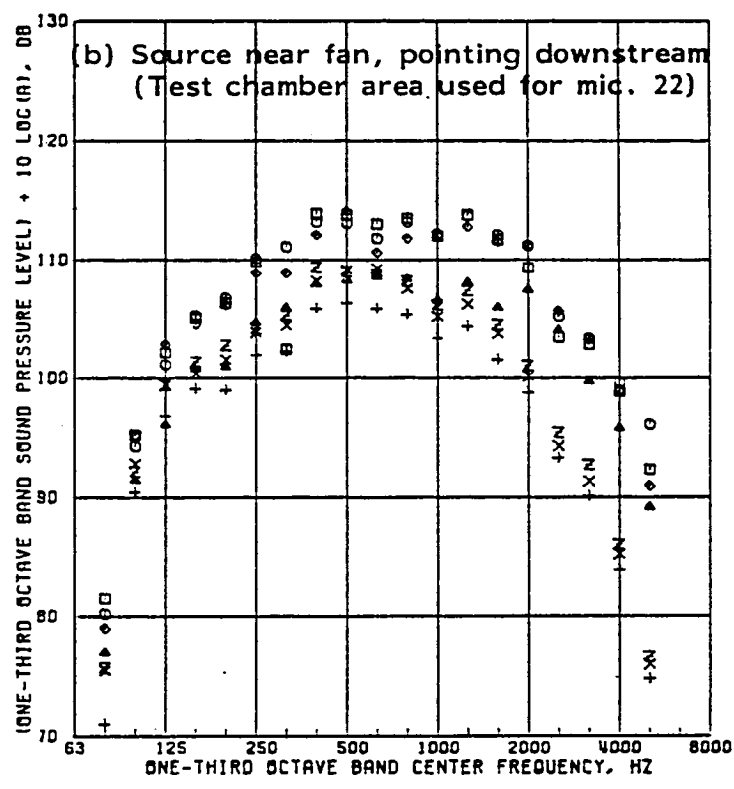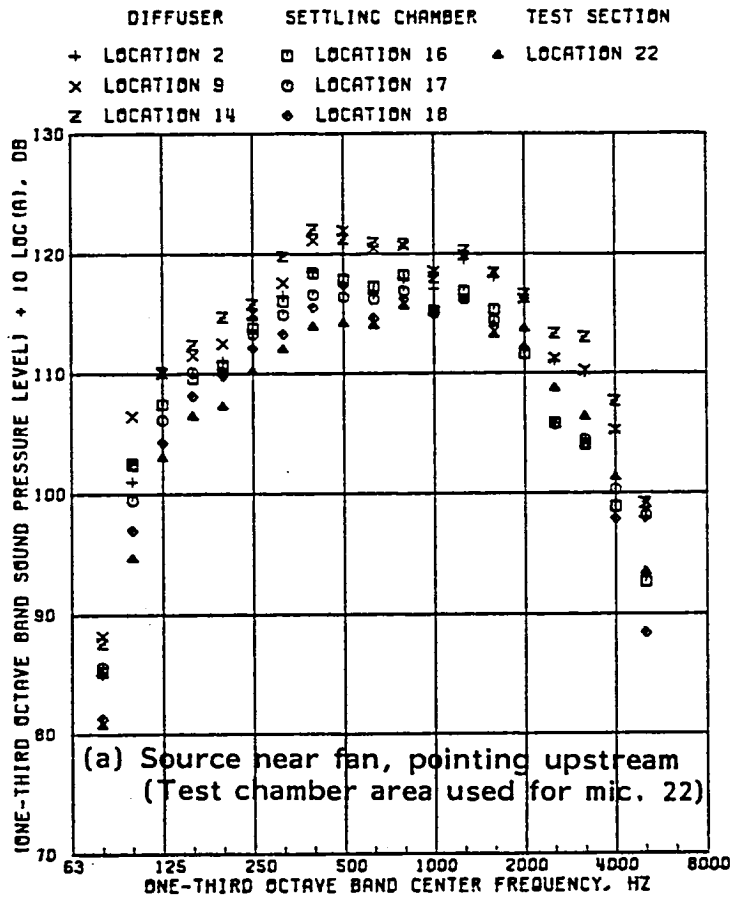
FIGURE 14. SOUND LEVELS IN TUNNEL NORMALIZED WITH RESPECT TO CROSS-SECTIONAL AREA (STEADY-STATE SOURCE).

(c) Source in nozzle, pointing downstream
(Test section area used for mic. 22)

FIGURE 14. CONTINUED

AZIMUTH RELATIVE TO TUNNEL CENTERLINE

ONE-THIRD OCTAVE BAND LEVEL RELATIVE TO CENTERLINE POSITION

FIGURE 15. ESTIMATED DIRECTIVITY OF NOZZLE AND COLLECTOR BASED ON NO-FLOW TESTS FOR MODELS IN FULL SCALE.

2.4 Cross-Correlation Measurements at Turning Vanes

Cross-correlation measurements were made using microphones located at either side of the turning vanes in the first and second corners of the tunnel. A steady-state sound source was used in each case and there was no flow in the tunnel. The measurements were used to determine the influence of the turning vanes and the flow control vanes. Results of the measurements are presented in Appendix E.

The main objective of the tests was to determine the importance of the turning vanes in reflecting sound waves around the corners. If the sound propagates through the vanes with little or no reflection or scattering, the sound waves will be reflected at the tunnel walls. An appropriate noise control method in such a case will involve the placement of sound absorbing material on the tunnel wall. On the other hand, if the sound waves are reflected by the turning vanes, the acoustic treatment on the walls will be bypassed and have little noise control benefit [3].

Examples of the ray tracing procedure performed for the first and second corner turning vanes are shown in Figure 16. These rays were constructed essentially for high frequency sound waves, so that they show paths associated with reflection by the vanes, although there are indications of direct transmission at some angles of incidence. In all cases the sound source and reference microphones were placed on the tunnel centerline; the secondary microphones were located at three positions across the tunnel. The postulated transmission paths will inevitably depend on the selected microphone and source positions. However, the general trend observed will be applicable to source distributions across the tunnel area.

(a) Microphone Pair 14-10
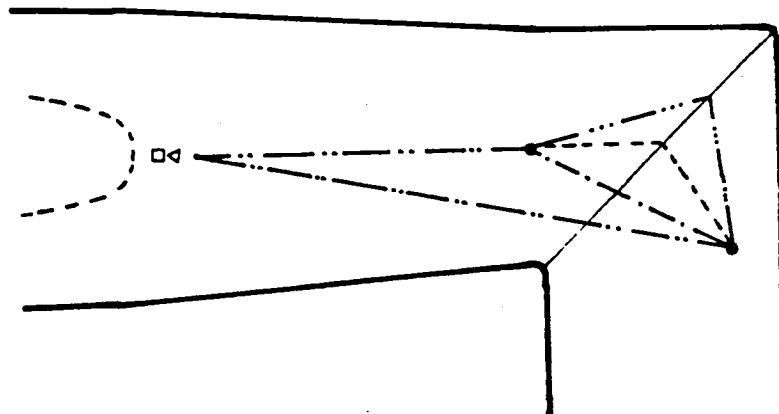
(b) Microphone Pair 14-9
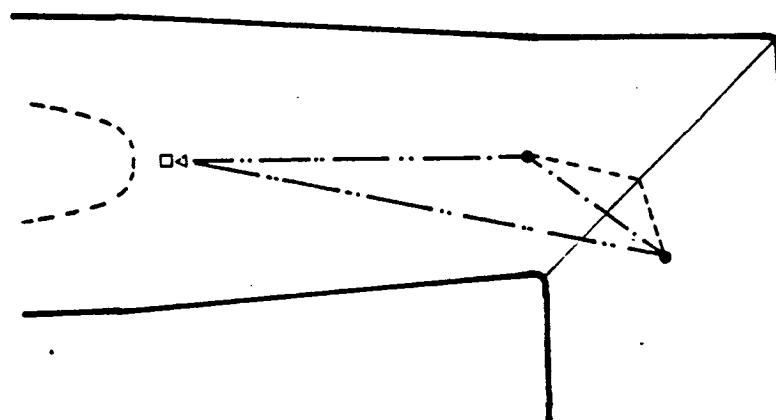
(c) Microphone Pair 14-8
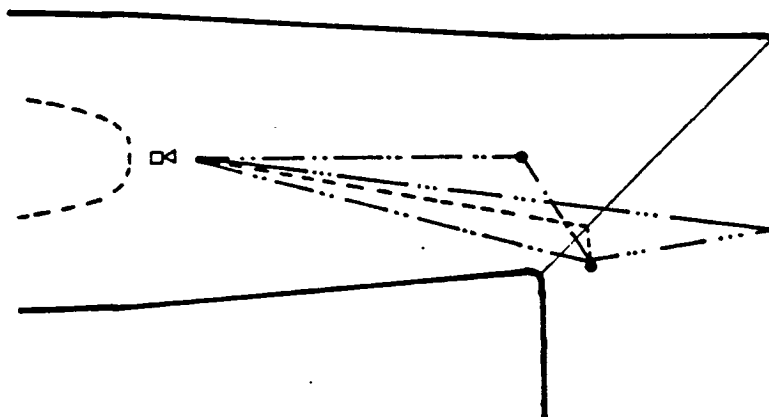
FIGURE 16. EXAMPLE OF RAY TRACING FOR TURNING VANES IN SECOND
CORNER.

Noise transmission tests were not performed in the settling chamber (third and fourth corners of the tunnel). However, the turning vanes in the third corner are identical in shape and size to those in the diffuser. Thus, the results for the first and second corner vanes should be directly applicable to the third corner.

The turning vanes in the fourth corner have a smaller chord and spacing than in the other three corners. Consequently they will have different noise transmission characteristics. It is expected, though, that appropriate scaling factors can be applied using vane chord and acoustic wavelengths as the relevant parameters. Thus the reflection characteristics of the diffuser vanes can be applied to the fourth corner vanes, with appropriate frequency scale.

There will be no distinct frequency boundary between waves that propagate through the vanes without reflection and waves that are fully reflected around the corner. Instead, there will be a fairly wide frequency range of transition. Thus it is possible to assign only a rather arbitrary demarcation frequency; data for the first and second corner turning vanes indicate that the demarcation frequency lies between 1000 Hz and 2000 Hz. In the NASA Ames 7x10-foot wind tunnel, Soderman [3] estimates that waves are fully reflected at frequencies above 2000 Hz when the turning vanes have a chord of 30 cm (12 inches).

The turning vanes in the fourth corner have a chord of about 33 cm (13 in) which is about half that of the vanes in the first, second and third corners. Consequently, the demarcation frequency will lie in the range 2000 Hz to 4000 Hz.

2.5 Coherence and Phase Measurements

The coherence and phase measurements involve the simultaneous recording of sound pressures at two closely-spaced microphones. The recordings are then replayed into a digital signal processor to obtain cross-spectral density information expressed in terms of the coherence function and phase angle spectra. These spectra can be interpreted in terms of propagating, reverberant and diffuse components, as is discussed in Appendix D. The objectives of the analysis are: the determination of the dominant direction of propagation, the magnitude of the reverberant component, the detection of incoherent sources generating a diffuse field, and the detection of acoustic components propagating in two opposing directions (upstream and downstream).

Coherence and phase spectra were measured under zero flow conditions with a single acoustic source present in the tunnel (Test 6), so that the acoustic field in the tunnel would be composed of propagating and reverberant components. The measurements were then repeated without the acoustic source but with the tunnel operating. The noise sources were then the fan, turbulent boundary layer, separated flow, and flow interaction with the turning vanes and flow control vanes. The generation mechanisms involved with the sources are discussed in Section 3; the discussion here is concerned only with the transmission of sound in the circuit and, at the same time, with estimates of the relative magnitudes of the different components.

The results of the coherence and phase measurements are presented in Appendix D, together with a brief review of the analytical models used in the data interpretation. The discussion in this section is concerned solely with the interpretation of the data.

First, consider the coherence and phase spectra measured
when the acoustic source was present and there was no flow in the
tunnel. Typical spectra measured in the diffuser and settling
chamber are shown in Figures 17 and 18 respectively. Super-
imposed on the measured spectra are curves predicted by means of
Eqs. (1) and (2) in Appendix D (see Sec. D.4 for explanation).
Values of the angle of propagation θ (see Figure D.1 for
definition of θ) were selected to fit the observed character-
istics of the phase spectra. Propagation in the downstream
direction (Figure 18) is associated with values of θ in the
range $-90^0 < \theta < + 90^0$ and a negative slope of the phase
spectrum. Propagation upstream (Figure 17) is associated
with $90^0 < \theta < 180^0$ and $-180^0 < \theta < -90^0$, and with a positive slope
of the phase spectrum; the selected values of θ were allowed to
have some variation with frequency.

Values of R, the ratio of pressure autospectral densities
for diffuse and propagating components were also selected on the
basis of the phase spectra, and were allowed some variation with
frequency. In the present case, with a single sound source in a
reverberant environment, an indication in the data of a diffuse
field component is interpreted as an artifact of the analysis
process. The discussion in Appendix D has shown how a rever-
berant field can show characteristics similar to those of a
diffuse field under certain data reduction conditions.

Straightline curves in the phase spectra of Figures 17 and
18 represent conditions where the acoustic field is purely
propagating, i.e., R=0. As R increases, the predicted phase
spectrum deviates further from the straightline. In Figure 17 a
value R=8 appears to give a reasonable fit to the measured phase
data at frequencies below about 800 Hz. However the data also
show a tendency to the (0, $\pm\pi$) pattern of a reverberant field.
Measurements in the settling chamber (Figure 18) show more of a

41
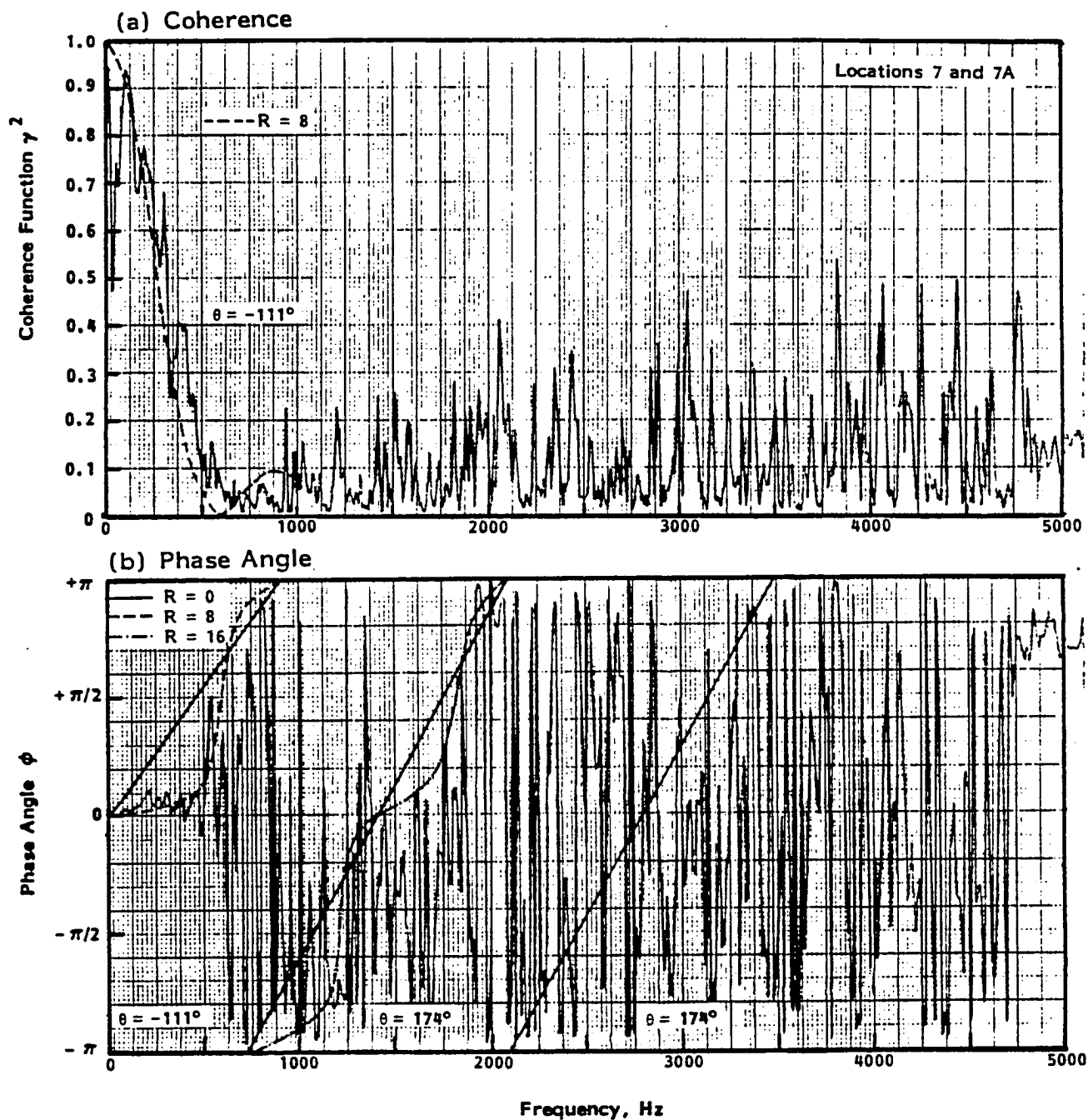
FIGURE 17. COHERENCE AND PHASE SPECTRA MEASURED IN DIFFUSER WITH SOUND SOURCE UPSTREAM OF FAN

42
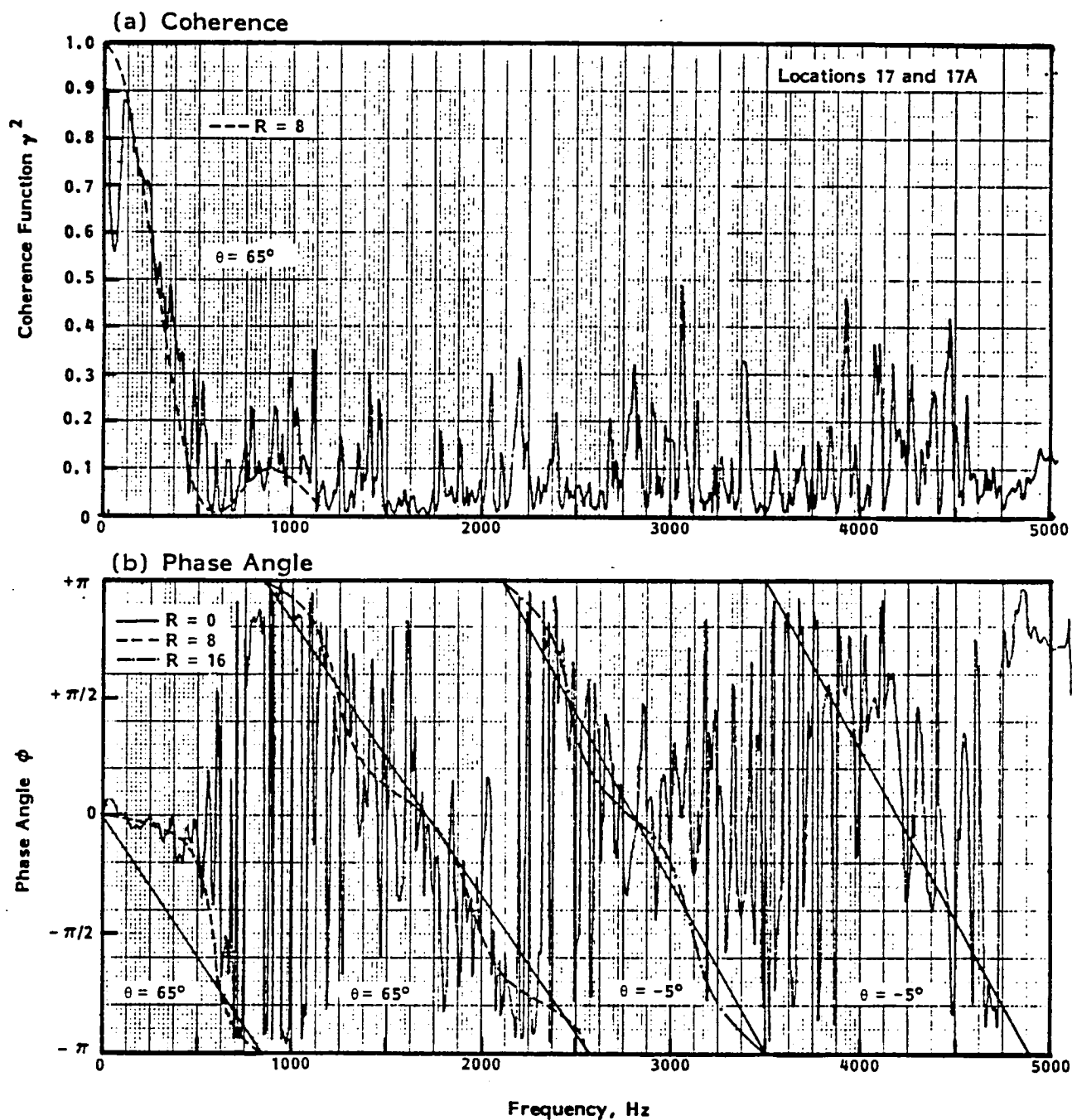
FIGURE 18.   COHERENCE AND PHASE SPECTRA MEASURED IN SETTLING
CHAMBER WITH SOUND SOURCE DOWNSTREAM OF FAN

43

propagating component. Again, appropriate values of R seem to be 8 at low frequencies, and 16 at intermediate frequencies.

Data for the test section are shown in Figures 19 and 20. In one case (Figure 20) the sound source was pointing in the downstream direction and the phase spectrum measured in the test section shows a component propagating in the downstream direction - at least for frequencies below 2000 Hz. When the sound source is pointing upstream, the test data indicate upstream propagating in the test section for frequencies above about 800 Hz (Figure 19) but at lower frequencies the downstream component is still dominant at the measurement location (microphone 22). The diffuse (or more correctly the reverberant) contribution is less in the test section than in the tunnel circuit. The values of R = 1, 2 or 4 are used to fit analytical curves to the measured phase spectra.

Corresponding coherence and phase spectra measured in the presence of flow are shown in Figures 21 through 22 for the diffuser, settling chamber and test section respectively. These sample spectra correspond to the same microphone arrangement (Configuration A) used for Figures 17 through 20, and are associated with a flow speed of 41 m/s (135 ft/sec, 80 kts) in the test section. The actual mean flow speed at location 7 is 14.5 m/s (48 ft/sec), and at location 17, 4.6 m/s (15 ft/sec).

Predicted coherence and phase angle spectra have been fitted to the measure data. Values of R are again selected to provide closest agreement with the measured spectra. It is observed first that the dominant propagation path is upstream (positive slope in the phase spectrum) in the diffuser and downstream in the settling chamber. In the case of the test section measurement location, the dominant direction is downstream at frequencies below about 700 Hz and upstream at higher frequencies.

44
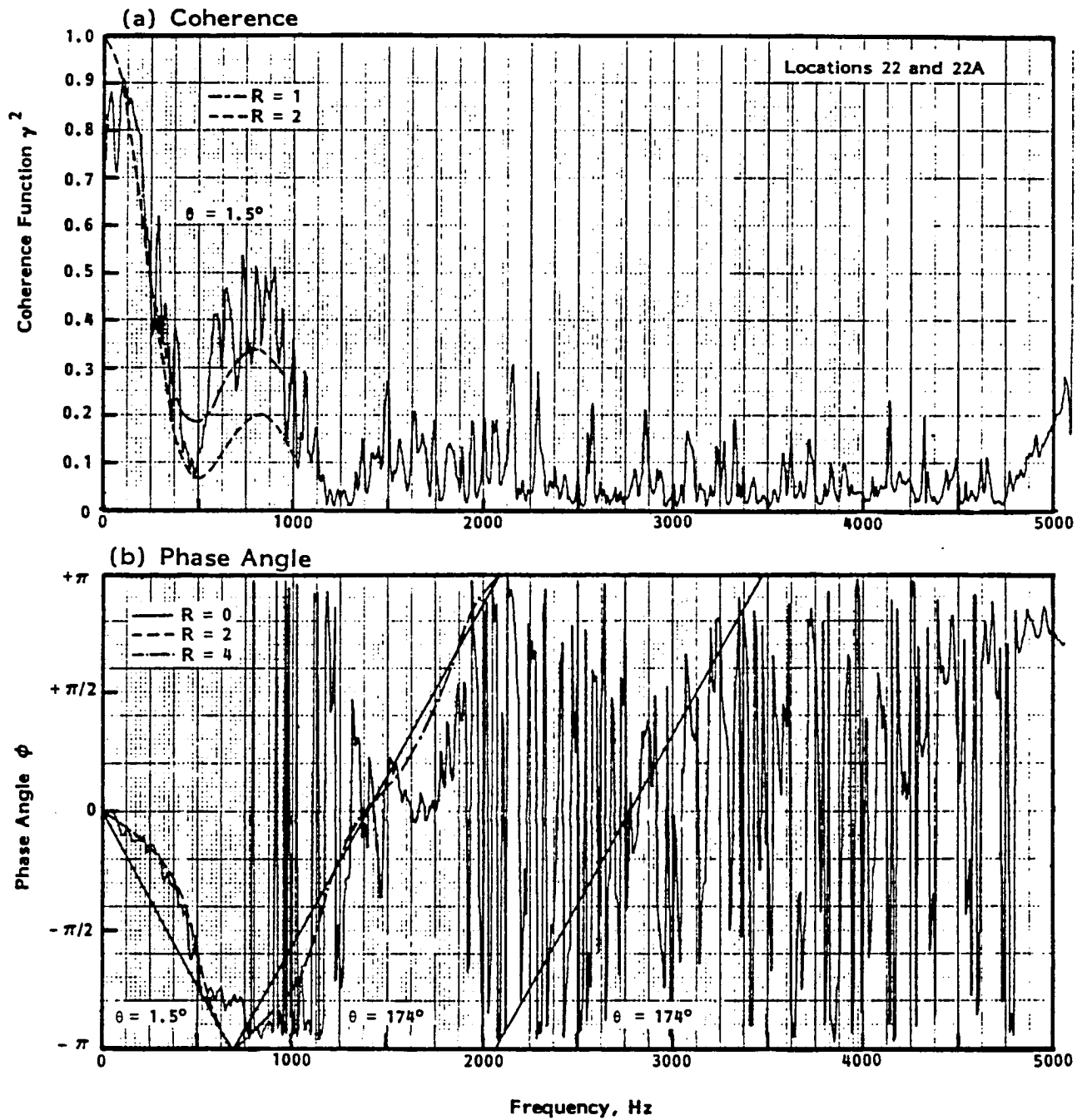
FIGURE 19. COHERENCE AND PHASE SPECTRA MEASURED IN TEST SECTION
WITH SOUND SOURCE UPSTREAM OF FAN

45
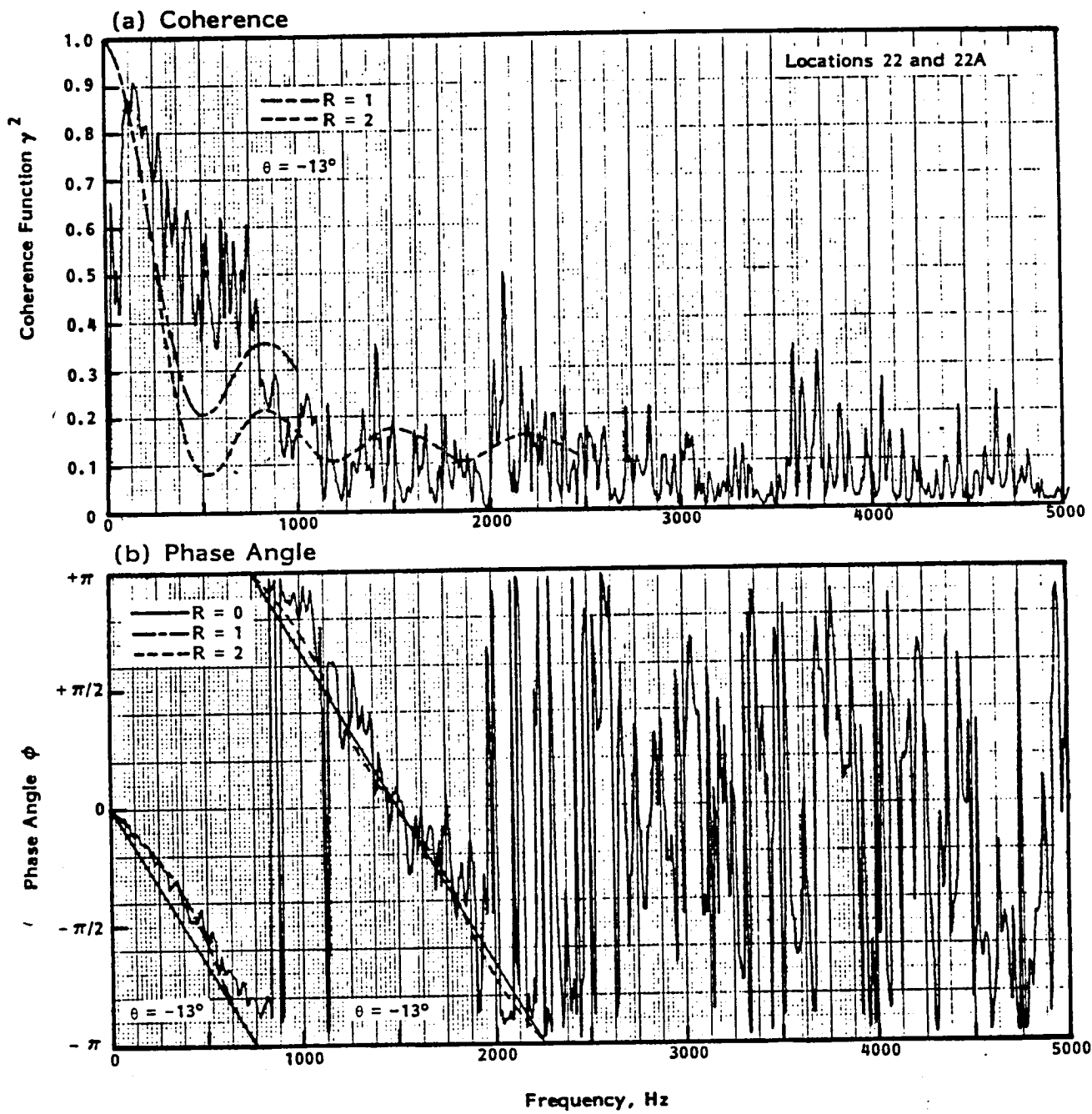
FIGURE 20. COHERENCE AND PHASE SPECTRA MEASURED IN TEST SECTION WITH SOUND SOURCE DOWNSTREAM OF FAN

46
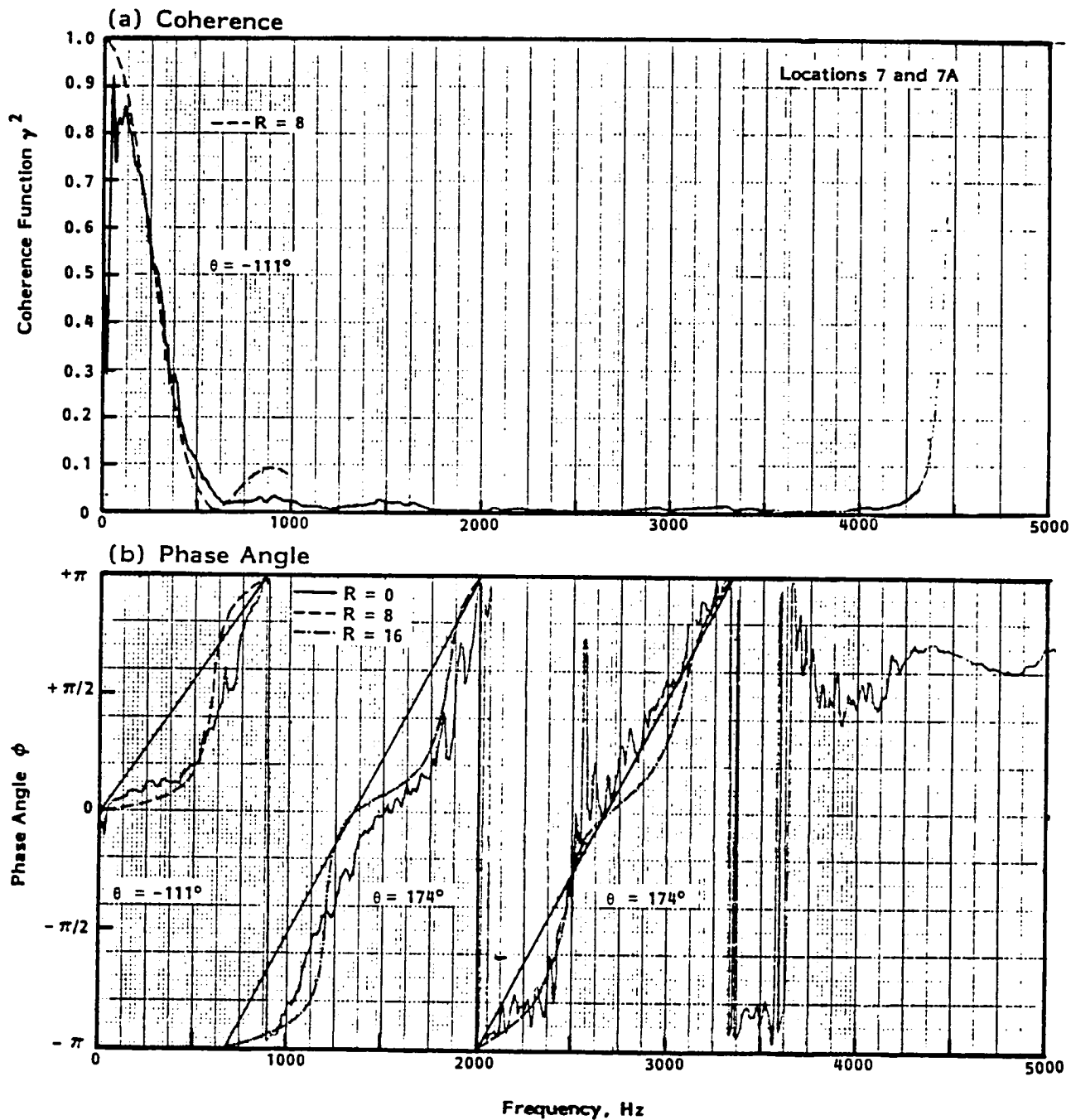
FIGURE 21. COHERENCE AND PHASE SPECTRA MEASURED IN DIFFUSER
(TEST SECTION FLOW SPEED = 41 m/s)

47
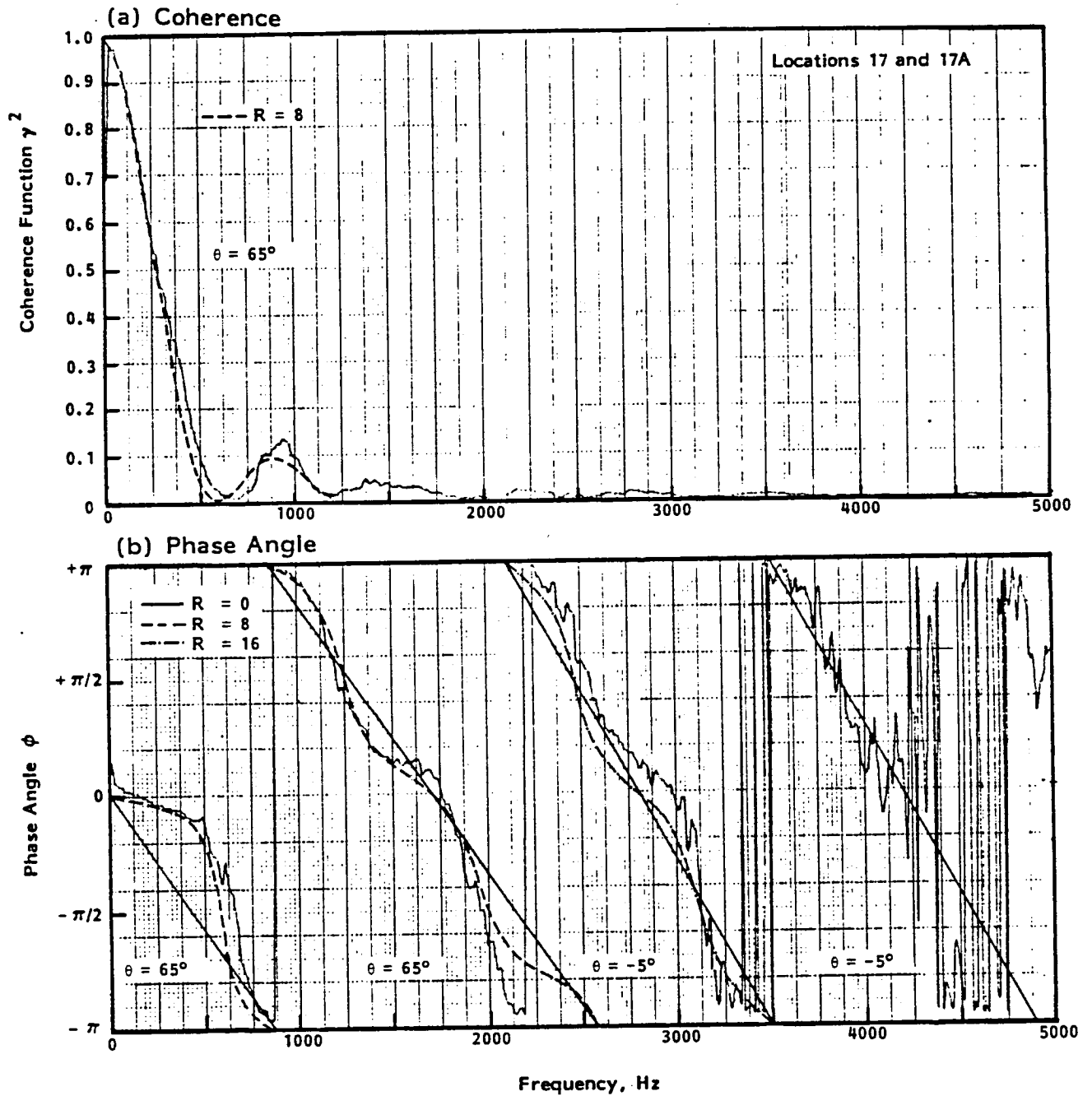
FIGURE 22. COHERENCE AND PHASE SPECTRA MEASURED IN SETTLING CHAMBER (TEST SECTION FLOW SPEED = 41 m/s)

48

However, it should be noted that, as shown in Figure D.4 of Appendix D, an indication of propagation in one direction does not mean that there is no acoustic power flow in the opposite direction. One interpretation of the data in Figure 23 is that, at frequencies above about 1000 Hz, the downstream propagating component is 6 to 10 dB below the upstream propagating component.

The values of R used to fit predicted spectra to the test data can be compared to corresponding values applied in the zero flow case. If the values of R are the same in both cases, then the data can be interpreted in terms of reverberation rather than diffusivity. If R is higher for the flow case, then the increase in value could be due to the presence of a diffuse acoustic field.

Consider first the measurements in the settling chamber. The values of R used to fit predicted curves to the measured values are the same (R = 8 or 16 depending on frequency) for the zero flow (Figure 18) and flow-on (Figure 22) cases. Consequently, it is deduced that the acoustic field in the settling chamber is reverberant with a component propagating in the downstream direction. This interpretation is consistent with the physical understanding - the flow speed is so low in the settling chamber that local aeroacoustic sources will make a negligible contribution to the acoustic field.

Now consider the diffuser. The situation is not so well defined in this case since, with zero-flow, results do not show an easily identifiable propagating component and it is difficult to fit a predicted spectrum with an assigned value of R. When flow is present the phase angle spectrum is quite different with well-defined propagating and diffuse components. It is possible that, with the sound propagating in an upstream direction, the sound waves are refracted towards the centerline of the tunnel,
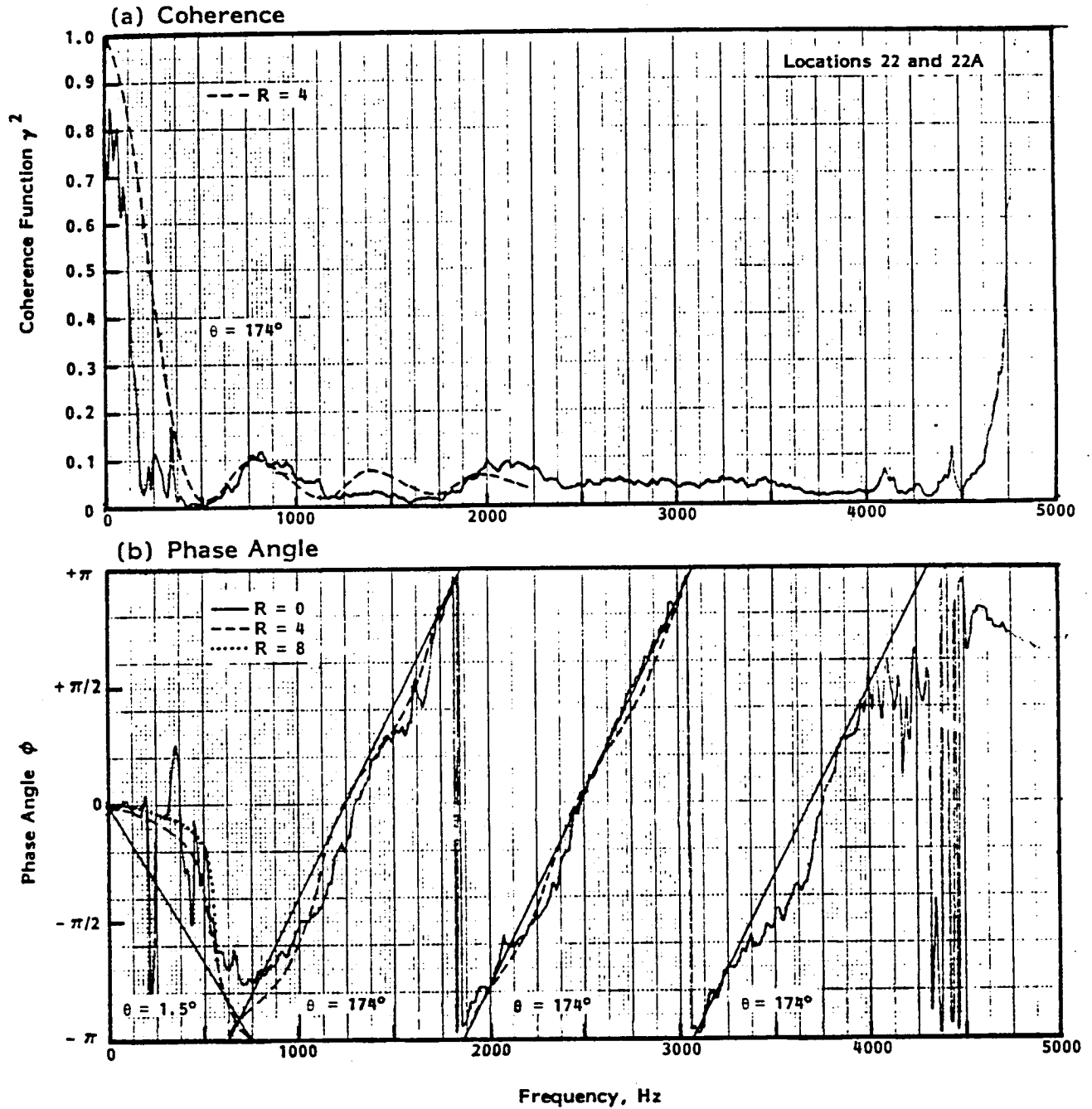
FIGURE 23.   COHERENCE AND PHASE SPECTRA MEASURED IN TEST SECTION
            (TEST SECTION FLOW SPEED = 41 m/s)

50

thereby reducing the reverberation effects. In addition sound
will be generated by the flow over the turning vanes and flow
control vanes, the mean velocity being three times larger than
that in the settling chamber. These additional noise sources
will add to the diffuse field component.

Measurements in the test section show that the effective
value of R is higher for the flow case (Figure 23) than for the
zero flow cases (Figures 17 and 20). Since there is no change in
reverberation, two explanations can be proposed for the differ-
ence in value of R. First, a diffuse sound field is generated at
the nozzle and collector in the test chamber. Secondly, the
propagating field contains components traveling upstream and
downstream. Both explanations are physically reasonable and
should be taken into consideration when designing noise control
measures.

2.6 Ray Tracing

The information acquired from analysis of the cross-
correlation and phase data has been used to construct possible
acoustic ray paths for the diffuser and settling chamber. These
paths are intended to provide a diagrammatical understanding of
the most likely transmission paths so that the effect of poten-
tial noise control methods can be assessed. Results from these
ray tracing studies are given in Figures 24 and 25 for the
diffuser and settling chamber respectively. In the case of the
diffuser, the frequency range is divided into "low" and "high"
regimes, with the bounding frequency being roughly that at which
the vanes reflect most of the acoustic power. Three frequency
regimes are used for the settling chamber analysis since the
vanes have different dimensions in the third and fourth corners,
and the bounding frequencies are different.

51
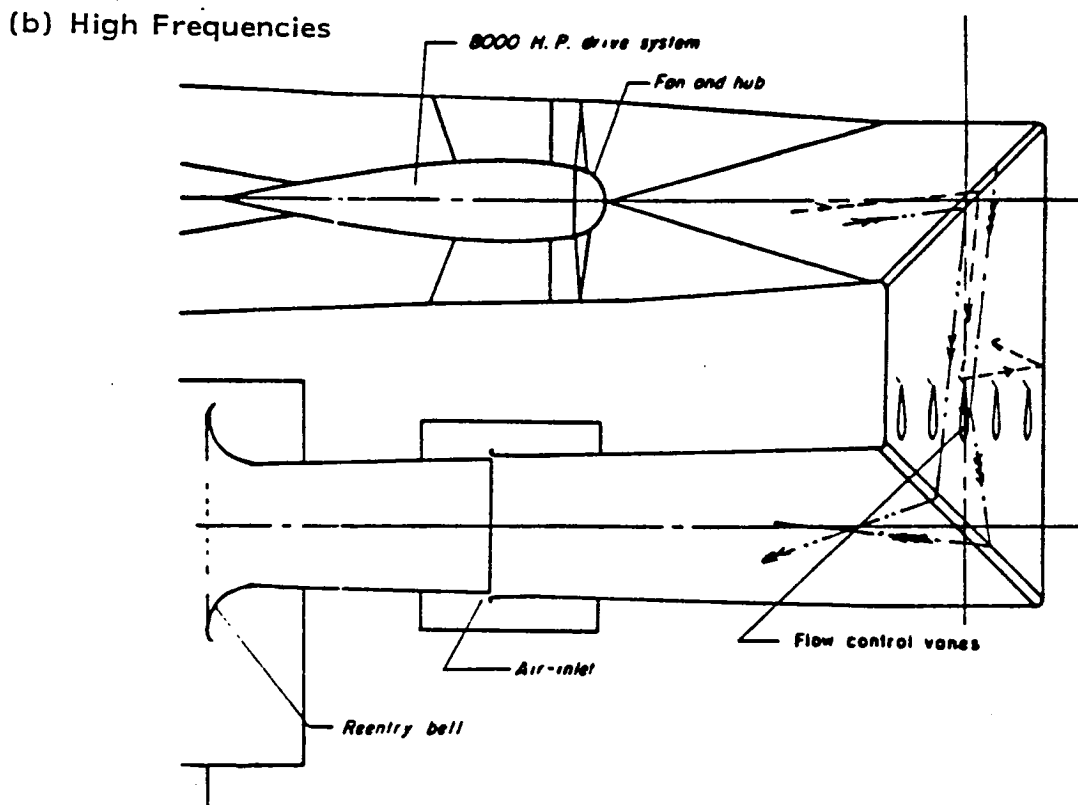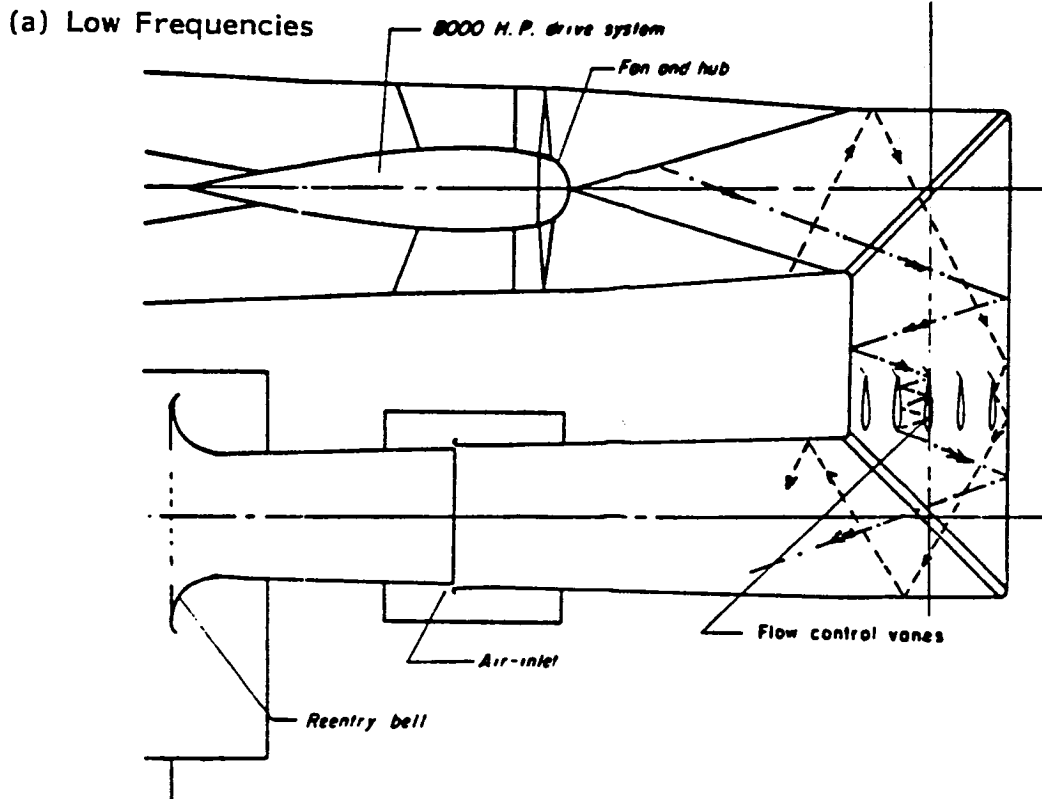
(a) Low Frequencies

FIGURE 24. DIAGRAMMATICAL REPRESENTATION OF ACOUSTIC RAY PATHS IN TUNNEL DIFFUSER

(a) Low Frequencies
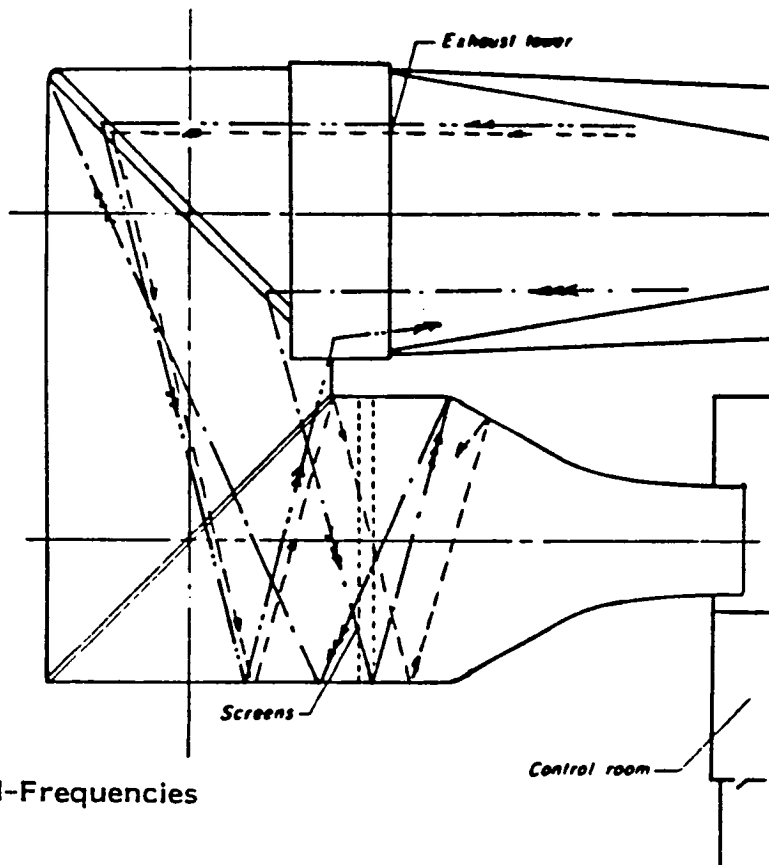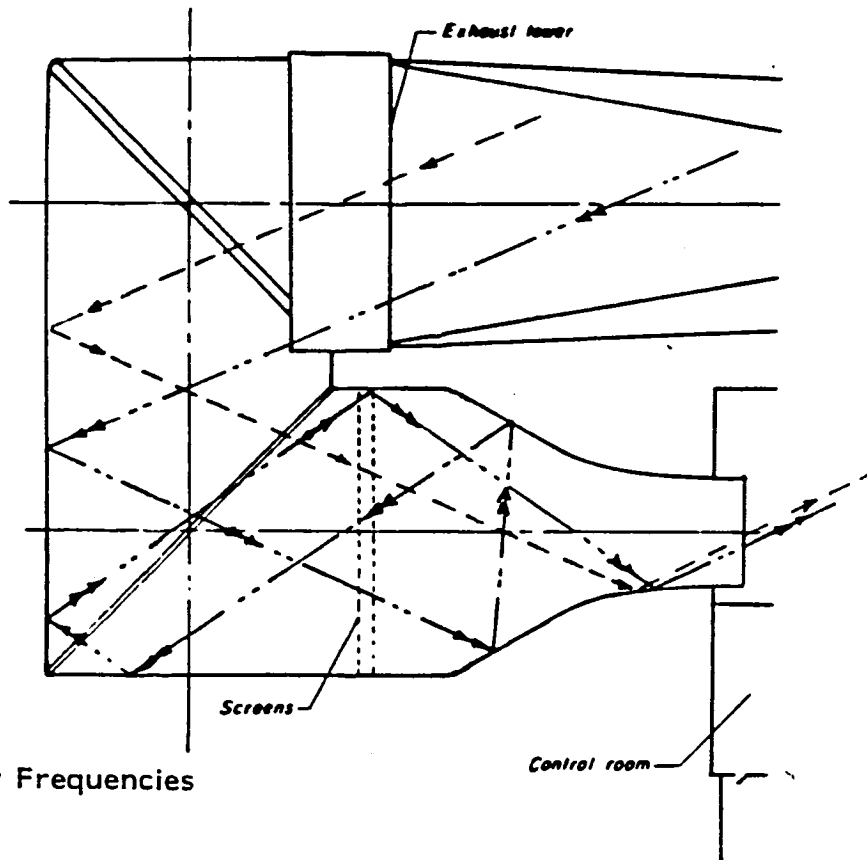
(b) Mid-Frequencies

FIGURE 25.   DIAGRAMMATICAL REPRESENTATION OF ACOUSTIC RAY PATHS
IN TUNNEL SETTLING CHAMBER

53

Exhaust tower

Screens

Control room
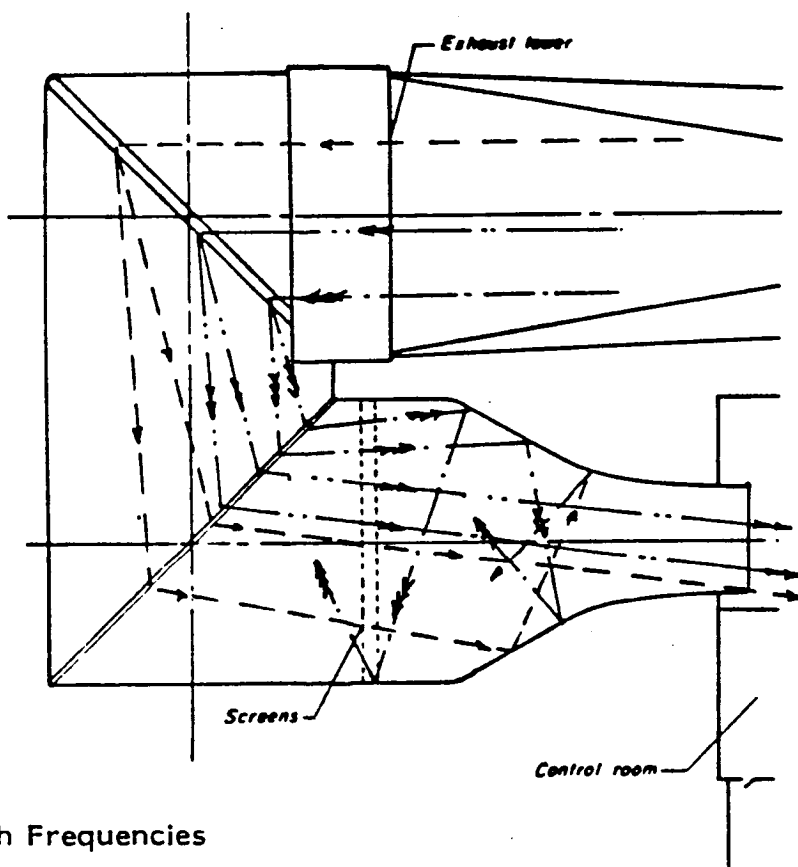
(c) High Frequencies

FIGURE 25. CONTINUED

54

The general trend of the ray patterns shown in the two figures is that of reflection from tunnel walls at low frequencies and reflection from the turning vanes at high frequencies. The presence of the flow control vanes in the diffuser provides an additional complicating factor. Then, in the settling chamber, mid-frequency acoustic rays are reflected at the third corner turning vanes but pass through the smaller vanes at the fourth corner without reflection (as do the low frequency components).

The conclusions drawn from the ray tracing analysis do not seem to be inconsistent with the steady state source measurements. Figure 14(b) shows that high frequency noise is transmitted from settling chamber to nozzle exit more easily than is the low and mid-frequency noise. However, the typical ray tracing patterns of Figure 25 show the same trend. At low and mid-frequencies the acoustic waves are not turned by the fourth-corner turning vanes and, as a consequence, there is significant reflection back upstream from the contraction area.

In contrast, the high frequency acoustic energy is turned by the vanes and aligned more readily with the nozzle axis. Thus it can propagate through the contraction and into the nozzle exit.

It should be recognized that the ray tracing patterns are somewhat subjective in that only a very small number of possible paths were selected for plotting. The intent is to show physical reasons for the high frequency selectivity in the noise transmission through the settling chamber and nozzle into the test section. Some rays will travel from settling chamber to nozzle exit at all frequencies, but there is a greater percentage at high frequencies. The rays plotted in Figure 25(b) for the mid-frequencies show no rays entering the nozzle exit. This is fortuitous because of the initial selection of rays entering the

third corner vanes in directions parallel to the tunnel center-
line. However, for other rays entering the third corner at other
angles, propagation through the nozzle opening is possible and
likely.

It is interesting to observe the influence of the contrac-
tion between the settling chamber and the test section. The rays
drawn in the figure show that a significant portion of the
acoustical·power can be reflected back through the settling
chamber in the upstream direction. Work performed earlier by BBN
in the NASA Ames 40 x 80 ft and 7 x 10 foot wind tunnels [4,5]
indicated that acoustic power did not pass easily from the
settling chamber into the test section. In both those cases the
contraction ratio was 14:1; coherence and phase measurements in
the test section of the 7 x 10 foot tunnel indicated that the
dominant propagation direction was upstream at all frequencies.
The contraction ratio in the 4x7 m tunnel has a lower value,
about 9:1, which may account for the evidence of significant
downstream propagation at low frequencies.

2.7 Acoustic Transfer Functions for Source-Path Calculations

In order to estimate the acoustic energy transmitted to the
test sections from each major source, the "propagation loss"
(change in space-averaged SPL) of each major path must be
estimated. The data discussed above and in Appendices B, C, and
D form the basis for such estimates. The no-flow propagation
tests with a steady-state source located at various points around
the circuit (Appendix B) provide the most readily-used data for
such calculations; unfortunately, these data can only provide
minimum values of the propagation loss since microphones remote
from the source generally measure sound which has propagated in
both direction around the tunnel circuit. Therefore, the

56

absolute value of propagation loss by the weaker path(s) will be masked by sound propagated along the stronger paths.

Figure 26 summarizes the propagation losses deduced from no-flow measurements for the two major sources in the circuit (fan and turning vanes in the first and second corners). These data show that for the fan and second corner sources, the upstream and downstream losses from microphone 14 (or 9) are predicted to be about equal below 800 Hz. From 1000 to 2000 Hz, the upstream path appears to be dominant by approximately 3 to 5 dB; at 2 kHz and above, the predicted path contributions are similar again. However, the data from the three source positions used either show ambiguities or are inconclusive for the downstream-propagating sound for frequencies below 400 Hz and above 2000 Hz. Further, the coherence and phase measurements clearly show dominant upstream propagation at all frequencies above 1 kHz (although measurement system limitations prevented explicit evaluation of propagation loss above about 4500 Hz by the coherence and phase method). The impulse data were not helpful in quantitatively resolving this issue due to the presence of many propagation modes and the low absorption in the circuit, which caused the energy arriving at the test section via the longer path to overlap with the energy arriving via the shorter path, thus complicating the quantitative interpretation of losses in each of the paths.

The data shown in Figure 26 are in some ways inconsistent with experience with other wind tunnels of similar general arrangement (i.e., similar fan location in circuit, similar nozzle configuration, free jet or partially-free jet arrangement in test section, nozzle contraction ratio in same range). Two of these tunnels have provided the opportunity to explicitly evaluate the average no-flow propagation loss through tests on scale models (in the range of .1 to .2 of full scale) in which one path
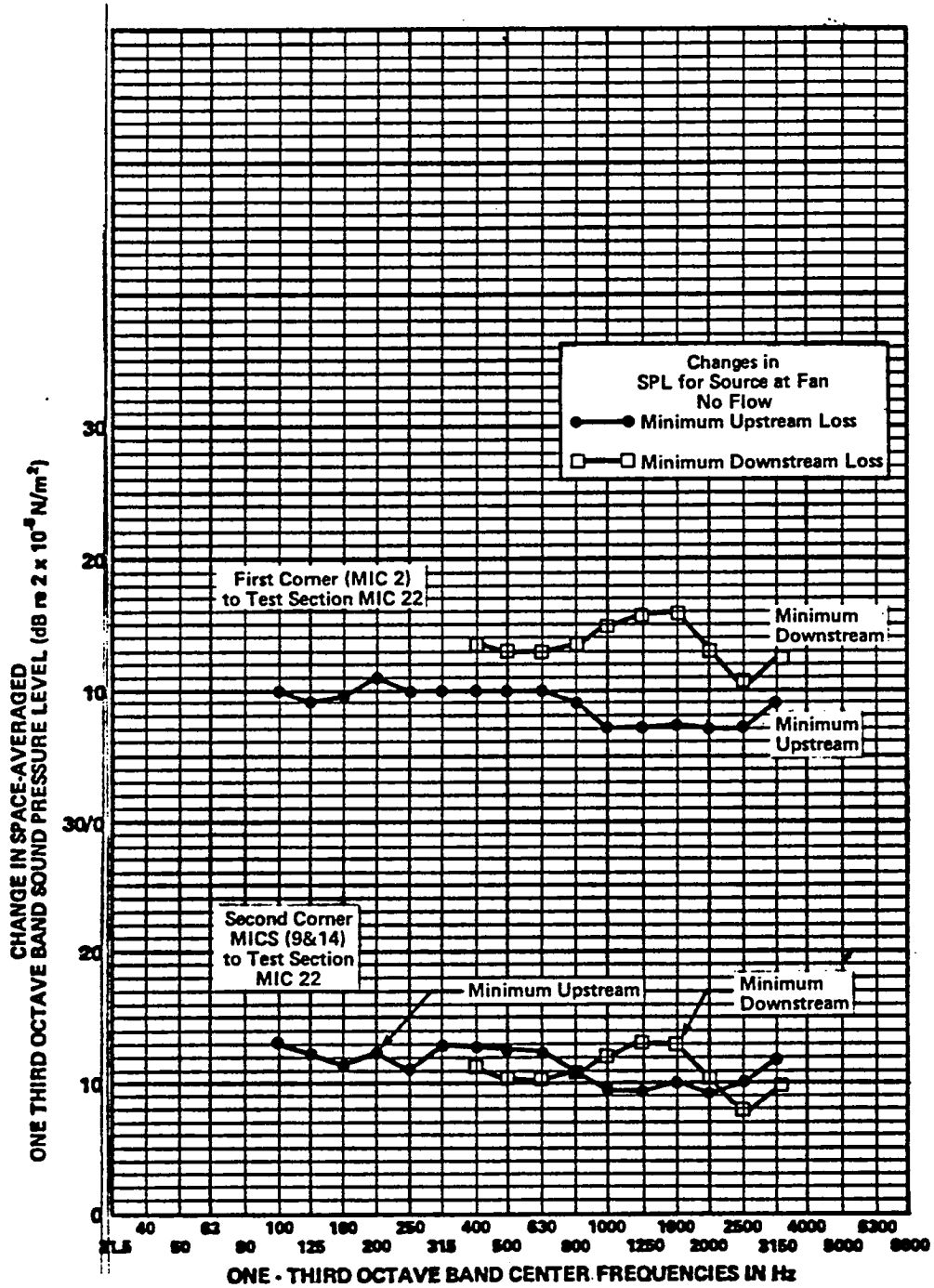
FIGURE 26. PROPAGATION LOSSES INFERRED FROM STEADY-STATE SOUND SOURCE DATA

could be "completely" eliminated by blocking off that part of the circuit. The model data can be converted to full scale by simply scaling frequencies by the scale factor. The data from the different tunnels can be compared by "scaling" the facilities to a similar scale (the nozzle exit area is used) and adjusting the measured losses by the area ratio between the "source" and the test section. Such a comparison has been made for two model tunnels, which have characteristics listed below:

TABLE 2

Tunnel	Test Section	Nozzle A.R.	$\sqrt{A_0}$	C.R.	A_0/A_2	V_T/V_O
4x7 m	3/4 Open	1.5	5.4 m	9:1	0.34	2.0
A	Fully Open	1.33	6.9 m	9:1	0.45	1.53
B	3/4 Open	1.72	4.7 m	6:1	0.58	2.12

A.R. = Aspect ratio (width/height)

A_0 = Exit area (m^2)

A_2 = Duct cross-sectional area downstream of second corner (m^2)

C.R. = Nozzle contraction ratio

V_T = Fan tip speed (kinematic)

V_O = Test section velocity

Note that Tunnel A had an anechoic test section, and Tunnel B had a relatively small open space around the flow path in the test section.

Figure 27 compares the adjusted model data with that measured in the 4x7 m, where full-scale frequencies have been adjusted to those of the 4x7 m by $\sqrt{A_0}$, and levels have been
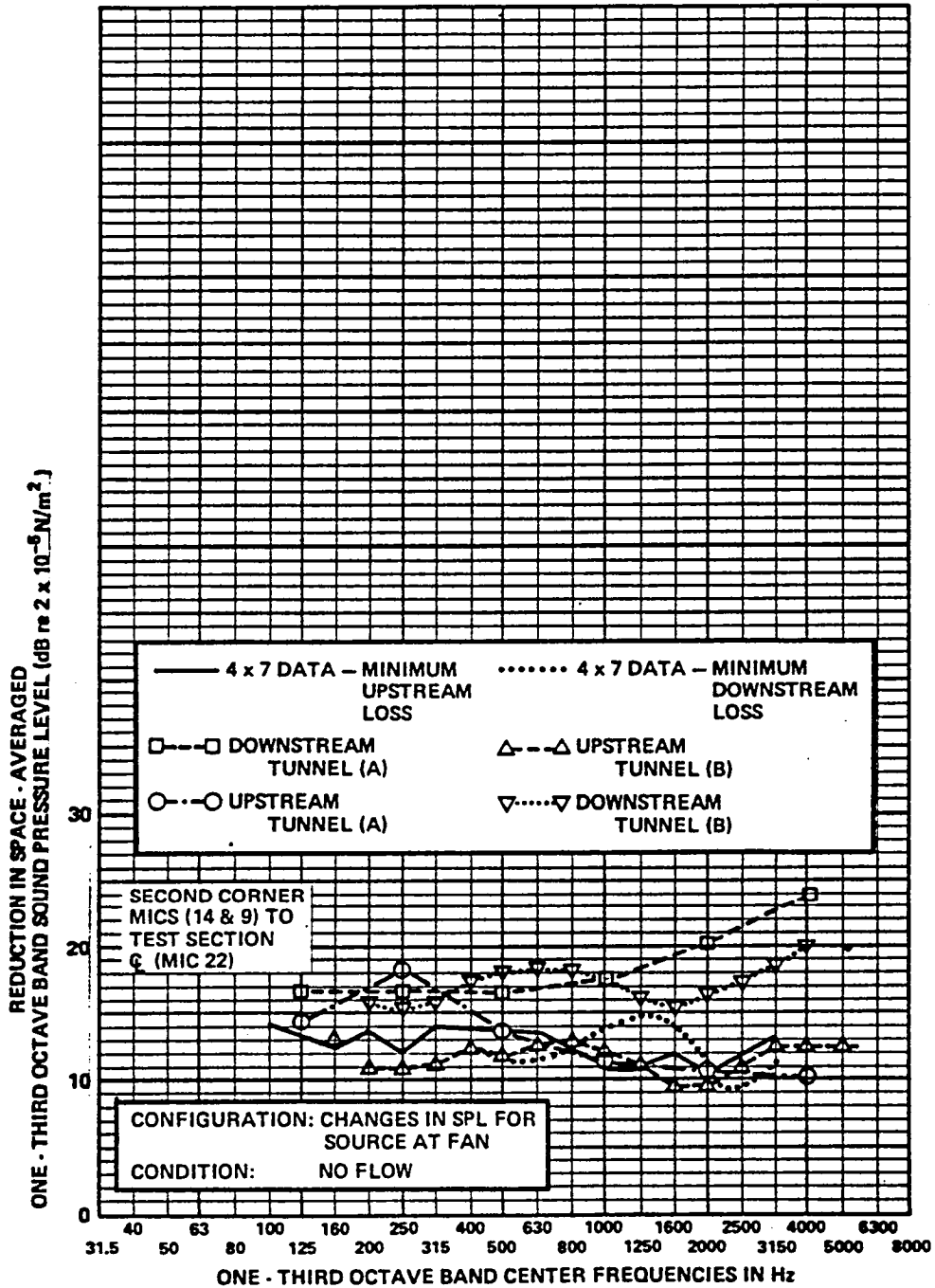
FIGURE 27. PROPAGATION LOSSES FROM THREE SIMILAR FACILITIES

60

adjusted to the 4x7 m by 10 log (A_0/A_2). No adjustments for nozzle aspect ratio or explicit corrections for contraction ratio have been made.

The comparisons clearly indicate that upstream propagation is dominant above 500 Hz, with the downstream losses rapidly increasing relative to the upstream losses at frequencies above 1000 to 2000 Hz. The high upstream loss measured in Tunnel A at 250 Hz may be an artifact of the test, since the model included treated vanes on the first corner (the measured insertion loss of these vanes has been deducted from the overall propagation loss, but residual effects of having the absorption in the upstream leg may be important).

The data strongly suggest that the measured 4x7 m downstream propagation losses (with the steady state sound source) are "contaminated" at high frequencies. It is therefore appropriate to "adjust" the 4x7 m data for frequencies above 1600 Hz to conform with the trends observed in other wind tunnels.

Figure 28 shows the estimated range of propagation loss from microphone position 14 to microphone position 22 in the 4x7 m tunnel. Figure 29 shows similar curves for microphone positions 2 and 22. The range shown includes the actual data from the 4x7 m tunnel (that which is considered valid) as a lower bound on the losses, and the more definitive data derived from the controlled tests in the scale models as an upper bound. Note that in the case of downstream propagation, Tunnel B was used in the high frequency regime since it's test section characteristics were more consistent with those of the 4x7 m. If the measured data from the no-flow tests in the 4 x 7 m tunnel were used, then the predicted test section levels would be higher, and noise reduction requirements greater. However, the impulse tests in the circuit showed systematically increasing absorption in the

61
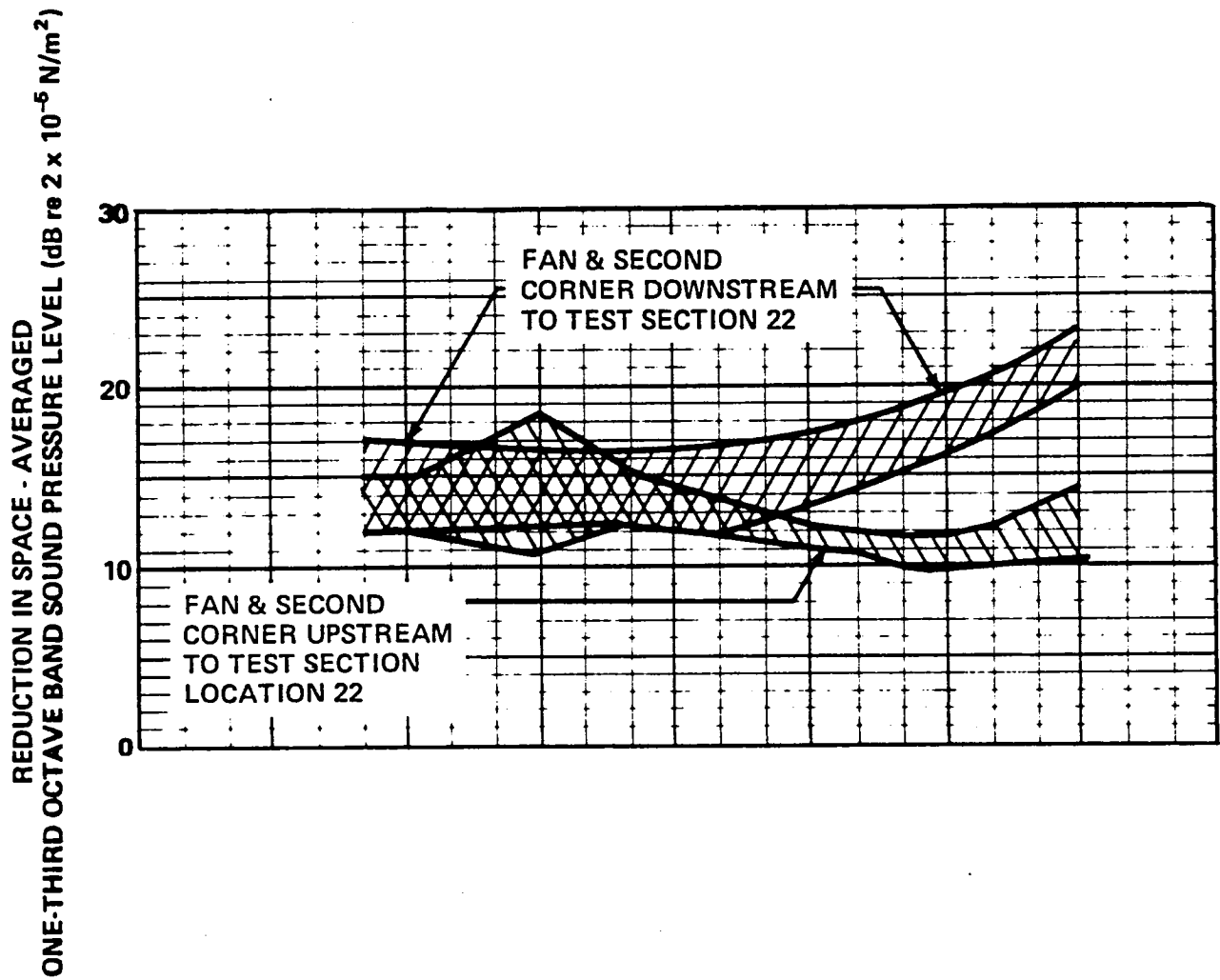
FIGURE 28. SUMMARY OF RANGE OF PROPAGATION LOSS BETWEEN
LOCATIONS 14 AND 22
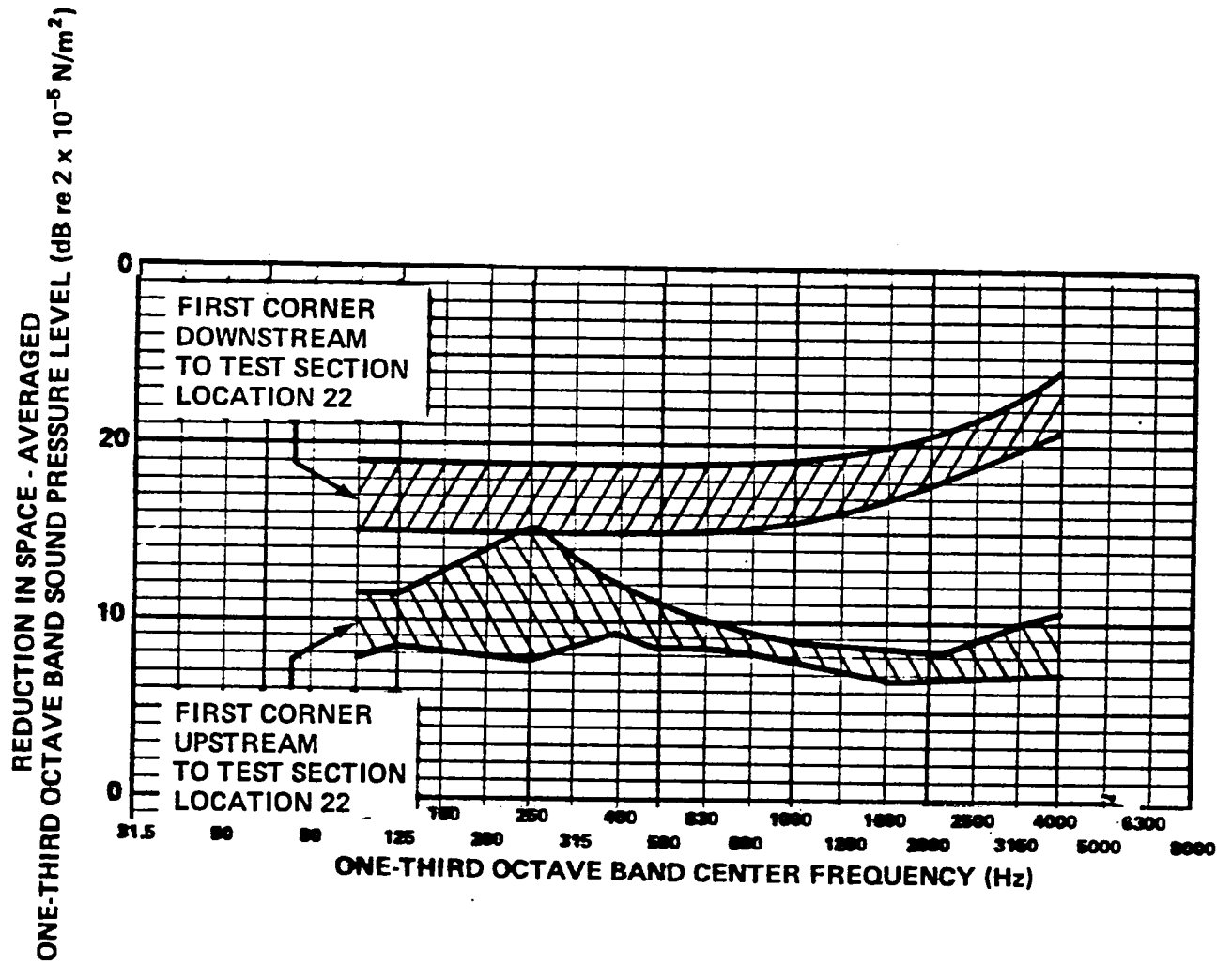
FIGURE 29 SUMMARY OF RANGE OF PROPAGATION LOSS BETWEEN
LOCATIONS 2 AND 22

circuit (see Table C.2, for example), thus lending support for the use of trends derived from scale model tunnels in which the path direction could be controlled, and in which low background noise levels existed during the tests.

3. SOURCE CHARACTERISTICS

Section 1 (Fig. 8) identified the most likely noise sources associated with the 4 x 7m circuit. In this section, the approach used to deduce source strengths is described. Almost exclusive reliance is made upon the measured data from the 4x7 m tunnel test, and from known scaling relationships for different source mechanisms. This approach was necessary since the flow information needed to perform meaningful detailed calculations of fan, turning vane, flap, and other aeroacoustic source noise levels were unavailable.

3.1 Normalization of Survey Data

The 1/3 octave band spectra (summarized in Appendix A) were normalized (to an 80 kt reference case) using a V^5 power law and Strouhal frequency scaling relationship. The rationale for this scaling procedure is that the broadband noise mechanisms expected from the dominant sources (fan blade/turbulence interactions, fan blade trailing edge and tip flow separation noise and turning vane noise) all are thought to roughly obey a V^5 power law at constant Strouhal number. Several cases are presented in Figs. 30-34.

It can be seen that the high speed data collapses reasonably well onto one curve using the V^5 relationship, and the low speed data scales well at the broadband peak, but not at those frequencies where machinery or other intrusive noise is unrelated to the aerodynamic mechanisms of the circuit. The data from the test section microphones are seen to contain one or two narrow bands in the vicinity of 2 kHz and 4 kHz (for the 80 kt condition). This noise was believed to be generated by the microphone support stands. That hypothesis was confirmed by removing only the in-flow microphones (22 and 23) and their stands and repeating the

65
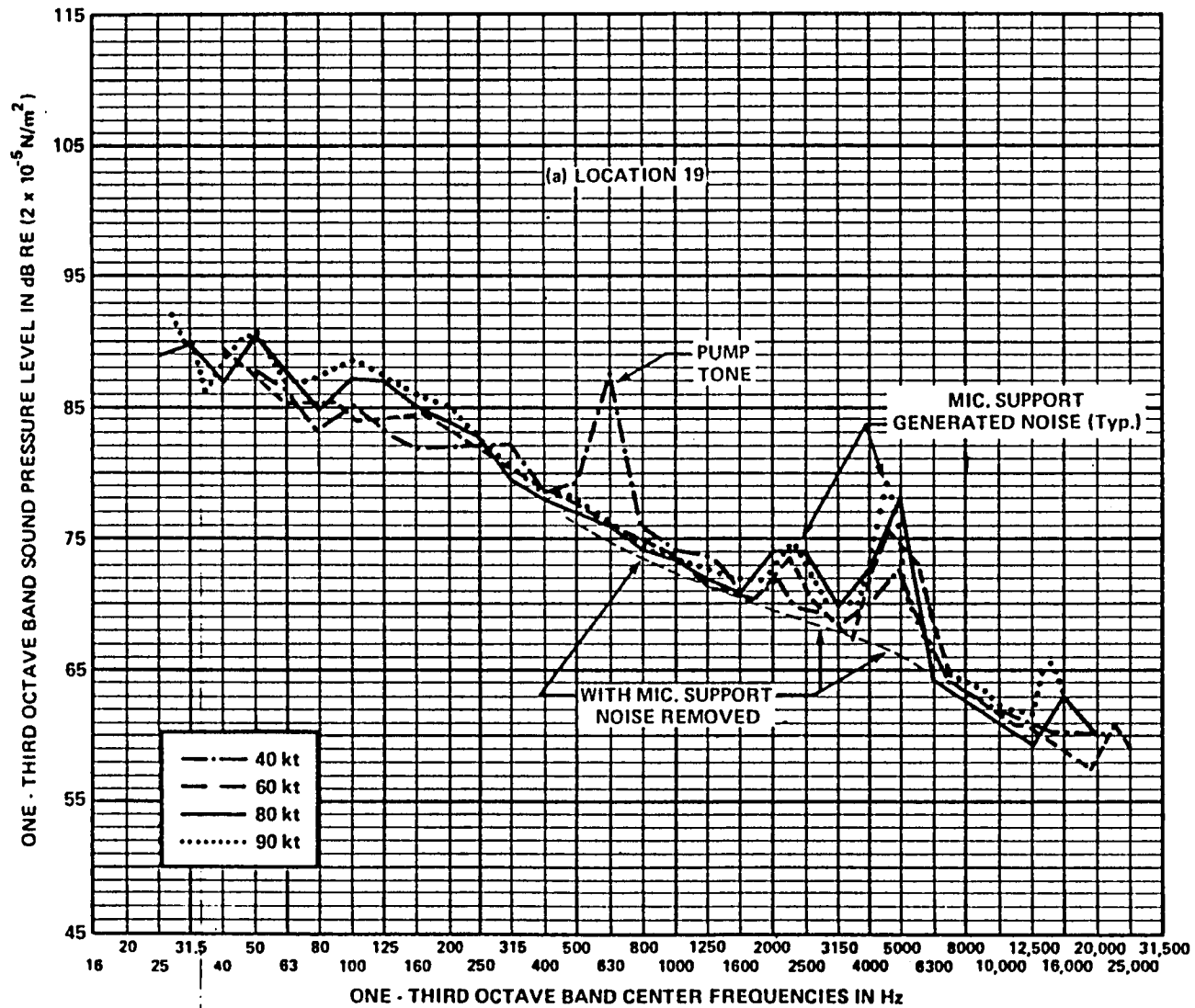
FIGURE 30. ACOUSTIC DATA SCALED TO 80 m/s USING V^5 POWER LAW AT CONSTANT STROUHAL NUMBER (LOCATION 19).
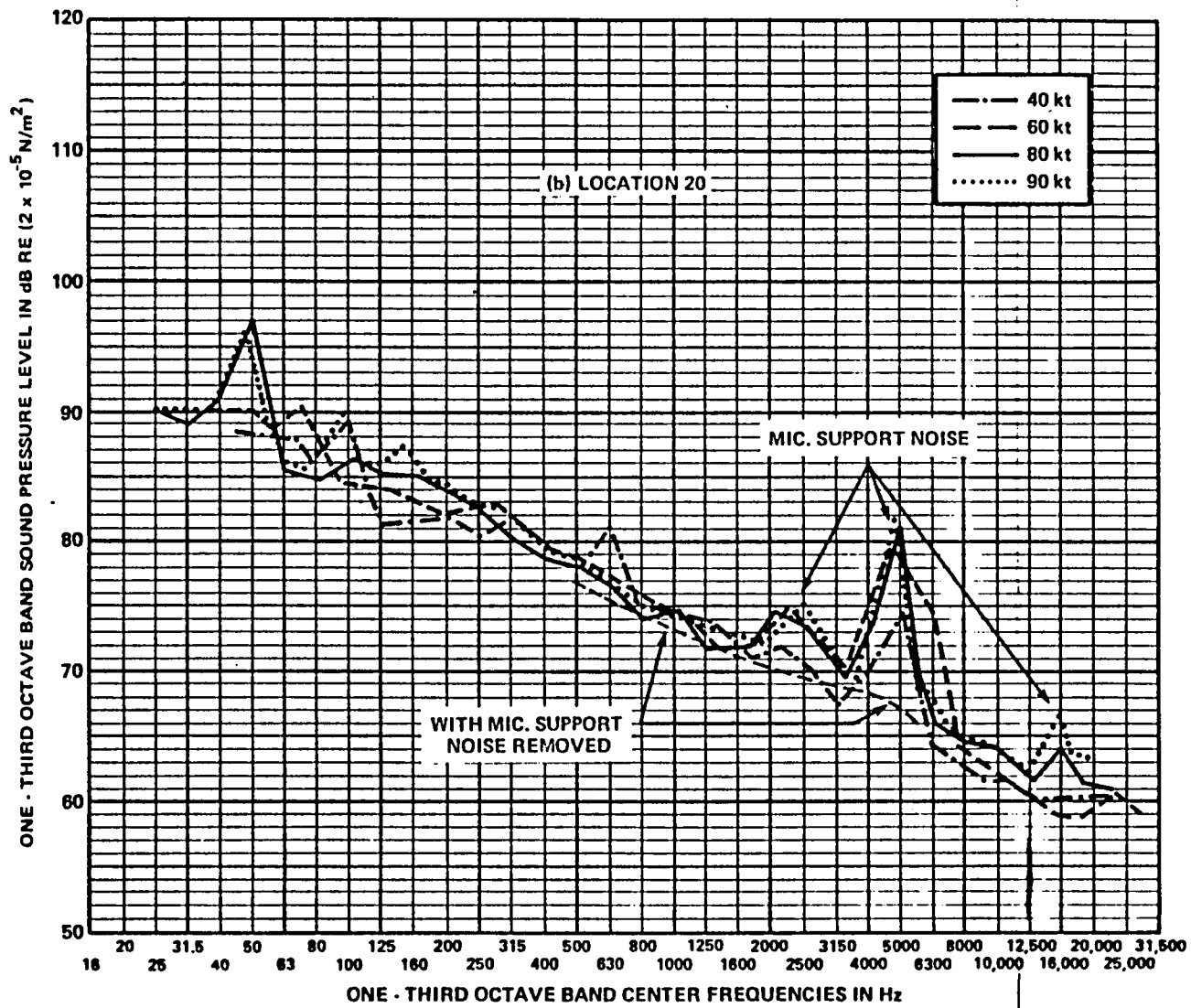
FIGURE 31.   ACOUSTIC DATA SCALED TO 80 m/s USING V^5 POWER LAW
AT CONSTANT STROUHAL NUMBER   (LOCATION 20).
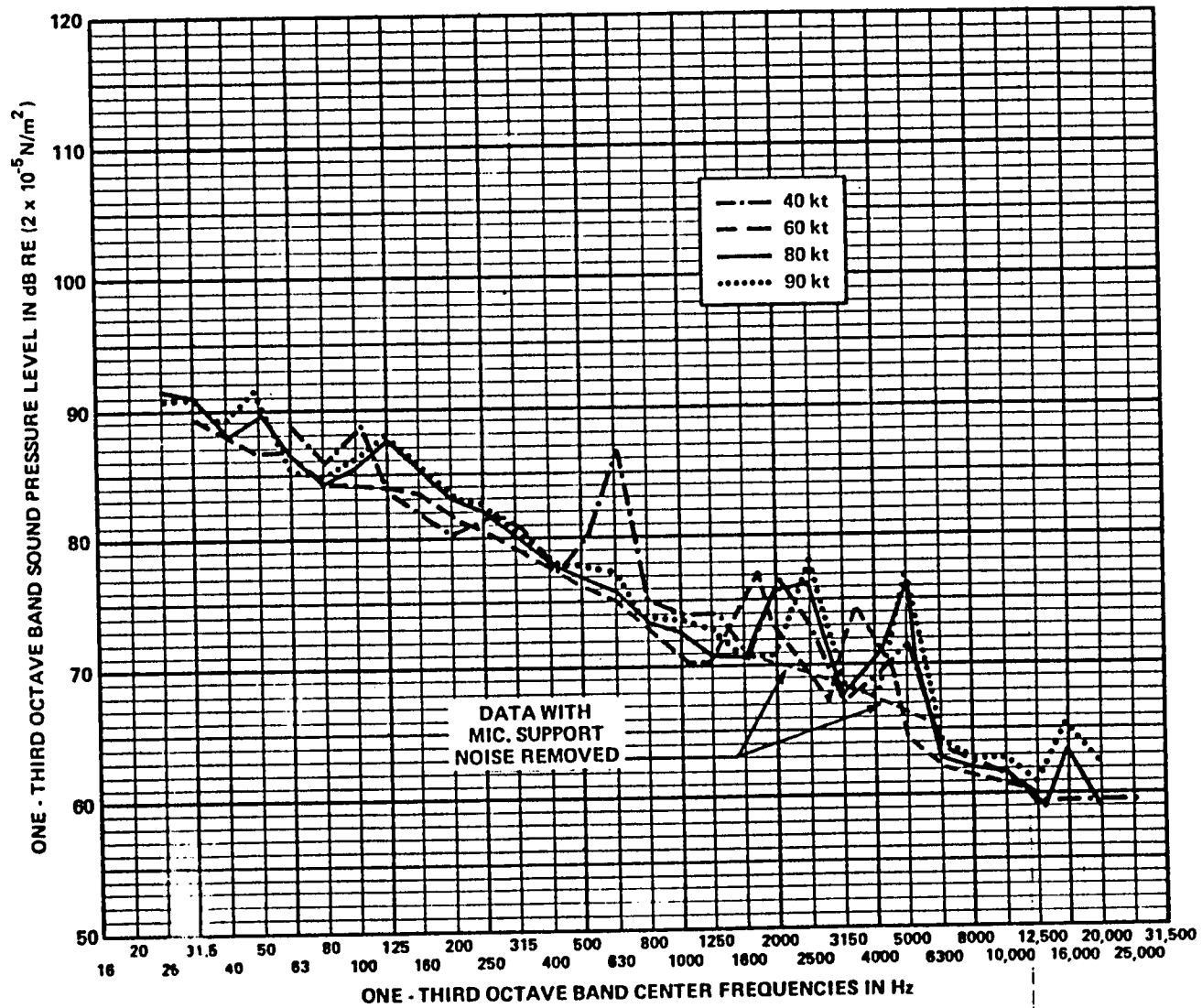
FIGURE 32. ACOUSTIC DATA SCALED TO 80 m/s USING V^5 POWER LAW AT
CONSTANT STROUHAL NUMBER (LOCATION 21).

89

ONE - THIRD OCTAVE BAND SOUND PRESSURE LEVEL IN dB RE (2×10^{-5} N/m^2)

(d) LOCATION 22

WITH MIC. SUPPORT
NOISE REMOVED

— · — 40 kt
— — 60 kt
——— 80 kt
········ 90 kt

ONE - THIRD OCTAVE BAND CENTER FREQUENCIES IN Hz

69
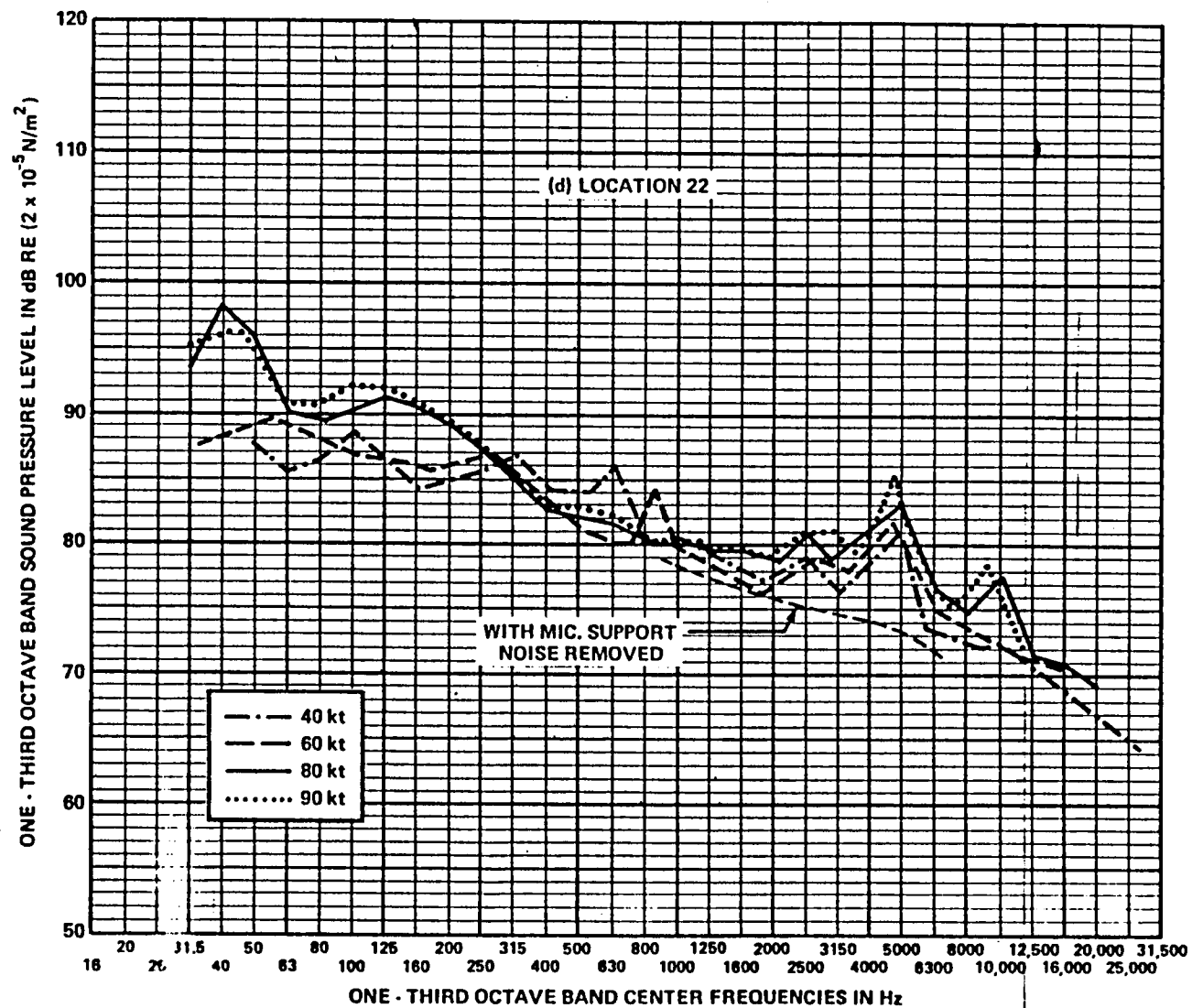
FIGURE 33. ACOUSTIC DATA SCALED TO 80 m/s USING V^5 POWER LAW AT CONSTANT STROUHAL NUMBER (LOCATION 22).
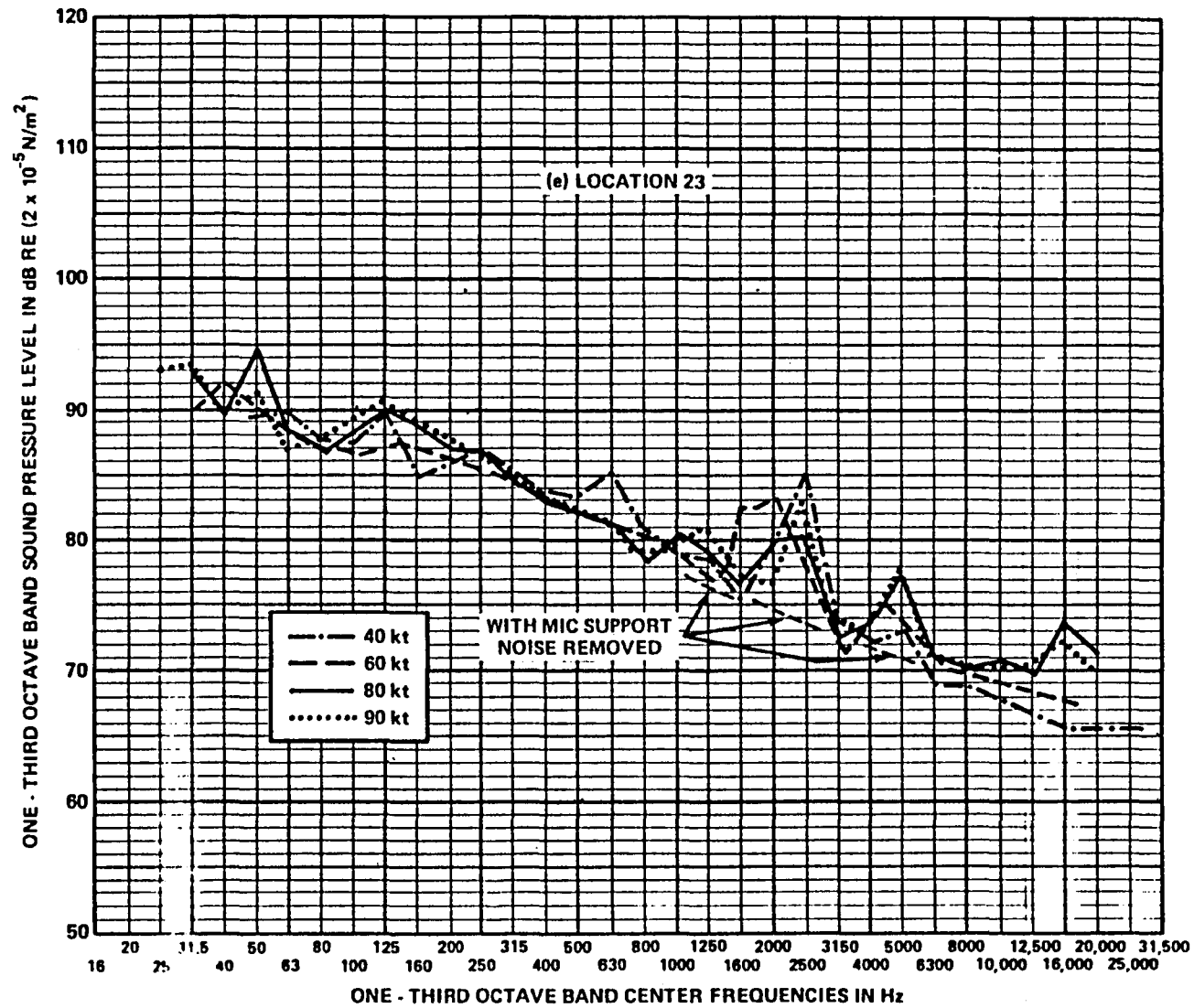
FIGURE 34. ACOUSTIC DATA SCALED TO 80 m/s USING V^5 POWER LAW AT CONSTANT STROUHAL NUMBER (LOCATION 23).

tests. Figures A.18 through A.22 (Appendix A) show typical comparisons between the cases with the stands in and out of the flow, clearly revealing the extraneous noise caused by the test stands. Therefore, it is appropriate to correct all test section data for this effect in order to obtain a realistic estimate of background noise caused by the circuit itself. However, the data serves as a reminder of a familiar problem associated with in-flow microphones and model supports; therefore, the issue of developing low noise microphone and model supports should remain as a priority for any wind tunnel acoustic measurements. While on the subject of microphone self-noise, it should be noted that the in-flow levels shown here were not dominated by self-noise (see App. G), but the levels at location 2 were only 6 dB above estimated self-noise levels.

Above 250 Hz, the data collapse well using the V^5 power law at constant Strouhal number. The data from microphones 19 and 22 show a systematic spread in the scaled curves from frequencies from about 80 to 200 Hz. The trend indicates in this frequency range is that a V^6 power law would be more appropriate. Such an indication is consistent with the variations in scaling laws from flow-surface interaction mechanisms from compact sources vs non-compact sources. The power radiated from an airfoil-like source which has dimensions small with respect to a typical acoustic wavelength obeys a V^6 law, while the power from edge sources - those which have wavelengths small with respect to the surface dimensions - varies as V^5. At 200 Hz, the wavelength of sound is approximately 1.7 m, which is approximately twice the typical chord of the fan blades and the turning vanes in the first and second corners. Thus, the transition between the two scaling "laws" might well be expected in that frequency range.

The scaled data indicate aeroacoustic sources associated with flow/surface interactions. The primary candidate sources

71

are the fan and the turning vanes. These are examined in more detail below. As mentioned above, there is little flow data available with which to calculate source spectra. Therefore, we will attempt to deduce the source spectra by first calculating the power spectra of the turning vanes using available empirical data, and then deducing the fan spectrum using the predicted vane power levels and transfer functions to obtain a comparison between the vane contribution and the total power measured.

3.2   Turning Vane Aeroacoustic Sources

3.2.1 Mechanisms

Turning vane noise generation involves complex mechanisms and is most difficult to treat analytically for multivane corners which are large with respect to typical acoustic wavelengths. However, in an attempt to develop scaling relationships, the mechanisms can be classified roughly as follows:

1) Unsteady turning forces: The fluctuation in the mean turning force of the corner as a whole, as well as individual vanes, results in a dipole source. At very low freqencies where the acoustic wavelength is on the order of or larger than the corner cross dimension, the behavior would be similar to a duct-enclosed "point" dipole, and would scale as V^6 and in direct proportion to the turbulence intensity. Once the wavelength becomes less than, the corner cross dimensions, individual vanes or groups of adjacent vanes act as local dipole forces, and there exists the possibility of degeneration of dipoles into higher order sources due to phase cancellation effects. Thus, the radiation efficiency could be reduced, but the speed scaling exponent could increase above V^6. When the wavelength becomes small with respect to the vane pitch

72

(spacing) and chord, then the sources become localized
at the leading and trailing edges, and the unsteady
turning force mechanism gives way to edge sources.

2) Edge Sources: Small scale eddies at the leading edges
    and trailing edges of the vanes produce so-called edge
    noise. The trailing edge noise mechanism has been
    studied extensively, and the relationship to gross flow
    field parameters as well as localized flow field details
    has been established [6,7]. To the first order, the
    trailing edge mechanism is directly proportional to:

    V^5,   where V is the local mean velocity,

    $\cos^3 \beta$,   where β is the angle of the mean flow with
                respect to the edge,

    $(v/V)^2$,   the local mean square turbulence
                intensity,

    ℓ_x,   the streamwise eddy length scale,

    ℓ_y,   the spanwise eddy length scale,

    ℓ_z, .   the eddy scale normal to the surface,

    W,   the span of the edge.

To calculate the sound produced by the turning vanes, the spatial
and spectral distribution of all the above parameters needs to be
known. Unfortunately, even the spatial distribution of V and
cos β is not well known for most parts of the tunnel circuit.
Therefore, it is quite futile to expect to accurately calculate
turning vane noise from "first principles." However, in order to
establish the order of magnitude of the noise of the vanes, a
calculation is undertaken below.

73

3.2.2 Semi-empirical correlation

In 1970, some work was carried out for Langley Research Center to provide guidance on the potential noise problems by obstructions in the air ducting being planned for the low noise facilities in the NASA ANRL [8]. This work involved testing various duct elements in a low noise reverberant room facility, and developing empirical correlations which would assist in evaluating large scale designs. One element tested was a right angle corner with circular arc turning vanes at a pitch-to-chord ratio of 0.174, the aerodynamically optimum ratio.

For fully-developed turbulent inflow, the turning vane tests led to a radiated noise correlation which has the following form

$$PWL \ (\frac{f\delta}{U}) \ (dB \ re \ 10^{-12}W) \ = \ PWL_N(\frac{f\delta}{U}) \ - \ 18.5 \ + \ 60 \ log \ (\overline{U})$$

$$+ \ 20 \ log \ [\frac{\sqrt{\overline{u^2}}}{\overline{U}}] \ + \ 10 \ log \ (n \ CH)$$

where $PWL_N \ (\frac{f\delta}{U})$ is an empirical correction which is a function of   Strouhal number $(\frac{f\delta}{U})$,

  $\overline{U}$ is the mean centerline velocity in the duct (fps)

  $\sqrt{\overline{u^2}}$ is the rms turbulence velocity at the Strouhal number

  C is the vane chord (in ft)

  H is the span (ft)

  f is the frequency (Hz) and

  δ is a typical length scale dimension (ft)

  N is the number of vanes.

For the purposes of the correlation, δ was originaly taken as half the duct diameter. Note that although a 60logU relation gave good data collapse at some Strouhal numbers, the scatter was such that a 50logU scaling law could also be justified. However, since the original data were taken over the same velocity range as occurs at the first and second corners of the 4x7 m tunnel, the velocity scaling issue need not be resolved here in order to use the empirical method to arrive at a calculation of vane noise.

Figure 35 shows the Strouhal spectrum of PWL_N (in 1/3 octave bands). Taking $PWL_N = 23$ as a reasonable mean value over the entire Strouhal number range, the spectrum of turning vane noise thus becomes primarily dependent upon the spectrum of turbulent inflow.

Using the turbulence spectrum shown in Fig. 36, which was measured at the time of the original tests and is now adjusted in overall amplitude to coincide with data from LaRC turbulence surveys in the 4x7 m tunnel, spectra can be predicted for the first and second corner vanes. Unfortunately, lacking information on eddy scales, one can arrive at almost any characteristic frequency for the spectrum, depending upon selection of δ. Using NASA velocity surveys as a guide, the characteristic δ is taken as being in the range of 1/4 to 1/2 the duct cross sectional dimension in the first diffuser. At the entrance to the second corner, where the flow should be more stable due to the smaller degree of diffusion in the second diffuser and the presence of the flow control vanes, δ is probably in the range of .1 to .3 times the duct diameter.

The resultant predictions are shown in Fig. 37; note that the levels predicted by the empirical correlation above have been adjusted by 6 dB from the freefield end condition of the original experiment to account for the image sources in the rigid tunnel walls.

75
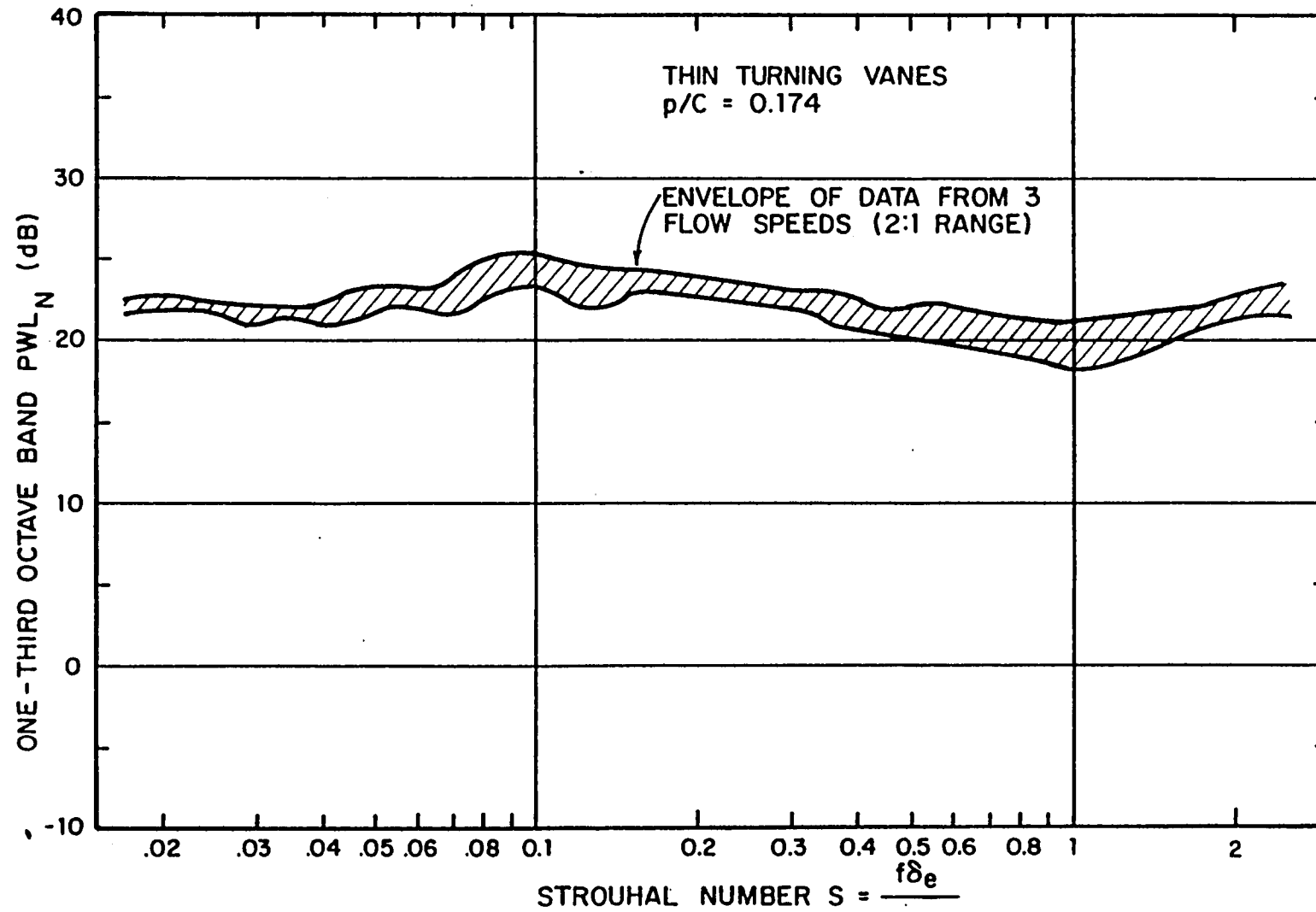
FIGURE 35. NORMALIZED POWER LEVEL FOR TURNING VANES FULLY DEVELOPED TURBULENT INFLOW (FROM REF. 7).
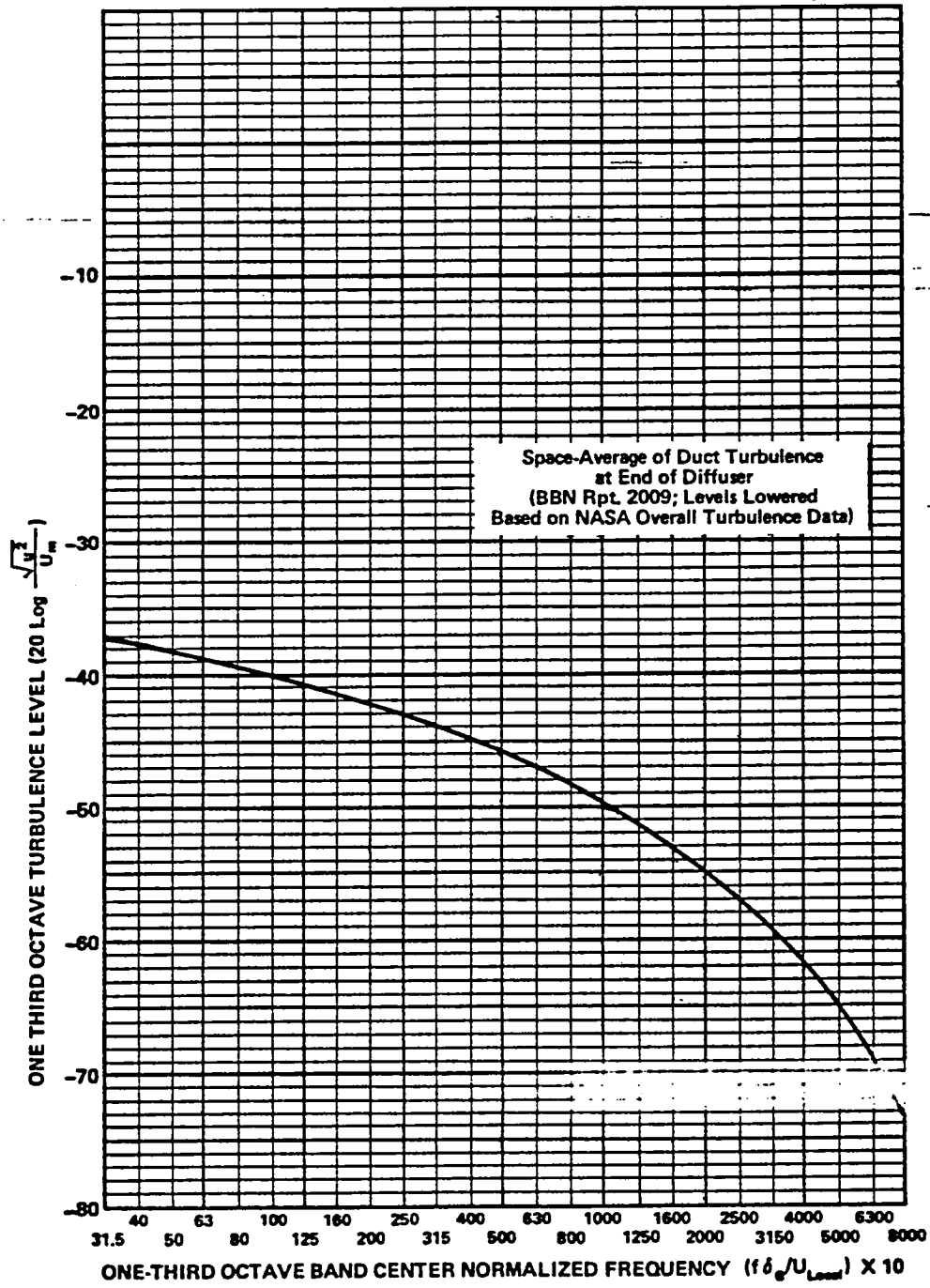
FIGURE 36. INFLOW TURBULENCE SPECTRUM FOR TURNING VANE NOISE CALCULATION

77
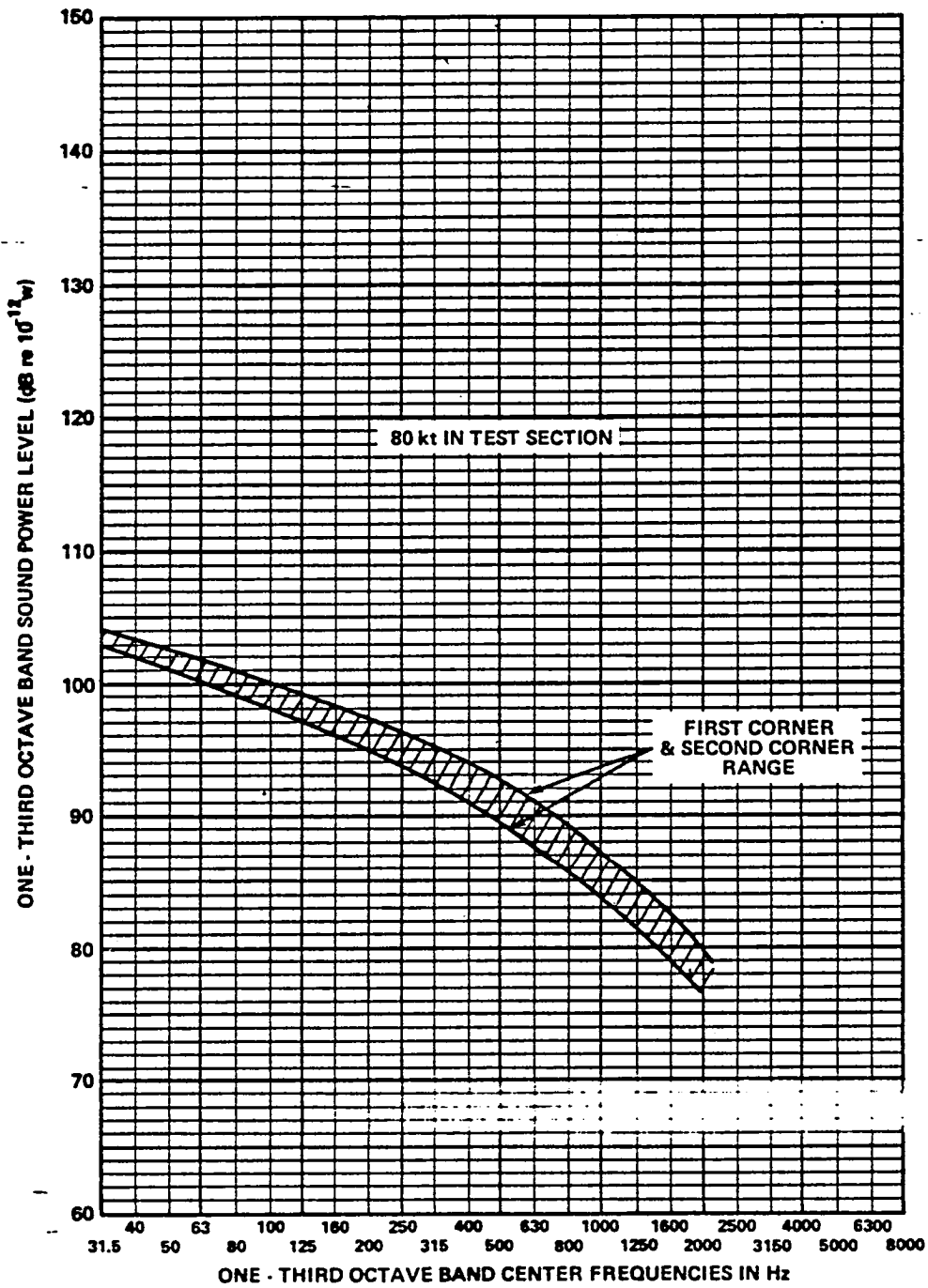
FIGURE 37. VANE ACOUSTIC POWER LEVEL.

3.3 Fan Broadband Noise

The tunnel drive fan generates noise primarily as a consequence of (1) rotor interaction with turbulent inflow which produces unsteady thrust and torque forces, (2) unsteady loads caused by flow separation in areas where local blade loading is excessive, (3) interaction of attached and separated flows with the trailing edge of the rotor blades, (4) interaction of the rotor mean and unsteady wake with the stator, and (5) turbulent flow interaction with the stator trailing edges. Due to the low blade passage rate (around 18 Hz for a test section velocity of 80 kt), the discrete frequency mechanisms associated with rotor stator interaction and rotor interaction with mean inflow distortions fall in a frequency range below that of primary concern. Therefore, we will concentrate on the broadband mechanisms of the rotor, since the relative velocity of the flow over the rotor blades is much higher than over the stator vanes.

The broadband noise due to turbulent inflow for a low-speed rotor has been consistently modeled as a dipole source in which the power radiated is proportional to the mean square fluctuating forces on the blades and the square of the frequency of the fluctuating forces. This model is also appropriate to describe radiation caused by large-scale flow separation on the blades themselves.

Regions of flow separation occur when the local blade loading (lift coefficient) is too high as a result of improper matching of local pitch angle to the inflow field. Stall usually occurs at the tip regions which often operate in low inflow velocities resulting from thick boundary layers on the tunnel walls (or even in flows that are themselves separated and thus contain reverse flow regions, such as sometimes occur on the inside legs of wind tunnel circuits). When stall occurs, the pressure fluctuations experienced by the surface are very

energetic relative to those in an unstalled airfoil at moderate coefficient. Since the sound radiated by flow/surface interactions has been clearly correlated with surface pressure fluctuations for a variety of mechanisms (e.g., whole-body fluctuating "lift", leading edge, and trailing edge interactions), it is clear that stall will increase the broadband noise if and when it occurs. Further, the broadband noise should increase systematically as the loading increases toward stall, since the fluctuating pressures do so (Ref. 6).

Flow surveys in the LaRC 4 x 7m wind tunnel have revealed that the blades are stalled over the outer 10% of the fan radius even when the circuit is operated in the closed circuit mode (Ref. 7). Since the inflow has even greater velocity deficits near the tunnel wall for the open circuit operation, it is a virtual certainty tht the fan is also stalled when the tunnel is operated in the open circuit mode, which is of primary interest for acoustic testing.

Lacking details on the inflow field, it is difficult to utilize the available theoretical relationships quantitatively. However, an order-of-magnitude calculation is in order. Let us assume an axial length scale, ℓ_x, of the inflow turbulence of about 3 m. The circumferential length scale ℓ_θ is normally .1 to .2 times the axial scale, so in this case, $\ell_\theta \approx$ .3 to .6 m. For the 80 kt reference case, the fan tip speed is around 80 m/s. Using the 3/4 span location as being representative of the overall blade, the characteristic frequency of encounter of the blades with the eddies is defined by the circumferential length scale and the local fan speed. In this case, that frequency is between 90 to 180 Hz, for the length scales assumed, which is in the range where data shows a broadband peak in the spectrum, as well as a tendency toward V^6 scaling relationships. An order-of-magnitude estimate of the power can be made using the simple free field point dipole expression

$$\Pi = \frac{\overline{F^2}\ \omega^2}{12\pi\ \rho c^3}$$

where $\overline{F^2}$ is the mean square fluctuating force,

   ω is the characteristic frequency,

   ρ is the medium's density, and

   c the local sound speed.

Applying this relation to the 4x7 m case cited gives a power level in the range of 120 to 130 dB (re 10^{-12} w) in the frequency range of 90 to 180 Hz. Applying a 6 dB correction to account for the enclosure of the source in a hard wall space gives a predicted SPL in the range measured, as shown in Fig. 38.

The order-of-magnitude of edge source levels are estimated from empirical data derived from [11] and [12]. Fig. 39 shows the empirical spectrum and the relationship used to calculate the power in a freefield environment. Using a characteristic boundary layer thickness of 2.5 cm on the lower surface and 5 cm on the upper surface produces the curve also plotted on Fig. 38. Stall noise is not estimated but would be expected to dominate the railing edge noise from the attached flow region. Obviously, the predictions reflect the crudeness of the input assumptions and should only be interpreted as showing the likelihood that the spectra measured are dominated by fan noise mechanisms.

3.4 Collector Noise

During a scale model study of the V/STOL tunnel (now 4x7 m Tunnel) [13], an investigation of collector shapes was conducted, aimed at reducing oscillations in the circuit. From data presented in Ref [13] the broadband noise of the collector can be inferred. Fig. 40 shows the spectrum at the center of the tunnel derived from measurements made with a corner-mounted microphone.
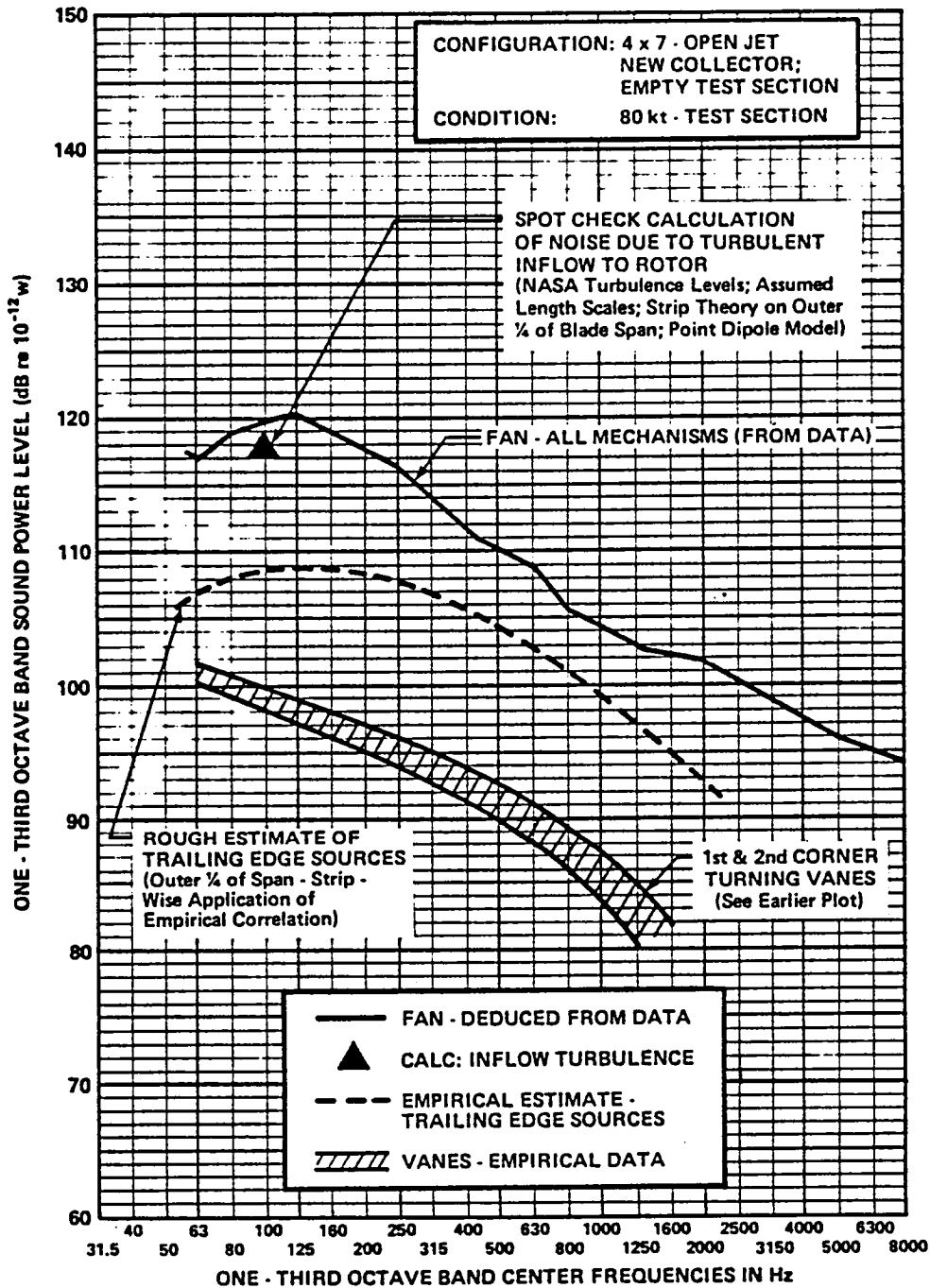
FIGURE 38. FAN BROADBAND SOURCE LEVEL.

82

NORMALIZED 1/3 OCTAVE BAND SPECTRA OF TRAILING EDGE NOISE
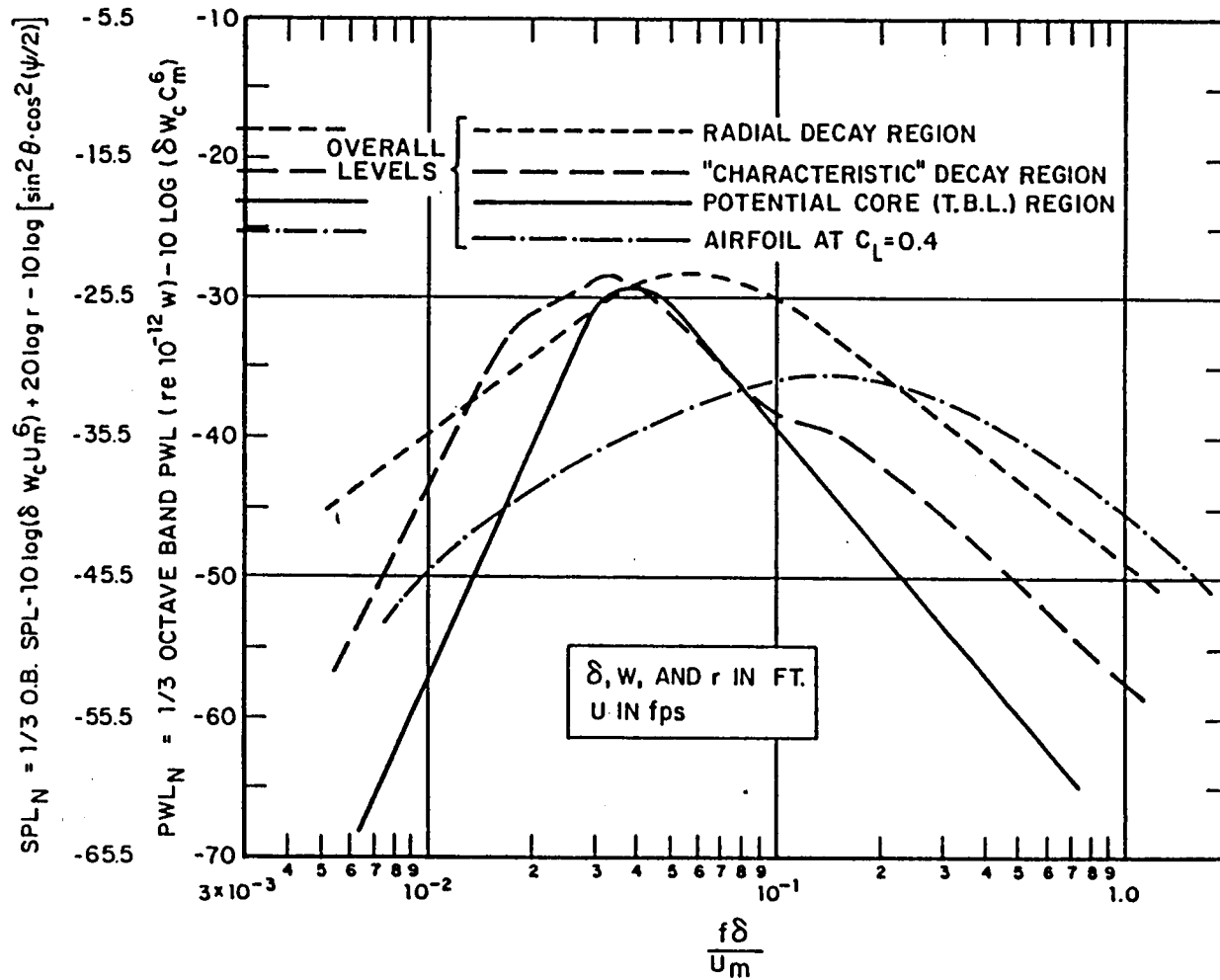
FIGURE 39. EMPIRICAL DATA FOR TRAILING EDGE NOISE ESTIMATE.
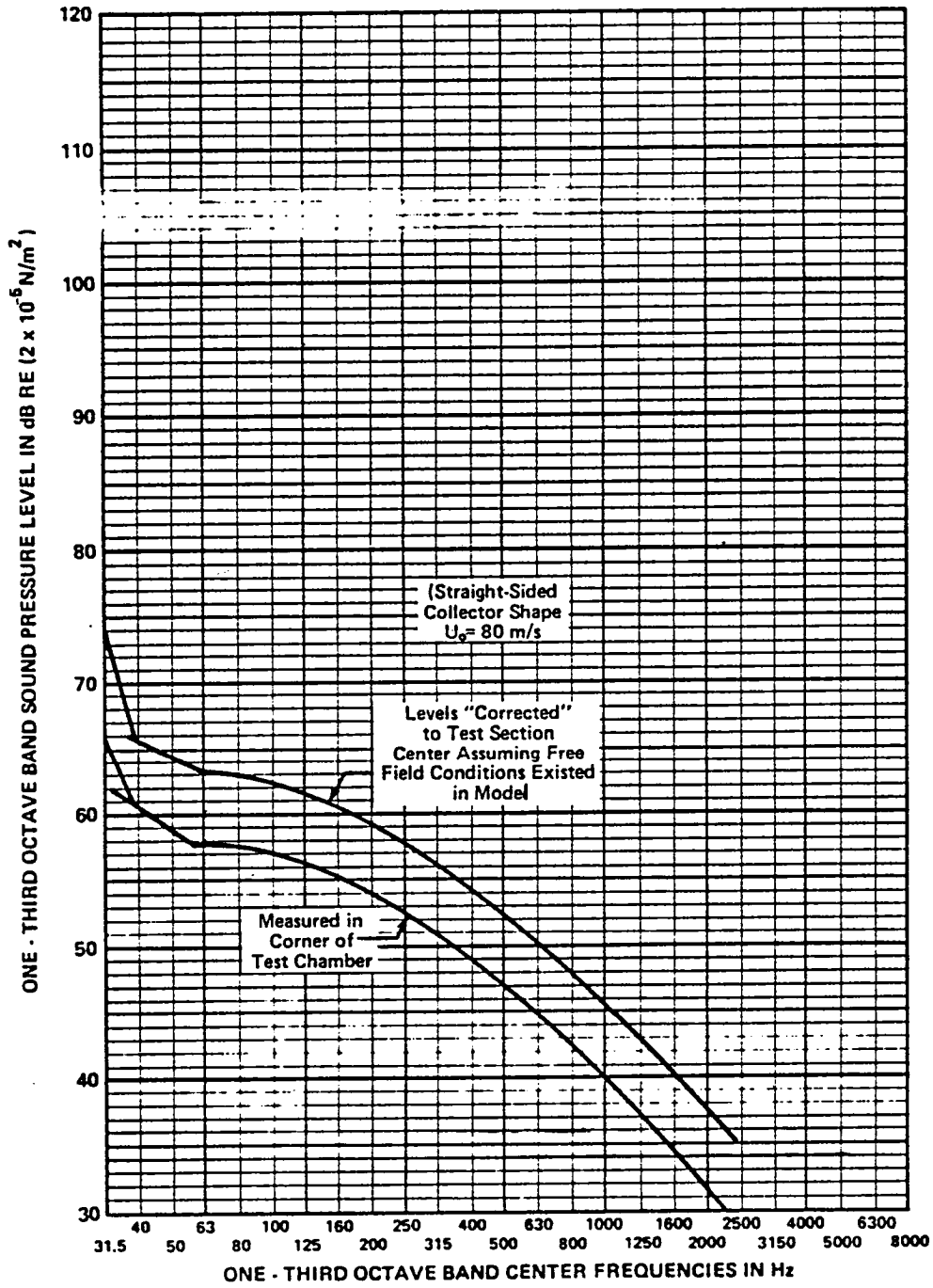
FIGURE 40. COLLECTOR NOISE LEVEL DERIVED FROM MODEL TEST.

84

The range shown reflects our uncertainty as to the acoustic characteristics of the model space (which was lined with 2.5 cm acoustic foam, but not calibrated acoustically since the detection of oscillations was of primary concern).

3.5 Other Sources

The contributions from other sources have not been estimated but can be inferred from the available data and from other data sources. The mechanical equipment noise associated with fan and motor auxiliary systems exceeds the noise goal, as shown by data in Appendix A.

Noise from the nozzle's turbulent boundary layer interacting with the nozzle lip has been observed by the DNW staff [2] in the DNW anechoic test section. If the flow field parameters were known, the methods of Howe [6] or of Brooks and Hodgson [7] could be used to calculate the spectra. In the absence of such data, the empirical correlation shown in Fig. 39 (from Ref [11] can be used, if appropriately modified for line source propagation effects. Using the curve for the moderately loaded airfoil as most representative of the lip. a line source approximation (which gives a $1/r$ spreading dependence (instead of $1/r^2$), the freefield sound pressure level at the Strouhal peak is calculated at typical sideline locations to be between 65 and 75 dB (re 2×10^{-5} N/m^2), and the frequency of the peak is calculated to be around 270 Hz. This level exceeds the goal by a large margin; the calculation is very crude but establishes the nozzle lip noise as a potenially-important mechanism to be studied further.

Flow interaction with the floor, model support, and acoustic treatment are other sources which may prove troublesome. However, if the circuit noise levels are not treated first, the test section sources are clearly unimportant.

85

4. ANALYSIS OF CONCEPTS TO REDUCE BACKGROUND NOISE

4.1 Overview

In general, noise reduction can be achieved at the source or along propagation paths. Both approaches are described below. The ultimate selection of an approach or combination of approaches depends upon a comprehensive tradeoff study involving consideration of aerodynamic performance penalties, structural and operational impacts, downtime required for the modifications, and, of course, cost. A study of acoustic and aerodynamic tradeoffs, potential operational impacts and rough costs of several treatment concepts has been undertaken in a preliminary fashion and is described below.

4.2 Test Section Acoustic Treatment

The test chamber must be improved as an acoustic space if any of the measurement objectives set forth by NASA in Ref. 1 are to be achieved. Such treatment will consist of anechoic wedges throughout the hall wherever they can be placed without being severely buffeted by the flow. Other surfaces must be covered with a flat (or appropriately-contoured) absorbing treatment securely anchored and having a surface which will minimize noise generation by flow over the treated surface.

Treatment of the chamber will also serve to reduce the reverberant buildup of levels in the chamber and thus will contribute to reducing the background noise. The impact on the in-flow locations may be negligible due to the proximity of these locations to the nozzle and collector openings; at most, a 5 dB reduction of levels at the mid-point between the nozzle and collector will be achieved. However, outside the flow, reductions of 5-10 dB can be expected, the larger reductions being achieved with increasing distance from the openings. In the analysis which

86

follows, the in-flow background levels will be assumed to be unchanged by the treatment, but the out-of-flow levels are taken to be 5 dB lower than in the present acoustic space.

4.3 Source Reduction

4.3.1 Overview

If the fan broadband noise is being dominated by inflow turbulence or tip stall, a lower speed operation or an inflow "cleanup" would both be potential means of noise reduction. The inflow cleanup would need to achieve reduced turbulence intensity, shorter length scales, and/or a reduced radial extent of the region of highly turbulent flow. Reduced speed operation would reduce the sound generation with or without inflow improvements. However, the speed reduction must be accomplished through changes in blade loading or rotor solidity in order to produce a given test section speed at a lower fan speed. The extent of the redesign may be limited by the motor capabilities and mechanical limits of the hub. The relative gain from this approach also depends upon how far the present fan's operating efficiency is from the optimum. Information supplied by NASA indicates that the present efficiency is around 75%, while fans in similar installations achieve efficiencies in excess of 90%; thus, it is believed that reduction of broadband noise from the 4x7 m wind tunnel fan could definitely be achieved by a blade redesign. Such a redesign would seek to optimize the distribution of blade loading by increasing chord lengths to allow reduced loading and tailoring the blade characteristics to the actual inflow to the fan, thus presumably increasing efficiency and allowing lower speed operation.

Reduction of turning vane noise at the source can be achieved by an inflow cleanup and a redesign of the vanes to substantially reduce their numbers, optimize the loading to

alleviate local separation and, if trailing edge noise is found to be important, to incorporate porous or serrated trailing edge configurations. A redesign to reduce the number of vanes by increasing chord length, using airfoil sections, etc. could be also used to incorporate sound-absorbing treatment, thus achieving the multiple benefit of reduced source levels, attenuation of fan-generated noise, and elimination of tendencies toward "guiding" sound around the corner which causes bypassing of wall treatments.

4.3.2 Fan Source Reduction

Section 3.3 postulated that the fan's predominant noise mechanisms were sound generated by local stall, blade interaction with inflow turbulence and trailing edge mechanisms (see Fig. 38). The discussion below explores the possibilities for fan noise reduction at the source and quantifies the benefits expected. The redesign of the fan to accomplish the noise reduction set forth is beyond the scope of the present study.

4.3.3 Techniques for and benefits of tip stall elimination

The basic requirement for tip stall elimination is the reduction of lift coefficients near the tip. A C_L of under 0.5 is generally regarded as safe for the entire span; however, it is usually desirable to reduce tip C_L's even further. The reduction of C_L can be accomplished by increasing axial velocity in the tip region through upstream flow path improvements or by redistributing the pitch and increasing the chord of the blades. The total thrust of the fan must and can be preserved through this process. Flow path improvement concepts which can lead to higher axial velocities near the tip include use of unevenly distributed turning vanes to force more flow along the walls, a tapered or an oversize bulbous nose cone to force high speed flow out of the

duct centerline toward the hub (essentially accomplishing an abrupt acceleration of the flow ahead of the fan), or air injection through blowing slots.

If the flow path modifications are insufficient or impractical, then a blade redesign is required. In the process of blade redesign, measured inflow velocity distributions would be used to set local pitch angles in such a way that stall would be avoided. If blade redesign was selected as a desired approach, then the opportunity could be seized to help improve other flow problems downstream of the fan through adjustment of fan outflow velocity distributions and swirl angles.
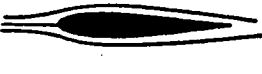
The fan redesign should also seek to substantially lower the blade tip speeds required to achieve a particular test section velocity since such a reduction will reduce noise due to blade interaction with inflow turbulence and "self noise" caused by trailing edge mechanisms. A reduction in tip speed must and can be accomplished without reducing the fan thrust for a given circuit flow requirement; increased chord lengths are required to reduce fan tip speed without overloading the blades.

4.3.4 Estimate of noise reduction achievable by elimination of tip stall and reduction of tip speed

Noise reduction achieved by elimination of tip stall will manifest itself in two direct ways:

1)   reduction of the intense pressure fluctuations associated with stall, and thus a reduction of the strength of the driving mechanism at the tip; and

2)   improved fan efficiency allowing for lower speed operation at a given test section velocity.

To estimate the potential reduction of noise due to elimination of tip stall, we resort to limited empirical data. First, consider the effect of C_L stall on the noise-producing surface pressure fluctuations. Heller, et al (Ref. 9) were concerned with detecting incipient airfoil stall through the use of surface pressure fluctuation measurements, and thus developed a large data base comparing surface pressure spectra between unstalled airfoils and those experiencing various stall mechanisms (e.g., trailing edge, leading edge, laminar separation, etc.). Figures 41 and 42 (from Ref. 9) illustrate the substantial variation in FPL spectra at two chordwise locations on an airfoil as a function of angle of attack. In general, when an airfoil experiences a separation bubble and when it ultimately stalls, there is a large increase in the amplitude of low frequency pressure fluctuations, and certainly an attendant large increase in the characteristic length scale. A direct calculation ofthe corresponding changes in radiated noise from a fan such as the 4x7m tunnel's drive fan requires a detailed knowledge of the "before and after" pressure fluctuation spectra, length scales, and spanwise extent of the stall region. Such data is not available for the 4x7 fan or for similar fans to our knowledge. However, the data in Figures 41 and 42 could be interpreted as first order indications of the relative fluctuating "lift and drag" on the blade tips and therefore, simple dipole source models would indicate a corresponding variation in the radiated sound from that region of the blade. Note that as one moves from hub to tip on a highly-loaded fan blade, the flow states (and thus the associated surface pressure fluctuations as illustrated in Figs. 42 and 43) traverse the full range of attached, partially-separated and fully separated flows. Thus to estimate the change in the radiated sound spectrum, one would need to account for the integrated effect over the full span of the blade. Therefore, from the surface pressure data shown, one

ANGLE OF ATTACK	0° → 1.5°	1.5° → 4°	4° → 13.5°	> 13.5°
FLOW REGIME	LAMINAR ATTACHED	INITIAL BUBBLE FORMATION; TRANSITIONAL FLOW	GROWTH OF SEPARATION BUBBLE	FULLY SEPARATED FLOW
FLOW PATTERN				

TWO-DIMENSIONAL FLOW PATTERNS ON "THIN AIRFOIL" (NACA 0006 PROFILE)
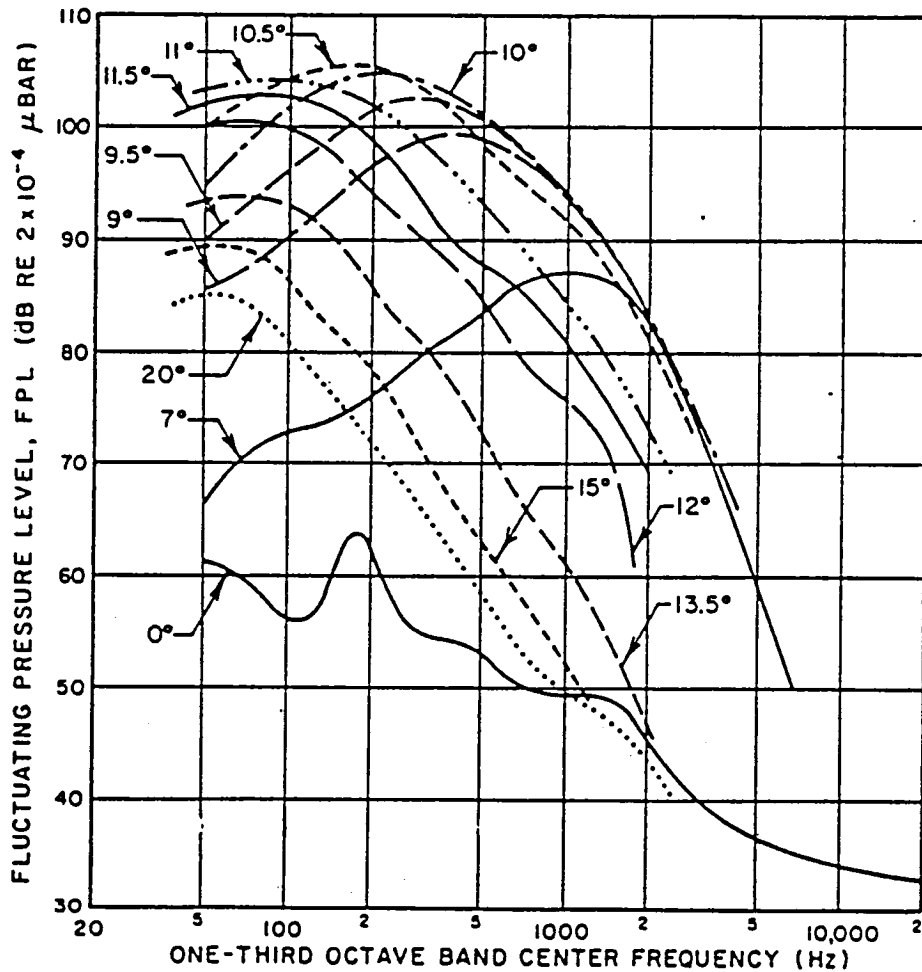
FIG. 41   SURFACE PRESSURE SPECTRA AT 20%-CHORD POSITION ON TOP SURFACE OF UNYAWED NACA 0006 AIRFOIL AT VARIOUS ANGLES OF ATTACK.   AT 36 fps AIRSPEED.   (Ref. 9)

91
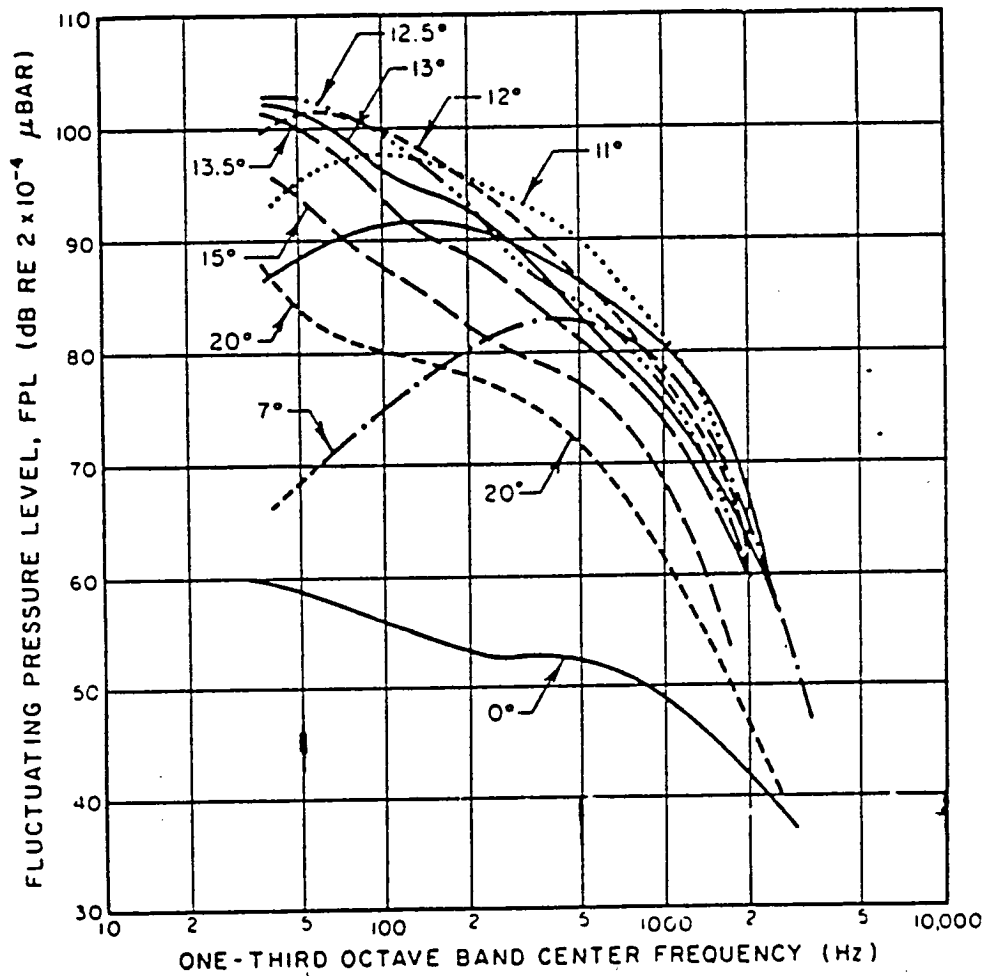
FIG. 42   SURFACE PRESSURE SPECTRA AT 70%-CHORD LOCATION ON TOP
SURFACE OF UNYAWED NACA 0006 AIRFOIL.   AT VARIOUS ANGLE
OF ATTACK.   AT 36 fps AIRSPEED.   (Ref. 9)
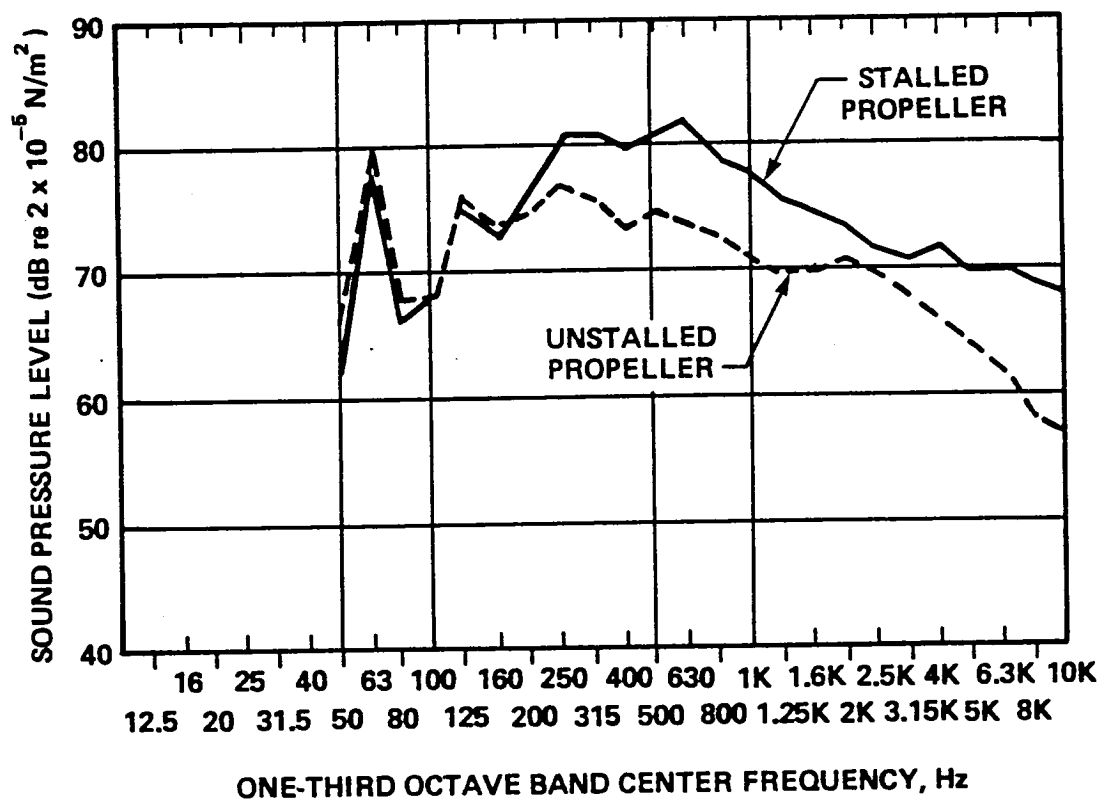
FIG. 43 COMPARISON OF 1/3 OCTAVE BAND SPECTRA FROM STALLED AND
UNSTALLED PROPELLERS (Static Conditions). (Ref. 14)

93

could expect changes in radiated sound from the outer part of the blade up to 20 dB in the low frequency regime with smaller changes in the high frequency regime. The spectrum details would depend upon the "severity" of the stall, which is a function of the spanwise (radial) location. The frequency regimes in which this data would be applicable can be roughly estimated by frequency scaling the data from Ref. 9 by U/C, where U is the local velocity and C is the chord. The tip velocity in the 4x7 m tunnel is approximately 82 m/s (272 tps) for an 80 kt (41 m/s) test section speed, and the fan blade chord at the tip is approximately 2.4 times that of the airfoil used in the tests. Thus, the frequency scale for the data to apply to the 4x7 fan should be multiplied by approximately 3; most changes from eliminating stall would reduce the radiated sound levels below 3000-4000 Hz, with the most dramatic changes probably occurring at frequencies below 1000-1500 Hz. It should be noted that at the very lowest frequencies, blade response to inflow turbulence may dominate the stall noise and thus no effect of eliminating stall would be evident.

To quantify the impact of eliminating stall on the noise from the complete fan, one would need to know in detail the relative source strengths of the noise due to turbulent inflow and trailing edge mechanisms. However, some data may be cited to provide an order-of-magnitude estimate of the noise reduction due to stall elimination. Figure 43 shows a comparison between stalled and unstalled propeller noise during a static (ground) test (Ref. 14). Presumably some turbulence and distortion existed in the inflow due to outdoor ground test conditions, so some inflow turbulence-induced mechanisms are present in both cases; no effect of stall is seen on the blade passage frequency and lowest harmonics. The 6-10 dB reduction in noise caused by eliminating stall occurs at frequencies above the lowest blade harmonics and covers a wide frequency band. Available data from

94

axial flow fans in ducts is not so definitive in characterizing the stall/unstall boundary, but consistent dependencies of noise on tip clearance have been noted in a variety of cases (15-17), the broadband noise being reduced as the clearance is reduced. Presumably the blades with large tip clearances experience recirculation around the tips which creates a locally stalled condition. Thus, the improvements of up to 6-10 dB by tip clearance reduction provide another measure of the "stall noise increment". For the present purposes, our assessment of the evidence suggests that at least 8 dB reduction of fan noise can be achieved at all frequencies below 3 kHz by eliminating tip stall, without taking credit for the reduction in fan speed which may accompany the increased efficiency attendant to stall elimination. Further evaluation of the flow environment and performance of the 4x7m fan in the open jet mode might reveal evidence that much larger reductions could be expected if the loading could be reduced by simultaneously increased blade chords and reduced local lift coefficients.

Noise reductions due to tip speed reductions can be expected to vary as 50 log V_T at constant Strouhal number. To effect a tip speed reduction while maintaining constant test section velocity and area (i.e., volume flow), the fan characteristics must be modified to match the tunnel characteristic at a more efficient point on the fan operating curve. If the tunnel loss characteristics and the inflow distribution to the fan are well-known, then the fan blade characteristics (pitch, chord, camber, and thickness distributions) can be altered to create optimum efficiency. Such efforts might also include changes in the blade number or hub/tip ratio.

In addition to a straightforward reduction in tip speed, optimizing the blade design apparently also reduces the strength of the hydrodynamic mechanisms producing "self-noise" of the

95

blade thus defining an optimum noise point (i.e., minimum-self) on the operating curve (Ref. 18). Mellin (Ref. 18) has shown that this optimum point spans a relatively modest range of flow coefficients and results in 8-9 dB less noise than operations near the stall boundary. Since the 4x7 fan is obviously "near" the stall boundary, such optimization could result in some reduction (say, 4-6 dB) at constant tip speed, (with the same chords being used) and additional benefits would accrue if the speed can also be lowered. One approach to "optimizing" the blade loading would be to simply repitch the present blades by reworking the attachment area. Another would be to utilize a nose cone ahead of the fan to alter the inflow (increase the advance ratio) and thus lower the blade loading. Both these changes may require increased tip speeds to maintain volume flow, so there will be some interplay between the effects of increased tip speed and the noise reduction resulting from the improved inflow environment and reduced blade loading. The need to increase tip speed may not exist if the fan moves to a more efficient operating point.

A straightforward example is worked out below to illustrate hypothetically the effect of stall elimination and speed reduction on the noise of the 4x7 fan. The data chosen as the baseline is the measured spectrum at location 9 for an 80 kt test section velocity. Figure 44 shows the baseline data (curve A) along with the same data lowered 8 dB to account for the effects of stall elimination (curve B). Data below 80 Hz is thought to be dominated by inflow turbulence so this data is "faired-in". Curves C and D show the effects of 25 and 50 percent speed reductions at the same working point on the fan performance characteristic curve. These curves are derived by reducing the level at constant Strouhal number by 50 log V_T and shifting the spectrum to lower frequencies by the tip speed ratio. Curves C and D would have to be adjusted for the effects of moving to
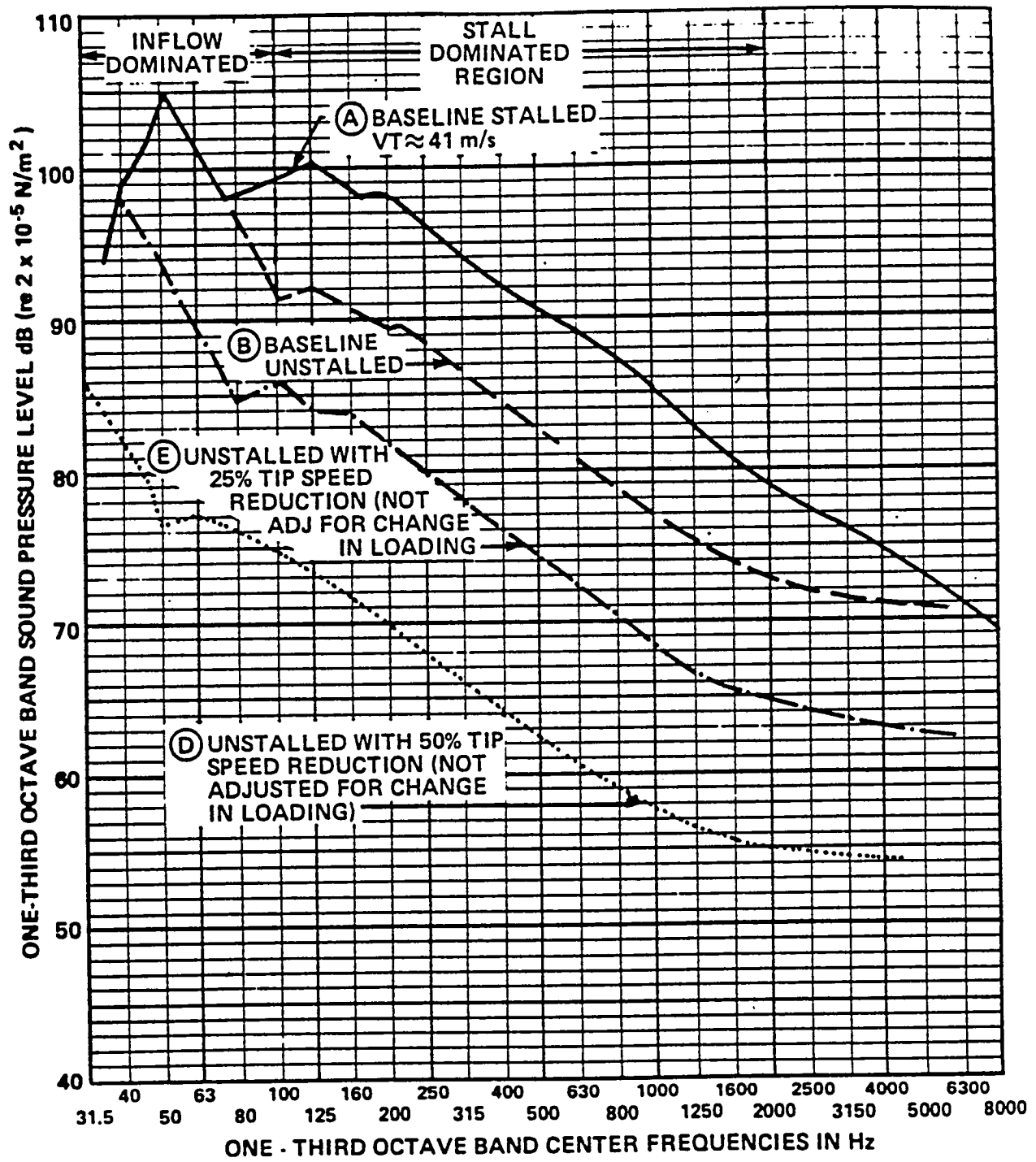
FIG. 44 SYNTHESIS OF SPECTRA FOR REDUCED NOISE FANS

97

another loading condition on the fan characteristic curve in order to accurately reflect the changes in the spectrum achievable at <u>constant</u> test section velocity. Since the present fan is already too heavily loaded, the speed reductions would only be possible if accompanied by an overall redesign of the blading system, a reduction in the tunnel system losses, or a decrease in the test section cross-sectional area to achieve high velocities in a smaller test section. The latter concept could prove most effective if the flow path will efficiently recover the head in the jet so that the fan does not sense the full impact of the high speed flow in the smaller test section. An analysis of altering the test section flow path is outside the scope of the present study.

In any event, it is obvious that if the fan could be redesigned to operate at an unstalled condition and fitted with alternate blading such that tip speeds could be reduced substantially, a great deal of noise reduction benefit will occur, with attendant reductions in power requirements.

4.3.5 Turning vanes

Turning vane noise reduction can be estimated from the parametric variables in the equation describing the sound generation (see Sec. 3). Without redesigning the present vanes, only a reduction in inflow velocity and turbulence levels will reduce source levels; however, a more subtle approach would be to reduce the response of the vanes to the turbulent inflow by providing a large leading edge radius and larger chord. This approach would also cause a reduction in the number of vanes, however, increasing the chord would lower the frequency at which "waveguiding" effects occur (see Sec. 2). Therefore, such vanes would have to be treated acoustically. Fortunately, as shown below, large-chord treated vanes are an attractive approach to

absorbing noise from other sources. At this point, no estimate has been made of source reduction attributable to long chord vanes with rounded leading edges. However, we are certain that if treated vanes are selected as an approach, the noise generation by these vanes will decrease substantially from present levels.

4.4 Evaluation of Various Sound Absorption Methods for Controlling Tunnel Noise

This section examines the performance of various concepts for absorbing sound between the circuit acoustic sources and the test section. Some of the calculations were carried out using a computer program which incorporates a number of theoretical and experimental results, such as described in references 19 through 25. Chapter 12 of Ref. 19 presents a succinct summary of the general methods used, although the computer program contains several refinements. In all cases, the analytical calculations have been compared with prior experience to obtain a final "high confidence" noise reduction estimate. The data presented below reflects such adjustments in the "raw" calculations.

Table 3 summarizes the insertion loss required as a function of frequency, in both "upstream" and "downstream" directions from the fan and the first corner vanes. The insertion loss requirements are presented for several fan speeds to reflect the impact that stall elimination and fan speed reduction would have on the attenuation requirements. Note also that different insertion loss requirements exist for in-flow vs sideline microphone positions. Adjustments have been made for the effects of proposed anechoic treatment in the chamber (0 dB for inflow; -5 dB for out-of-flow).

In all cases, the absorption required is broadband, and thus highly-tuned absorbers have been ruled out. The performance

TABLE 3. SUMMARY OF PATH NOISE REDUCTION REQUIREMENTS FOR PRIMARY SOURCES

	Insertion Loss in Octave Band					
	Octave Band Center Frequency (Hz)					
I. Upstream - Propagating Sound	125	250	500	1K	2K	4K

A. REQUIRED (C_L IN-FLOW/SIDELINE OUT OF FLOW - ANECHOIC)

A. Fan-to-Test Section (T.S.)

	125	250	500	1K	2K	4K
1. Nominal Speed (N_O)	39/29	38/28	28/18	19/9	10/0	4/0
2. Unstalled at N_O	31/21	30/20	19/9	12/2	5/0	0/0
3. Unstalled at 0.75 N_O	23/13	21/11	13/3	5/0	0/0	0/0
4. Unstalled at 0.50 N_O	11/1	10/0	10/0	0/0	0/0	0/0
B. 1st Corner Turning Vanes-to-Test Section	22/12	18/8	13/3	10/0	3/0	0/0

II. Downstream - Propagating Sound

REQUIRED: (C_L IN FLOW/SIDELINE OUT OF FLOW-ANECHOIC)

A. Fan-to-Test Section

	125	250	500	1K	2K	4K
1. Nominal Fan Speed (N_O)	37/27	35/25	27/17	17/7	6/0	0/0
2. Unstalled at N_O	29/19	27/17	19/9	9/0	0/0	0/0
3. Unstalled at 0.75 N_O	24/14	19/9	11/1	2/0	0/0	0/0
4. Unstalled at 0.50 N_O	12/2	8/0	1/0	0/0	0/0	0/0
B. Turning Vanes	(No. I.L. Needed if Fan Paths Treated)					

Note: **Bold** figures refer to the insertion loss required to reduce levels at a point on the **wind tunnel centerline midway between the nozzle and collector**; the figures in normal type refer to reductions needed to only meet the sideline out-of-flow background noise goal in a high quality anechoic space.

100

estimates for the absorbers are all based upon the optimum
impedance for the bandwidth required and physical space avail-
able, and for the effects of flow. The concepts presented below
are treated separately, although in practice they may be combined
in various ways to achieve the total insertion loss required
between the sources and test section. Section 4.4.3 discusses
some of the limitations and uncertainties involved in combining
the individual elements. Section 4.5 presents suggested combina-
tions for the 4x7m tunnel.

4.4.1 Summary of sound-absorbing concepts

The sound absorption concepts applicable to the 4 x 7m wind
tunnel circuit can be broadly classified as:

A. Non-Intrusive Liners: absorbing surfaces which do not
   modify the contours of the flow path and therefore do not
   represent sources of potentially-significant aerodynamic
   losses;

B. Splitters: large-chord streamlined surfaces which
   effectively cut the ducts in half, but which represent
   relatively little blockage and thus relatively small
   aerodynamic penalties;

C. Baffles: traditional industrial-type closely-spaced
   acoustically-absorbing "splitters" which are acoustically
   effective but aerodynamically inefficient;

D. Treated Turning Vanes: long-chord airfoil-shaped turning
   vanes which contain acoustic treatment; such vanes have
   inherently low aerodynamic losses if designed according to
   good aerodynamic practice.

Figures 45 and 46 illustrate the application of non-
intrusive liners to the 4x7 m tunnel at several locations. In

101
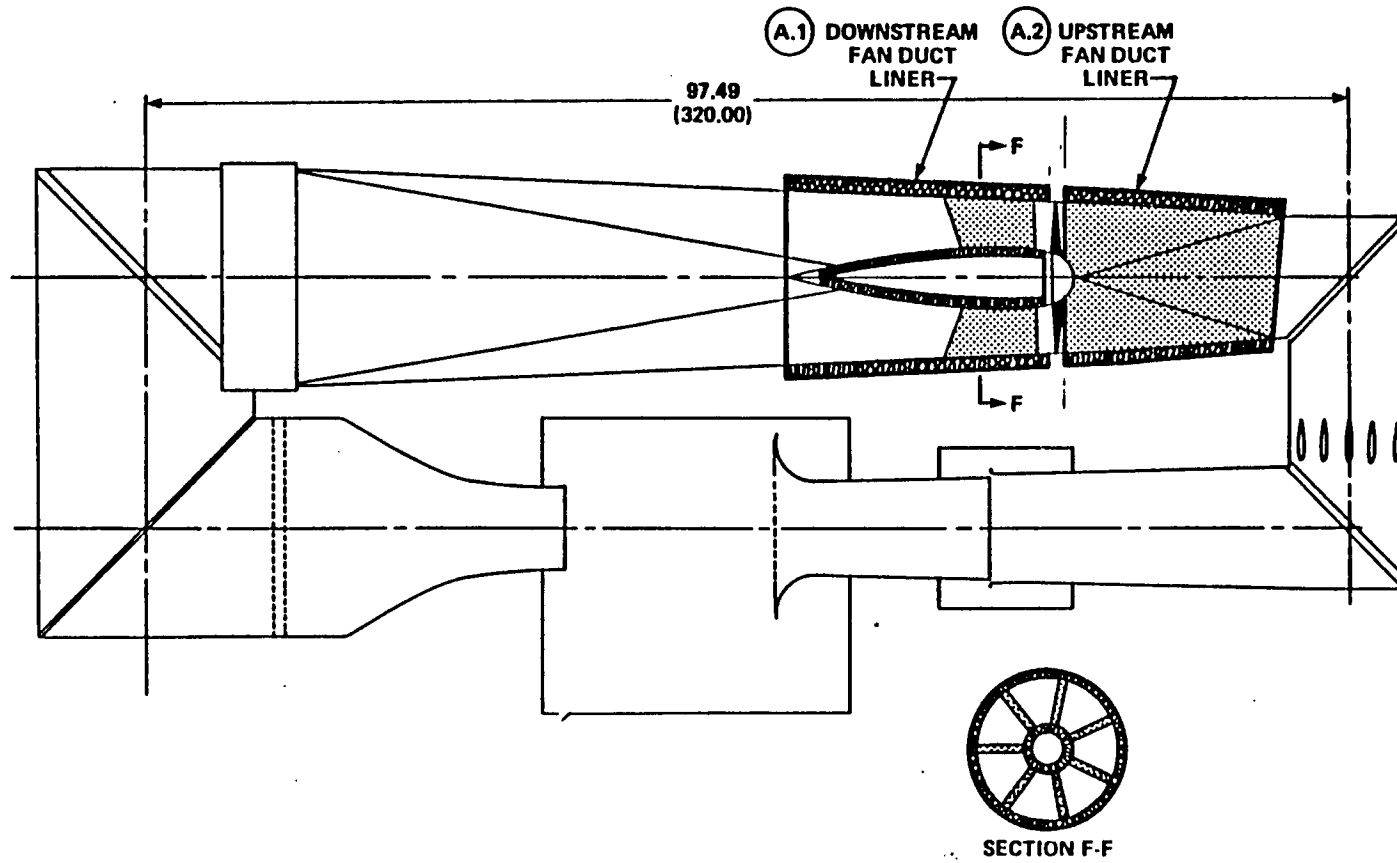
FIGURE 45.   NON-INTRUSIVE LINER APPLIED TO FAN DUCTS.
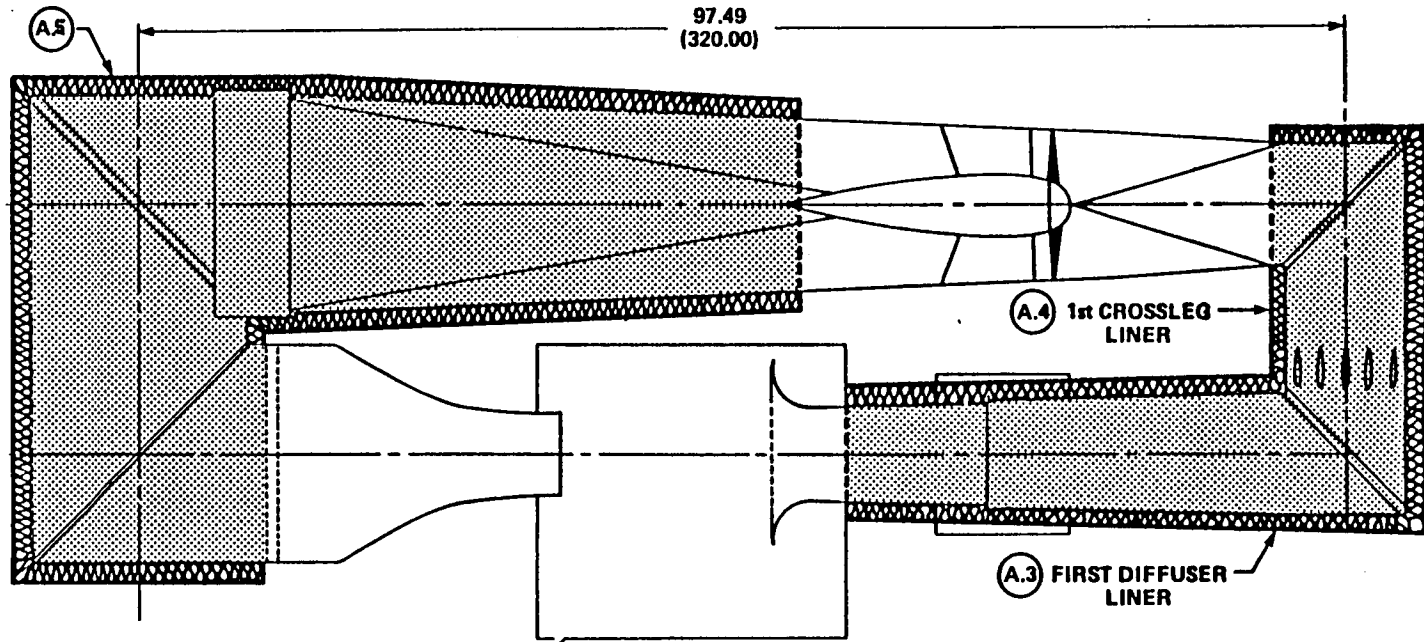
FIGURE 46. NON-INTRUSIVE LINER APPLIED TO FLOW PATH.

Figure 45, a fan duct liner is shown in two parts. The upstream segment (A.2) consists of a liner, approximately 0.4-0.5 m thick, recessed into the wall extending roughly from the rotor plane to the second corner. This liner could be augmented with a lined centerbody if, as suggested in Sec. 3.3, aerodynamic considerations indicate some associated benefit on the fan performance. Such a centerbody would increase the insertion loss as well as reducing the source strength if it could help eliminate stall. A further improvement in acoustic performance could be achieved by adding a treated "ring" between the centerbody and the wall. These additions are shown in Fig. 47, and their performance is analyzed in Sec. 4.4.3.

The downstream fan duct liner (A.1) shown in Figure 45 consists of an outer wall lining treatment (0.4-0.5m deep; recessed to preserve the original flow path), a lined centerbody (fan tail-cone), and stator vanes treated to act like sound-absorbing splitters. This treatment could also be improved with a treated "ring" between the centerbody and the outer wall, as shown in Fig. 47.

Figure 46 also illustrates recessed liners applied to the first diffuser (A.3), the second diffuser (A.4), and the fourth and fifth diffusers (A.5). These treatments consist of recessed absorbers with a perforated surface which follows the original flow path. As discussed in Sec. 2 and below, such treatments may be bypassed at frequencies above 1 kHz as a result of waveguiding by turning vanes, and therefore may be economically inefficient.

Simple treated splitters can be combined with the non-intrusive wall liners as shown in Figure 48. The splitters would typically be 0.5-1.5 m thick and would incorporate aerodynamic features (streamlined nose and tail) to minimize losses. The construction normally includes internal structural members to support and stabilize the splitter. One variation on the simple
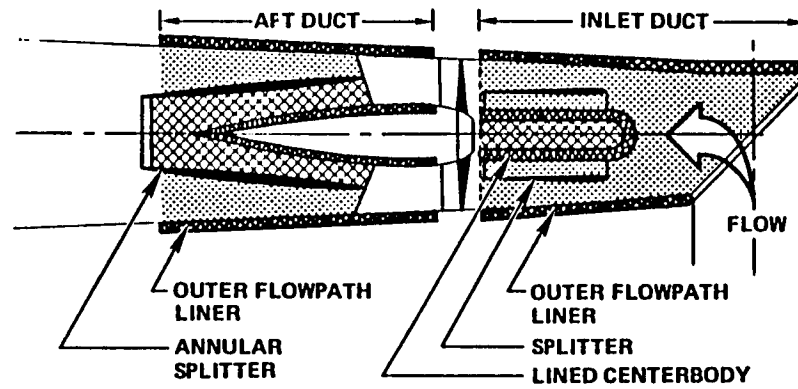
FIGURE 47. SCHEMATIC OF LINED CENTERBODY AND ANNULAR SPLITTERS
APPLIED TO FAN INLET AND OUTLET DUCTS.
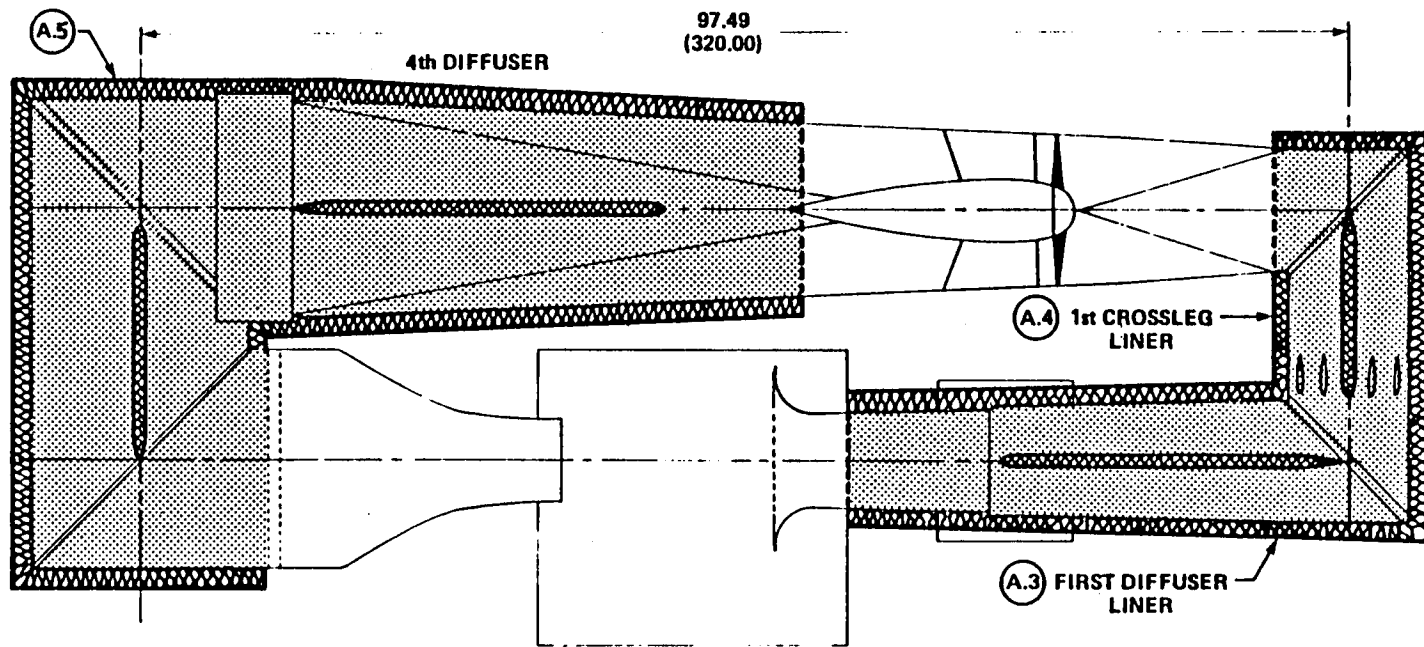
FIGURE 48. SIMPLE "SPLITTERS" USED IN COMBINATION WITH WALL TREATMENTS.

splitter is the cruciform (Fig. 49), which essentially incorporates two perpendicular splitters, each approximately 1-1.5 m thick. The cruciform would again increase effective length-to-width ratio of the duct, thus increasing the attenuation per unit length. However, blockage is increased by this muffler and thus aerodynamic losses may be unacceptable in some parts of the circuit.

Parallel baffles derived from traditional duct silencing applications may be placed at several locations around the circuit (Fig. 50). These baffles tend to provide high attenuation at the expense of considerable aerodynamic penalty. However, the performance of such "silencers" is well-understood and thus design estimates are usually very reliable.

One approach to achieving the benefits of closely-spaced parallel baffles is to utilize the turning vane stages at one or more corners. Since turning vanes perform optimally when the pitch-to-chord ratio is between 0.2-0.4, the close spacing provides an ideal situation for application of parallel baffle technology. In order to effectively incorporate a silencer "bank" into a turning vane stage, an adequate thickness and length of treatment is required. Thus, the existing thin circular arc vanes with chord lengths of 0.6-0.7 m would be replaced with airfoil-shaped vanes with a maximum thickness of approximately 0.5 m. A schematic of such a vane is shown in Fig. 51. To incorporate this thickness over the length required for effective sound absorption, and also to maintain a constant cross-sectional area for the flow through the corner, the chord length required is approximately 5 m. A typical arrangement of these vanes is shown in Fig. 52. Other advantages of the treated vanes are (1) that they effectively prevent "waveguiding", (2) reflection of sound generated by the test object is reduced, and (3) noise generation is reduced in the frequency range of

107
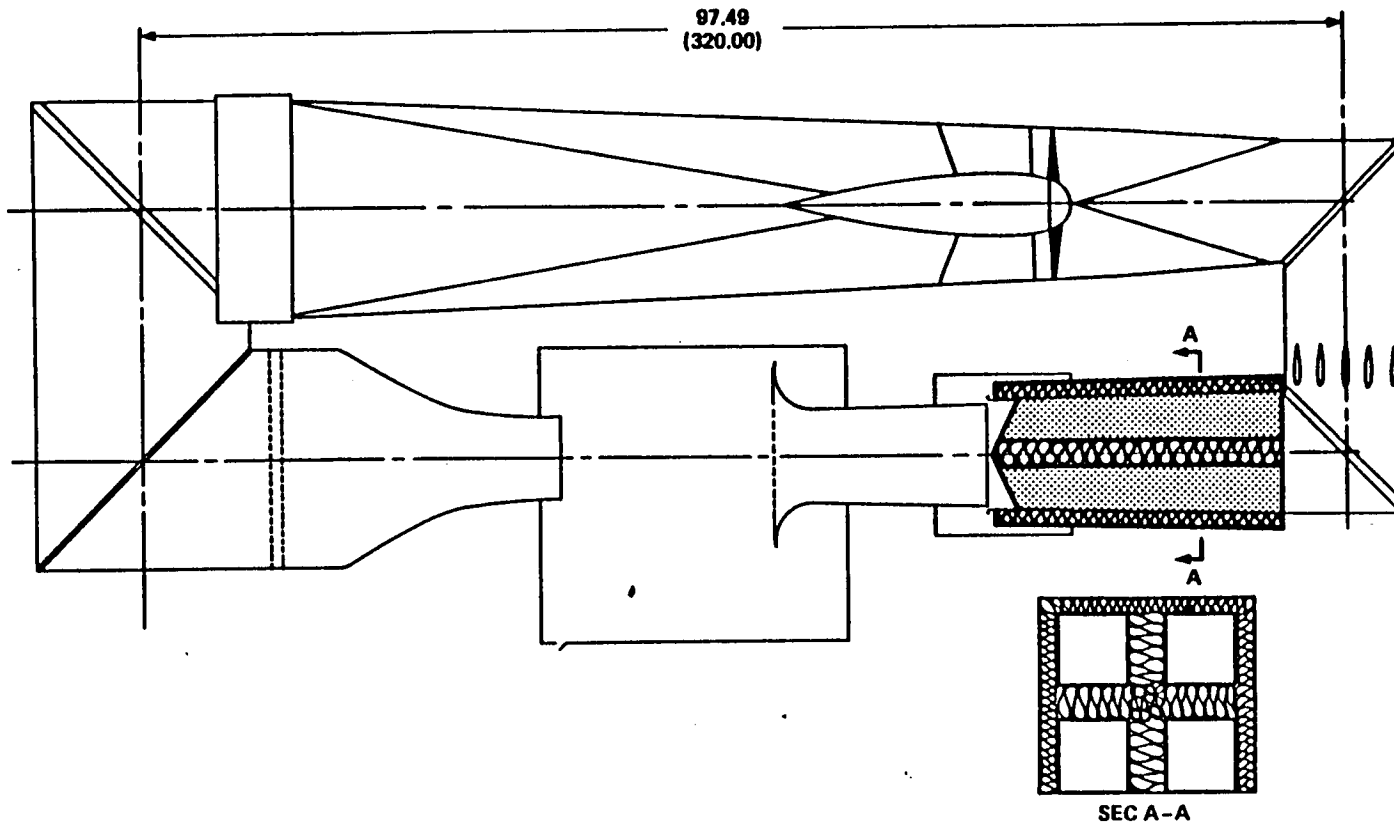
FIGURE 49. "CRUCIFORM" ABSORBER APPLIED TO FIRST DIFFUSER.

97.49
(320.00)

4th DIFFUSER

2nd DIFFUSER

1st DIFFUSER

109
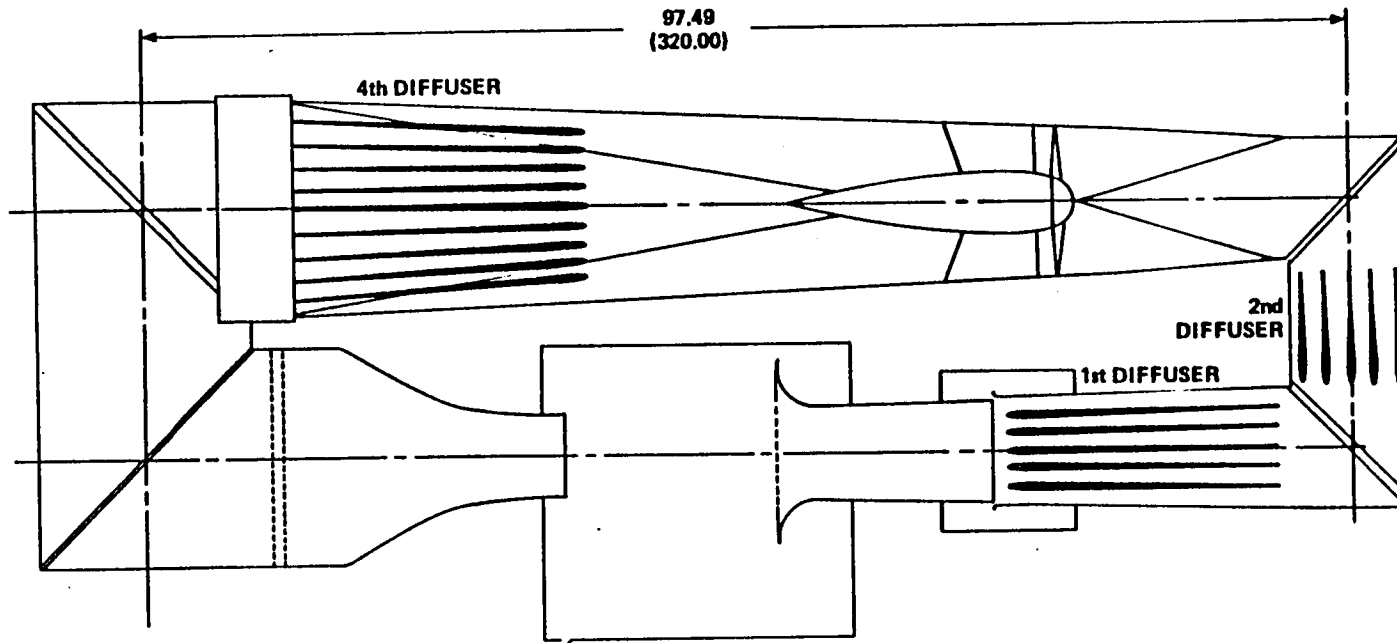
FIGURE 50. SCHEMATIC OF PARALLEL BAFFLE SILENCERS APPLIED TO THE 4x7 m
TUNNEL CIRCUIT.

SHORT
EXTENSION |←→|

FLOW

LEADING EDGE
RADIUS COULD
BE LARGER

CORE CAN BE
BULK ABSORBER
OR "NO-FUZZ"

TRAILING EDGE
EXTENSION WILL
IMPROVE
AERODYNAMICS

SHORT
EXTENSION
RECOMMENDED
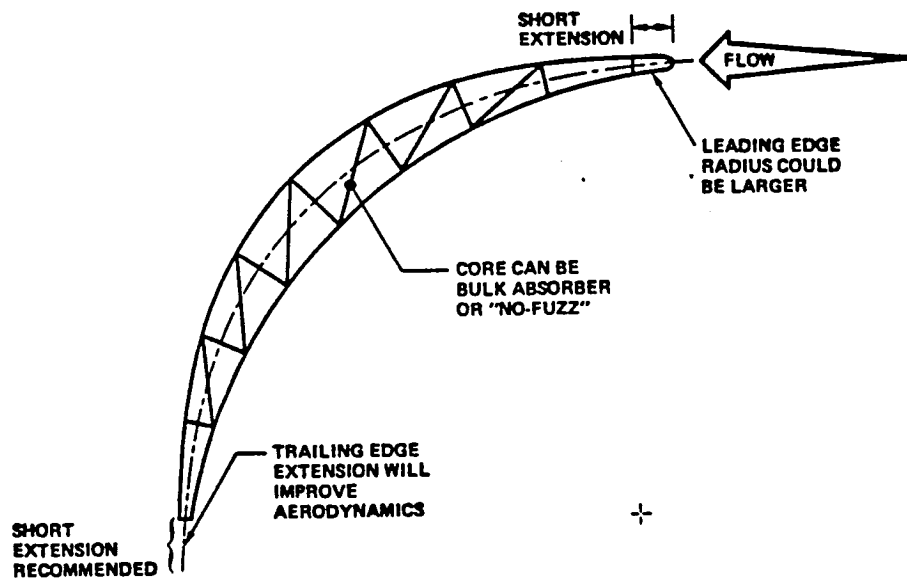
FIGURE 51.   SCHEMATIC SECTION OF TREATED TURNING VANE.
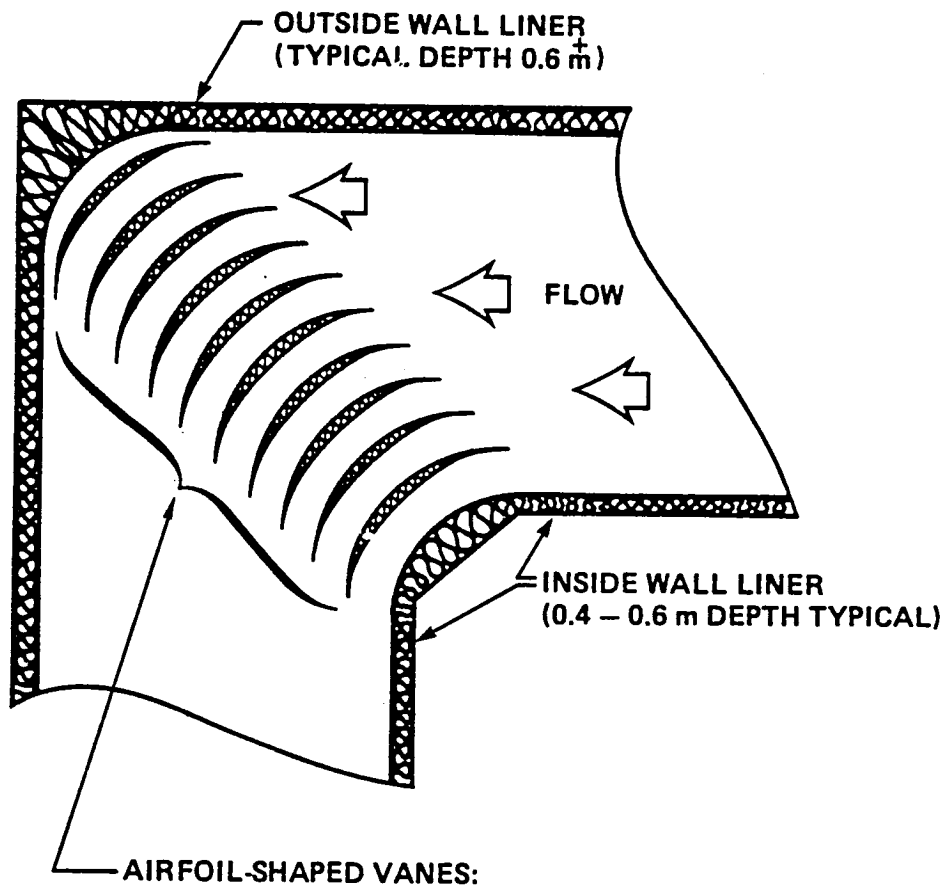
110

OUTSIDE WALL LINER
(TYPICAL DEPTH 0.6 $\overset{+}{m}$)

FLOW

INSIDE WALL LINER
(0.4 – 0.6 m DEPTH TYPICAL)

AIRFOIL-SHAPED VANES:

- Chord $\approx$ 5 m
- Maximum Thickness $\sim$ 0.4 – 0.6 m
- Number of Vanes Dictated by Best
  Aerodynamic Performance (p/c $\approx$ 0.2)
- Perforated Facings Both Sides;
  Variable Geometry Cavities Inside, With
  Absorption as Needed; or Bulk Absorber.

FIGURE 52. SCHEMATIC OF CORNER FITTED WITH LONG-CHORD TREATED
TURNING VANES

interest due to rounded leading edges, longer chord lengths
(which reduce response to turbulent inflow and create lower
frequency trailing edge noise than untreated vanes), and the
reduced number of sources (vanes).

4.4.2 Treatment detailing

Broadband absorbers for wind tunnels or other flow-carrying
ducts are traditionally constructed of a fibrous bulk absorber
material contained between a surface layer consisting of
perfortated metal sheets backed up by a layer of fiberglass cloth
and a screen. Figure 53 illustrates such a detail. Note that
there are periodic structural elements which serve two essential
purposes - (1) provision of structural support, and (2) preven-
tion of internal sound propagation which can "short-circuit" an
extended length of treatment.

The open area ratio of the perforated surface may be varied
over a range from about 15% to 50%. If the flow resistance of
the internal elements are not varied at the same time the open
area ratio is varied, there will be variations in the effective
bandwidth of the attenuation provided (see Fig. 12.22 of Ref. 19
for illustration). However, the relationships between all the
elements of a bulk absorber of the type shown are well-understood
and therefore silencers which incorporate these concepts can be
designed with a high degree of confidence.

The primary objections to the bulk absorber concept for wind
tunnels are (1) the gradual erosion of the glass fibers which may
fill the tunnel circuit and also lead to changes in acoustic
performance, and (2) susceptibility to contamination by oil and
dirt, thus leading to changes in performance and possible fire
hazards. Also, when immersed in high speed flow, the perforated

112

FILL (4^{lb}/ft^3 MINERAL WOOL OR EQUIVALENT)

FIBERGLASS CLOTH

WIRE MESH (∼.01 in. dia. wire)

GALVANIZED SHEET METAL FACING PERFORATED; ∼30% OPEN 16 - 18 GAGE HOLES ≈ 1/8" dia.

.7 – .8 m
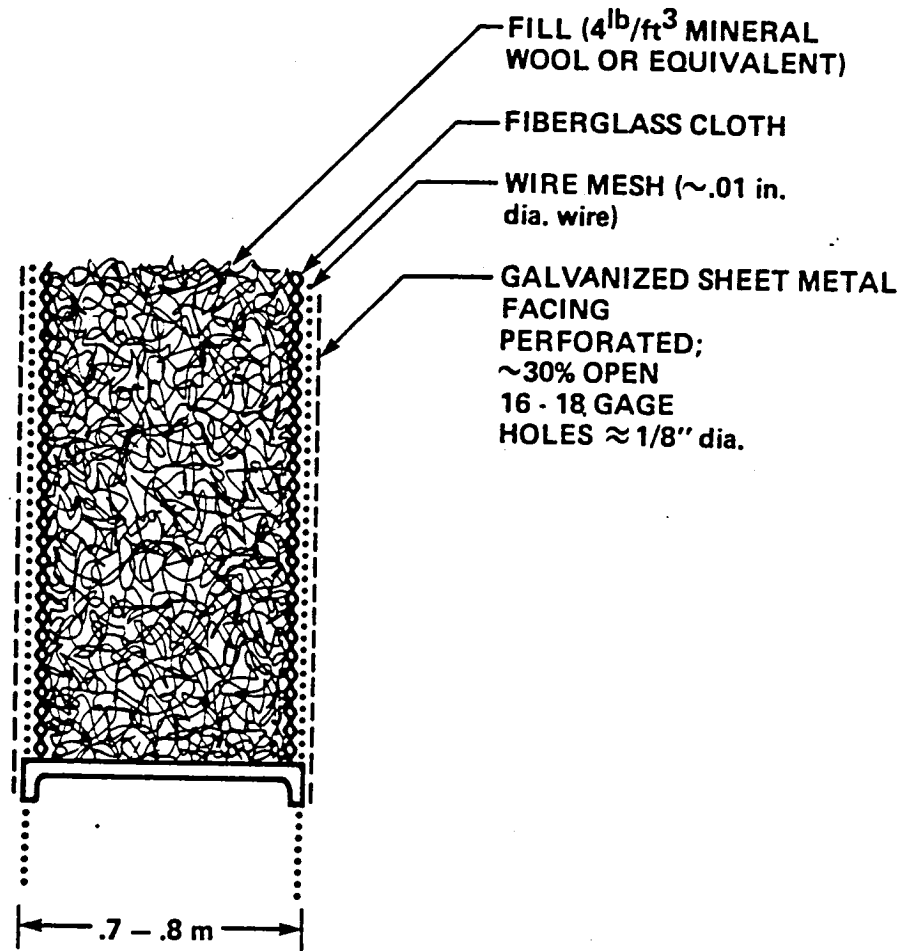
FIGURE 53. TYPICAL SECTION DETAIL OF A BULK ABSORBER

sheets generate high frequency "self-noise" which may offset their attenuation benefits.

One alternative to the bulk absorber is a silencer concept which has as its acoustic elements a thin perforated sheet with sparsely spaced small holes and a variable-geometry cavity backing up the sheet as the reactive element. This so-called "no-fuzz" design has been utilized in the NASA Ames 40x80/80x120 retrofit and is described in detail by Soderman (Ref. 26). Figure 54 shows a typical section of the "no-fuzz" concept (which actually contains a thin layer of porous material ("fuzz") bonded to the diagonal baffle plate which creates the variable depth cavity). The purpose of the porous material is to suppress high frequency tones excited by flow interaction with the perforations which couple to the backing cavity. The "no-fuzz" silencer concept has been shown to provide insertion loss comparable to the bulk absorber concept. However, the impedance of the perforated surface/cavity combination is affected by flow due to the small size of the perforations. Thus, the insertion loss of a "no-fuzz" muffler will vary with flow speed. Therefore, when considering use of a no-fuzz design, it is essential to select the flow speed range of interest and optimize the details accordingly. A second drawback to the "no-fuzz" silencer is the susceptibility to contamination by dirt and oil. Since the concept uses small perforations as an essential part of the design, any change in the orifice geometry, such as caused by dirt or oil, will cause change in the acoustic performance. However, due to the absence of fibrous material immediately beneath the skin, cleaning of the surfaces is straightforward and will, of course, restore the original acoustic characteristics.

PLAN SECTION

SOLID DIVIDER

ABSORPTIVE MATERIAL

STRUCTURAL SUPPORT/DIVIDER

PERFORATED FACING SHEET (4 – 5% OPEN)
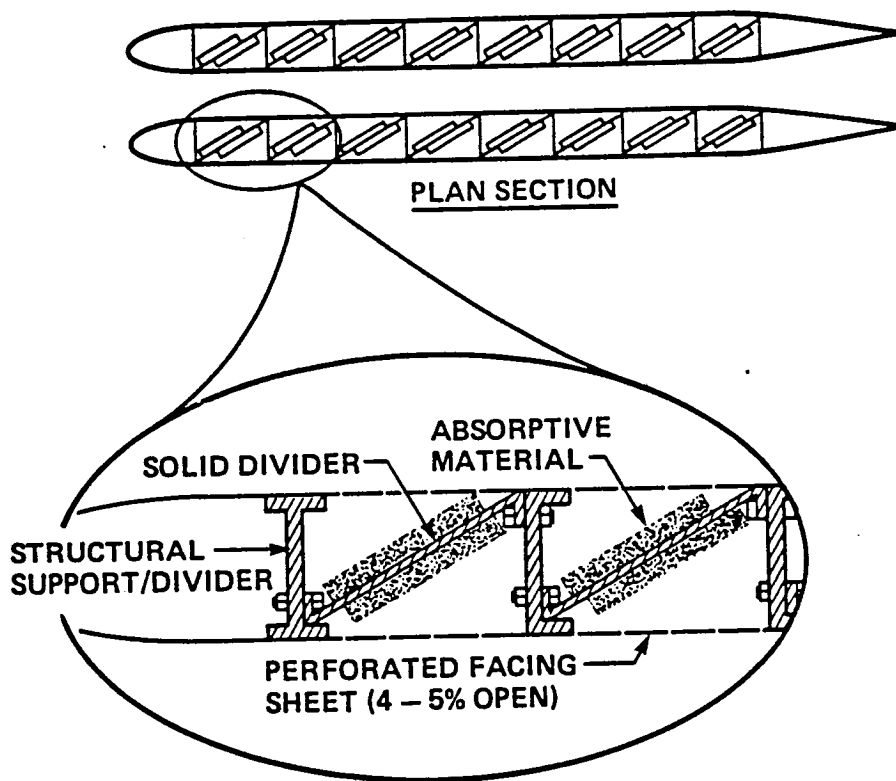
FIGURE 54. TYPICAL DETAIL OF "NO-FUZZ" ABSORBER CONCEPT [REF 26]

115
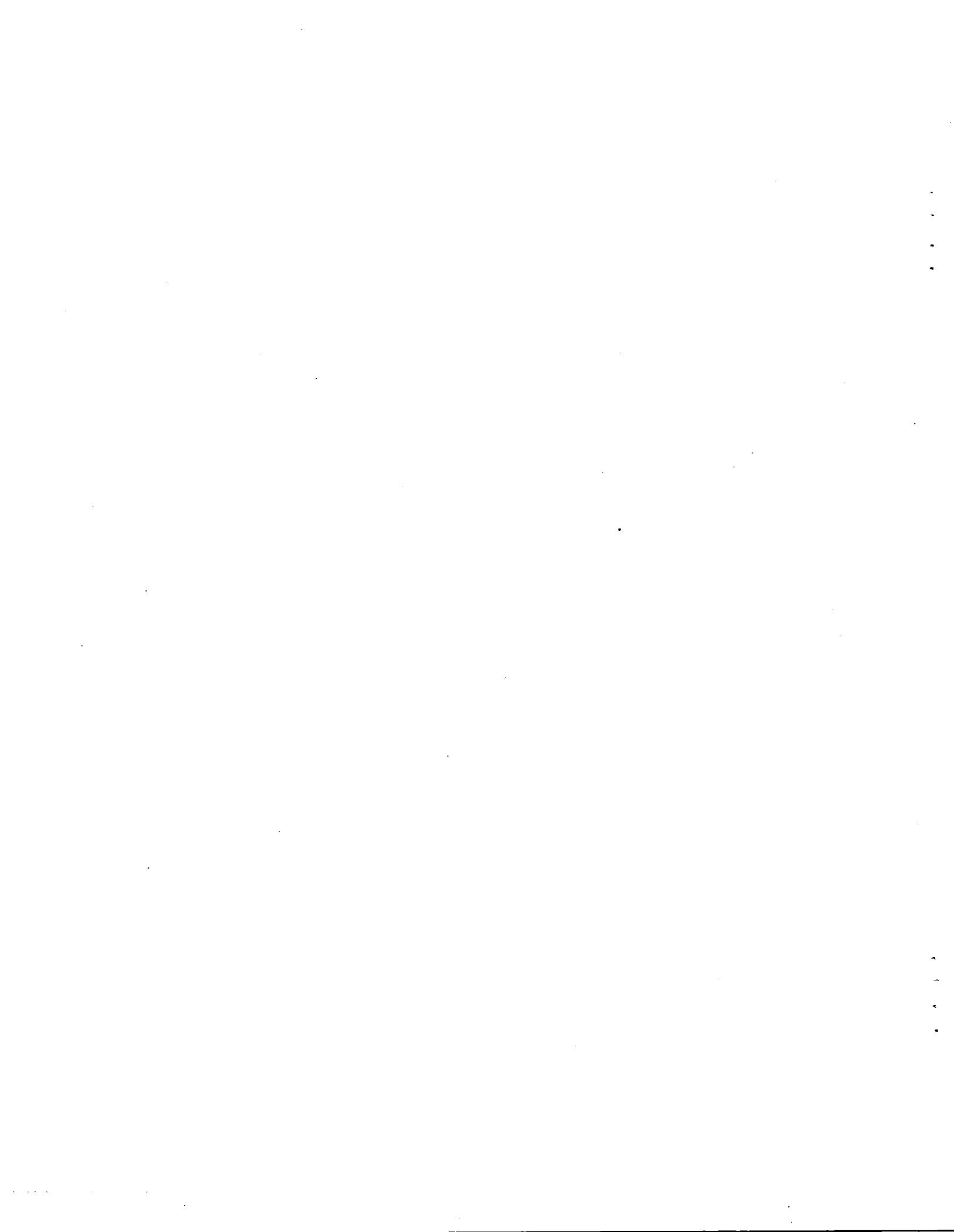
Fan Inlet Duct Treatment

Three possibilities were developed for absorbing forward-propagating sound generated by the fan, before such sound reaches the second corner turning vanes. These concepts are sketched in Table 4, and are also shown in Figures 45 and 47.

The first was a non-intrusive wall liner in which the present surfaces would be replaced with a perforated metal surface which is backed up by an acoustic layer 0.4 - 0.6 m deep. Such a liner would be installed from the fan rotor plane forward to the corner on all surfaces. In the frequency range of interest, the primary acoustic benefit comes from "random incidence" effects, since the surfaces are too far apart to provide significant plane wave attenuation. However, this effect should reduce fan-generated noise by about 10 dB; aerodynamic losses would be minimal.

Adding a treated nose cone (non-rotating) to the wall treatment provides a considerable improvement in the low frequency insertion loss while maintaining the random incidence benefits at high frequencies. Such a nose cone is also desirable from an aerodynamic standpoint since a redistribution of inflow to the fan is needed to reduce the loading and eliminate stall (see Sec. 3). For a given length of nose cone, the exact contours of the nose cone could be dictated by aerodynamic considerations without substantial effect on the acoustic performance, as long as the approximate diameter was maintained.

A further (and more dramatic) improvement is achieved by adding a treated, streamlined annular ring between the nose cone and the wall. The predicted effect of this combined treatment would be to reduce the upstream-propagating fan noise contribution to the test section to the desired goal (recall that the first and second corner vanes may also require treatment between

117

TABLE 4 . TREATMENT SUMMARY

Concept: ___Upstream Fan Duct Liners___

Section of Tunnel Treated: ___2nd corner to rotor___

Approximate Length of Treatment (m): ___(a)16.5(55ft); (b)12(40ft); (c)12(40ft)___

Surface Area (m^2): (a)734(8000ft^2); (b)800; (c)100 (incl a & b)

Typical Depth (m): ___0.4-0.6 (sidewall and nose cone); 0.2-0.4 splitter___

Sketch of Typical Section of Treatment
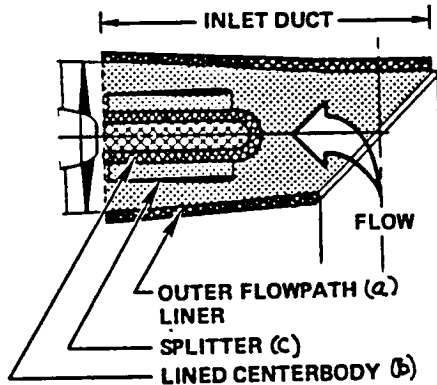
Scheme (1) wall treatment only (a)
Scheme (2) (1) + centerbody (b)
Scheme (3) (2) + ring (c)

Aerodynamic Performance Effect ($\Delta q/q_o$):
Insertion Loss of Section Treated:

(a) 0^+ (nominal)
(b) .013
(c) .04 (includes (b)).

| | Octave Band Center Frequency (Hz) | | | | | | | |
	125	250	500	1K	2K	4K	8K	FOM
Scheme (1)	11	10*	10*	10*	10*	5-10*	5-10*	.055
Scheme (2)	19	14.3	10	10	10 .	10	10	.066[1]
Scheme (3)	35	35	26	11.5	10	10	10	.107[1]

Will this treatment be bypassed in any way due to propagation anomolies?
o Refraction may cause sound to bend away from duct wall.
o High frequency performance depends on source directivity and cross-mode content in duct.

Will there be deleterious effects of flow on performance?
No. If "no-fuzz" concept is used, optimum liner performance depends on flow velocity.

Other comments:
[1] Extended nose cone (and ring) can be configured to modify flow field entering fan, thereby eliminating stall or near-stall conditions; ring wake deficit could be filled with trailing edge blowing.

the vanes and the test section). This could be achieved with an aerodynamic penalty of $\Delta q_o/q_o \approx 0.04$, neglecting potential off-setting benefits of improved fan performance.

If fan performance improvements are realized, or if other treatments are used upstream for the first corner vane source, the extent of the treated ring and nose cone could be reduced with an accompanying reduction in aerodynamic losses. Alternatively, it might be possible to omit outer wall treatment if other upstream sources of absorption are used in conjunction with controlling vane-generated noise (these other absorbing areas will of course also provide reduction of fan-generated sound).

Fan Exhaust Duct Treatments

A similar set of options is available for treating the downstream-propagating fan noise, although the existing tailcone provides a more favorable baseline for treatment. In Figure 47, a treatment was shown in which the baseline treatment consists of replacing all existing duct, tailcone, and stator surfaces with sound-absorbing areas. Table 5 summarizes the predicted perform-ance for this scheme (Scheme 1). The calculations indicate that treating the existing surfaces will realize about 10 dB of random incidence absorption and some plane wave attenuation at low frequencies. If the stator vanes were not treated, the axial mode attenuation would be reduced by about 6 dB in the 125 Hz band, and 2 dB in the 250 Hz band; also, some of the random incidence benefits might be lost due to the relatively short length of treated duct (i.e., short in terms of duct height). The addition of a streamlined treated ring could enhance the attenuation of downstream-propagating sound as shown in Table 5 (Scheme 2). The ring could also be used to redistribute flow into the fourth diffuser, thus providing some overall benefit to the circuit aerodynamic performance and flow quality. The

TABLE 5. TREATMENT SUMMARY

Concept: <u>Downstream Fan Duct Liner</u>

Section of Tunnel Treated: <u>Fan duct, centerbody & stators</u>

Approximate Length of Treatment (m): <u>23 m (75 ft)</u>

Surface Area (m^2): <u>(a) 1600m^2(approx.; includes stator vanes) (b) 2400 (incl(a))</u>

Typical Depth (m): <u>0.4 - 0.6 m</u>
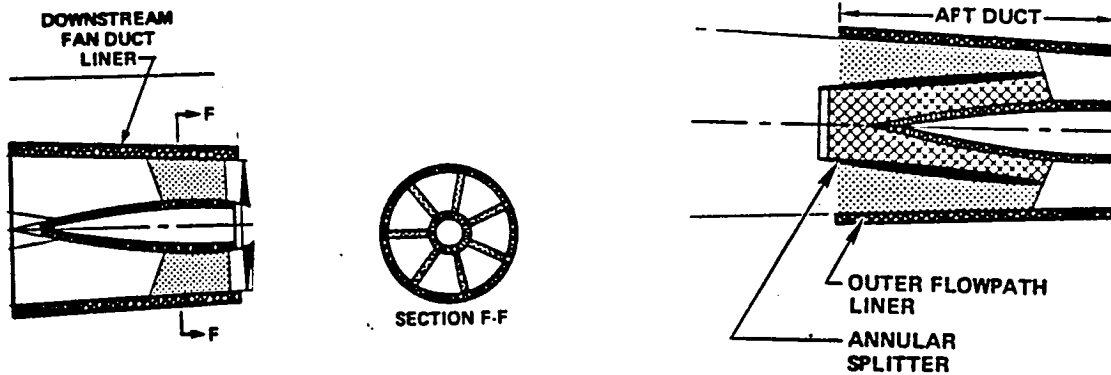
Sketch of Typical Section of Treatment

Scheme 1.   Scheme 2.

(a) nominal (skin friction)

Aerodynamic Performance Effect $(\Delta q/q_o)$:(b) .01 - .015

<u>Insertion Loss of Section Treated</u>:   (<u>Note</u>: local q not well-defined)

Octave Band Center Frequency (Hz)

		125	250	500	1K	2K	4K	8K	FOM
Scheme	1	30	15	10	10*	10*	9-10*	5-10*	.040
Scheme	2	40	30	12	10	10	10	10	.038

Will this treatment be bypassed in any way due to propagation anomolies?

*High frequency performance depends on source directivity and cross-mode content in duct.

Will there be deleterious effects of flow on performance?

No. If "no-fuzz" concept is used, optimum liner performance depends on flow velocity.

Other comments:

Ring could be configured to improve 4th diffuser flow; especially forcing some high speed flow toward walls.

120

estimated losses in test section q caused by this scheme are
0.01-0.015 times the test section q. However, the details of the
flow field in the aft region of the fan should be studied further
to refine this estimate.

Non-Intrusive Liners

The "wetted" surfaces of the flow path can be lined with
sound-absorbing treatment by removing the existing skin, replac-
ing it with a perforated sheet of appropriate open area ratio and
hole configuration, and installing an acoustically-treated cavity
behind the skin between the existing structural members of the
tunnel shell. The exact sequence of this replacement would
depend upon further study of the many tradeoffs between install-
ing the acoustic cavity treatment from the outside or from the
inside.

Figure 46 showed schematically such treatments applied to
the first, second, and fourth diffusers and the second crossleg/
settling chamber. For the purposes of the analysis, these
treated areas have been considered separately, since their
relative effectiveness and cost of treating each part of the
tunnel is expected to vary.

Table 6 summarizes the predicted performance of each treat-
ment showing that the primary benefit is in diffuse field absorp-
tion rather than axial mode attenuation. However, the diffuse
field benefit could be cancelled as a result of "wave-guiding"
effects of turning vanes, which begin to occur at acoustic
wavelengths which are less than twice the chord. Thus, for the
specific geometry of the 4x7 tunnel, the wall treatment may be
bypassed at frequencies above 1 kHz (see Sec. 2).

One should also note that in successive treated lengths of
ductwork, diffuse field "entrance" effects are not always

TABLE 6.   TREATMENT SUMMARY

Concept: Non-Intrusive Liners

Section of Tunnel Treated: 1st diffuser, 2nd diffuser, "big end"

Approximate Length of Treatment (m): (1) :29m;(2) :38m; (3):30m (4) 80m

Surface Area (m²): (1) 1010; (2) 1080; (3) 2200 (4) 2400

Typical Depth (m): 0.4 - 0.6m

Sketch of Typical Section of Treatment
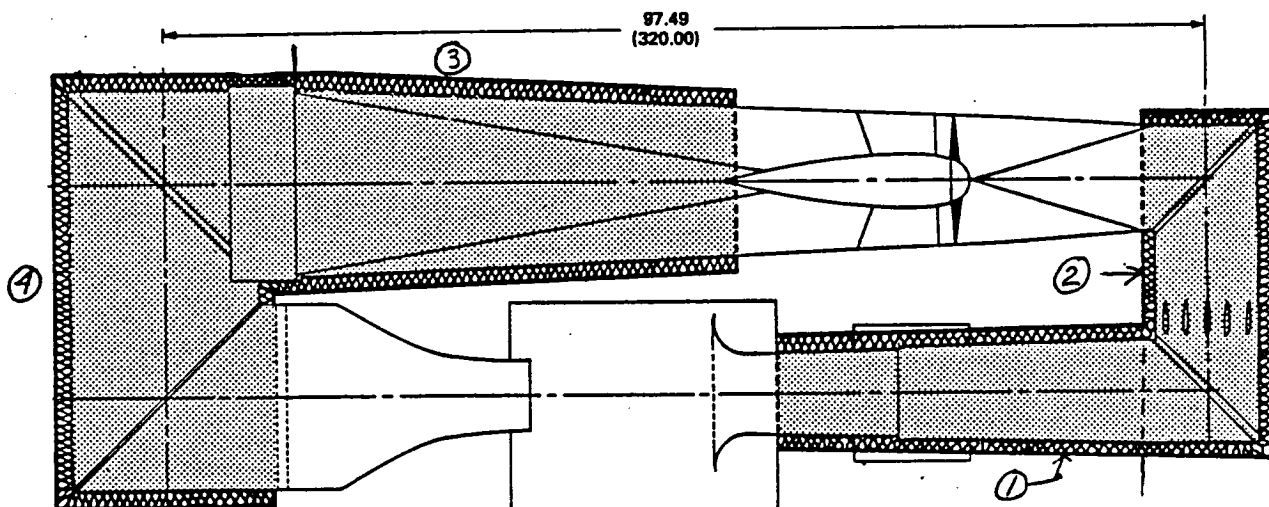
Aerodynamic Performance Effect: Nominal - change in skin friction only.

Insertion Loss of Section Treated:

| | Octave Band Center Frequency (Hz) | | | | | | | |
	125	250	500	1K	2K	4K	8K	FOM
Scheme 1	18	12	10*	5-10*	5-10*	5-10*	5-10*	.047
Scheme 2	14	11.5*	10*	10*	0**	0**	0**	.042
Scheme 3+4	14	11	10*	5*	0-5**	0-5**	0-5**	.008

Will this treatment be bypassed in any way due to propagation anomolies?
**Turning vanes may bypass treatement completely above 1 kHz

Will there be deleterious effects of flow on performance?
1) Refraction may reduce effectiveness of (1) and (2)
2) If "no fuzz" concept is chosen, optimum impedance depends on
   flow velocity.
Other comments:
*1) Diffuse field losses depend on effects of turning vanes and cannot be
    fully taken for adjoining section (i.e., both (1) and (2) include 10 dB
    of random incidence loss, but in practice, one would expect much less
    than 20 dB for sound propagating through both sections).
**2) Assumes treatment will be bypassed by turning vanes.
  3) Treatment of 4th diffuser (upstream of 3rd corner) is very ineffective.

122

realized in an additive sense; this is because the first section of treated ductwork absorbs many of the crossmodes leaving only quasi-axial and axial modes propagating toward the next section.

Simple Splitters (Baffles) Used in Conjunction with Treated Walls

The wall treatment described above can often be made more effective by the addition of simple splitters as shown in Fig. 48. Such splitters double the effective length of treated duct (in terms of duct widths) and move the ratio of duct width-to-wavelength to a more favorable value in terms of attenuation per unit length of duct (see Ref. 19). Table 7 shows calculated performance for such splitters located in various parts of the circuit. As can be seen from the table, these single splitters do not improve the low frequency performance except in the first diffuser and are also vulnerable to being bypassed by high frequency sound "guided" by turning vanes. Losses of test section q caused by a splitter in the first diffuser are estimated to be approximately 1.5-2% of the nominal q; however, one could expect that the splitter could be used to improve the distribution of flow at the end of the diffuser, thus lessening the overall impact on the circuit performance.

Cruciform Splitter

An extension of the splitter concept was considered. This scheme involved the formation of a cruciform splitter such as shown in Figure 49 and Table 8. Such a splitter may increase low frequency performance but does not provide substantial improvement in attenuation of high frequency axial modes.

123

TABLE 7 TREATMENT SUMMARY

Concept: <u>Simple splitters in combination with wall treatment</u>

Section of Tunnel Treated: <u>(1) 1st diff; (2) 2nd diff; (3) 4th diff.(4) sell chbr</u>

Approximate Length of Treatment (m): Splitter only (1) 30; (2) 12; (3) 30; (4) 18

Surface Area (m^2): <u>Splitter & walls: (1) 1700 (2) 1400; (3) 3020 (4)3500</u>

Typical Depth (m): <u>1-2m</u>

Sketch of Typical Section of Treatment
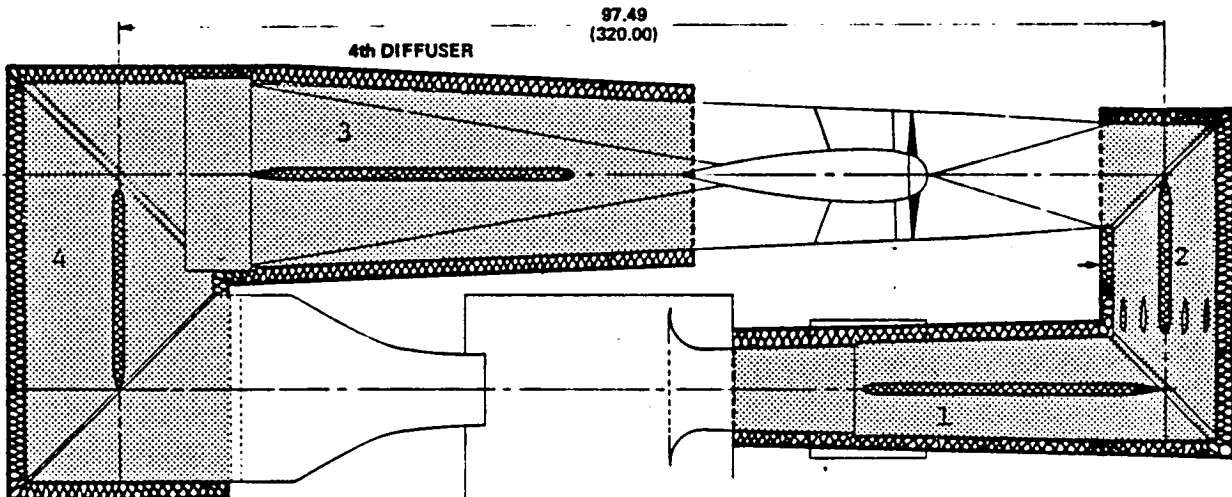
Aerodynamic Performance Effect ($\Delta q/q_o$):
<u>Insertion Loss of Section Treated</u>:

(1)	.020
(2)	.019
(3,4)	0^+ (Nominal)

Octave Band Center Frequency (Hz)

	125	250	500	1K	2K	4K	8K	FOM
Scheme 1	38	17	5-10*	5-10*	5-10*	5-10*	5-10*	.040
Scheme 2	16	12	11	5-10*	0**	0**	0**	.033
Scheme 3+4	18	14	11	5*	0**	0**	0**	.007

Will this treatment be bypassed in any way due to propagation anomolies?
**Turning vanes may bypass treatment completely above 1 kHz

Will there be deleterious effects of flow on performance?
1) Refraction may reduct effectiveness of 1 and 2.
2) If "no-fuzz" concept is chosen, optimum impedance depends on
   flow velocity.

Other comments:
*1) Diffuse field losses depend on effects of turning vanes and cannot be
   fully taken for adjoining section (i.e., both (1) and (2) include 10 dB
   of random incidence loss, but in practice, one would expect much less
   than 20 dB for sound propagating through both sections).
**2) Assumes treatment will be bypassed by turning vanes.
 3) Treatment of 4th diffuser (upstream of 3rd corner) is very <u>ineffective</u>.

124

TABLE 8 TREATMENT SUMMARY

Concept: ___Cruciform Splitter___

Section of Tunnel Treated: ___1st diffuser___

Approximate Length of Treatment (m): ___30m___

Surface Area (m^2): ___1600 m^2___

Typical Depth (m): ___1.-1.5m___

Sketch of Typical Section of Treatment

SEC A-A
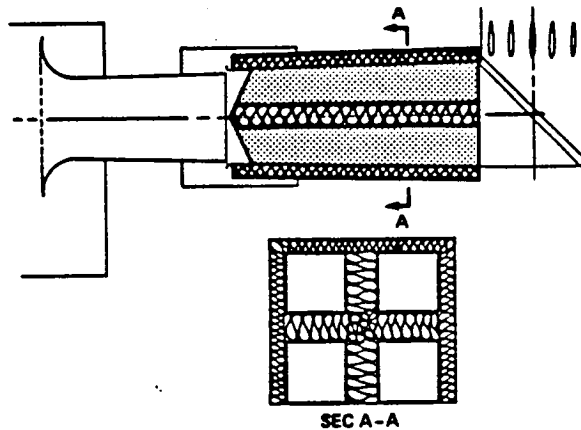
Aerodynamic Performance Effect($\Delta q'/q_o$): .02-.03 (depends on overall effect on diffuser

Insertion Loss of Section Treated:

		Octave Band Center Frequency (Hz)							
		125	250	500	1K	2K	4K	8K	FOM
Scheme	1	35-40	12	5-10*	5-10*	5-10*	5-10*	5-10*	.041

Will this treatment be bypassed in any way due to propagation anomolies?
Refraction may affect attenuation adversely.

Will there be deleterious effects of flow on performance?
If "no-fuzz" concept is used, optimum impedance is a function of flow velocity.

*Other comments:
1) Cruciform in first diffuser will cause aerodynamic losses but could be used to help redistribute flow entering first corner.
2) Diffuse field effects depend on details of sound field entering treated section.

125

Parallel Baffle Silencers

Parallel baffle silencers were analyzed for possible placement in the first, second and fourth diffusers, as shown in Fig. 50. Table 9 summarizes the expected performance of these "silencers", again showing good low frequency performance but with potential deficiencies at high frequencies.

These silencers will produce significant losses in the first diffusers ($\Delta q_o/q_o \approx 0.1 - 0.15$). In the second diffuser, the losses could be minimized (relative to the present case) if the baffles were integrated into the present flow deflectors (note that greater length would be required than presently exists with the deflectors).

In the fourth diffuser, the silencers create less pressure drop, but the physical dimensions of the treatment become very large. However, relatively few acoustically-efficient options are available for treating the downstream-propagating sound, so the baffles in the fourth diffuser may ultimately represent the most reasonable choice.

Treated Turning Vanes

Turning vanes were analyzed in the same way as the parallel baffle silencers except that full "credit" for diffuse field entry effects was taken. For the first, second, and third corner vanes, the geometry proposed in Fig. 52 would be appropriate. The configuration shown arises from four interlocking considerations:

(1) a minimum thickness is required to achieve attenuation at the lowest frequency of interest;

(2) a minimum length is required to achieve the low frequency attenuation;

126

TABLE 9   TREATMENT SUMMARY

Concept: __Parallel Baffle Silencers__

Section of Tunnel Treated: <u>1st or 2nd diffuser (1) and (2)
4th diffuser (3)</u>

Approximate Length of Treatment (m): <u>(1) 30; (2) 20:. (3) 20</u>

Surface Area (m^2): <u>(1) 2060; (2) 1650; (3) 4770</u>

Typical Depth (m): <u>1(a) or 2(a) 0.50;.1(b) or 2(b) 0.57; (3) .57</u>

Sketch of Typical Section of Treatment
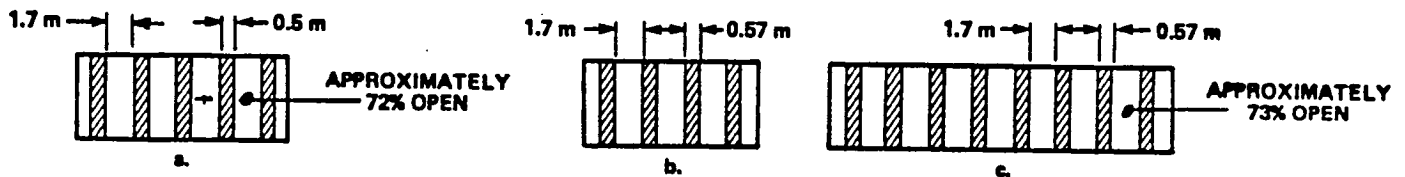
Note: Schemes (a) and (b) are applicable to first and second diffusers
      Scheme (c) is applicable to fourth diffuser

Aerodynamic Performance Effect ($\Delta q/q_0$):
(a) .1-.15 (first diffuser)
(b) .04-.06 (second diffuser)
(c) .02   (fourth diffuser)

Insertion Loss of Section Treated:

Octave Band Center Frequency (Hz)

	125	250	500	1K	2K	4K	8K	FOM
Scheme 1	35	40-50	10	5-10*	3-10*	0-10*	0-10*	.047
Scheme 2	35	38-40	10-12	0-10*	0-10*	0-10*	0-10*	.055
Scheme 3	35	45±	10-12	5-10*	0-10*	0-10*	0-10*	.02

Will this treatment be bypassed in any way due to propagation anomolies?
No, but random incidence (diffuse field) correction will depend on
characteristics of. sound field entering silencer.

Will there be deleterious effects of flow on performance?
1) Some refraction may occur
2) If "no-fuzz" detail is used, optimum impedance will be a function of
   flow velocity.
Other comments: 3) High frequency self-noise may result from high speed regions.

*(1) Random incidence (diffuse field) attenuation "credit" depends on
     details of sound field entering diffuser.

(3) aerodynamic losses can be minimized if a constant cross-
    sectional area is maintained through the vane stage and
    if appropriate leading and trailing edge extensions are
    provided; .

(4) for a given vane configuration the optimum pitch is
    between 0.2 and 0.4 times the chord length (this happens
    to be desirable range of spacing from the acoustical
    point of view). The vanes would be either filled with
    bulk absorber material (see Fig. 53) or an acoustically-
    equivalent construction, or could be of the "no-fuzz"
    design (Fig. 54).

Table 10 shows the predicted performance, which has its
maximum attenuation in the 250 Hz range. Estimated test section
q losses from treating the first corner are in the 1-2% range.
Lower losses would be expected at other corners. One benefit of
the acoustically-treated turning vanes is that they absorb
incident sound rather than guiding such sound around the corner;
therefore, their acoustic benefits are additive around the cir-
cuit. Furthermore, when applied at the first and fourth corners,
treated vanes will minimize reflections of sound generated in the
test section by the models, thereby reducing one potential
measurement problem. Also, as mentioned in Sec. 4.2, the vane
stage as depicted in Figure 52 and Table 10 is likely to produce
less aerodynamically-generated noise than the current configura-
tion, and thus may provide the double benefit of absorbing fan-
generated sound and reducing a significant source of sound in the
circuit. Prior to counting on such a double benefit, model tests
should be conducted to confirm both the source levels and the
absorption performances.

TABLE 10   TREATMENT SUMMARY

Concept: __Acoustically-Treated Turning Vanes__

Section of Tunnel Treated: ___Corners___

Approximate Length of Treatment (m): __4-5m (1st, 2nd, 3rd cor.); 1.2-1.5m (4th cor.)__

Surface Area (m^2): __Typ~800 - 1st & 2nd corners; 4900 - 3rd; 3600 - 4th__

Typical Depth (m): __.5 m at maximum thickness point ≠ 1st-3rd cor.; .15 - 4th cor.__

Sketch of Typical Section of Treatment ·

AIRFOIL-SHAPED VANES:
- Chord ≈ 5 m
- Maximum Thickness ~ 0.4 — 0.6 m
- Number of Vanes Dictated by Best Aerodynamic Performance (p/c ≈ 0.2)
- Perforated Facings Both Sides; Variable Geometry Cavities Inside, With Absorption as Needed; or Bulk Absorber.

OUTSIDE WALL LINER (TYPICAL DEPTH 0.6 m)

FLOW

INSIDE WALL LINER (0.4 — 0.6 m DEPTH TYPICAL)
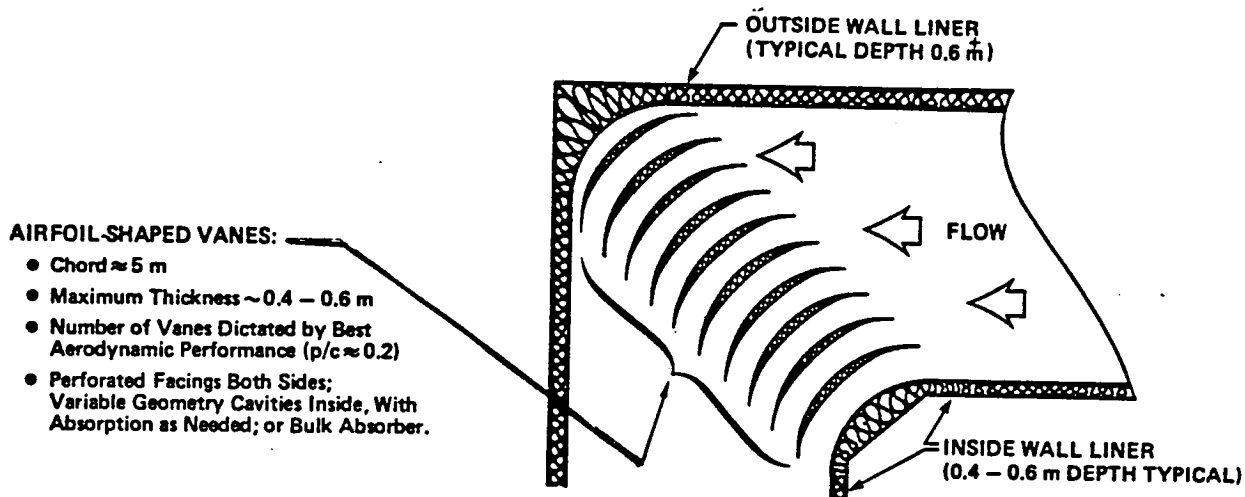
Aerodynamic Performance Effect ($\Delta q/q_o$):   1st & 2nd Corner: 0.015
                                                    3rd & 4th Corner: negligible

Insertion Loss of Section Treated:

Octave Band Center Frequency (Hz)

	125	250	500	1K	2K	4K	8K	FOM
One Corner	8	12	10	10	10	5-10	5-10	.0496
Two Corners	16	24	20	20	20	10-20	10-20	.0496

(Note: Frequency of peak absorption can be adjusted by changing geometry.)

Will this treatment be bypassed in any way due to propagation anomolies?
 Probably not, except at very high frequencies where refraction effects
 may become important.

Will there be deleterious effects of flow on performance?
 If "no-fuzz" design is used, optimum impedance is a function of
 flow velocity.

Other comments: (1) Inside (concave) surface may be subject to contamination but
 treating this surface is important to achieving acoustic performance.
 (2) Use of this concept could eliminate turning vanes as a noise source since
 fewer vanes will be used, rounded leading edge and long chord reduces
 response to inflow turbulence and trailing edge sources will be low
 frequency.

129

4.5 Comparison of Performance and Cost of Various Treatment Combinations

4.5.1 Summary of requirements and treatment performance

The foregoing sections have provided the basis for devising alternative schemes for achieving the reduction in noise control required in the test section of the 4x7m wind tunnel. The analysis is summarized in Tables 11 and 12 below. Table 11 deals with requirements and techniques for reducing upstream-propagating sound from the fan and first corner turning vanes. Table 12 deals with requirements and techniques for reducing sound propagating downstream from the fan to the test section.

In both tables, two sets of figures are provided for the noise reduction requirements. The **first figure** in each set (in **bold** type) is the noise reduction (insertion loss) required between the source and the test section centerline (in-flow) location to achieve NASA's background noise goal; recall that although the test section surfaces must be fitted with anechoic treatment to make the space suitable for discrete frequency measurements, no substantial reduction of the centerline in-flow background noise levels are expected due to the proximity of the nozzle and collector openings. The out-of-flow locations are assumed to be as close to the treated walls as possible; as such, these positions will receive full benefit of nozzle and collector directivity effects in a free field and therefore are estimated to be typically 10 dB below the centerline levels.

The "REQUIRED" insertion loss portions of Tables 11 and 12 show the strong effect of unstalling the fan and of reducing its speed. The advantages of the fan improvements are that they can simultaneously achieve noise reduction and cut power requirements, without adversely impacting the circuit aerodynamics. The fan can be unstalled without reblading, although an adjustment in the

130

TABLE 11. COMPARISON OF TREATMENT PERFORMANCE VS REQUIREMENTS.

	Insertion Loss in Octave Band						Impact on Test Section q
	Octave Band Center Frequency (Hz)						Net $\Delta q_o/q_o$
Upstream – Propagating Sound	125	250	500	1K	2K	4K	
I. REQUIRED (C_L IN-FLOW/SIDELINE OUT OF FLOW – ANECHOIC) A. Fan-to-Test Section (T.S.)							
1. Nominal Speed (N_o)	39/29	38/28	28/18	19/9	10/0	4/0	–
2. Unstalled at N_o	31/21	30/20	19/9	12/2	5/0	0/0	0*
3. Unstalled at 0.75 N_o	23/13	21/11	13/3	5/0	0/0	0/0	0*
4. Unstalled at 0.50 N_o	11/1	10/0	10/0	0/0	0/0	0/0	0*
B. 1st Corner Turning Vanes-to-Test Section	22/12	18/8	13/3	10/0	3/0	0/0	–
II. PREDICTED FOR CONCEPT LISTED: A. Fan Duct Liner							
1. Treated Walls Only	10	10	10	10	10	10	0[+]
2. Walls + Nose Cone	19	14	10	10	10	10	0.013
3. (2) + Ring	35	35	26	12	10	10	0.04
B. 1st Diffuser							
1. Lined Flow Path	18	12	10	5-10**[†]	5-10**[†]	5-10**[†]	0[+]
2. (B.1) + Splitter	38	17	5-10**	5-10**[†]	5-10**[†]	5-10**[†]	0.018-0.020
C. Cruciform in 1st Diffuser	38	12	5-10**	5-10**[†]	5-10**[†]	5-10**[†]	0.02-0.03
D. 2nd Diffuser							
1. Lined	14	11	10	0-5[†]	0[†]	0[†]	0[+]
2. (1) + Splitter	18	16	12	0-5[†]	0[†]	0[†]	0.019
E. 1st or 2nd Corner Vanes	8	12	10	10	10	10	0.015
F. 1st and 2nd Corner Vanes	16	24	20	20	20	20	0.03
G. Parallel Baffles-1st Diff.	35	40	10-12**	5-10**	0-10**	0-10**	0.10-0.15
H. Parallel Baffles-2nd Diff.	35	40	10-12**	5-10**	0-10**	0-10**	0.04-0.05

* Δq for reduced fan speed depends on method used to reduce fan speed.
**Diffuse field attenuation depends upon structure of sound field entering treated section.
[†]Treatment may be bypassed by turning vane waveguiding effect.

131

TABLE 12. COMPARISON OF TREATMENT PERFORMANCE VS REQUIREMENTS.

Downstream – Propagating Sound	Insertion Loss in Octave Band						Impact on Test Section q
	Octave Band Center Frequency (Hz)						Net $\Delta q_0/q_0$
	125	250	500	Test Section 1K	2K	4K	
I. REQUIRED: (c_L IN FLOW/SIDELINE OUT OF FLOW-ANECHOIC)							
A. Fan-to-Test Section							
1. Nominal Fan Speed (N_0)	37/27	35/25	27/17	17/7	6/0	0/0	–
2. Unstalled at N_0	29/19	27/17	19/9	9/0	0/0	0/0	0*
3. Unstalled at 0.75 N_0	24/14	19/9	11/1	2/0	0/0	0/0	0*
4. Unstalled at 0.50 N_0	12/2	8/0	1/0	0/0	0/0	0/0	0*
B. Turning Vanes	(No I.L. Needed if Fan Source Treated)						
II. PREDICTED FOR CONCEPT LISTED:							
A. Fan Duct Liner							
1. Present Flow Path	30	15	10**	10**	10**	10**	<0.01
2. With Ring Added	40	30	12**	10**	10**	10**	0.01–0.015
B. 4th and 5th Diffuser Lined	14	11	10**	5**	0-5**†	0-5**†	0^+
C. (B) + Baffles in 4th & 5th	18	14	11**	5**	0-5**†	0-5**†	0^+
D. 3rd or 4th Corner Vanes Lined	8	12	10	10	10	10	0^+
E. 3rd and 4th Corner Vanes Lined	16	24	20	20	20	20	0^+
F. Parallel Baffles-4th Diff.	35	45	11	5-10**	0-10**†	0-10**†	0.02

*Δq for reduced fan speed depends on method used to reduce fan speed.
**Diffuse field attenuation depends upon structure of sound field entering treated section.
†Treatment may be bypassed by turning vane waveguiding effect.

collective pitch setting may be required (by a minor rework of the blade root attachment region). However, to achieve 25-to-50% reductions in tip speed while maintaining the same volume flow through the test section, new blades will be required. The practical extent to which the rotor blade chord length can be increased in the present fan system may be governed by motor torque limitations and the ability of the foundations and shaft supports to carry a larger overhung mass. If a fixed nose cone is included as we have recommended, a new shaft support bearing could be included as part of the nose cone apparatus, thus relaxing the requirements on the present fan drive system bearings and structural supports.

Part B of the "REQUIRED" sections of Tables 11 and 12 deals with turning vane noise reduction requirements. For upstream-propagating noise (Table 11) the first corner vanes represent a source which must be treated either at the source or in the first diffuser. The sound levels produced by the second corner vanes are predicted to be below that of the first corner vanes; there-fore, the treatment of the upstream propagating sound from the first corner vanes will also be sufficient to alleviate contributions from the second corner vanes. Downstream-propagating sound from both sets of turning vanes will be fully absorbed by fan treatment, unless the fan is redesigned to allow unstalled operation at 50% of the present speed, in which case provision for absorption of turning vane noise would be required.

The second parts (II) of Tables 11 and 12 summarize the estimated insertion loss for each of the treatment concepts developed above; also shown is the estimated total relative reduction in test section dynamic pressure caused by the treatment.

From these tables, and the source-path diagnosis presented in Sec. 3, one can devise combinations of treatments which will provide the necessary reduction of background noise in the test section. Note that in such an analysis, one must account for the multiplicity of source/path combinations contributing to the test section background levels; i.e., if in a given location, the contributions of several sources/path combinations are predicted to be equal, then additional source reduction or treatment insertion loss will be required.

4.5.2 Feasible Combinations of Treatments

The treatments devised above may be combined in various ways to see which combinations will produce the desired background noise in the test section. The final selection of treatment combinations which are feasible depends upon which fan source noise spectra are assumed (and thus upon the extent of fan re-design or stall alleviation), and whether or not the in-flow background noise criterion can be relaxed (since sideline out-of-flow levels are predicted to be 10 dB lower than on the tunnel centerline). For the present purposes, we will assume that the fan will operate either in its current (stalled) condition (levels given on line I.A. 1 in Tables 11 and 12) or in an unstalled condition but retaining the present blades and hub and thus the present ratio of fan tip speed to test section velocity (levels given on line I.A. 2 in Tables 11 and 12); we will also assume that the background noise requirement cannot be relaxed. If some other assumptions are made, Tables 11 and 12 provide all the necessary information with which to explore the consequences of such assumptions.

Treatments to Control Upstream-Propagating Noise

Two primary sources must be controlled in the path between the fan and the test section:

- fan system
- first corner turning vanes.

In any treatment scheme, the noise from the first corner turning vanes must be controlled or eliminated, which will also provide attenuation of fan-generated noise. The residual amount of insertion loss required for fan noise must then be achieved somewhere in the path between the fan and the test section.

If the present first corner vanes are retained, none of the treatments proposed for the first diffuser (e.g., treatments B.1; B.2; C; or G in Tables 11 and 12) adequately deals with the predicted noise of the vanes in the mid-frequency range (500 Hz band), although parallel baffles (treatment G) provide nearly enough attenuation and could perhaps be modified slightly to provide more attenuation in that band. Even if parallel baffles were used in the first diffuser, careful examination of Table 11 shows that at least two or three other (substantial) treatments would be required to alleviate all the residual noise from the stalled fan in the mid-frequency range; also excessive low frequency attenuation is provided. Of the candidates for these additional treatments, treated turning vanes provide the most attenuation in the 500 Hz and 1 kHz bands. Therefore, since we expect that use of long-chord airfoil shaped vanes will substantially eliminate turning vane noise as an important source (at least for the sideline out-of-flow microphone positions), it is logical to establish a treated first corner vane set as the baseline treatment for upstream-propagating sound.

With the first corner vanes treated, several options exist for achieving the additional attenuation required:

Option 1: Treat the second corner vane set, the second diffuser walls and add a splitter in the second diffuser (i.e., Treatments F and D.2 in Tables 11 and 12);

Option 2: Treat the second corner vanes, add a fan duct liner and an acoustically treated nose cone (Treatments F and A.2 in Tables 11 and 12);

Option 3: Treat the second corner vanes, treat the first diffuser walls and add a splitter (Treatments F and B.2);

Option 4: Apply the full fan inlet treatment (Treatment A.3; no second corner treatment required);

Option 5: Treat the second corner vanes and add parallel baffle silencers to either the first or second diffusers (Treatment F plus either G or H).

Note that Options 2 and 4 should also be able to reduce or eliminate fan stall if aerodynamic considerations are integrated into the design; therefore, selection of these options could provide a multiple benefit, both acoustically and aerodynamically. If the predicted benefit of stall elimination (i.e., 8+dB reduction in fan noise) is realized, then the extent of the treatments could be reduced somewhat (most notably, the fan duct wall liner could probably be eliminated, thus mitigating the need to cut into that part of the tunnel shell).

In reviewing the Figure-of-Merit (FOM) calculations shown in Tables 4-10, Option 4 is clearly the most cost-effective, followed by Option 2, then by Options 3 and 1 in that order; Option 5 is clearly the least cost-effective and also involves the greatest aerodynamic penalty. Therefore, the recommended

136

approaches to treating upstream-propagating noise are:

(1) Replace first corner vanes with long-chord acoustically-treated vanes;

(2) Provide for a fan inlet duct with a long treated nose cone and a treated splitter ring, and possibly a full complement of duct wall treatment.

Alternatives to Part 2 of the above recommendation include Options 2 or 3 above in that order.

Treatment of Downstream-Propagating Fan Noise

In order to control background noise arriving in the test section through the nozzle, noise associated with fan sources must be controlled along the downstream path between the fan and the test section. If the baseline (stalled) fan or an unstalled fan operating at the nominal speed (N_o) is used, treatment of fan noise will also adequately control noise from other sources upstream of the fan which would otherwise contribute to background levels via the downstream path(s).

As was done for the upstream-propagating sound, we will assume that the fan is operating in its present stalled condition and that the background noise criterion is rigorously applied on the tunnel centerline. Thus, the required insertion loss is given by the bold figures in line I.A.1 of Table 12.

Examination of treatment options listed in Table 12 reveals a lack of treatments with effective mid-frequency performance, and those which have reasonable noise reduction potential in the mid-frequency range are susceptible to being bypassed as a result of the waveguiding effects of the third and fourth corner turning vanes. Although the third and fourth corner turning vanes are

137

not considered to be significant noise sources, they must be treated to avoid the effects of waveguiding. We thus again establish <u>treated turning vanes</u> as the <u>baseline treatment</u> for downstream-propagating sound.

The only treatments which are effective in combination with one or two sets of treated turning vanes are:

o parallel baffles in the fourth diffuser (Treatment F in Table 12); or

o lining of the aft fan duct, tail cone, and the addition of a treated annular ring between the wall and the fan tail cone (Treatment A.2 in Table 12).

Note that parallel baffles cannot be considered for the fifth diffuser (i.e., second crossleg) since there·is insufficient length available along the inside part of that section.

In analyzing the effectiveness of the above treatments in combination with one or two stages of treated turning vanes, it is evident that the low frequency requirement can be "overkilled", but that insufficient attenuation of the sound in the 500 Hz band is achieved with a single vane stage. Thus, if the baseline assumptions are used, two stages of treated vanes will be needed in conjunction with one of the other two candidate treatments. Reviewing the Figure-of-Merit (FOM) calculations in Tables 4-10 reveals that the fan-duct treatment would be a somewhat more efficient treatment. Note that the fourth corner vanes can be made with a smaller chord reduced thickness (relative to the third corner), and trailing edge extensions to minimize effects on test section flow quality. The effect of such changes would

be to increase the frequency at which peak attenuation occurs, which is beneficial in this case.

Note that if the <u>upstream</u> treatment included means to eliminate fan stall (such as the nose cone) or if the blades were re-set to accomplish the same result, then the insertion loss requirements would be those given on line I.A.2 of Table 12, and only one set of turning vanes would be required. if this were the case, we would recommend treatment of fourth corner vanes to eliminate reflections of noise generated by test objects. It is also recommended that the wetted surface of the outer wall of the second crossleg be treated with a flat treatment to reduce reflection of low frequency sound generated by test objects and to provide some reduction of reverberant buildup from the fan sources. Such treatment would also reduce the requirements on the treatment concept selected for controlling fan-generated noise; e.g., stator vanes might not need treatment; length of treated ring could be reduced; or length of parallel baffles could be reduced.

Therefore, the treatment recommendations for controlling downstream-propagating noise from the fan are as follows:

o **Baseline Treatment:**

   (A) Treated fourth corner vanes (1.5-2 m chord)

   (B) Flat wall treatment on second crossleg

o **Complementary Treatments:**

   Option 1: Full fan duct treatment (A.2)

   Option 2: Parallel baffle silencers (F).

If the fan was operated in an unstalled condiiton at the nominal speed (N_o), the treatment requirements would become:

139

o **Baseline Treatment:**

   (A) Treated fourth corner vanes (1.5-2 m chord)

o **Complementary Treatment:**

   Option 1: Treated third corner vanes (long chord) plus full treatment of second crossleg (lined surfaces plus single baffle; Treatment C)

   Option 2: Treated fan duct flow path (Treatment A.1 in Table 12).

Note that these options as listed in the table do not always provide all the insertion loss indicated as required in all bands, but the concepts selected can be fine-tuned in the final design stages to alter their performance slightly.

4.5.3 Preliminary cost estimates for treatments

The range of expected costs of fabricating and installing the treatments described above have been estimated through use of industry "rules-of-thumb". The final costs will depend upon the extent of structural re-work required to accomodate treatments such as long-chord treated turning vanes, non-intrusive liners and fan duct treatments. Therefore, the "high end" of the range quoted to us by manufacturers and installers has been used to provide some allowance for the structural re-work; however, such cost estimates must be revised after detailed design studies have been made. The available cost data is considered to be sufficiently reliable to allow comparisons of treatment options and to develop an order-of-magnitude estimate for the total cost of the 4x7 m tunnel noise control project.

140

Unit Costs:

The approximate unit costs of <u>installed</u> treatments of the
types described above are as follows:

o Test Section Anechoic Treatment, with suitable
   protection from flow, 100 Hz cutoff $400/m^2

o Flat Wall Treatment (bulk-absorber type) $100-200/m^2

o Splitters and Parallel Baffle Silencers $250-300/m^2

o Treated Turning Vanes $350-400/m^2

Note that the area referenced is the total "wetted" surface area
of the treatment, except in the case of the anechoic wedges for
which the reference area is that of the untreated wall.

Costs of various treatment concepts

The above unit costs can be combined with the surface area
estimates shown in Tables 4-10 to develop estimates for costs of
various treatment combinations. Note that by use of Figures-of-
Merit in selecting among various treatment options, the rough
cost ranking has already been partially factored into the
development of the options recommended in Section 5.4.2.

For the purpose of summarizing the relative costs of various
treatment combinations, the above unit cost figures have been
combined with the appropriate surface areas to provide the data
shown in Table 13. From this table, the range of baseline treat-
ment costs is seen to be $3.75M-$4.2M. We believe, at this stage
of analysis of the project, that a 33% contingency is advisable,
bringing the range of estimated costs to around $5-5.5M for
treatment concepts which do not involve re-work of the fan blades
and hub.

141

TABLE 13: COSTS OF TREATMENT OPTIONS

Treatment	Range of Costs
(1) Baseline Treatment of Test Section...	$1000K

(2) Treatments for Upstream Paths (see Sec. 4.5.2 for key):

    Option (1).........$ 940K
    Option (2).........$ 900K.....Recommendation #2 ⎫
    Option (3).........$ 920K   ⎬ $750-900K
    Option (4).........$ 750K.....Recommendation #1 ⎭
    Option (5).........$1300K

(3) Treatments for Downstream Paths (see Sec. 4.5.2 for key):

Stalled Fan:

    Option (1): (Baseline (A) + (B) + Compl. Option 1)...$2300K (Rec.)... $2300K
    Option (2): (Baseline (A) + (B) + Compl. Option 2)...$3100K

Unstalled Fan:

    Option (1): (Baseline (A) + Compl. Option 1)...$4700K
    Option (2): (Baseline (A) + Compl. Option 2)...$2000K (Rec.)........ $2000K

Note: No provision for preliminary engineering or structural re-work included.

4.6 Summary of Noise Reduction Concepts and Options

The analyses in Sections 4.1-4.5 of this report have shown the following:

(1) Fan stall elimination is highly desirable to reduce circuit background noise, and may provide additional benefits in flow quality and operating costs; stall reduction can probably be achieved without altering fan blades or the fan hub.

(2) Fan speed reduction is a powerful means of reducing circuit background noise, and should improve operating efficiency since the new blading required to achieve significant tip speed reductions can be tailored to the existing inflow.

(3) Several feasible concepts exist for attenuating fan-generated noise in the circuit, but the relative effectiveness varies widely; concepts which treat the areas immediately upstream and downstream of the fan are most effective, but must be augmented with long-chord treated turning vanes in the upstream path since turning vane self-noise and "wave-guiding" are viewed as significant problems.

(4) Sound transmitted through the "downstream" paths is by far the most expensive to control, due to the large cross-sectional areas and large amounts of surface area to be treated; significant reduction in the cost of treatment for the downstream leg will require fan source reductions through reduced speed.

(5) The estimated cost of treating the circuit with the fan operating in its present stalled condition, and with the in-flow (centerline) background noise criterion as stated by NASA, is between $5M and $5.5M.

As a final tradeoff exercise, it is interesting to explore the impact of redesigning the fan such that it could be operated

unstalled at around 50% of its present speed. The estimated
insertion loss requirements are shown in line I.A.4 of Tables 11
and 12 and are essentially 10-11 dB in bands below 500 Hz, and 0
above 500 Hz. Note that first (and presumably second) corner
turning vane noise must still be treated; therefore, the only
treatment necessary in the upstream paths would be long-chord
treated vanes at the first and second corners. On the downstream
path, non-intrusive treatment of the walls of the second crossleg/
settling chamber would provide enough random incidence loss to
achieve the necessary insertion loss in the downstream direction
(note that reflections of test object noise by fourth corner
vanes could still be a problem). The costs of this option are
summarized below:

o Test Chamber Anechoic Treatment $1000K
o Fan Re-work and Nose Cone $1500K
o 1st and 2nd Corner Vanes $ 640K
o 2nd Crossleg/Settling Chamber Flat Wall Treatment $ 580K

Subtotal $3720K

To this subtotal, one should add the 33% contingency applied to
the earlier estimates, which brings the total estimated cost to
$4.95M; i.e., on the low end of the previously-stated range.
Model studies could show that second corner vane treatment is not
necessary, thus reducing this figure by $425K. The estimate for
the fan re-work was derived from recent vendor quotations for a
similar fan in a closed circuit wind tunnel; however, substantial
changes in the motor are not included.

The latter option outlined above represents a significant
improvement over those which involve reducing noise without
dealing with the fan source for the following reasons:

o Noise control by source reduction involves few aerodynamic
  penalties (and possibly some benefits), low risk of treat-

144

ment degradation, and in this case, probable improvement in power usage.

o Physical disruption of the tunnel circuit is minimized, and installation time is much reduced.

o Treatment maintenance is virtually non-existent.

The fan re-design is certainly within the state-of-the-art and can be carried out with the aid of scale model tests which will provide the inflow details from which optimum blade loading, geometries, and setting angles can be derived.

5. CONCLUSIONS AND RECOMMENDATIONS

5.1 Conclusions

(1) The test chamber acoustic characteristics are unsuitable for discrete frequency measurements and must be improved by the addition of anechoic treatment.

(2) The test section noise background levels exceed those selected as an interim goal by 35-40 dB at low frequencies, and less at high frequencies.

(3) At frequencies below 2 kHz, the in-flow criteria for background noise is well below the range of self-noise levels produced by modern microphones fitted with streamlined nose cones and low-noise supports; therefore, this criterion could be relaxed, or development of low self-noise microphones should be initiated.

(4) Fan broadband noise is the predominant sound source. This noise reaches the test section by both upstream and downstream paths. Below 800 Hz, the downstream path appears to be approximately equal to the upstream path. Above 800 Hz, the upstream path is dominant. Fan noise may be able to be reduced by a redesign of the fan blading to lower speed through increased efficiency and by reducing tip stall noise sources.

(5) Turning vane noise is not dominant, but may present a barrier to reaching the desired levels in the test section. The present prediction is not viewed with a high degree of confidence and steps are needed to refine this estimate.

(6) Auxiliary machinery noise exceeds the interim goal. Noise produced by an oil pump is dominant in several frequency bands.

146

(7) Sources in the test section itself represent the ultimate barrier in reaching the interim goal. The collector noise levels appear to be in the vicinity of the goal. Noise generated by microphone stands and model supports can clearly exceed the goal.

(8) The circuit noise sources are treatable with extensive absorption in the form of various combinations of wall linings, parallel baffles, and treated turning vanes.

(9) The most effective noise reduction concepts are elimination of fan stall; reduced blade loading and reduced tip speed of the fan; treated turning vanes; and use of treated walls, centerbodies and annular splitters in the fan inlet and exhaust ducts.

(10) The major approaches for achieving the necessary background noise reduction are summarized in Table 14.

(11) The manufacturing and installation cost of treatments or fan modifications which achieve the desired background noise level and provide a high-quality acoustic space in the test section is estimated to be between $4.9M and $5.5M. This estimate is subject to a selection of a final approach and follow-up studies of certain options.

5.2 Recommendations

(1) Devise and procure a high quality anechoic treatment for the test section.

(2) Re-examine the question of in-flow acoustic measurements in the context of minimum achievable self-noise levels of microphones as compared with the background noise criterion.

TABLE 14   SUMMARY OF APPROACHES TO BACKGROUND NOISE REDUCTION AND IMPACTS OF EACH

IMPACT ON FACILITY CAPABILITIES AND OPERATIONS

APPROACH*	BACKGROUND NOISE GOAL	FLOW QUALITY PLANNED FLOW QUALITY	MAXIMUM q_0 CURRENT MAXIMUM q_0	RELATIVE INTIAL COST	RELATIVE OPERATING COSTS	MAINTENANCE REQUIRED	DOWNTIME FOR CONVERSION	ADDITIONAL STEPS NEEDED
① Maintain Current Fan; Add Acoustic Treatment to Circuit	Can Meet or Exceed	Possible Minor Degradation (or Minor Improvement	May Reduce by 8–10%	High	Increase $\propto \Delta q/q_0$	Periodic Cleaning of Certain Treatment	Substantial (to Be Determined)	● Model Tests ● Design ● Procurement
② Rebuild Fan	Probably Can't Meet Without Some Treatment in Circuit	Could Improve	Could Increase	Low	Below Current Costs	Probably Below Current Levels	Substantial (to Be Determined)	● Model Tests ● Full Scale Flow Measurements ● Design ● Model Test ● Procurement
③ Rebuild Fan and Add Acoustic Treatment to Circuit	Could Exceed Goals by Large Margin	Could Improve	Could Increase	High to Highest	Below Current Costs	FAN: Less Than Current TREATMENT: Periodic Cleaning	Substantial	① + ②

* All choices assume that suitable anechoic treatment will be installed in test section.

(3)   Improve estimates of key variables which are presently dominating the assumptions regarding the required treatment (first and second corner turning vane noise levels, and random incidence performance of various wall treatments).

(4)   Carry out model tests and analyses to determine extent to which the fan can be re-worked and to quantify the attendant benefit.

(5)   Carry out model studies to validate performance of various treatments and optimize their specification.

(6)   Once the results of (4) and (5) are in-hand, update the specifications of additional noise control treatments.

APPENDIX A

NOISE DATA TAKEN AROUND TUNNEL CIRCUIT
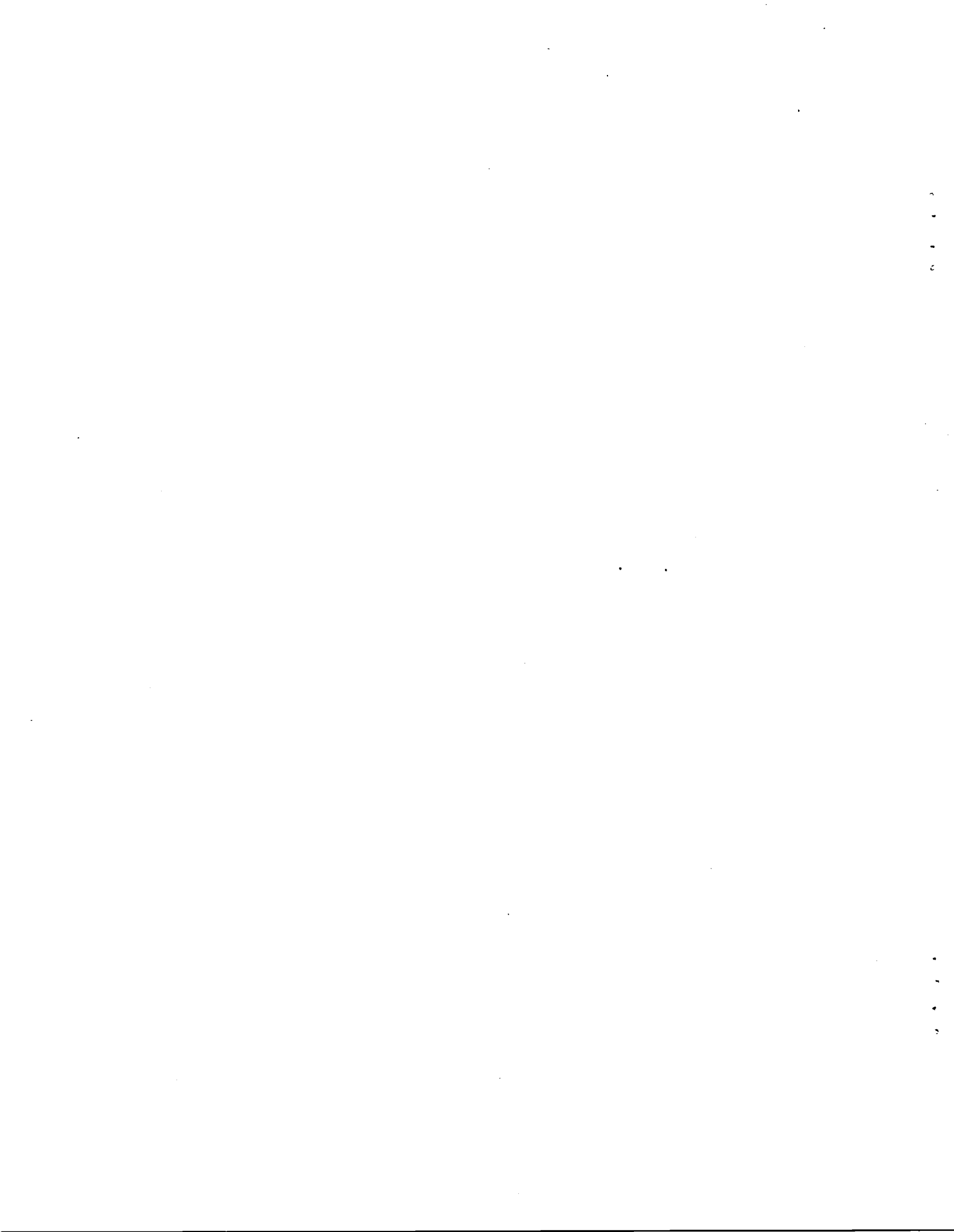
APPENDIX A

NOISE DATA TAKEN AROUND TUNNEL CIRCUIT

This appendix presents a summary of acoustic measurements taken around the tunnel circuit for various operating conditions. The principal conditions summarized are for the case of an empty test section. Data were also taken with a helicopter model operating in the test section. This was done in order to introduce realistic disturbances into the flow, thus allowing assessment of the effects of such disturbances on the source levels of the turning vanes and fan. However, the helicopter selected was uncharacteristically noisy and the data taken around the circuit were thus often "contaminated" with noise from the model.

The microphone locations tested are depicted in Fig. A.1 All microphones were mounted on 6 ft poles, except Microphone 18, which was mounted 20 ft above the floor of the settling chamber. The microphones were 1.27 cm (0.5 inch) condenser microphones filled with bullet shaped nose cones to reduce the susceptibility to extraneous signals being generated by flow-induced pressure fluctuations. Appendix G discusses the flow noise issue in greater detail.

A.1 Ambient and No-Flow Noise Levels

Figures A.2 through A.5 summarize ambient noise levels measured in the circuit under no-flow conditions with and without tunnel-related machinery running. It was observed during the week of testing that several nearby facilities caused increases in the ambient noise level. However, due to conflicting facility schedules, it was not possible to arrange a controlled test in which adjacent facilities were operated while 4 x 7 ambient levels were being measured. This aspect of the background noise issue should be investigated further. In Figs. A.2 through A.5,

a predominant tone occurs in the 315 Hz band, with a harmonic in the 630 Hz band. This tone is associated with the oil pump supplying the fan and motor lubrication.

A.2 Spectra for Each Location For Various Speeds

The tunnel was operated at 20, 40, 60, 80, and 90 knots (test section velocities) in the open jet mode with the new collector mockup in place. Testing at speeds above 90 kts was ruled out due to concerns about the structural integrity of the mockup. Figures A.6 to A.17 summarize the 1/3 octave spectra at each location for the various speeds tested. The spectra are seen to be broadband in nature over the frequency range of interest, except for intrusive tones associated with the oil pump. Note that only limited data are presented for microphone 14 which was located just upstream of the fan. During the tests, the output of this microphone showed characteristics of extreme buffet and attempts to correct the problem by adjustments in the microphone support apparatus were largely unsuccessful. However, from transfer function tests, it is believed that the data at Microphone 9 is representative of that at Microphone position 14.

The test section data contain several narrowband humps in the 1000 to 4000 Hz range (depending upon speed). These peaks were believed to be associated with sound radiation by flow interaction with the in-flow microphone support poles and cables (Microphones 22 and 23). This hypothesis was verified by removing the two in-flow microphones and repeating the tests. With the test stand supports removed, the high frequency narrowband peaks disappeared. The "corrected" spectra" of background noise coming only from the circuit are shown in Figures A.18 through A.22 for 40 and 80 kt test section speed. It is believed that these "corrected spectra" are otherwise representative of the true acoustic pressures at these locations, since estimates of

flow-induced pressures showed such levels to be below the measured levels.

Narrowband analysis of the data in the circuit did not provide any additional insight into sources of background noise or propagation paths. In these analyses, the machinery tones were clearly visible.
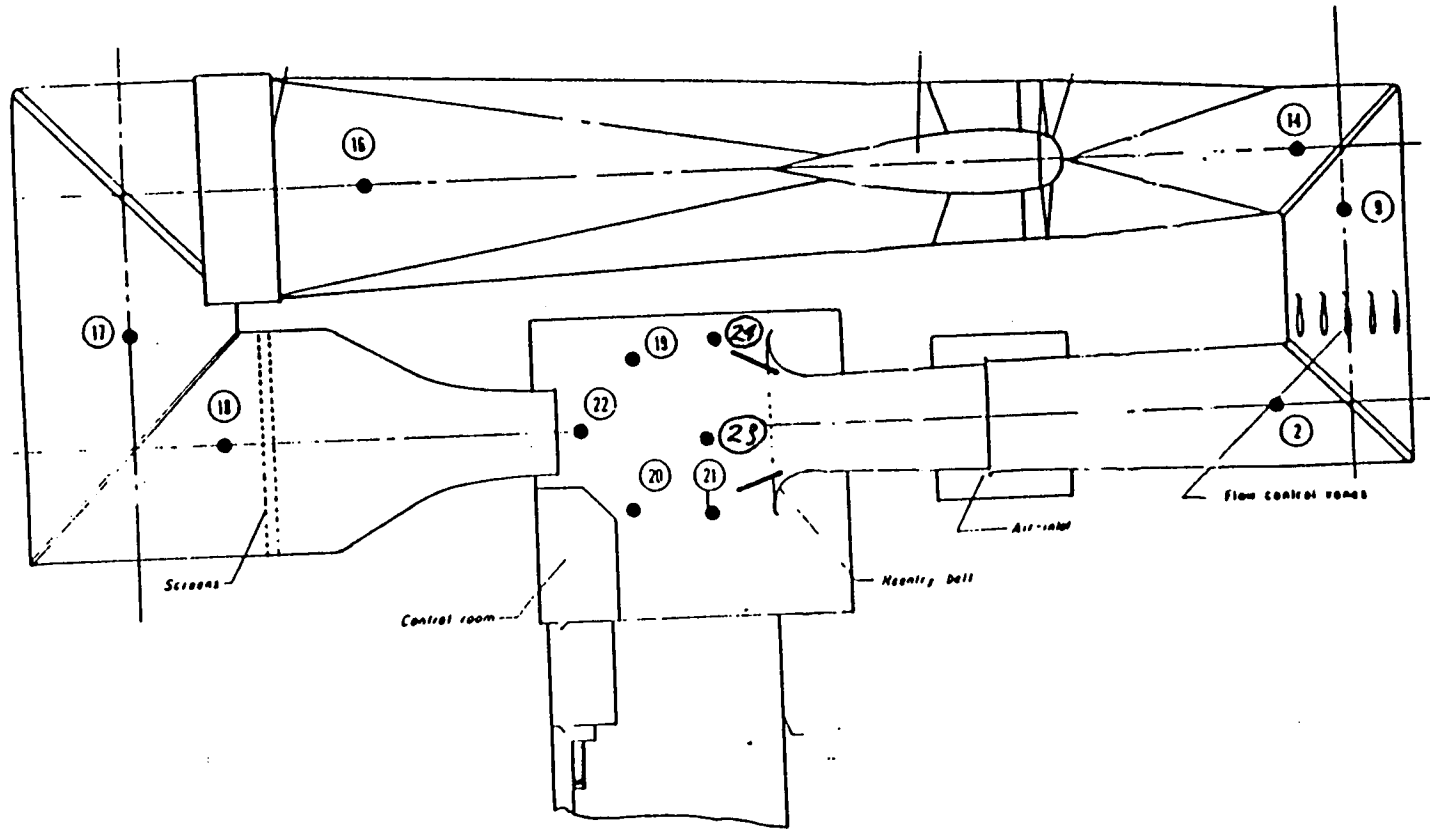
FIG. A.1 MICROPHONE AND SOURCE LOCATIONS FOR BACKGROUND NOISE TESTS
TEST 8
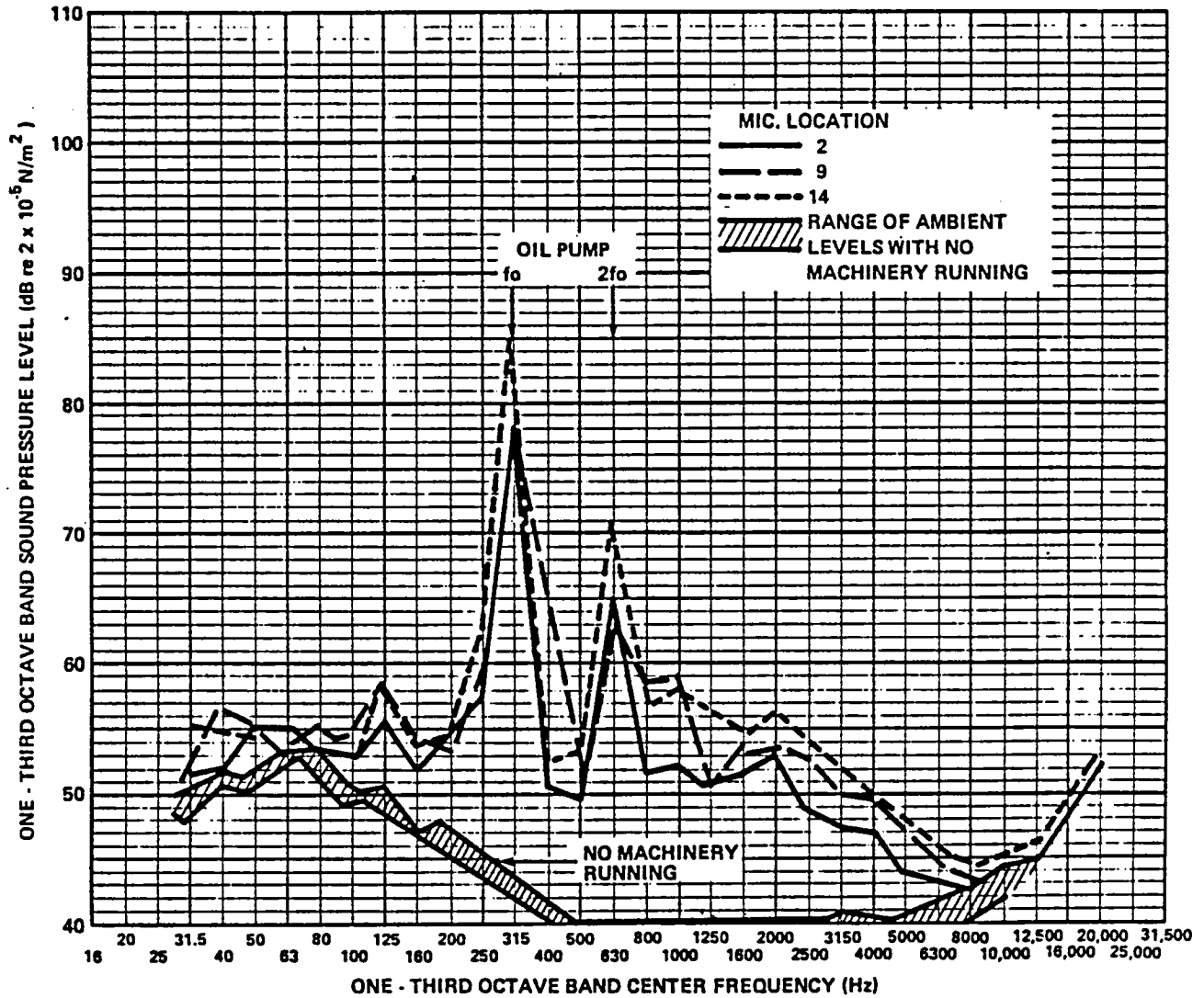
FIG. A.2 AMBIENT NOISE LEVELS WITH AND WITHOUT AUXILIARY
MACHINERY RUNNING (LOCATIONS 2, 9, & 14).

A-5
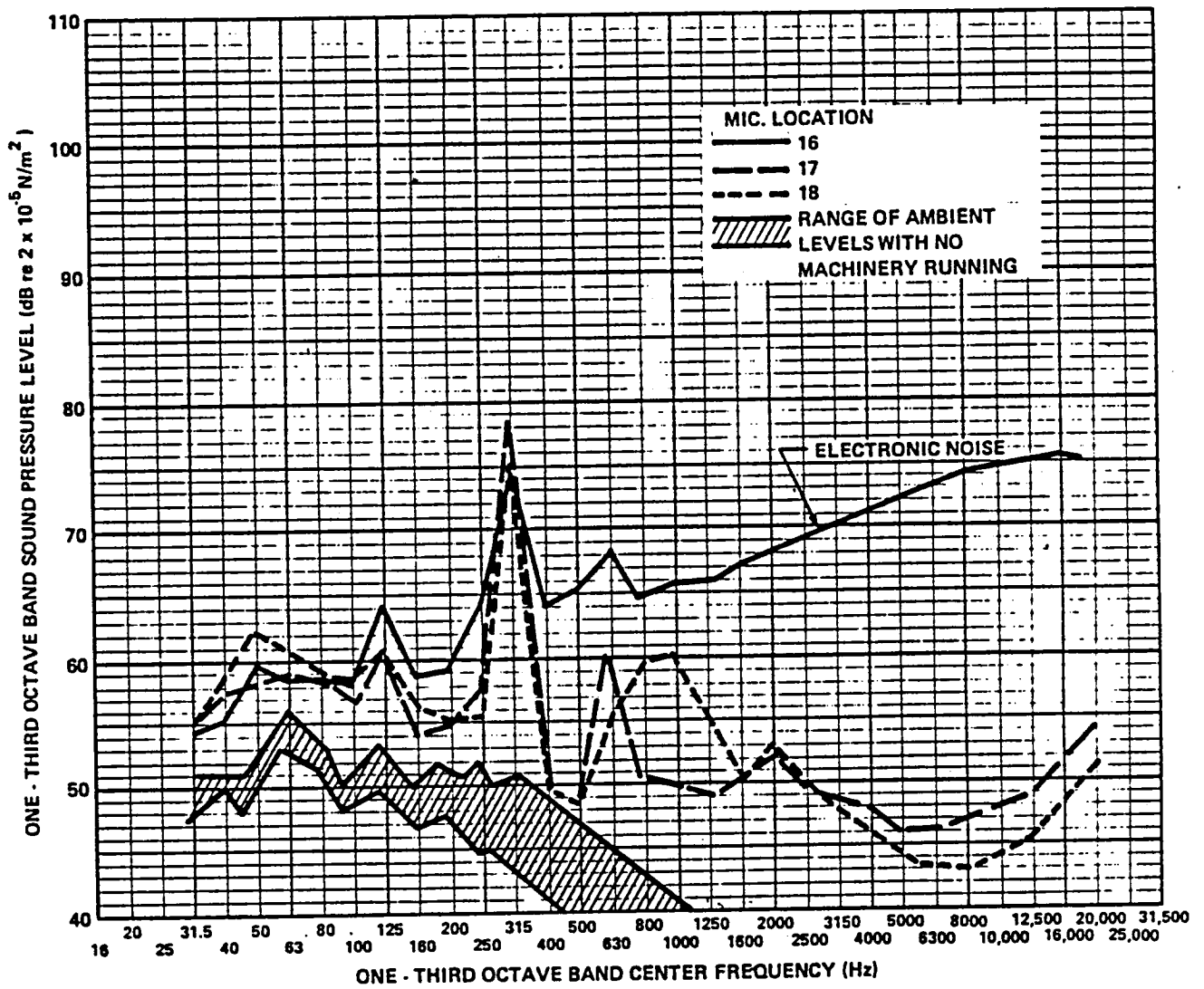
FIG. A.3 AMBIENT NOISE LEVELS WITH AND WITHOUT AUXILIARY MACHINERY RUNNING (LOCATIONS 16, 17 & 18).
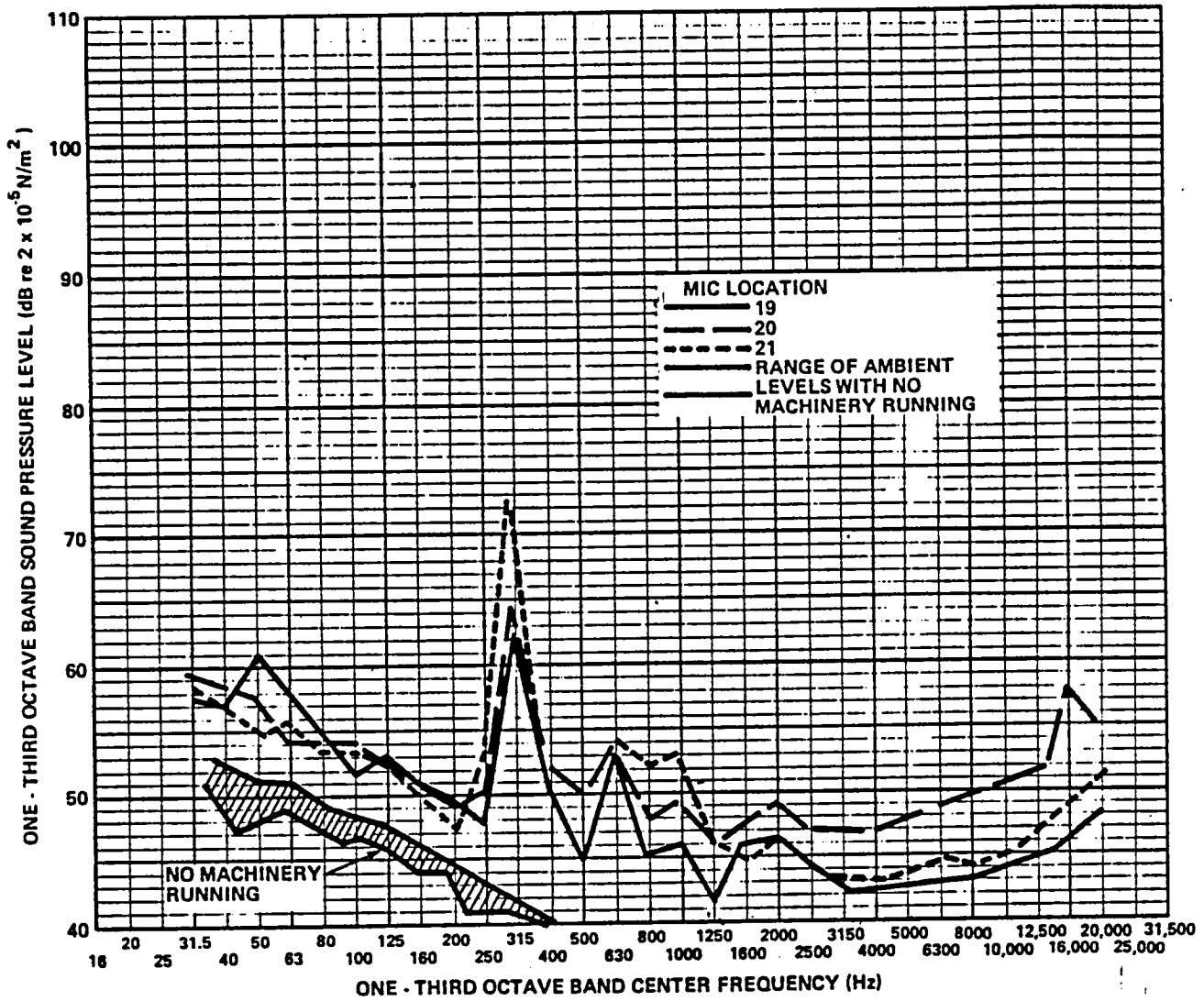
FIG. A.4.   AMBIENT NOISE LEVELS WITH AND WITHOUT AUXILIARY
MACHINERY RUNNING (LOCATIONS 19, 20 & 21).
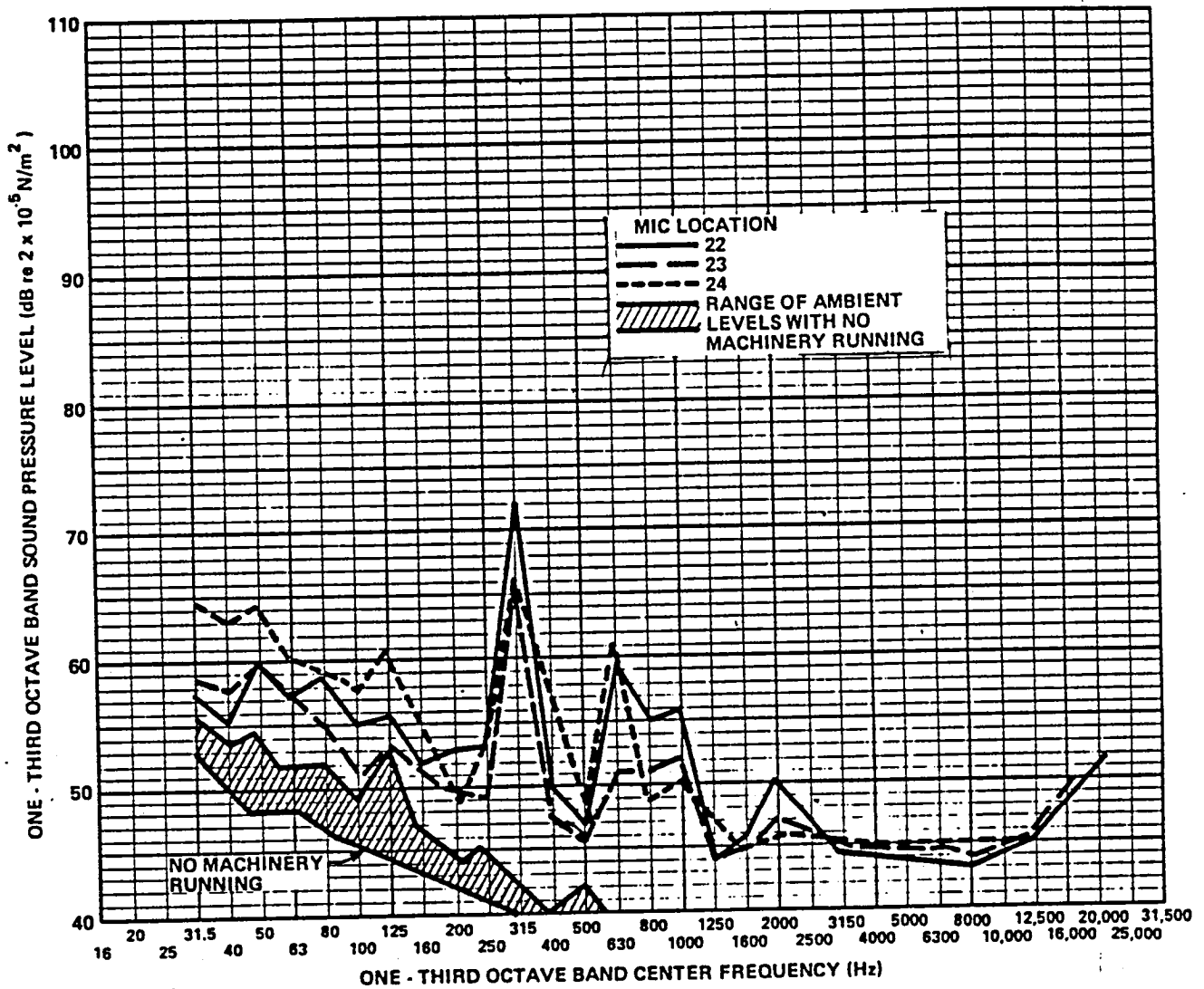
FIG. A.5. AMBIENT NOISE LEVELS WITH AND WITHOUT AUXILIARY
MACHINERY RUNNING (LOCATIONS 22, 23 & 24).
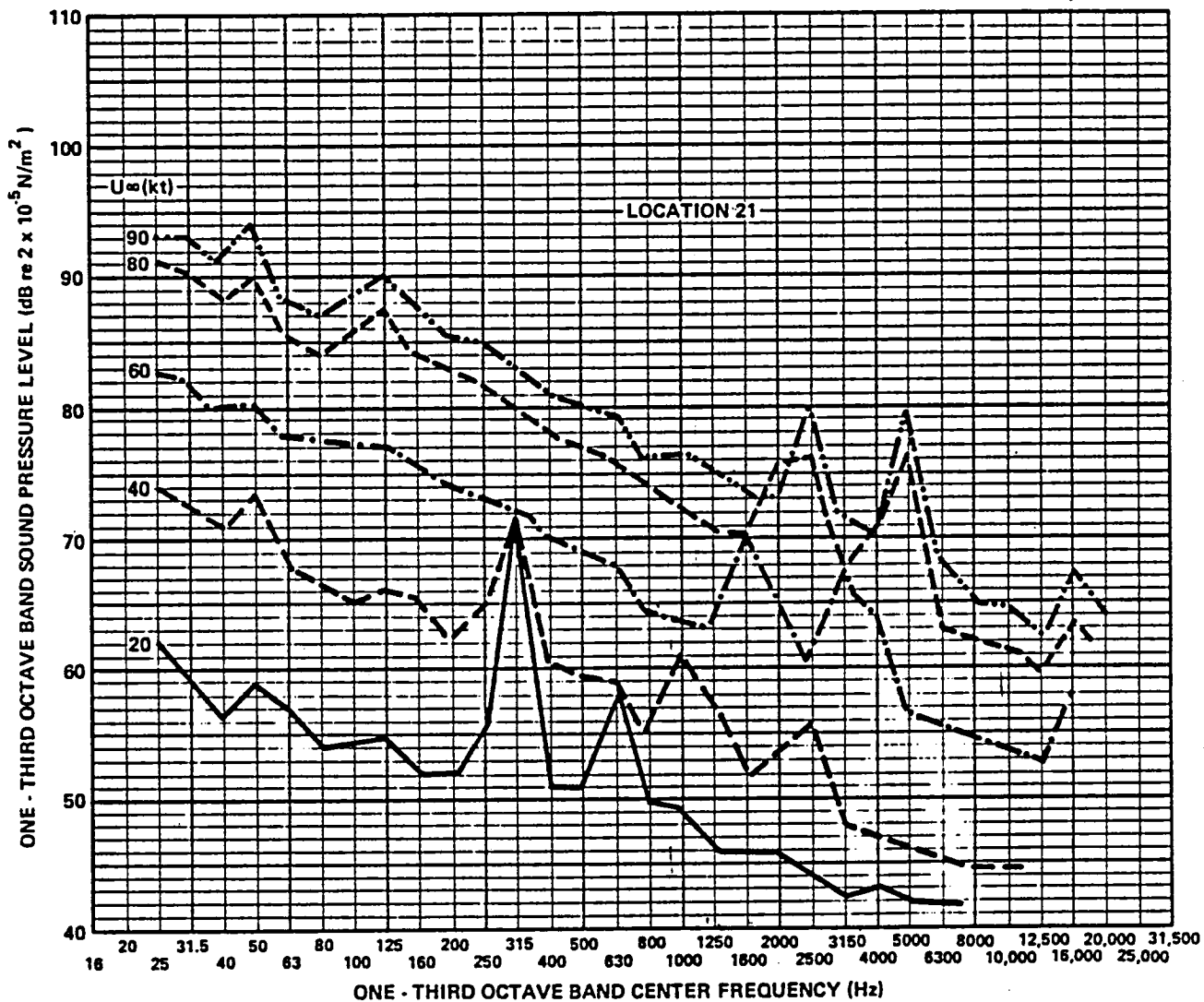
A-8
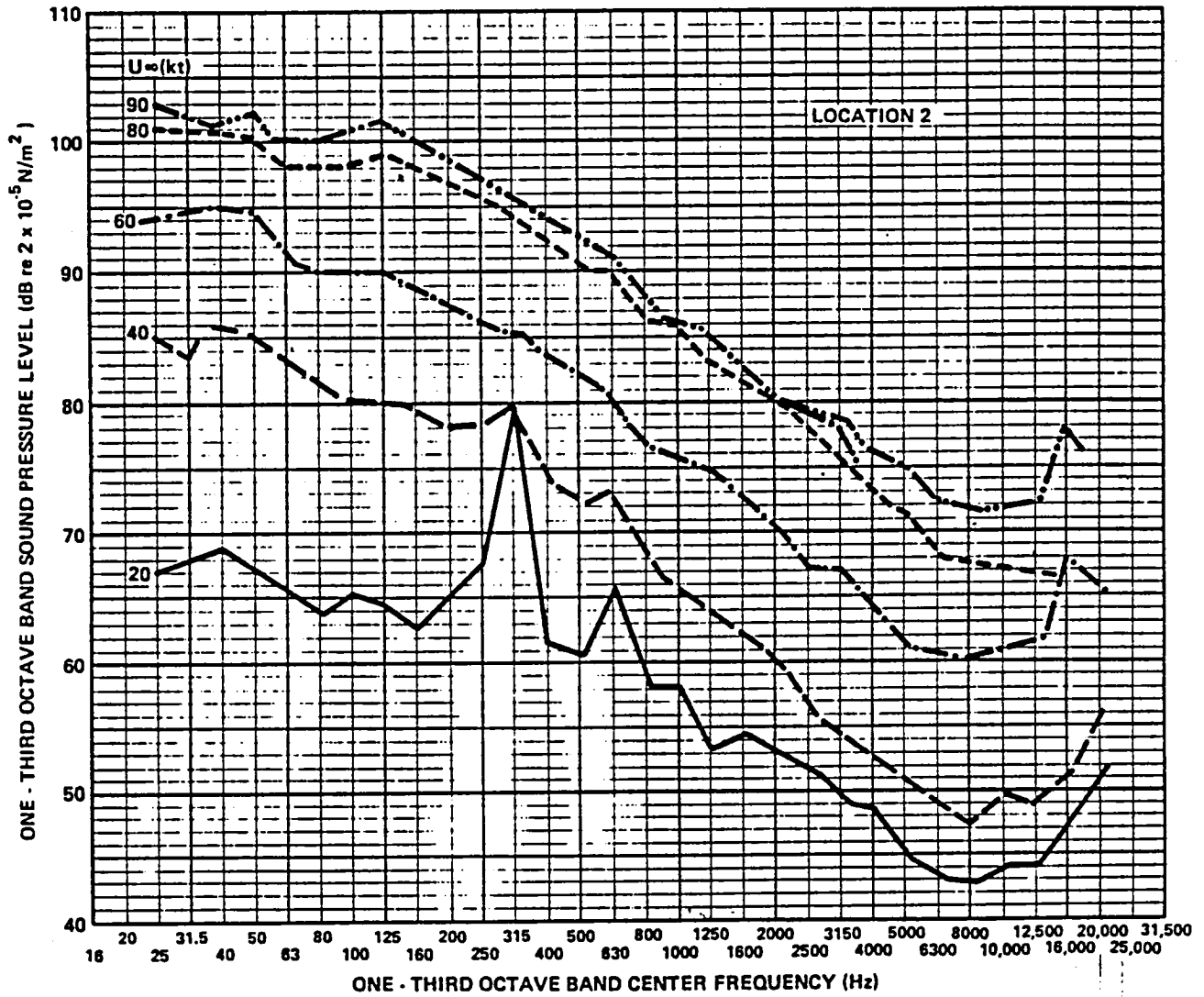
FIG. A.6 BACKGROUND NOISE IN 4X7 M WIND TUNNEL CIRCUIT AT 5 SPEEDS (LOCATION 2).

A-9
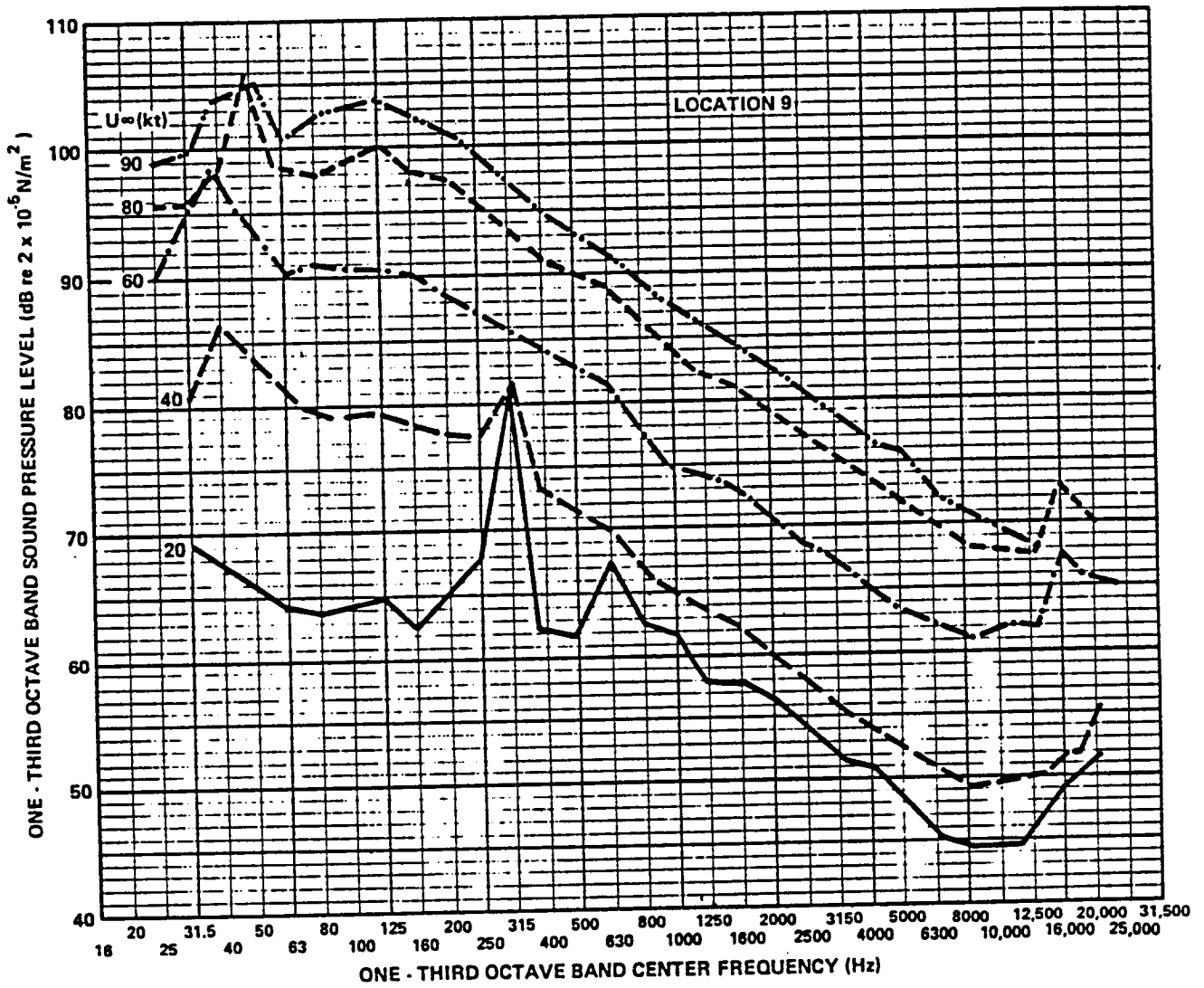
FIG. A.7.   BACKGROUND NOISE IN 4X7 M WIND TUNNEL CIRCUIT AT
5 SPEEDS (LOCATION 9).
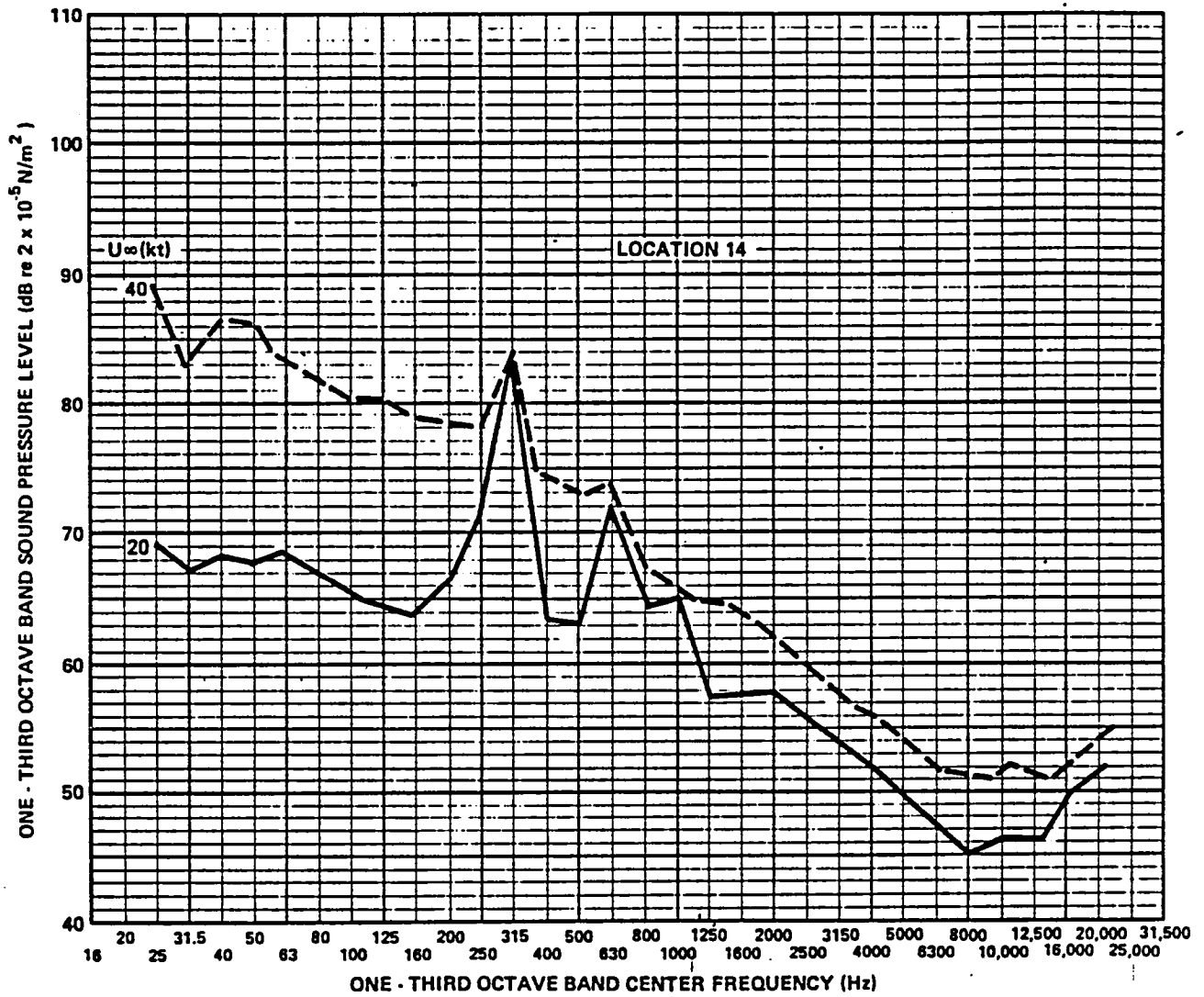
FIG. A.8.   BACKGROUND NOISE IN 4X7 M WIND TUNNEL CIRCUIT AT
            5 SPEEDS (LOCATION 14).

A-11
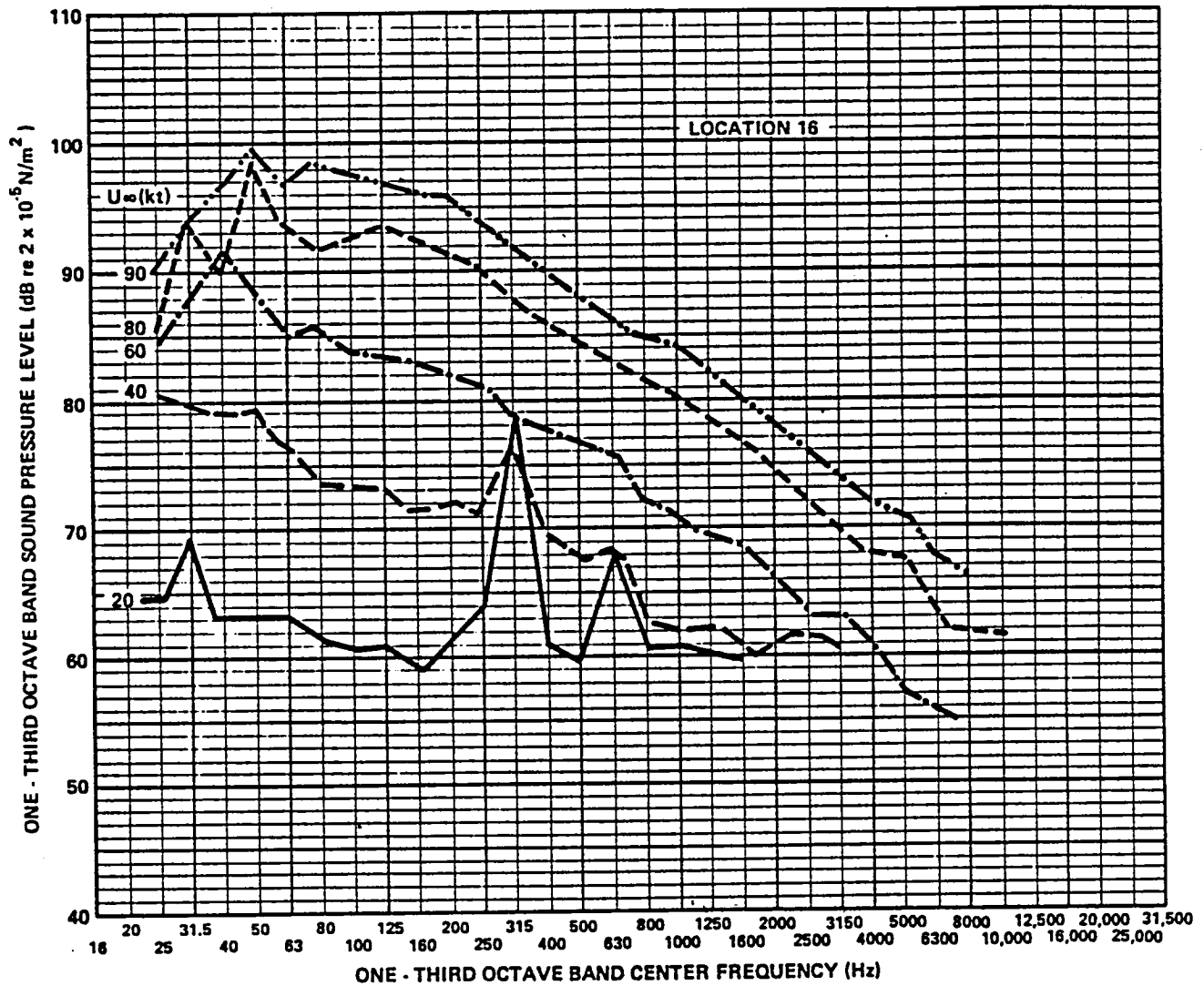
FIG. A.9. BACKGROUND NOISE IN 4X7 M WIND TUNNEL CIRCUIT AT
5 SPEEDS (LOCATION 16).
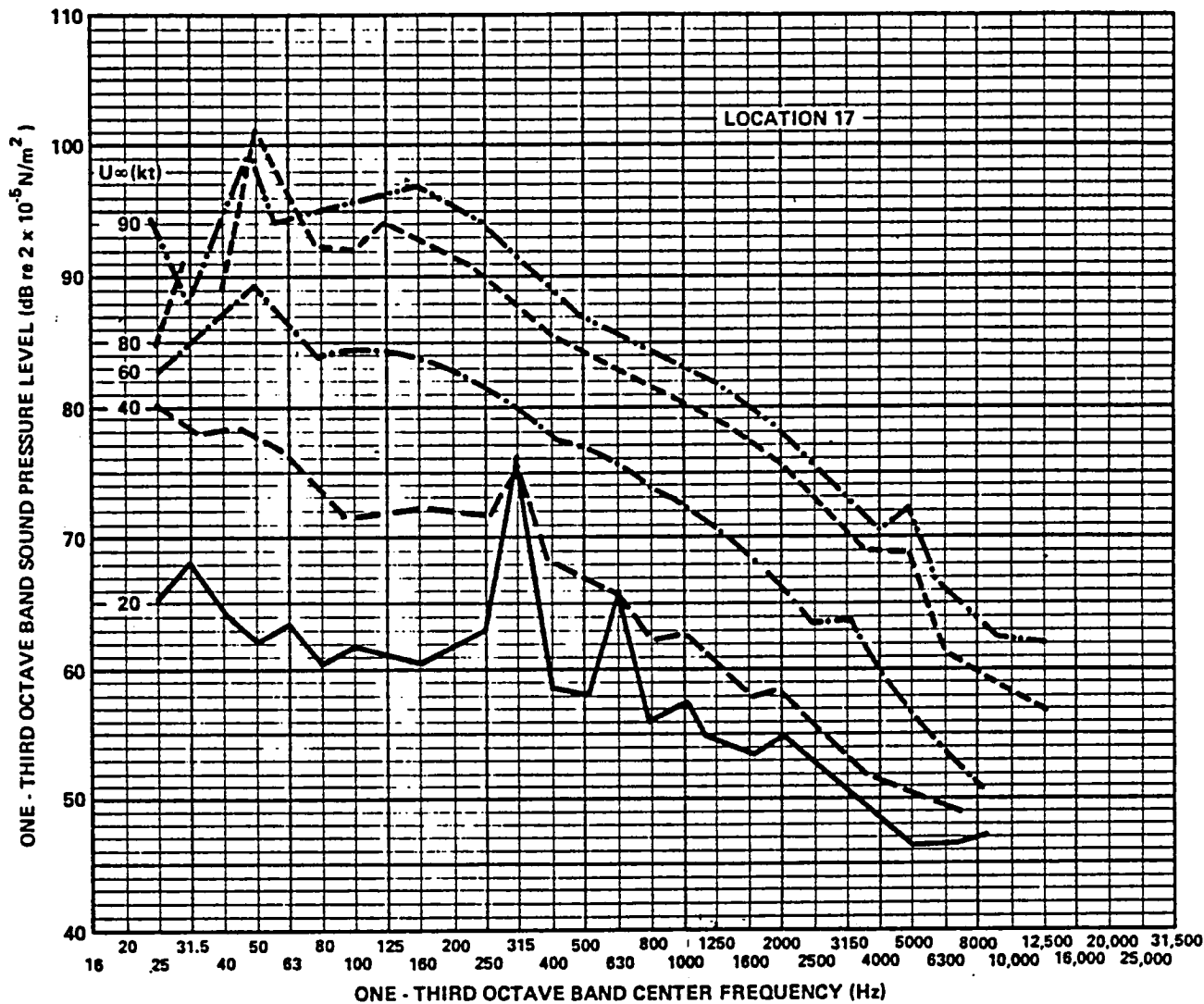
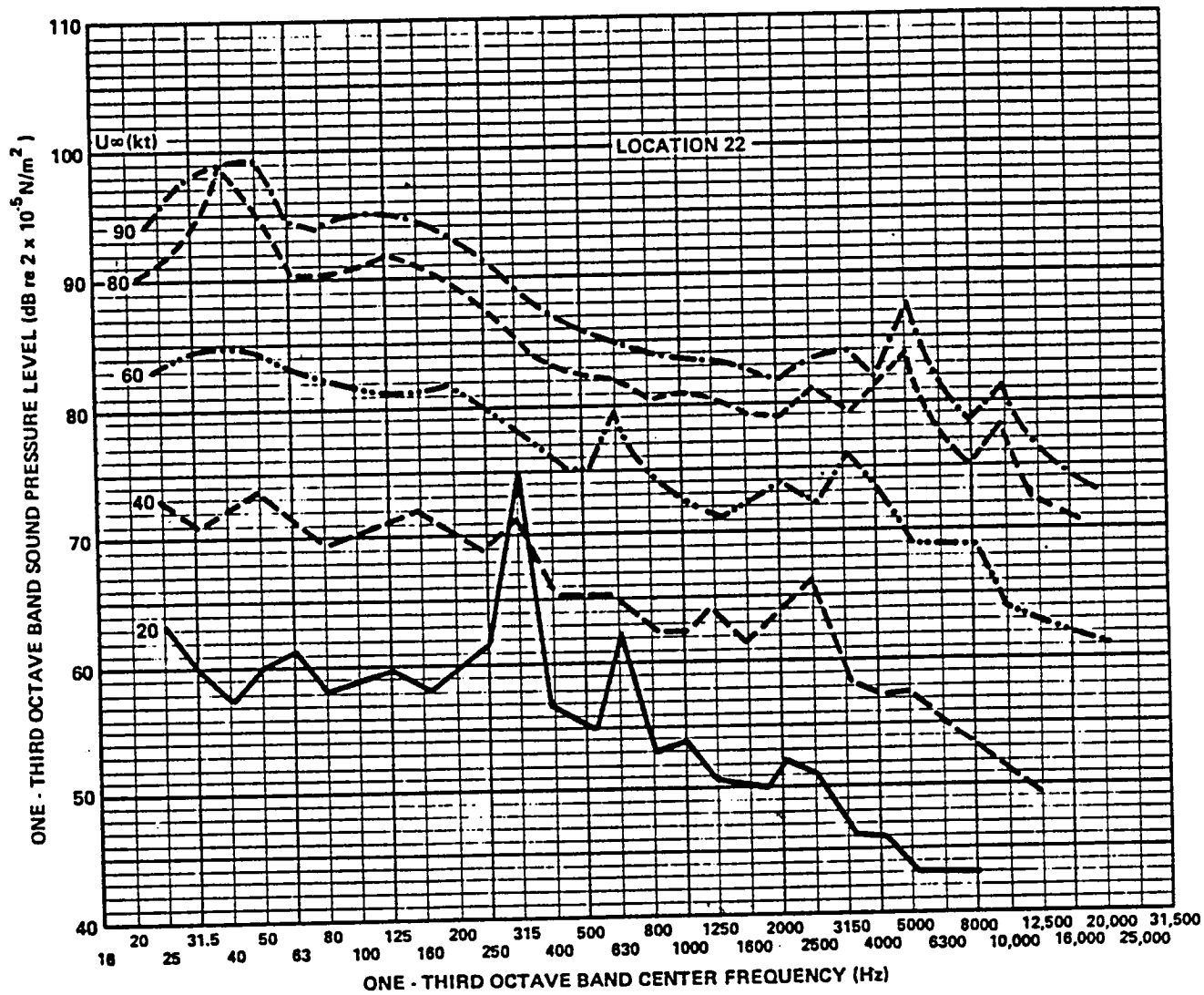FIG. A.10. BACKGROUND NOISE IN 4X7 M WIND TUNNEL CIRCUIT AT 5 SPEEDS (LOCATION 17).
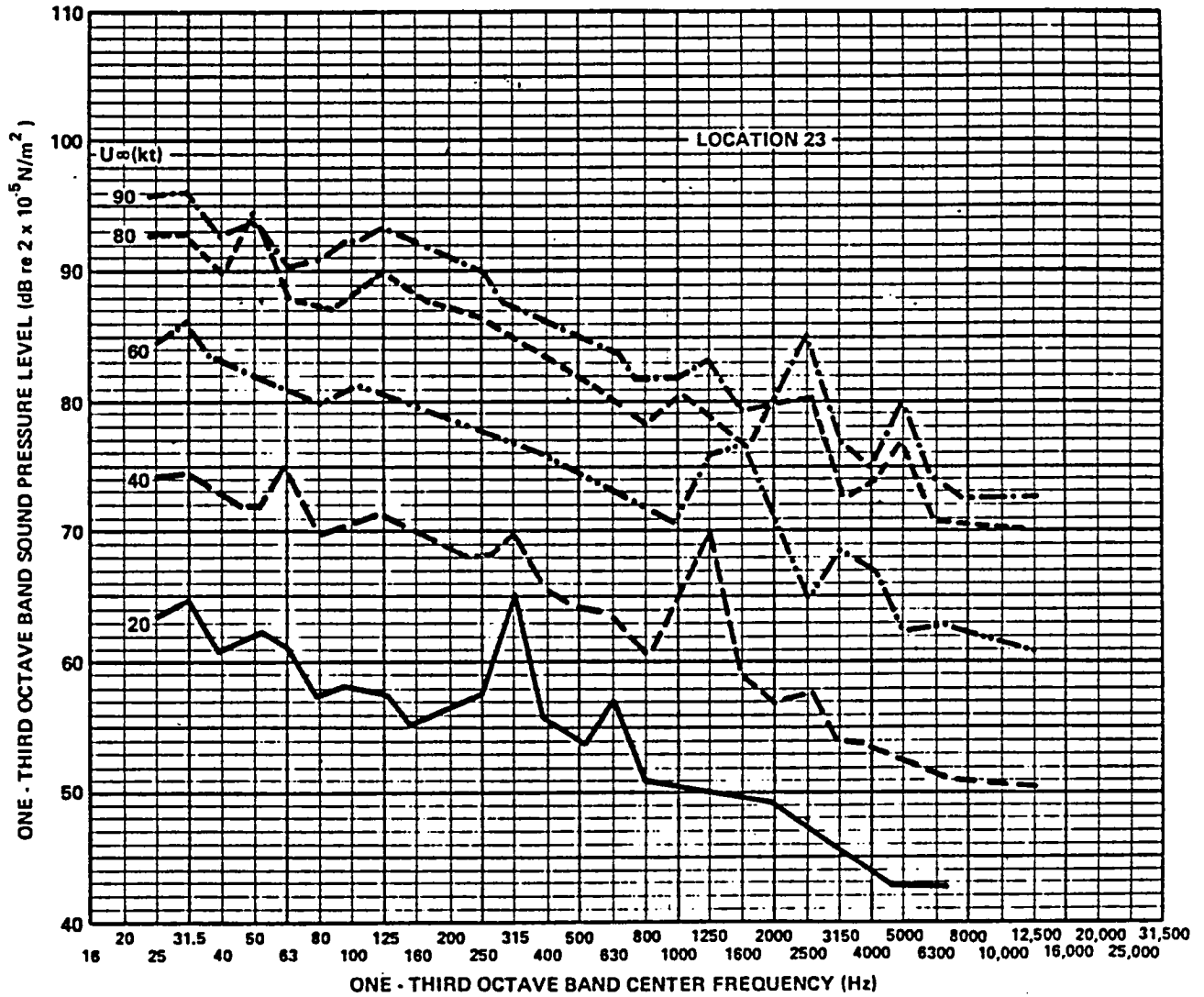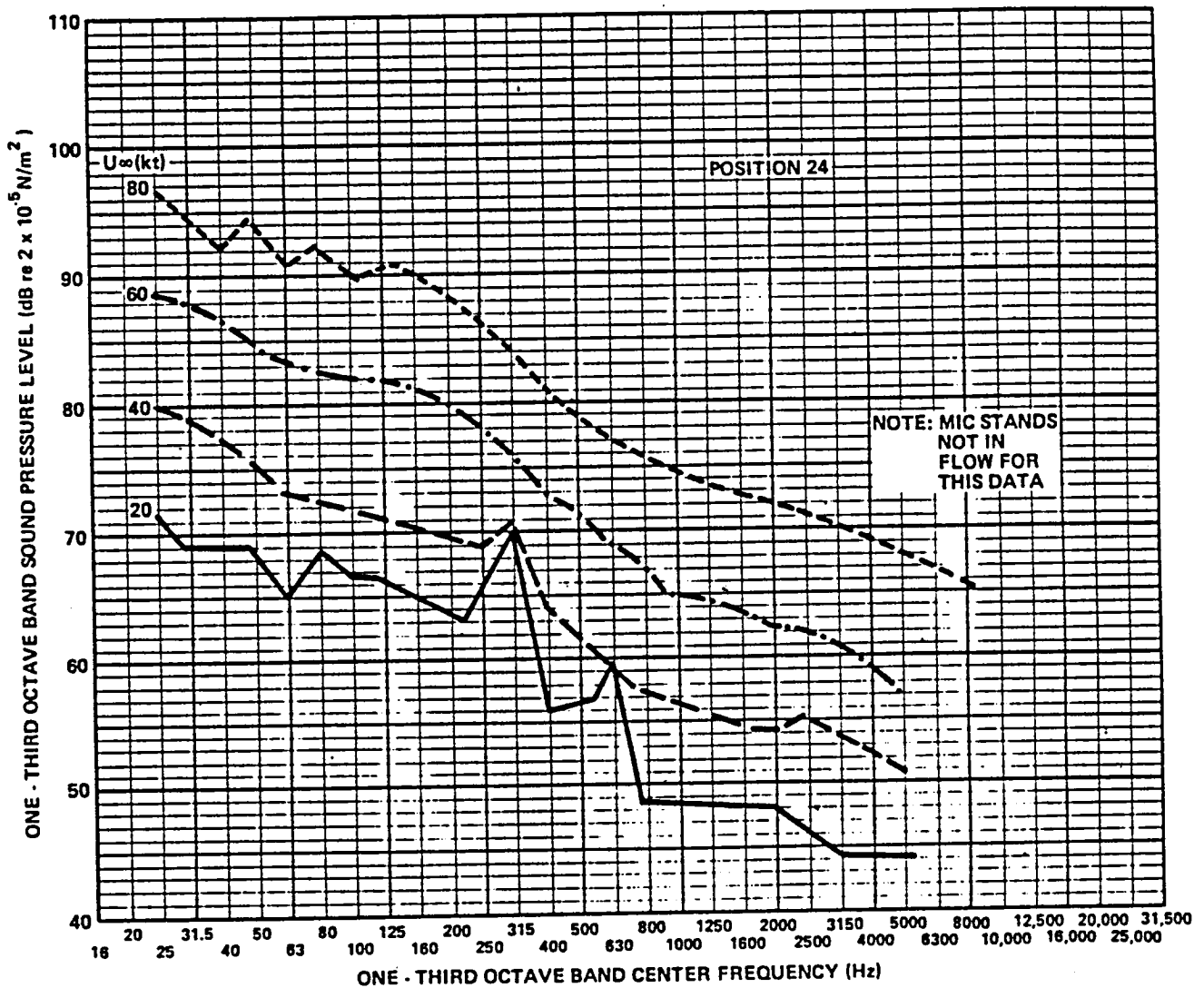
A-13
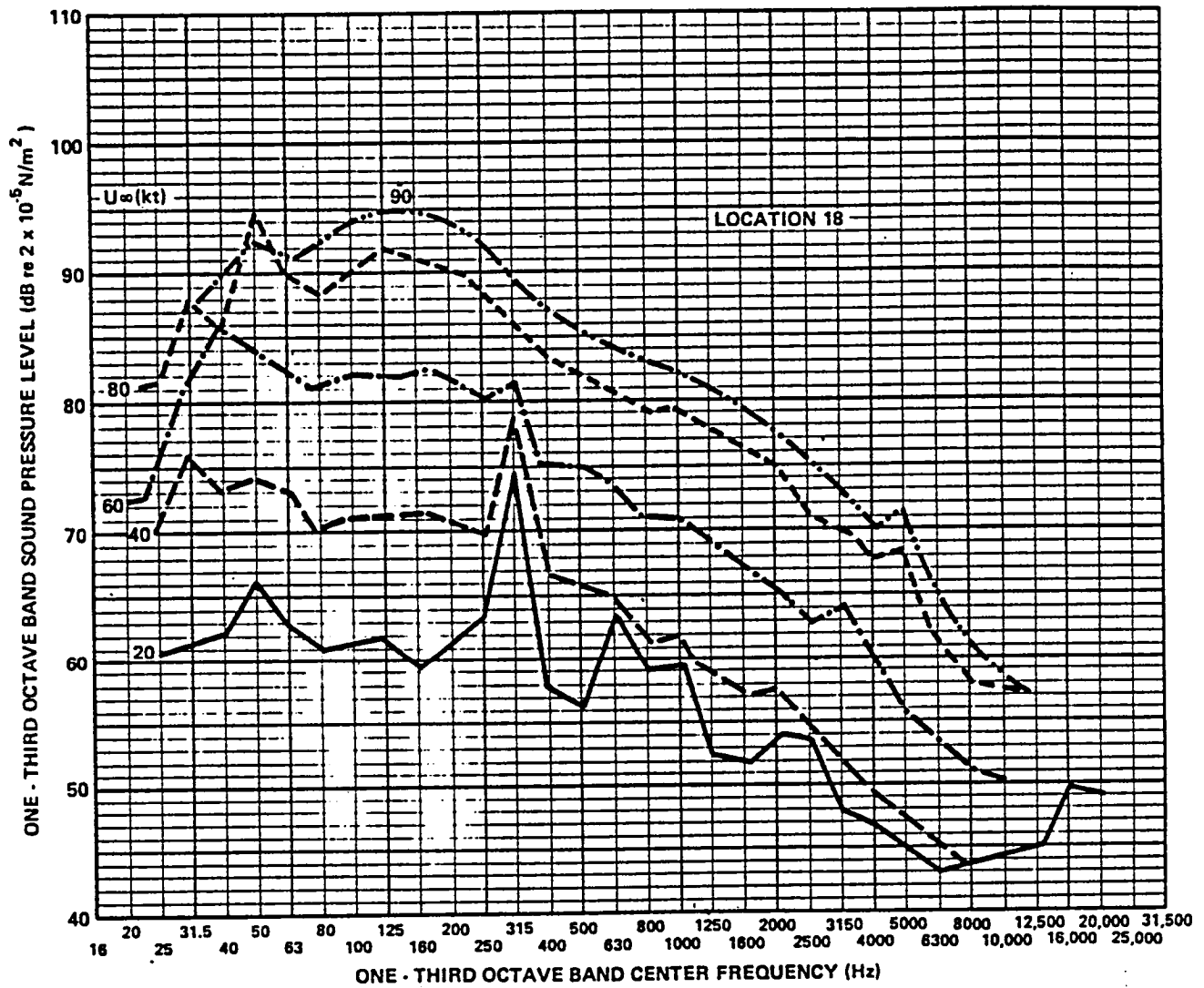
FIG. A.11. BACKGROUND NOISE IN 4X7 M WIND TUNNEL CIRCUIT AT
5 SPEEDS (LOCATION 18).

A-14
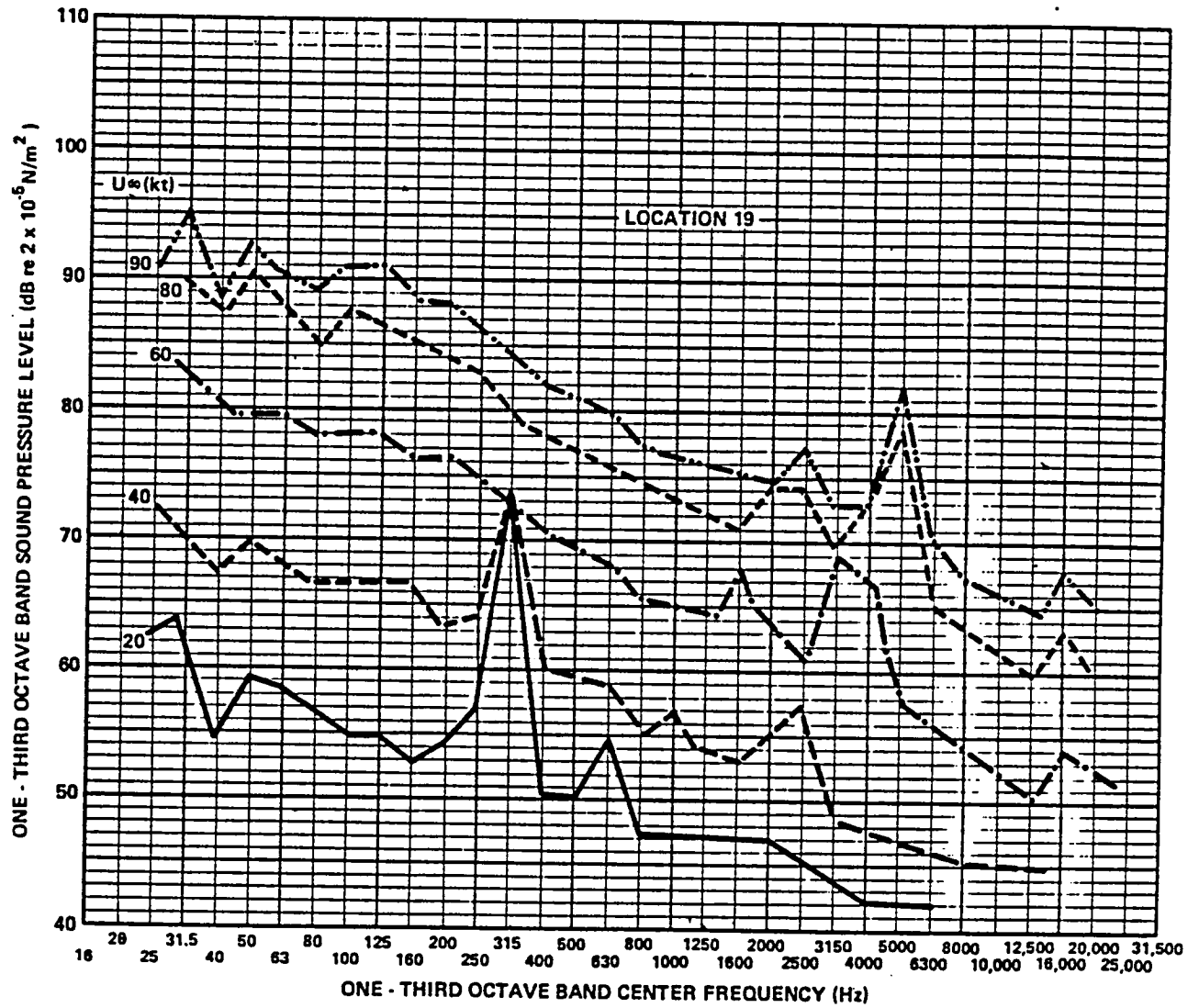
FIG. A.12. BACKGROUND NOISE IN 4X7 M WIND TUNNEL CIRCUIT AT
5 SPEEDS (LOCATION 19).

A-15
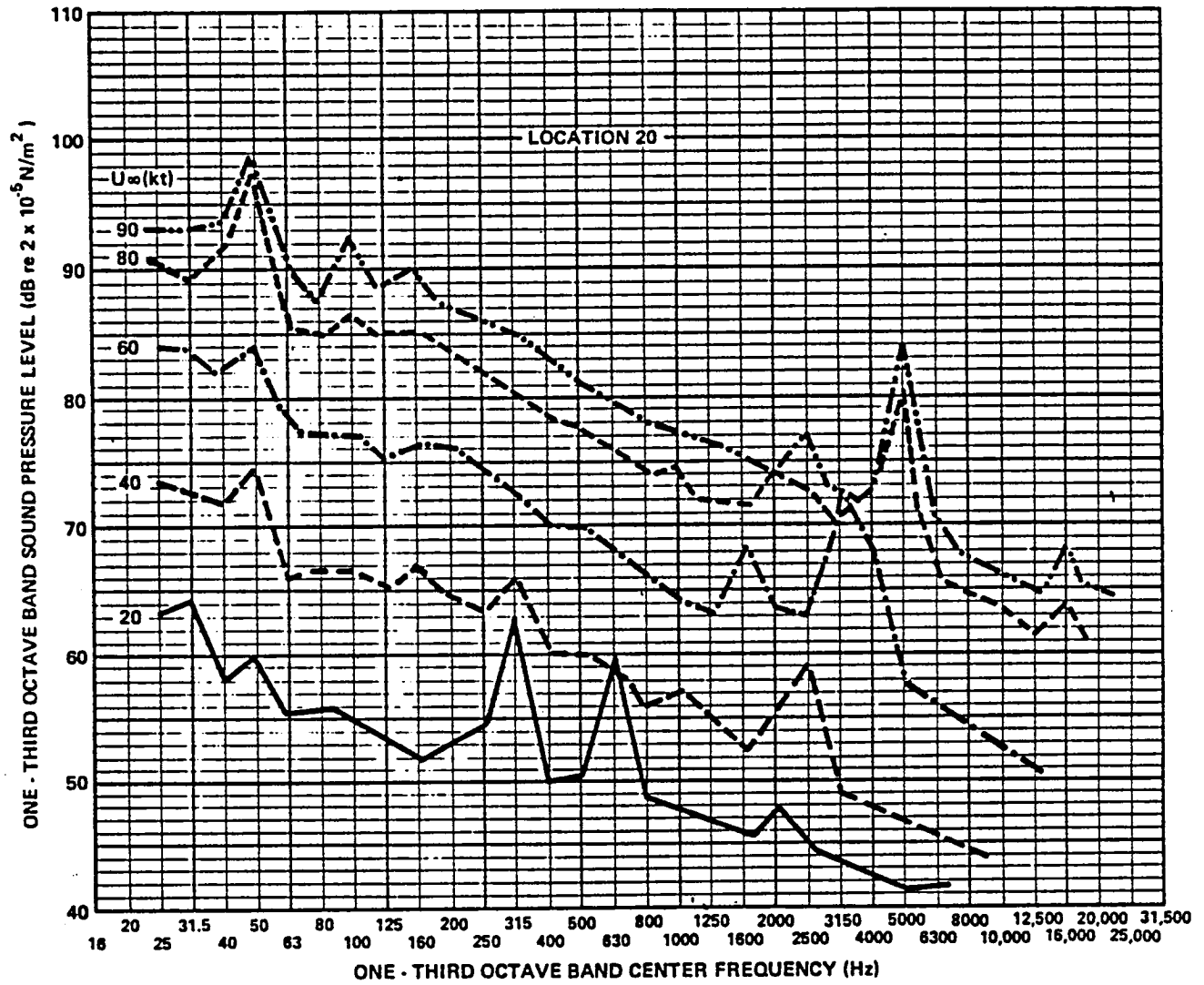
FIG. A.13.   BACKGROUND NOISE IN 4X7 M WIND TUNNEL CIRCUIT AT
             5 SPEEDS (LOCATION 20).

A-16

FIG. A.14. BACKGROUND NOISE IN 4X7 M WIND TUNNEL CIRCUIT AT
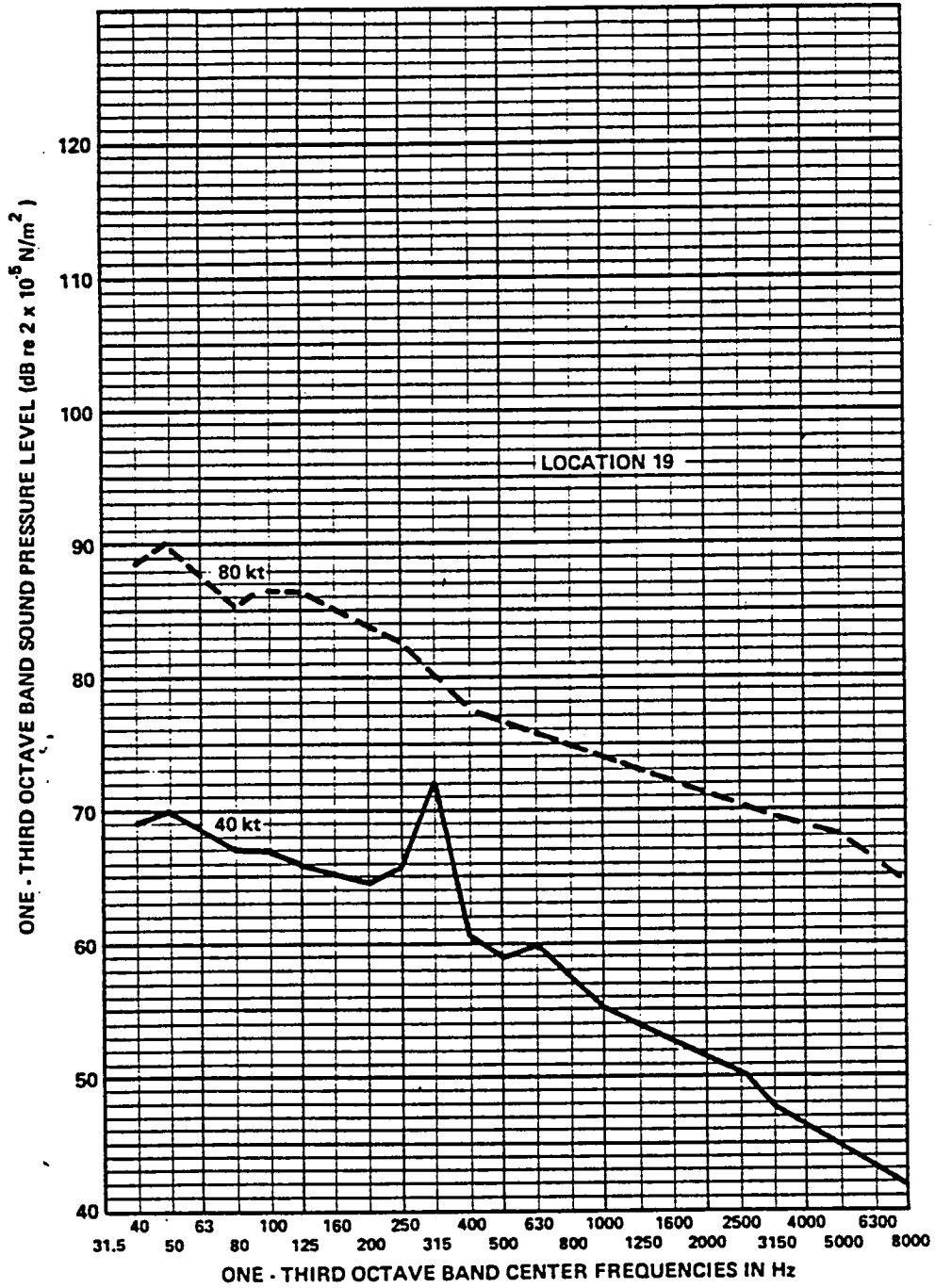5 SPEEDS (LOCATION 21).

A-17

FIG. A.15. BACKGROUND NOISE IN 4X7 M WIND TUNNEL CIRCUIT AT
5 SPEEDS (LOCATION 22).

A-18

FIG. A.16. BACKGROUND NOISE IN 4X7 M WIND TUNNEL CIRCUIT AT 5 SPEEDS (LOCATION 23).

A-19

FIG. A.17. BACKGROUND NOISE IN 4X7 M WIND TUNNEL CIRCUIT AT
5 SPEEDS (LOCATION 24).

A-20

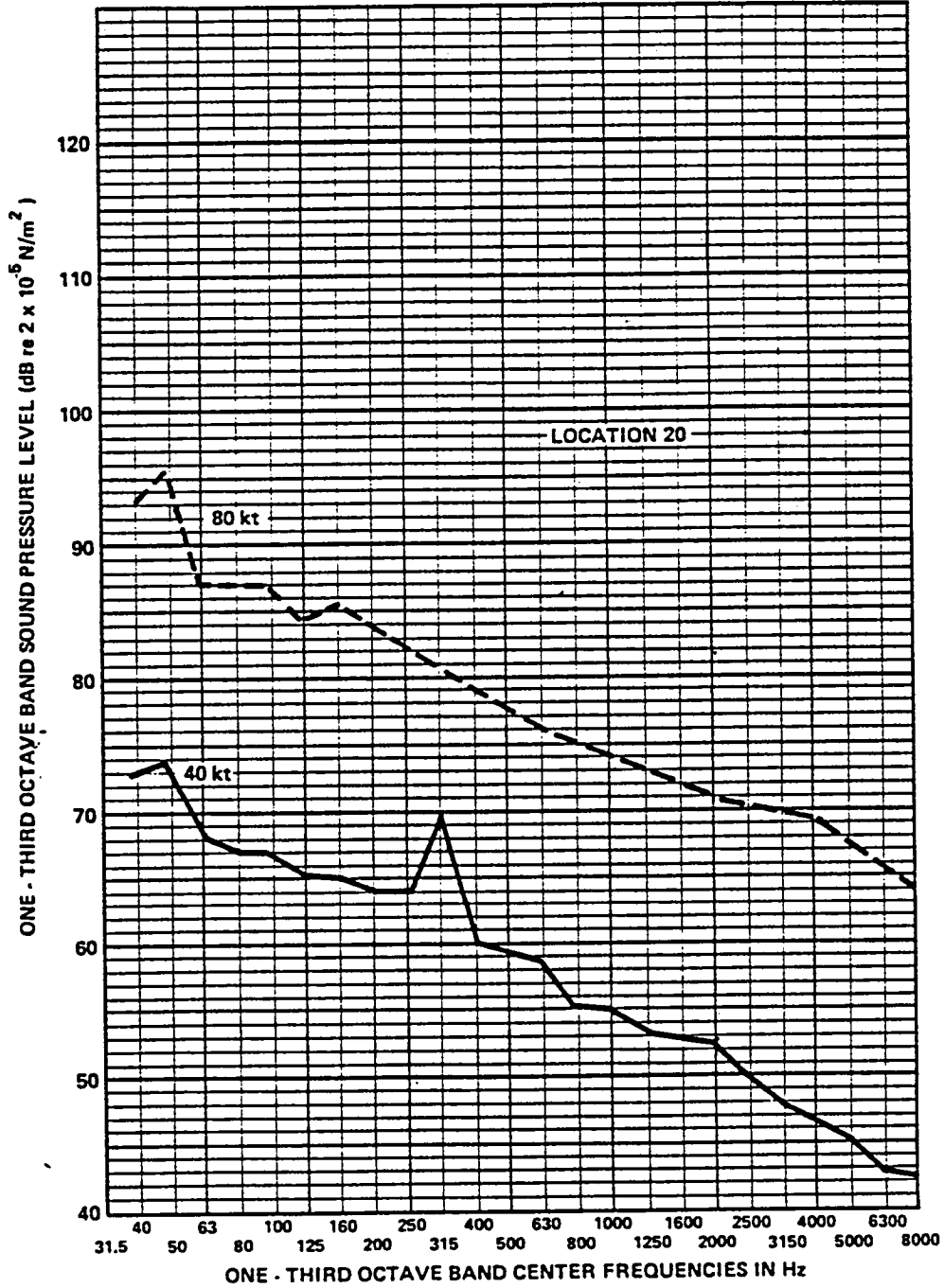FIG. A.18. BACKGROUND NOISE IN TEST SECTION WITH MICROPHONE TEST STAND REMOVED (LOCATION 19).

A-21

FIG. A.19. BACKGROUND NOISE IN TEST SECTION WITH MICROPHONE TEST STAND REMOVED. (LOCATION 20).
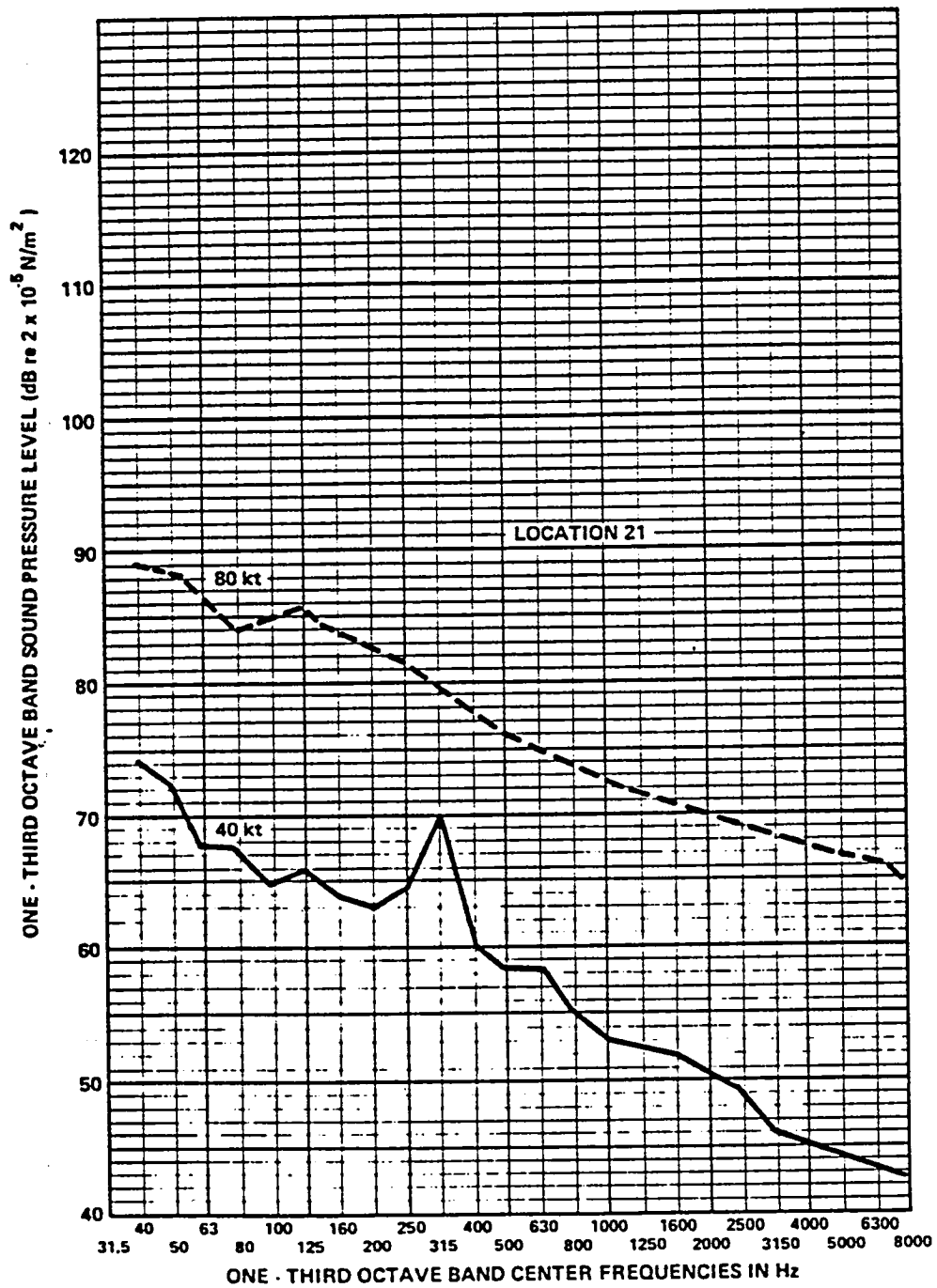
A-22

FIG. A.20. BACKGROUND NOISE IN TEST SECTION WITH MICROPHONE TEST STAND REMOVED (LOCATION 21).
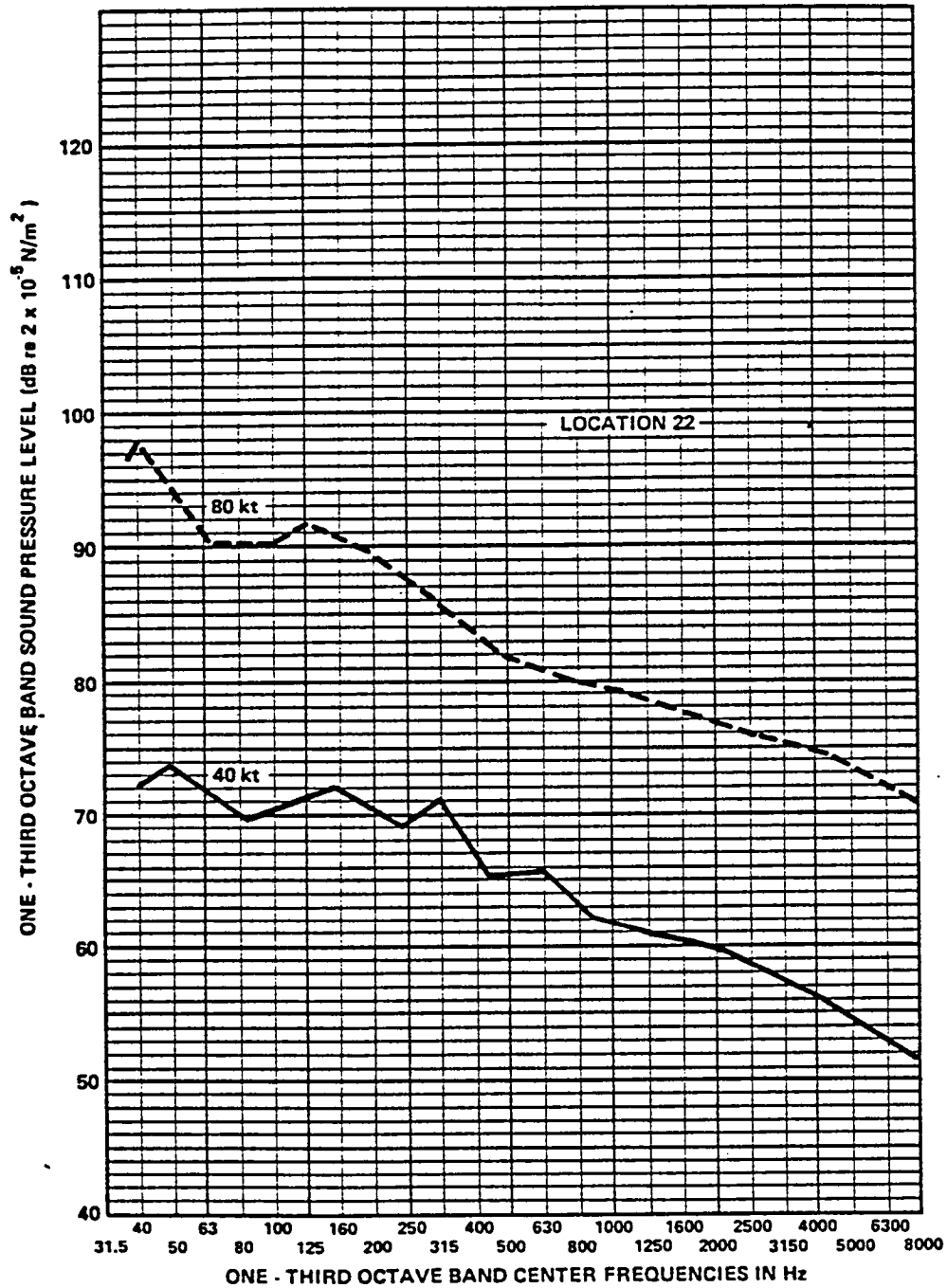
A-23

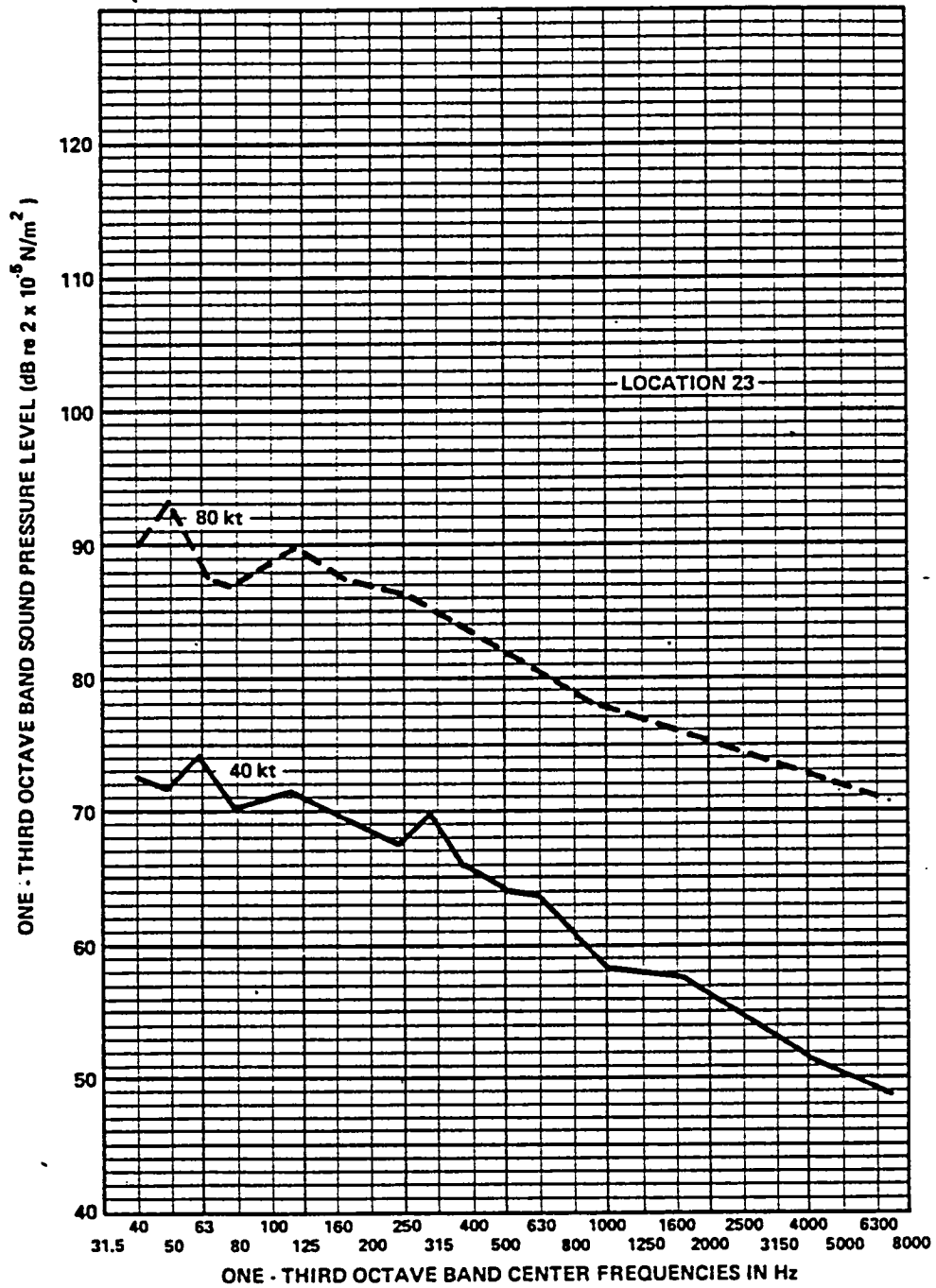FIG. A.21. BACKGROUND NOISE IN TEST SECTION WITH MICROPHONE TEST
STAND REMOVED (LOCATION 22).

A-24

FIG. A.22. BACKGROUND NOISE IN TEST SECTION WITH MICROPHONE TEST STAND REMOVED (LOCATION 23).

A-25

FIG. A.23. BACKGROUND NOISE IN TEST SECTION WITH MICROPHONE TEST STAND REMOVED (LOCATION 24).
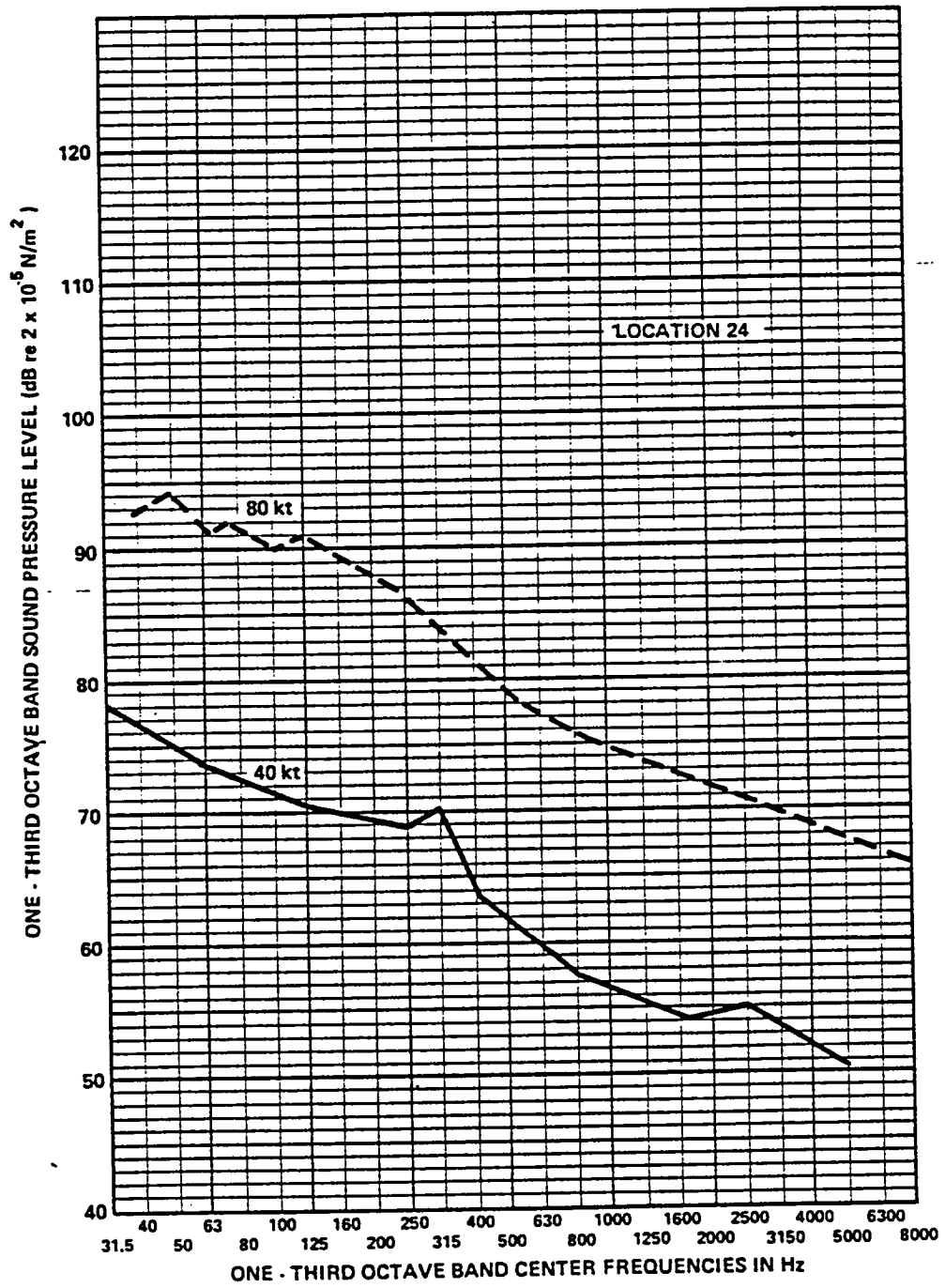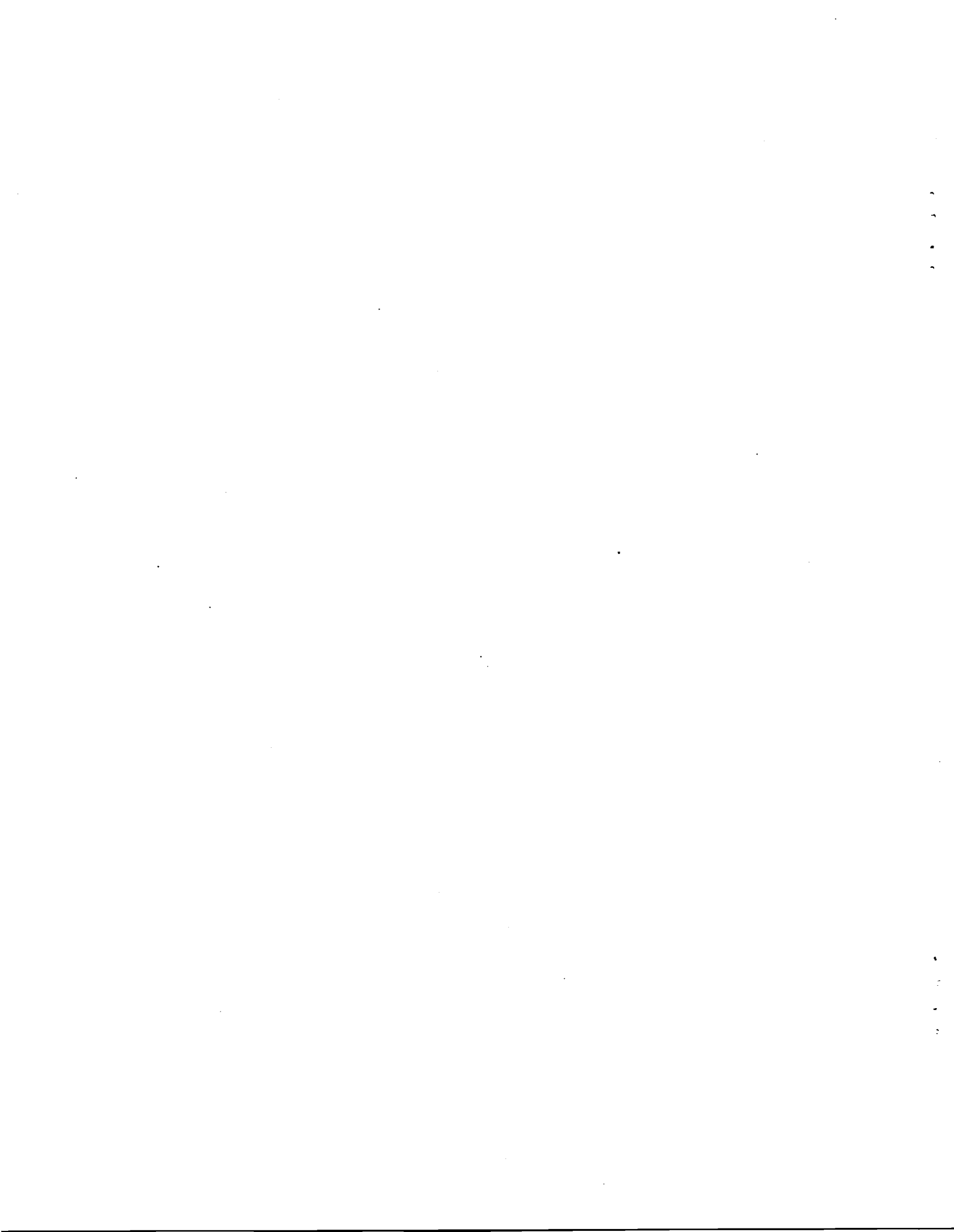
A-26

APPENDIX B

SOUND PROPAGATION AROUND TUNNEL CIRCUIT WITH STEADY-STATE SOURCE

APPENDIX B

SOUND PROPAGATION AROUND TUNNEL CIRCUIT WITH STEADY-STATE SOURCE

B.1. Introduction

In order to obtain an estimate of the propagation losses around the circuit, sound pressure levels were measured at a number of locations in the tunnel when an electro-acoustic sound source was placed in the fan section of the circuit or in the nozzle exit. The ten microphone locations used for the test are shown in Figure B.1; three locations (2, 9, 14) were in the diffuser, three (16, 17, 18) in the settling chamber, and four (19-22) in the test section. The microphone height was 6 feet above the tunnel floor except at location 18 where it was 12 feet. The three source locations, identified as 2-1, 2-2, and 2-3, are shown in Figure B.2 At each location the horn of the source was oriented at three angles to the tunnel centerline, 0, 30°, and 60° for configurations 2-1 and 2-2, and 0, ±30° for configuration 2-3. The input signal to the sound source was pink noise with a high pass filter at 80 Hz and a low pass filter at 5000 Hz.

B.2 Analysis of Test Data ($\theta-0^0$)

One-third octave band sound pressure levels measured at the six locations in the tunnel circuit and at location 22 in the test section are compared in Figure B.3 through B.5 for the three source locations with the source directed along the tunnel centerline. At frequencies below 80 Hz and above 5000 Hz, the data were contaminated by instrumentation noise.

When the source is located just upstream of the fan rotor (configuration 2-1) the sound levels in the diffuser group together and are 8 to 10 dB higher than the levels in the settling chamber. Sound levels at location 22 in the test

section are slightly lower than those in the settling chamber. When the source is downstream of the fan, the sound pressure levels in the diffuser and settling chamber appear to cluster together; levels in the test section are lower. Finally, when the source is in the tunnel nozzle and pointing into the test section, the highest sound levels occur at locations 22, and the lowest levels are in the settling chamber.

One approach to the interpretation of the data is to assume that the sound pressure level (SPL) is uniformly distributed across a given cross-section of the tunnel and that the acoustic energy is propagating around the tunnel circuit. The acoustical power (PWL) at any location in the tunnel would then be given, approximately, by

$$PWL = SPL + 10 \log A \quad dB \ (re \ 10^{-12}W) \quad .$$

where A is the cross-sectional area in square meters. The data in Figures B.3 through B.5 have been adjusted in this manner and the resulting spectra are plotted in Figures B.6 through B.8. The appropriate values for A are well-defined except for location 22 in the test section. If the test section had been closed at the time of the measurements the appropriate value of A would be 29.5 sq.m. However, with the test section open it is possible that the value of A should be that of the chamber cross-section, i.e., 314 sq.m. Both values of A have been used in adjusting the data measured at location 22 for test configuration 2-1 and 2-2 where the noise source was in the fan section of the tunnel circuit. For test configuration 2-3, when the noise source was in the nozzle and very close to the microphone at location 22, only the value of A for the nozzle exit was used in the analysis.

The spectra in Figures B.6 through B.8 show that there is a reasonably good collapse of the data for configurations 2-1 and

2-2 when data for location 22 are adjusted on the basis of test chamber area. In the case of configuration 2-3 the data collapse is reasonably good when the nozzle area is used to adjust the data for location 22. Thus it is concluded that, when the sound source is in the tunnel circuit and at some distance from the test section, the sound levels in the test section are about 10 dB lower than they would be in a closed test section. The reduction in level is due to dispersion and dissipation of the acoustical power in the test chamber.

Considering the sound levels in the diffuser and settling chamber, it is found that, when adjusted for area, the data collapse quite well for test configurations 2-1 and 2-3. The average range of the data for any given one-third octave band is about 6 dB. For configuration 2-2, the data collapse is not as good, with the data range being about 10 dB for any one-third octave band; data for the diffuser and settling chamber apparently collapse onto different spectral bands.

B.3. Test Data for Source Orientations Off-Axis

When the source was oriented at an angle to the tunnel centerline at locations 2-1 and 2-2, the test results were essentially the same as for source orientation along the centerline. Example spectra are shown in Figures B.9 and B.10. Apparently, the reverberation effects were sufficiently strong to mask the effects of source directivity.

However, significant differences were observed for source location 2-3. In this case, the environment surrounding microphone 22 is much less reverberant than it is elsewhere in the tunnel and the directivity of the source becomes more important. This is particularly true at frequencies above 5000 Hz as can be seen in Figure B.11. Part of the acoustic power generated by the

source is directed away from microphone 22 and, at the same time, away from the entry to the diffuser. Consequently the acoustic power does not enter the tunnel circuit and the sound levels in the tunnel are lower than when the source is oriented along the tunnel centerline.

The data presented above will be used to derive "transfer functions" to predict test section contributions resulting from noise sources in various parts of the circuit. The data themselves suggest that for acoustic sources located in the first corner, first crossleg, second corner and at the fan, the predominant path to the test section is upstream. However, the exact contribution of each path is not clear since acoustic power can flow through the test section thus presenting the possibility that the measurements in the circuit will consist of sound traveling in both directions. Coherence and phase analyses will assist in such interpretations.

B.4 Nozzle and Collector Directivity

Analysis of the sound pressure levels measured by the four microphones in the test section/chamber show that the levels are higher at the locations closer to the tunnel centerline. This suggests that directivity effects associated with the nozzle and collector may be influencing the data. Such directivity effects have been observed in other free-jet wind tunnels in which the surrounding room was highly absorptive or anechoic. Such effects have practircal significance in terms of both developing estimates for noise reduction requirements and planning measurement strategies for particular test items.

Analytical predictions of such effects using simple classical models are not particularly meaningful since (a) in the frequency range of interest, the propagation characteristics of

the duct consist of a large number of non-axial modes, thus making plane wave or piston radiation models inappropriate, and (b) most points in the room surrounding the nozzle and collector are in the geometric near field of the openings thus making the definition of the effective origin of the sound ambiguous (although one could, in principle, carry out the nearfield calculation). Available empirical methods indicate that for an unbaffled opening of the size of the 4x7 m nozzle (or collector), the levels at 45° from the opening at the typical microphone sideline distance tested would be 2 to 5 dB below the level on the centerline.

With this in mind, the no-flow data can be examined in terms of sideline rather than polar distributions. Microphones 19, 20, and 21 were, respectively, 5.6m (18.5 ft), 6.3m (20.7 ft) and 6.5m (21.3 ft) from the tunnel centerline; the average distance was 6.1m (20.2 ft), or approximately 0.87 times the nozzle width off the centerline. Microphone 22 was on the tunnel centerline. Sound pressure levels measured at microphones 19, 20, and 21 have been normalized relative to levels at microphone 22, without performing any adjustment (such as inverse square law) for distance. The normalized levels for the three sideline micro-phones were then averaged for each one-third octave frequency band. The resulting spectrum is plotted in Figure B.13. When averaged over all frequencies the sideline sound pressure levels are approximately 4.5 dB lower than the tunnel centerline values.

Measurements could not be made at greater distances from the tunnel centerline because of the presence of hardware in the test section/chamber. However, some indication of the probable spatial variation of sound pressure levels can be obtained from Ref. B1, where it was found that the hall radius had an average value of about 4.9m (16 ft). (The hall radius is the distance from the source at which the direct and reverberant acoustic

fields make equal contributions to the sound pressure levels). This result suggests that the sound pressure levels will not differ much from those measured at locations 20 and 21. Thus, in the absence of flow, the sound levels throughout the test chamber will be about 5 dB below corresponding values on the tunnel centerline.

One inherent difficulty in interpreting the 4x7m data is the inability to unambiguously separate the sound propagating through the nozzle from that propagating "upstream" through the collector. To help clarify this matter, we examined unpublished data from out files in which a scale model free jet tunnel was tested. One test was a no-flow test similar to that described above, with a known sound source located near the fan. The chamber surrounding the nozzle and collector was anechoic and no floor plane was present. Otherwise, the general arrangement was quite similar to the chamber in the 4x7m tunnel, although the aspect ratio of the nozzle in the model was 30% greater than the 4x7. In the model tests, the direction of propagation could be isolated by alternatively blocking the nozzle and collector openings; thus, the directivity of each could be separated. Two sideline microphone locations were tested, one approximately 1.5 nozzle widths to the side of the centerline, midway between the nozzle and collector planes, and another above the nozzle at a distance from the centerline equal to 1.5 times the nozzle height.

The data from the model are shown in Figure B.14, scaled in frequency to correspond to full scale dimensions. When the propagation is via the nozzle, the sideline and overhead levels are 7-9 dB below the centerline levels; when the propagation is via the collector, the corresponding reductions are 3 to 9 dB.

Since the field points tested in the model are almost in the geometric far field of the openings, these data can be normalized to a constant distance from the center of the openings to determine the approximate "directivity" indices. Figure B.15 shows the results of such scaling, along with the azimuthal locations of microphones 19, 20, 21 and 22 in the 4x7 tests. Also shown is a data point for the 4x7 normalized in a similar way. The results are consistent and clearly illustrate that off-axis propagation of noise originating in the tunnel circuit will result in lower levels than that on-axis, the reductions being a function of azimuth and frequency. Note that in a room which is relatively reverberant, such as the 4x7 test chamber, the full impact of directivity effects will not be observable, but that in an anechoic or semi-anechoic chamber, the effects can be used to advantage when designing experiments in which low background noise is essential. At this point we have not considered the effects of shear layer refraction in modifying the above results.

REFERENCES

(for Appendix B)

1. Ver, I.L., "Acoustical Evaluation of the NASA Langley V/STOL Wind Tunnel", NASA CR-145087, 1976.

Exhaust tower

8000 H.P. drive system

Fan and hub

Screens

Control room

Reentry bell

Air-inlet

Flow control vanes

Model preparation and
static test area
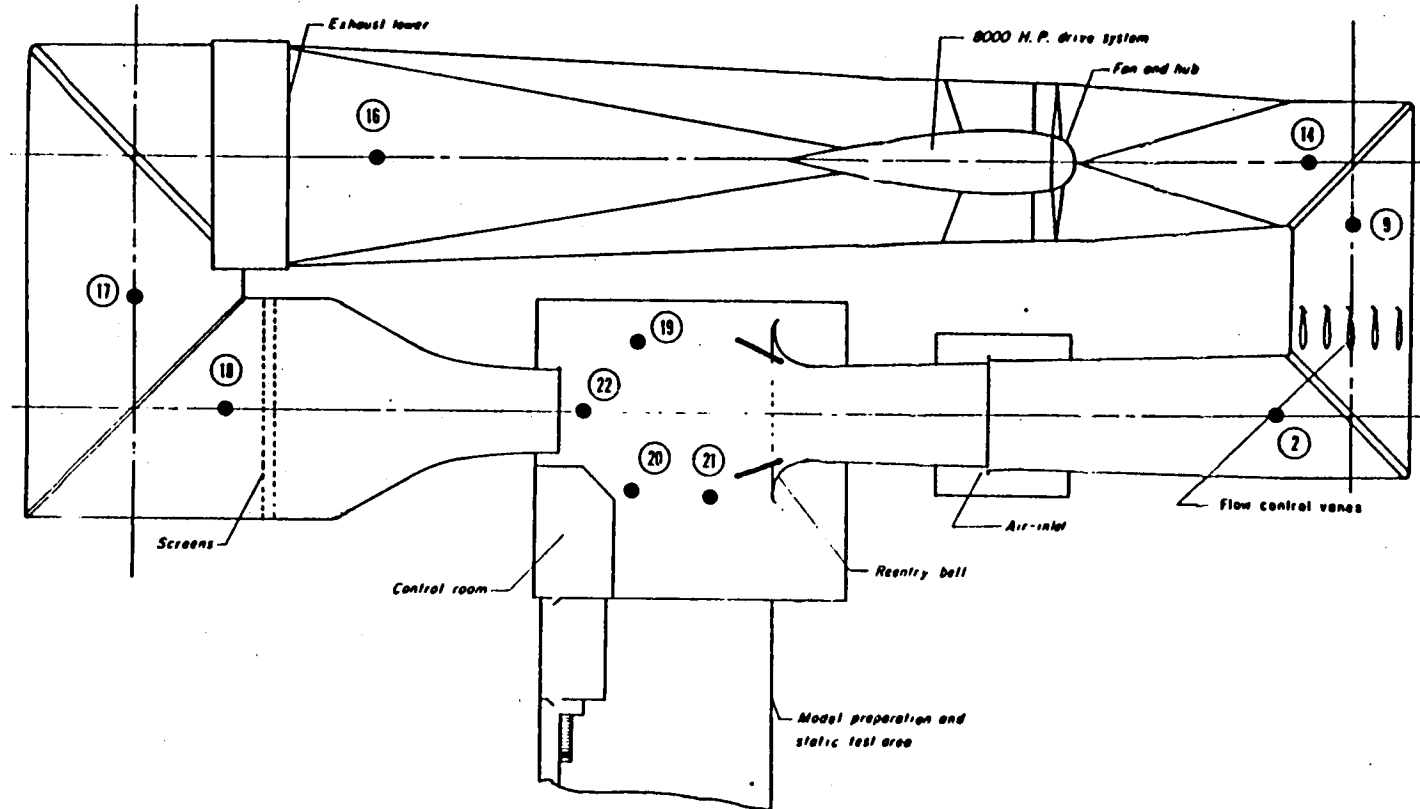
**FIGURE B.1 MICROPHONE LOCATIONS FOR STEADY-STATE NOISE PROPAGATION
TESTS (TEST 2)**

Exhaust tower
8000 H.P. drive system
Fan and hub
30°
30°
2-2
2-1
30°
30°
2-3   30°
30°
Screens
Air inlet
Flow control vanes
Control room
Reentry bell
Model preparation and
static test area
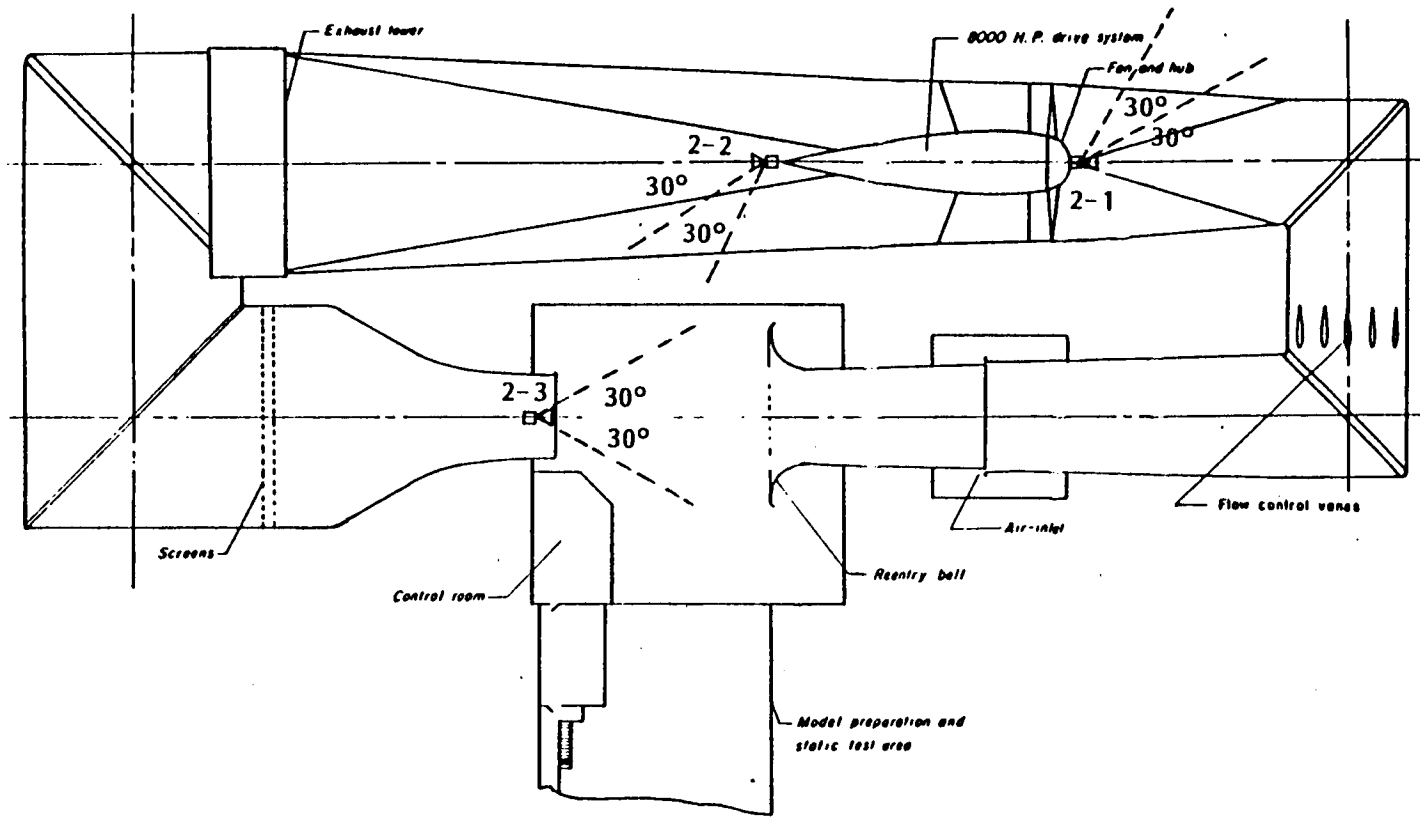
FIGURE B.2 SOURCE LOCATIONS FOR STEADY-STATE NOISE PROPAGATION
TESTS (TEST 2)
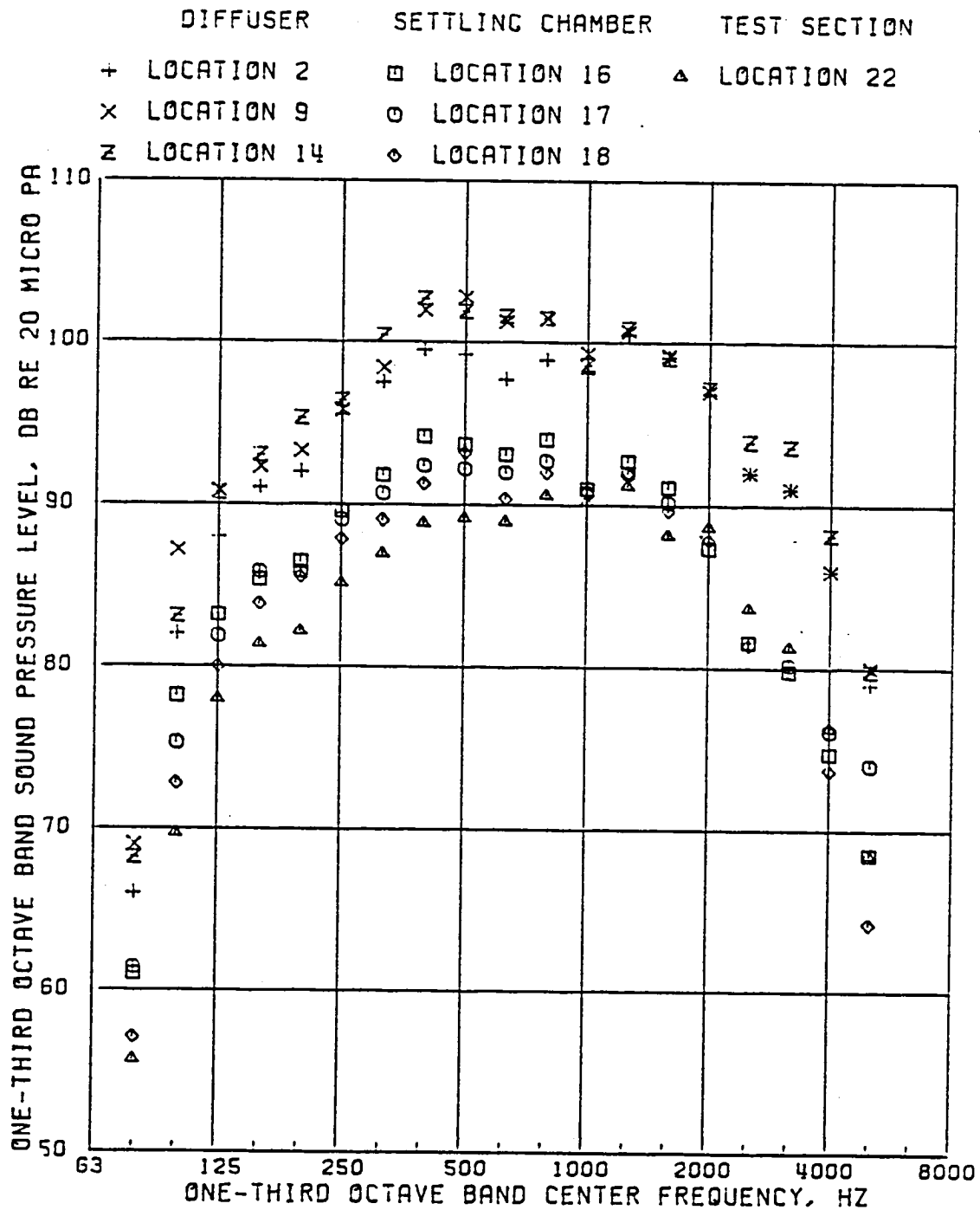
FIGURE B.3 SOUND PRESSURE LEVELS MEASURED IN TUNNEL WITH
SOURCE CONFIGURATION 2-1
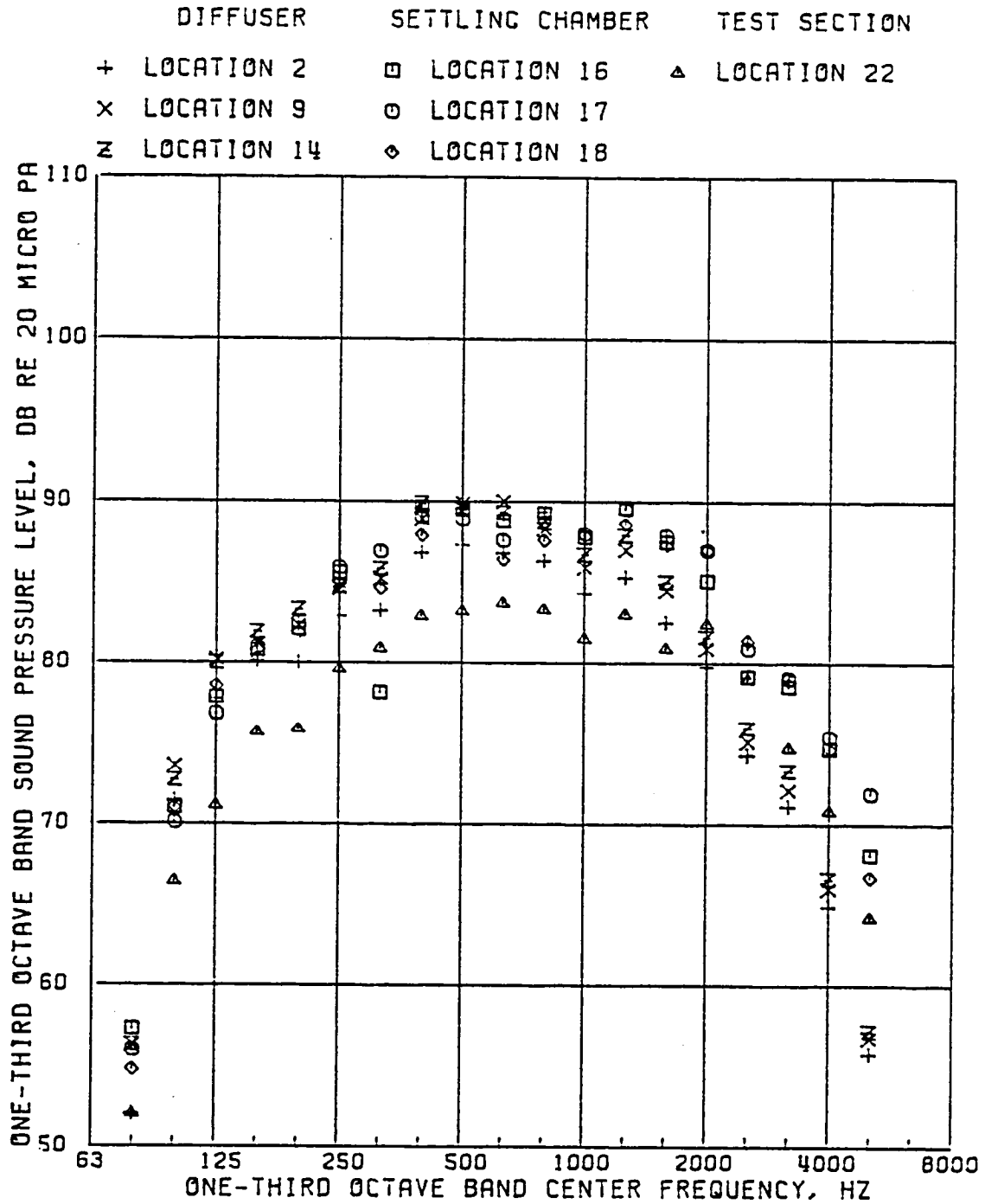
FIGURE B.4 SOUND PRESSURE LEVELS MEASURED IN TUNNEL WITH SOURCE CONFIGURATION 2-2

FIGURE B.5 SOUND PRESSURE LEVELS MEASURED IN TUNNEL WITH
SOURCE CONFIGURATION 2-3
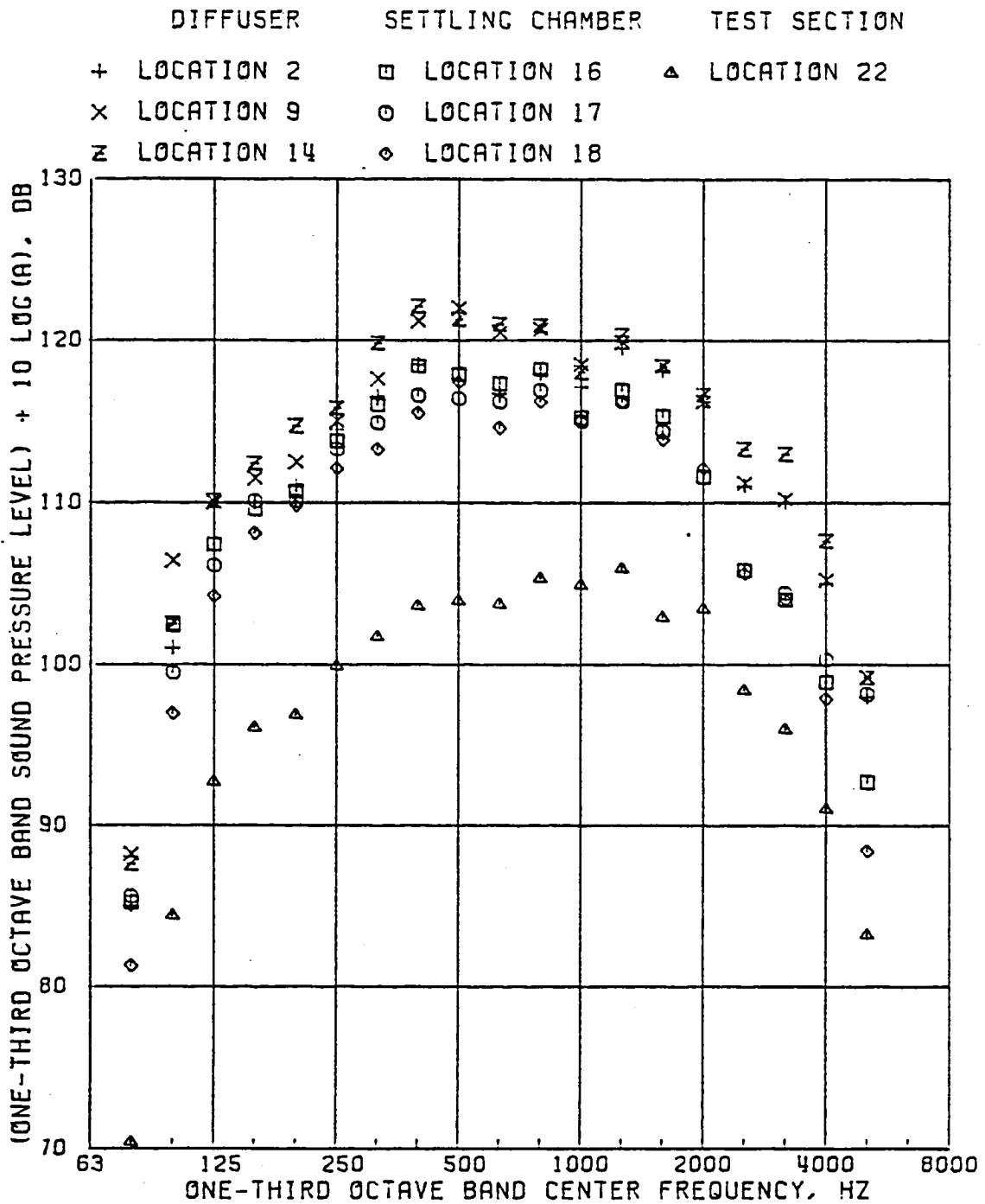
FIGURE B.6 SOUND LEVELS IN TUNNEL ADJUSTED FOR TUNNEL AREA
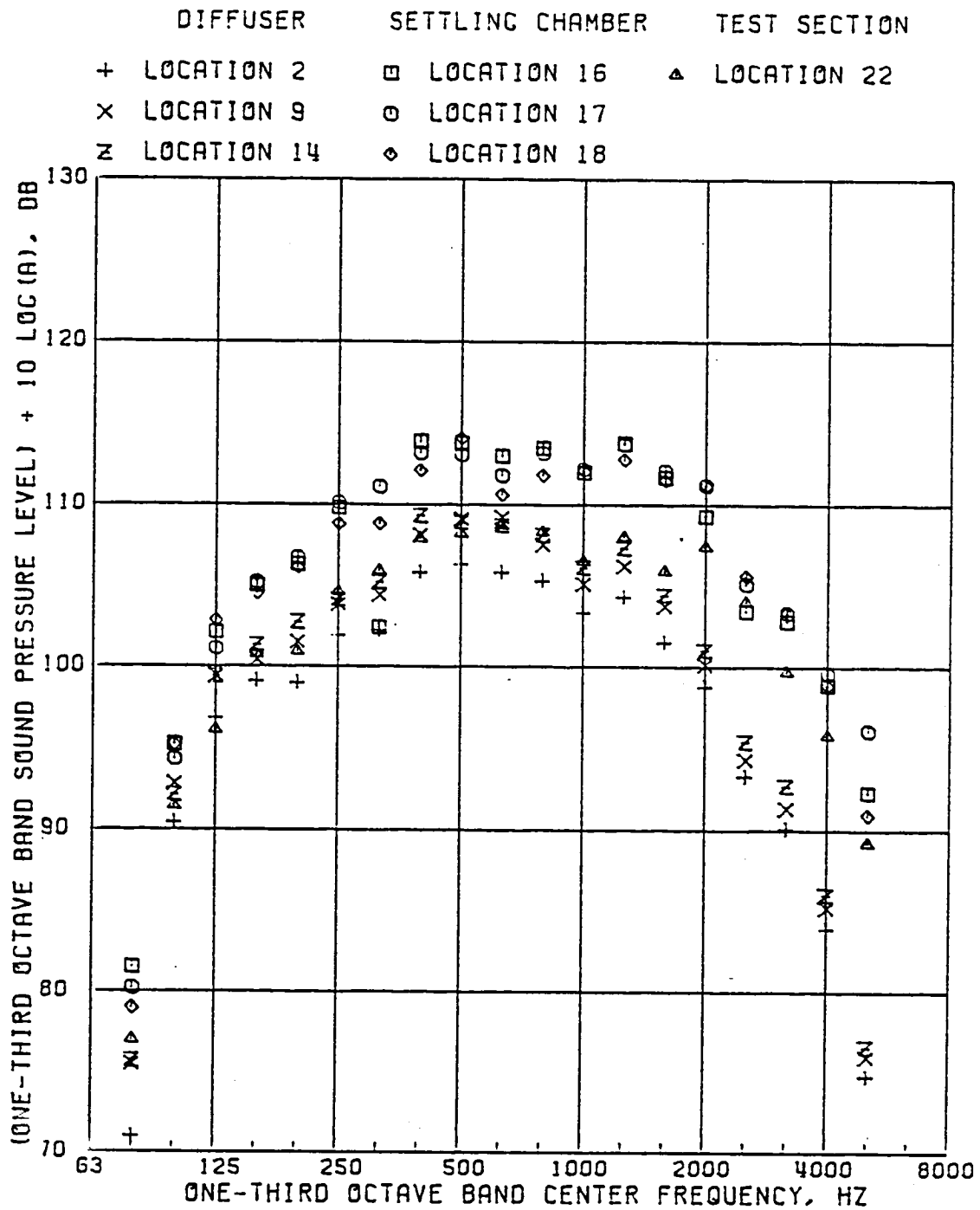(SOURCE CONFIGURATION 2-1)

(a) Test Section Area Used For Microphone 22

B-14

DIFFUSER   SETTLING CHAMBER   TEST SECTION

+ LOCATION 2   ⊡ LOCATION 16   ▲ LOCATION 22
✕ LOCATION 9   ⊙ LOCATION 17
☒ LOCATION 14   ◇ LOCATION 18
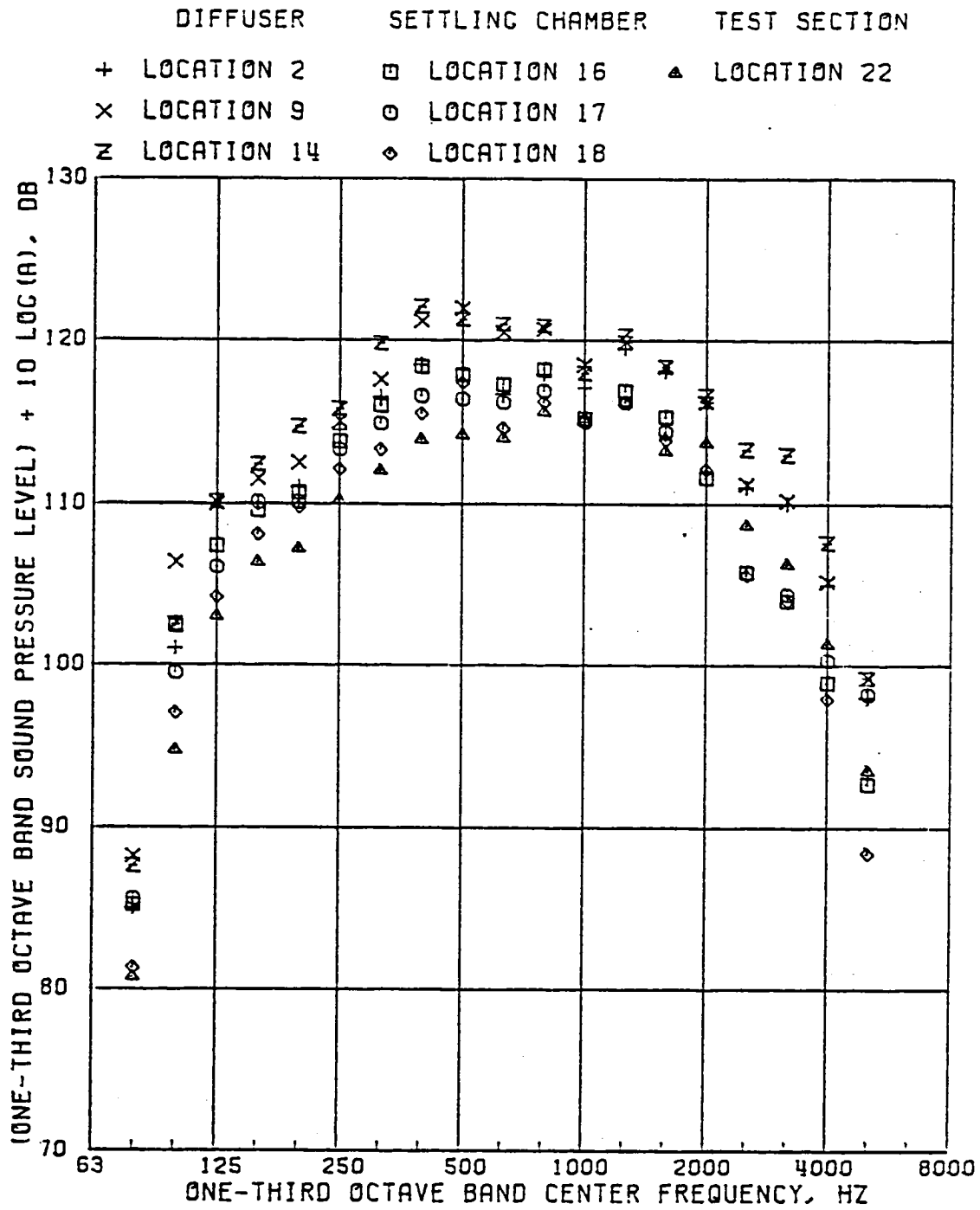
FIGURE B.6 Continued

(b) Test Chamber Area Used For Microphone 22

B-15
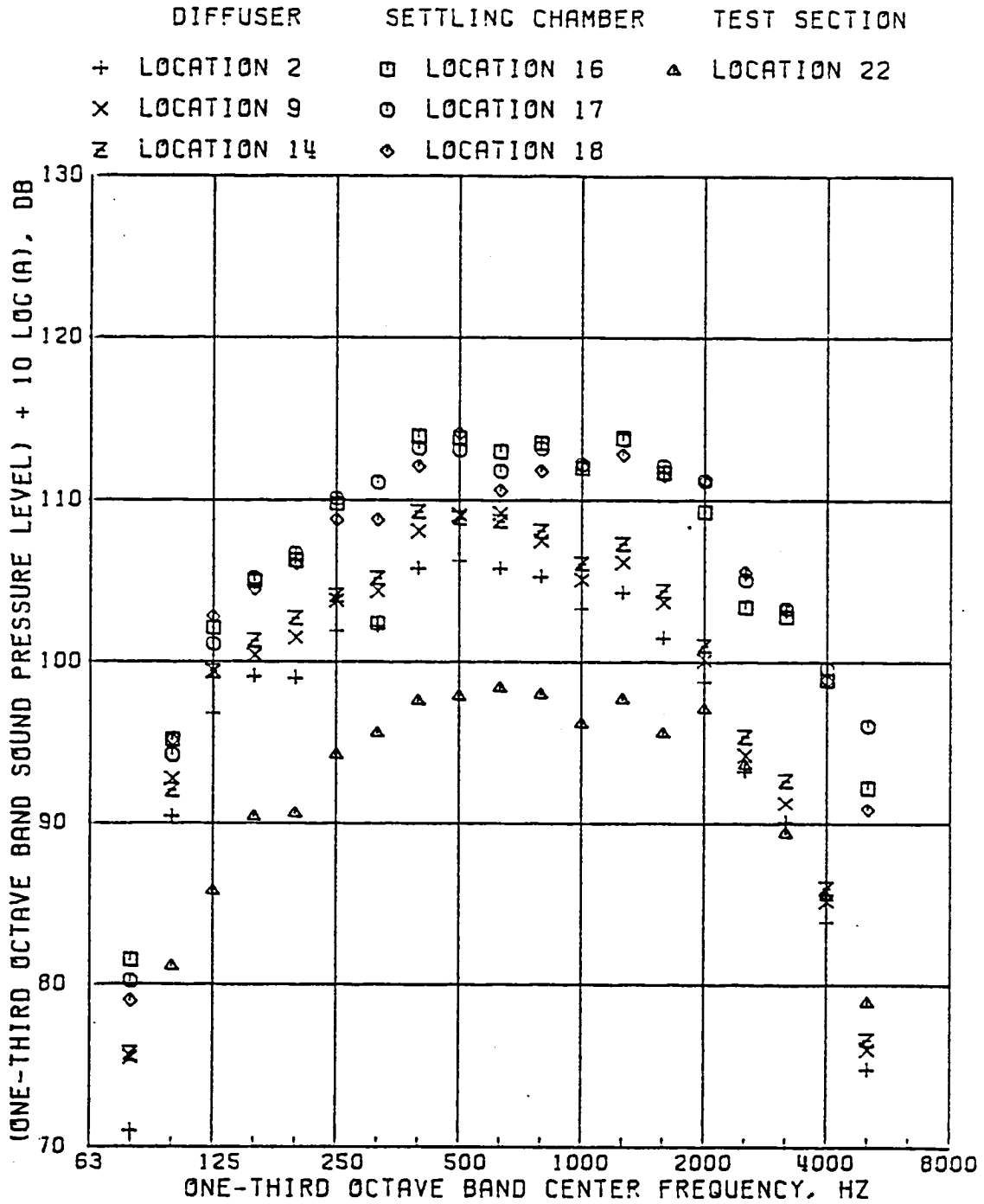
FIGURE B.7 SOUND LEVELS IN TUNNEL ADJUSTED FOR TUNNEL AREA
(SOURCE CONFIGURATION 2-2)

(a) Test Section Area Used For Microphone 22

B-16

DIFFUSER   SETTLING CHAMBER   TEST SECTION

+ LOCATION 2   ⊡ LOCATION 16   ▲ LOCATION 22

X LOCATION 9   ⊙ LOCATION 17

Z LOCATION 14   ◇ LOCATION 18

FIGURE B.7 Continued

(b) Test Chamber Area Used For Microphone 22
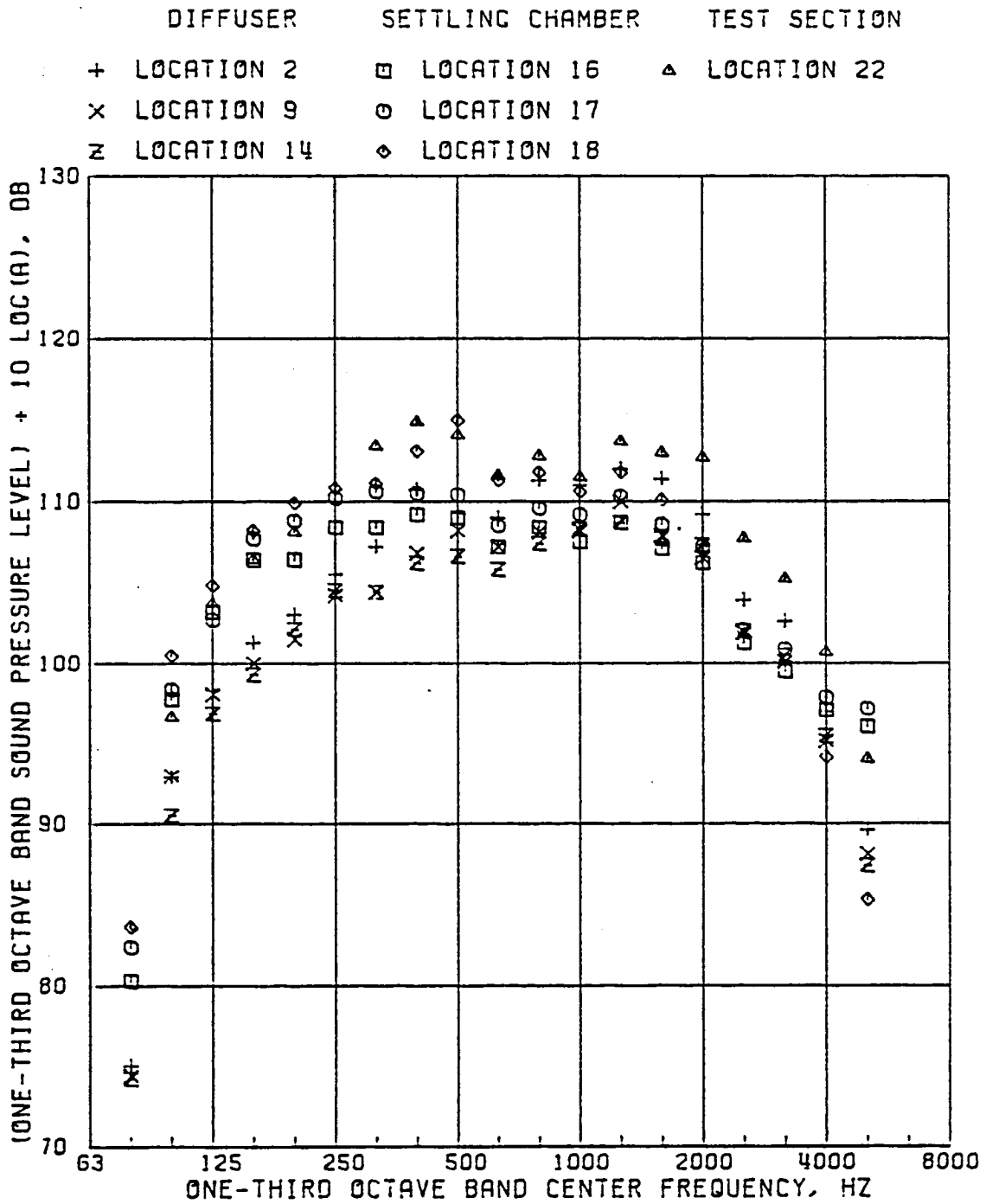
FIGURE B.8 SOUND LEVELS IN TUNNEL ADJUSTED FOR TUNNEL AREA
(SOURCE CONFIGURATION 2-3)
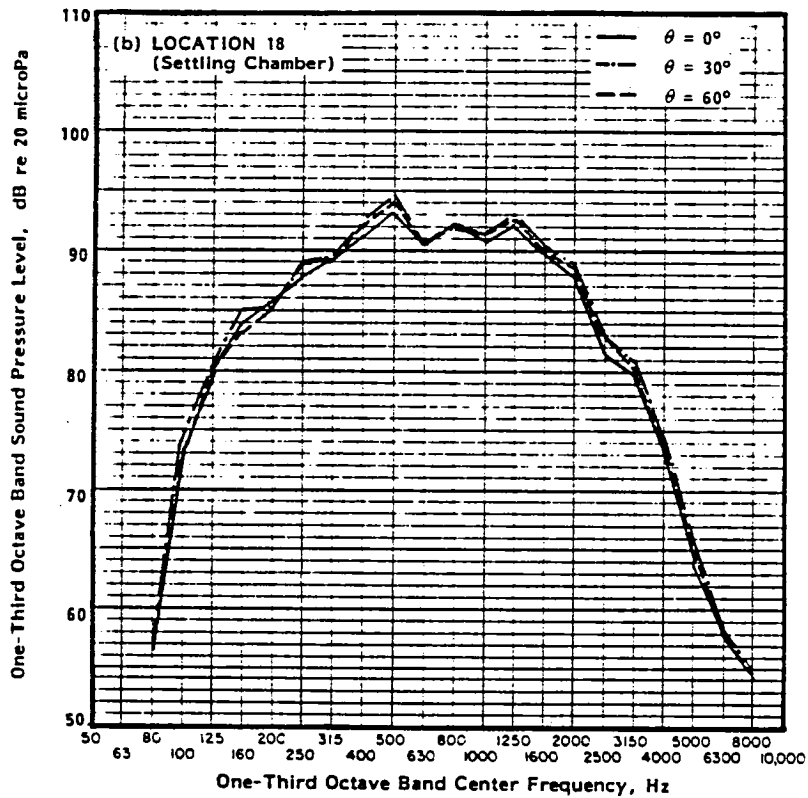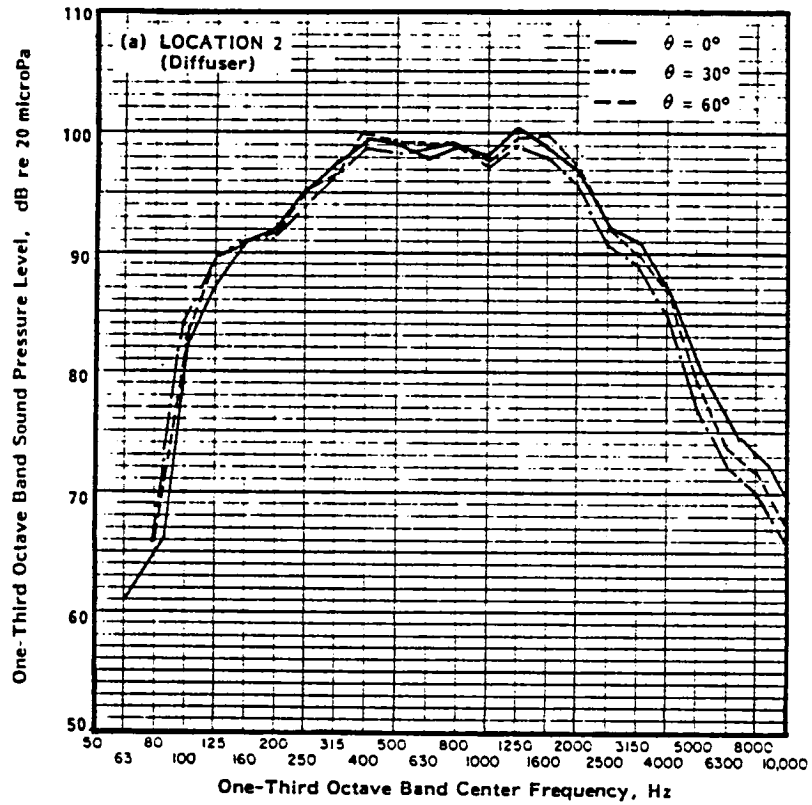
FIGURE B.9. SOUND LEVELS IN TUNNEL WITH SOUND SOURCE AT DIFFERENT ANGLES TO TUNNEL CENTERLINE (CONFIGURATION 2-1)
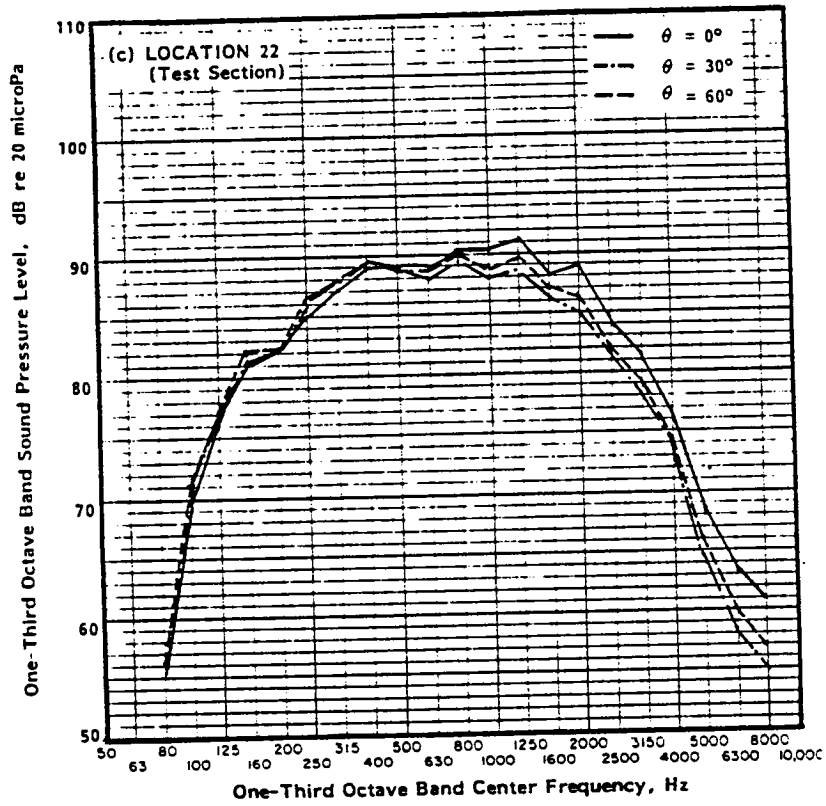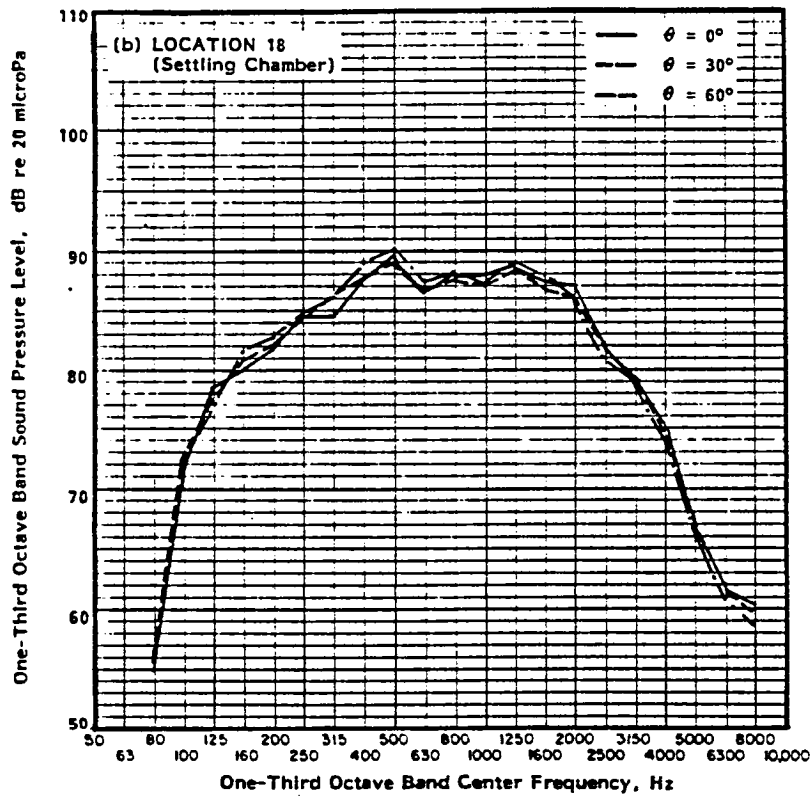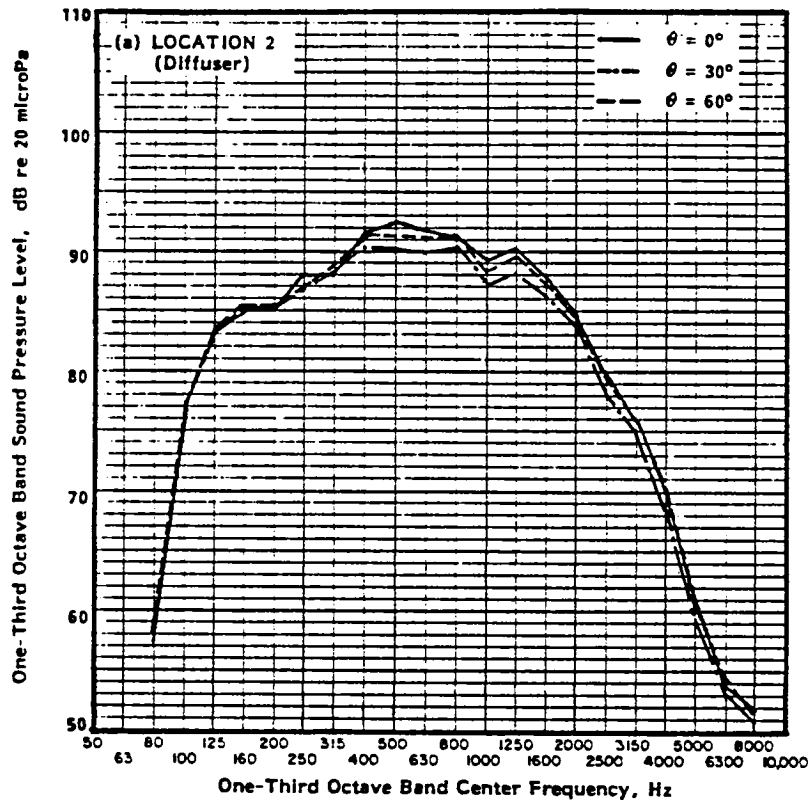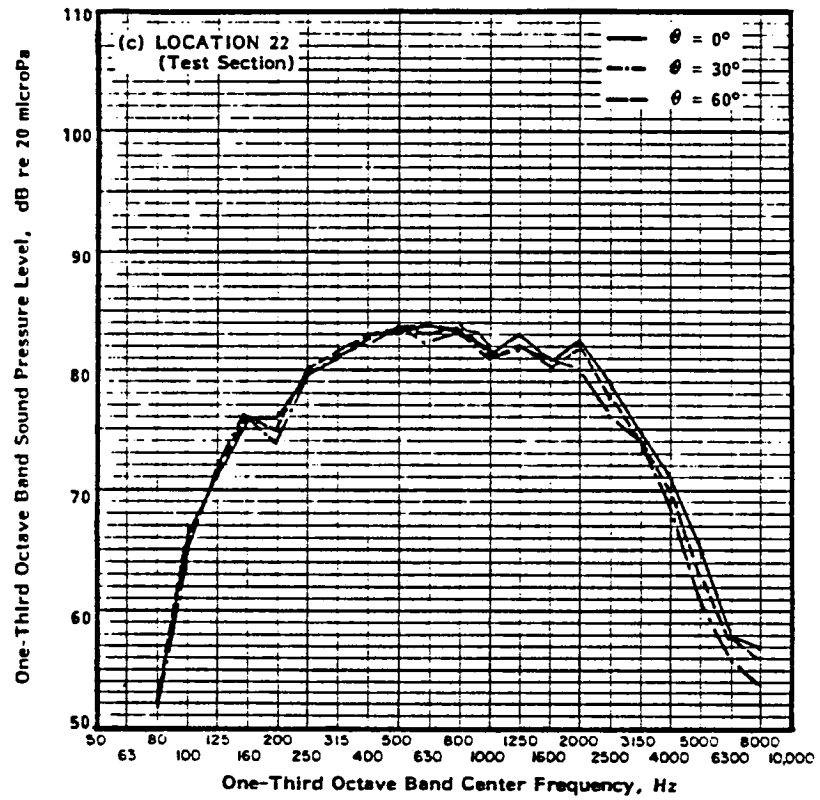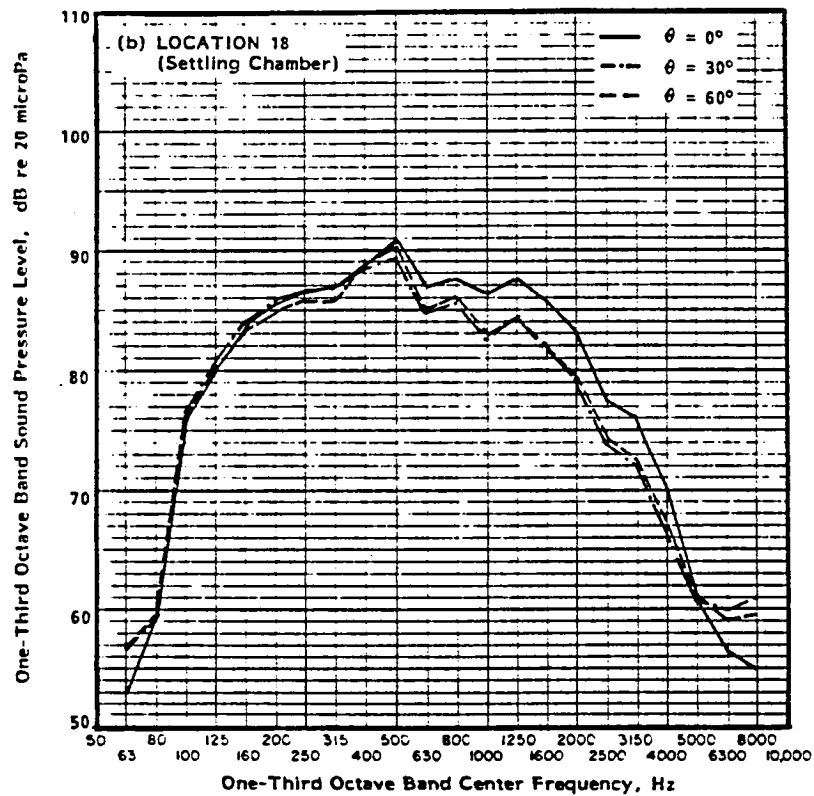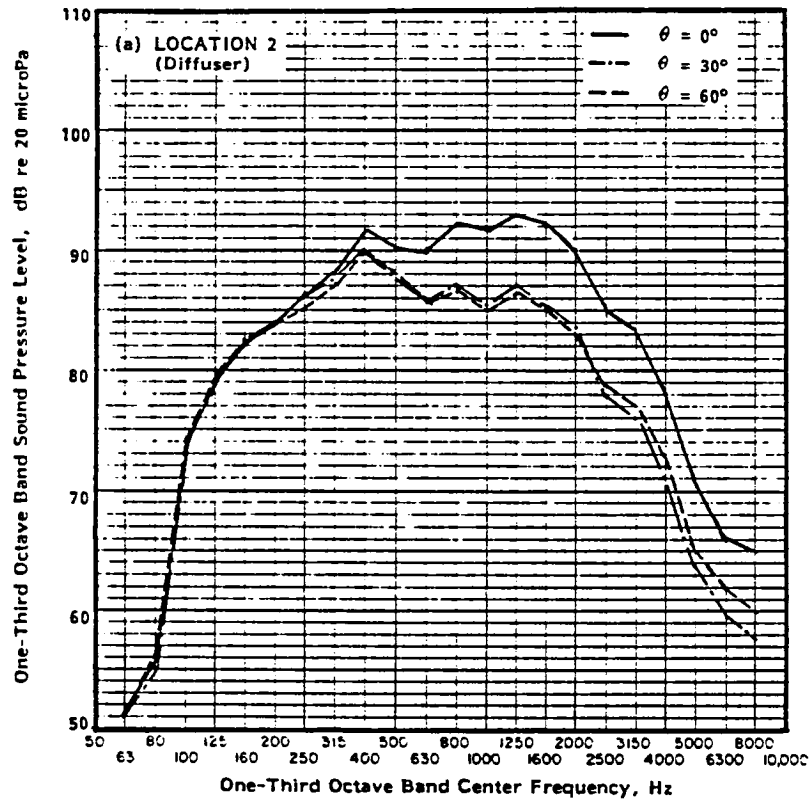
FIGURE B.9.   CONTINUED

FIGURE B.10.   SOUND LEVELS IN TUNNEL WITH SOUND SOURCE AT
DIFFERENT ANGLES TO TUNNEL CENTERLINE
(CONFIGURATION 2-2)

B-21

FIGURE B.10. CONTINUED

FIGURE B.11. SOUND LEVELS IN TUNNEL WITH SOUND SOURCE AT DIFFERENT ANGLES TO TUNNEL CENTERLINE (CONFIGURATION 2-3)
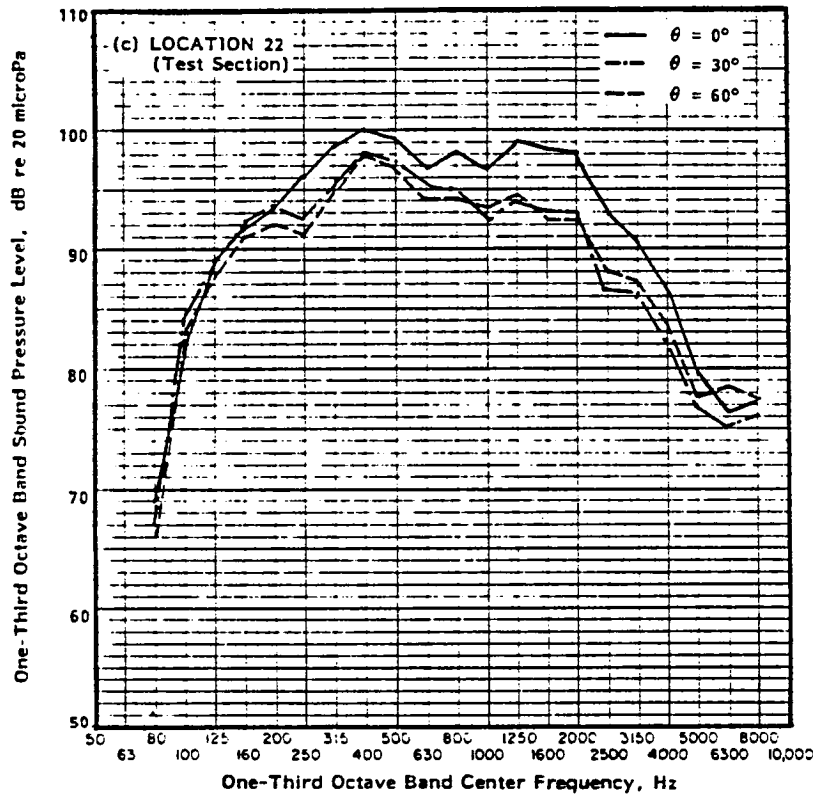
B-23

FIGURE B.11.   CONTINUED
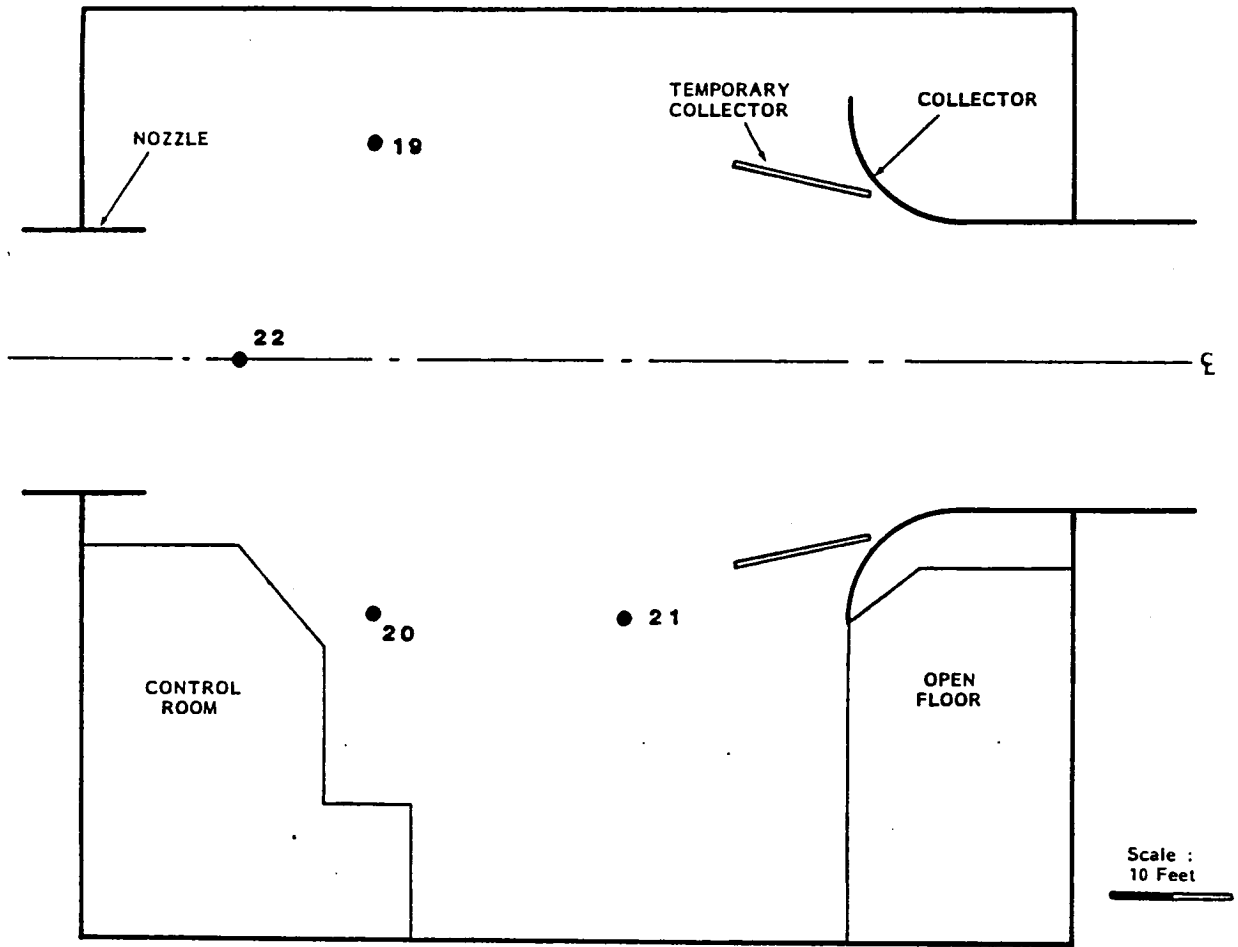
B-24

NOZZLE

●19

TEMPORARY
COLLECTOR

COLLECTOR

22

€

CONTROL
ROOM

●20

●21

OPEN
FLOOR

Scale :
10 Feet

FIGURE B.12 MICROPHONE LOCATIONS IN TEST SECTION/CHAMBER
FOR TEST 2

The graph shows:
- Y-axis: ONE-THIRD OCTAVE BAND SOUND PRESSURE LEVEL RELATIVE TO CENTERLINE LEVEL (dB), ranging from -30 to 30
- X-axis: ONE - THIRD OCTAVE BAND CENTER FREQUENCIES IN Hz (31.5 to 8000)
- Curve labeled: 4 x 7 m TUNNEL – NO FLOW; AVG OF 3 MICROPHONES 6.1 m (20.2 ft) FROM TUNNEL CENTERLINE
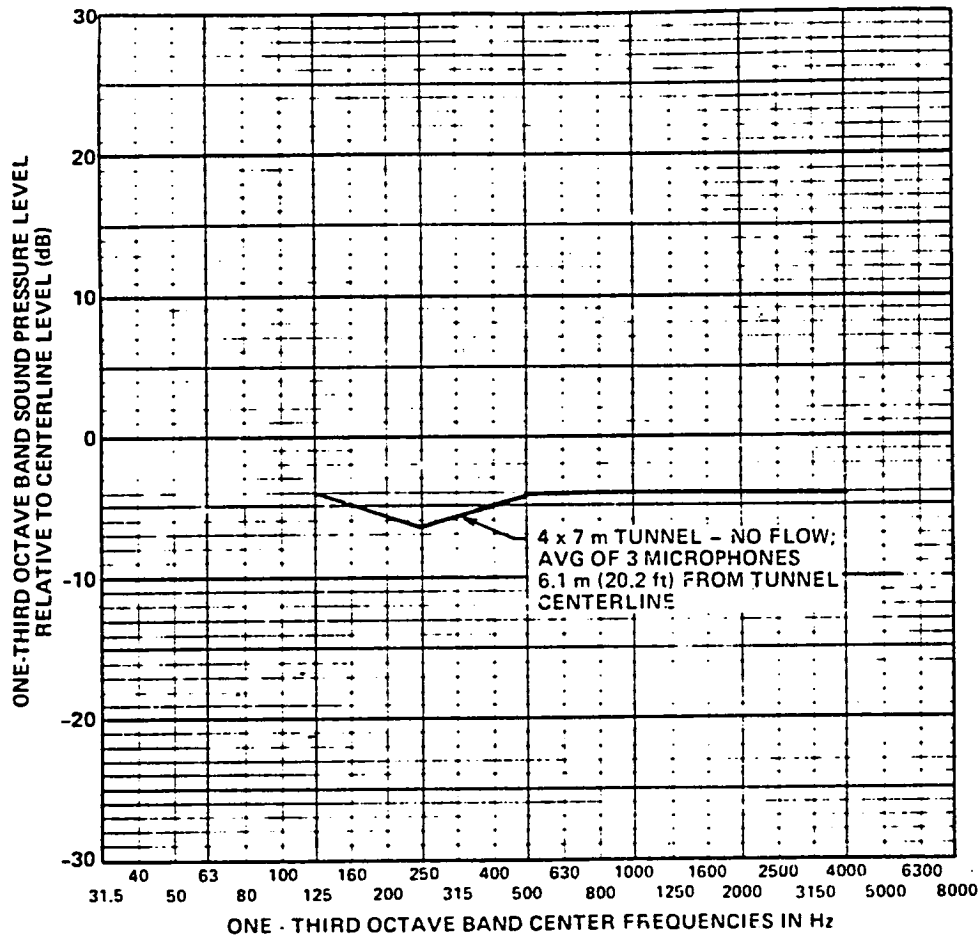
FIGURE B.13.   DIFFERENCE BETWEEN SIDELINE AND CENTERLINE SPL'S IN 4X7 M TUNNEL TEST SECTION WITH NO FLOW AND WITH AN ACOUSTIC SOURCE LOCATED IN THE TUNNEL CIRCUIT.
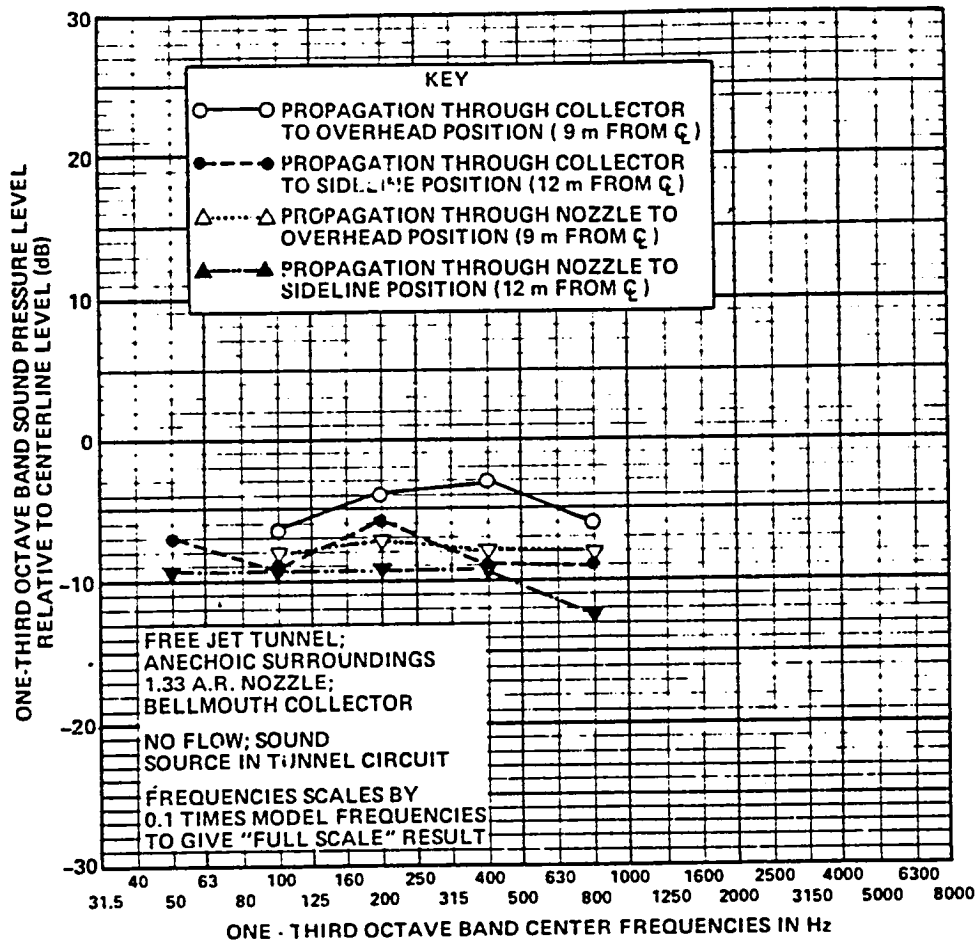
B-26

FIGURE B.14. DIFFERENCE BETWEEN SIDELINE, OVERHEAD AND CENTERLINE SPL'S FOR MODEL FREE JET WIND TUNNEL WITH NO FLOW AND A KNOWN ACOUSTIC SOURCE LOCATED AT THE FAN.
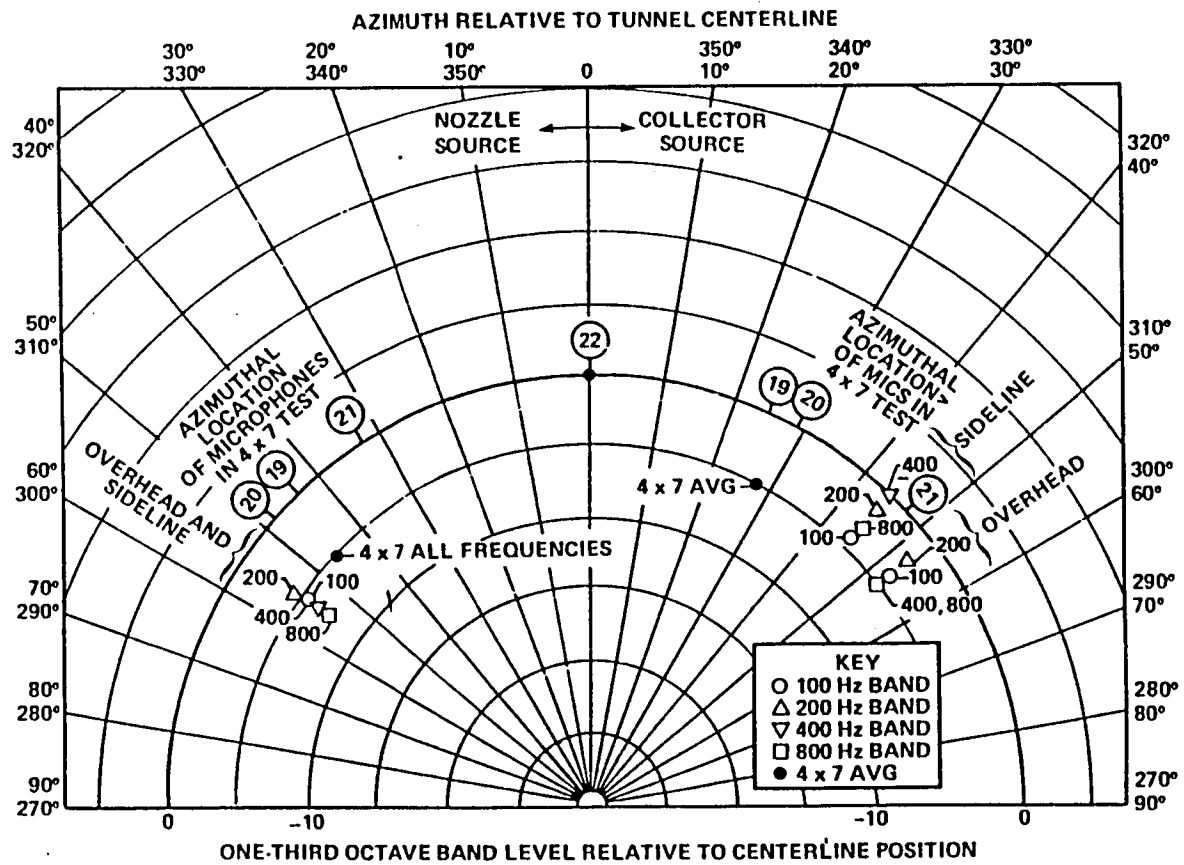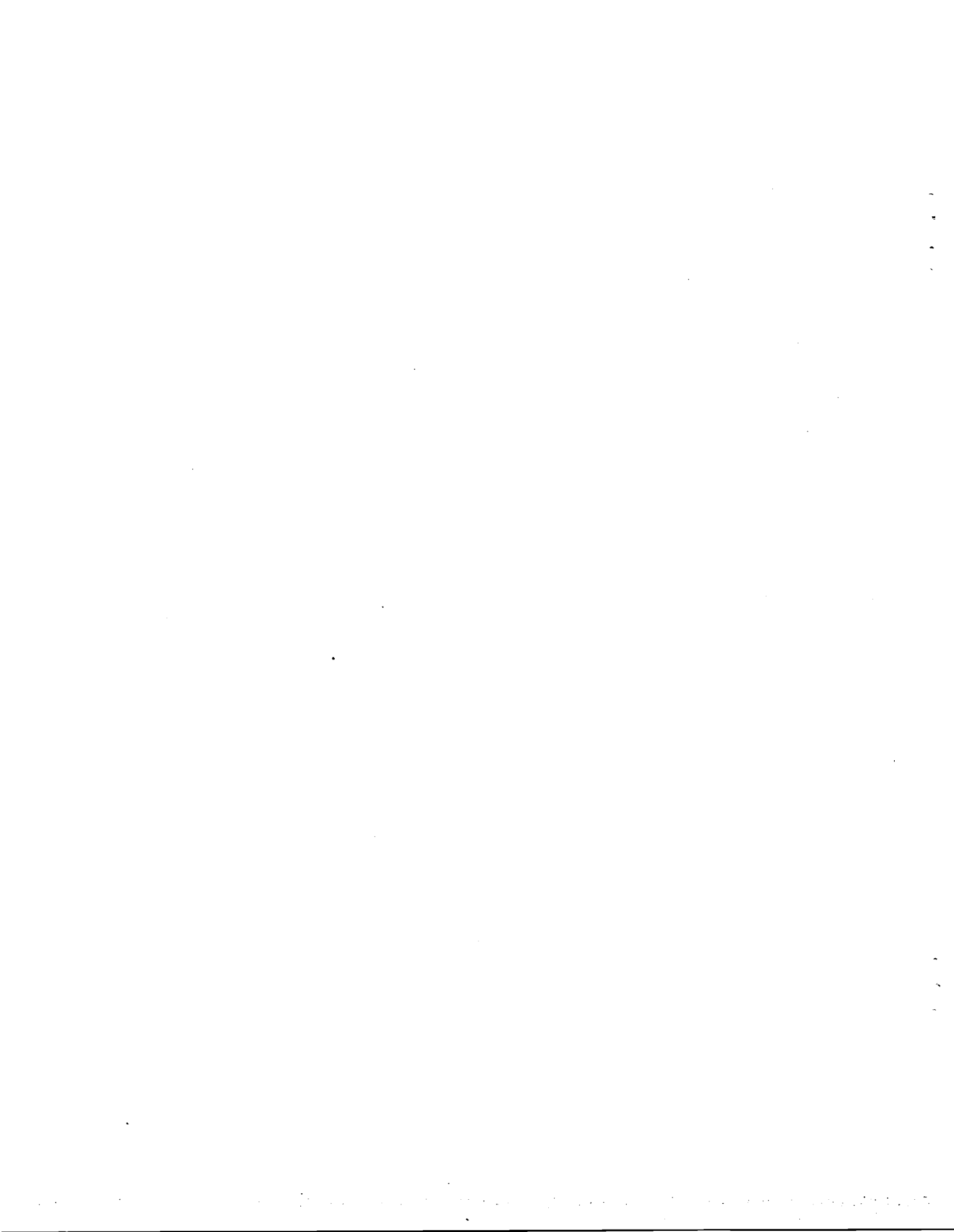
FIG. B.15 "DIRECTIVITY" OF WIND TUNNEL NOZZLE AND COLLECTOR WITH
BROADBAND SOURCE IN CIRCUIT FAR REMOVED FROM OPENINGS.

APPENDIX C

IMPULSE TESTS

APPENDIX C

IMPULSE TESTS

An impulsive source was used to facilitate the assessment of absorption inherent in various parts of the tunnel. The use of an impulsive source can (in principle) also provide information on the relative strengths of different paths around the circuit.

The source used was a yachting cannon which was fired at five different locations around the circuit, shown in Fig. C.1. The time history of the resultant acoustic signal was recorded for microphones located around the circuit, also shown on Fig. C.1. A typical time history shows a buildup of acoustic energy, followed by a short period of nearly constant overall levels (waves are arriving from many different modes) and then a long period of decay. A plot of level vs time is shown in Fig. C.2 for a typical location.

The reverberation time (T_R) determined from these plots is summarized in Table C.1. From these data, average absorption coefficient, $\bar{\alpha}$, can be determined by:

$$\bar{\alpha} = \frac{0.161V}{S \ T_R} \tag{C.1}$$

where V is the volume of the portion of the tunnel circuit of interest (m^3)

S is the surface area of the segment (m^2)

T_R is the reverberation time (sec)

$\bar{\alpha}$ is the average Sabine absorption coefficient.

The tunnel circuit was divided into two major segments defined by elements of similar character and the absorption calculations performed using the above expression (the fan and test section

C-1

were used to divide the tunnel into two parts). The results are summarized in Table C.2 for each "half" of the circuit. No results for the test section are presented here inasmuch as the reverberation measured there probably was dominated by reverbera-tion from the circuit for those positions at which measurements were made. Also presented in Table C.2 is the difference between power level (PWL, dB re 10^{-12} w) and space-averaged sound pressure level (SPL, dB re 2×10^{-5} N/m^2), which is useful in interpreting acoustic data measured in the circuit as well as in applying calculated source levels to the circuit.

TABLE C.1. REVERBERATION TIMES – CANNON IN 1ST DIFFUSER DOWN-STREAM OF TEST SECTION.

T_R, Reverberation Time (Sec)

Octave Band Center Frequency (Hz)	No. 2 First Corner	Microphone Number and Position			
		No. 14 Upstream of Fan	No. 17 Settling Chamber	No. 21 Test	No. 19 Section
D/A	8.1	8.5	13.4	7.5	8.6
125	7.4	8.3	10.6	6.6	8.4
250	8.6	8.6	13.6	9.2	8.8
500	8.4	9.5	13.9	10.3	9.6
1000	7.0	8.8	11.3	9.1	8.4
2000	4.8	6.3	7.7	6.4	5.9
4000	3.2	3.8	4.9	4.3	3.9
8000	1.8*	1.7*	2.9*	4.6	4.6

*Decay taken very early in decay record, i.e., probably mostly "local" reverberation. All other decays taken later in delay record, i.e., "total tunnel" reverberation.

TABLE C.2. APPROXIMATE ABSORPTION COEFFICIENTS.

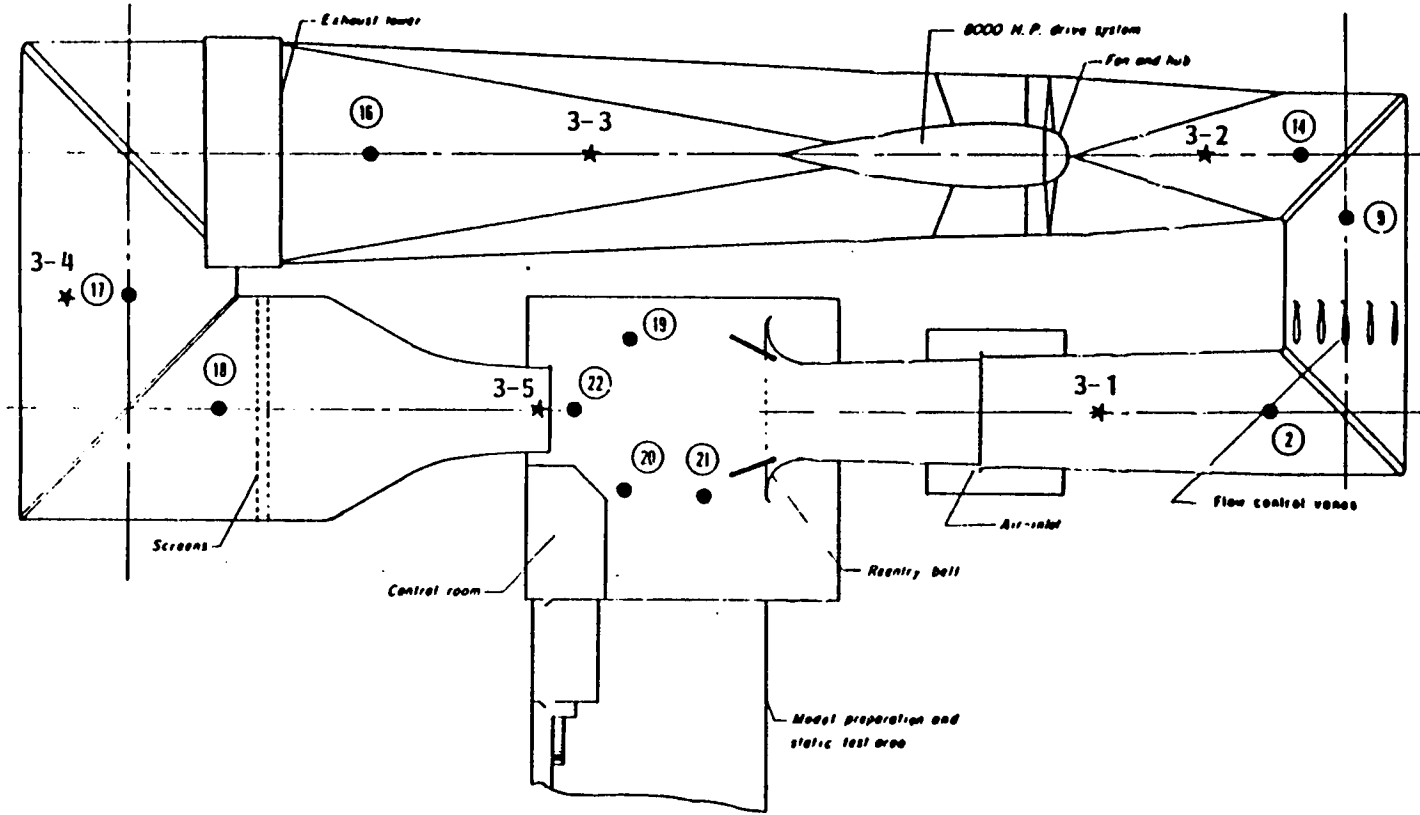| Octave Band Center Frequency (Hz)	Absorption Coeff ($\bar{\alpha}$) (Sabines)		PWL-SPL (dB)	
	1st & 2nd Diff	Settling Chamber	1st & 2nd Diff	Settling Chamber
OA	.065	.044	14.3	16.0
125	.070	.056	14.6	17.0
250	.063	.044	14.1	16.0
500	..061	.043	14.0	15.9
1000	.070	.052	14.6	16.7
2000	.100	.077	16.1	18.4
4000	.157	.121	18.1	20.4
8000	.320	.205	21.1	22.7

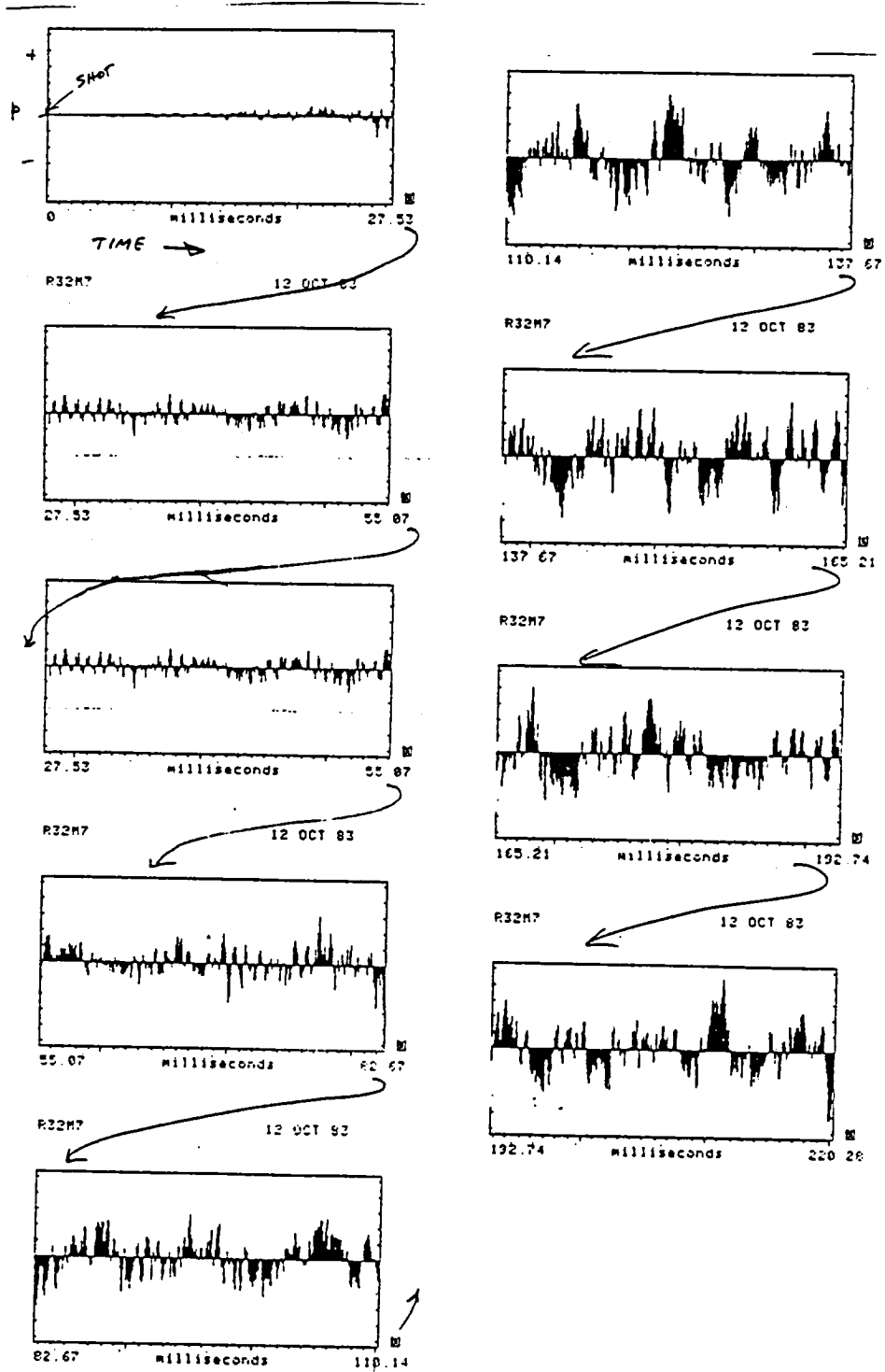FIGURE C.1 MICROPHONE AND SOURCE LOCATIONS FOR IMPULSIVE SOUND
TESTS (TEST 3)

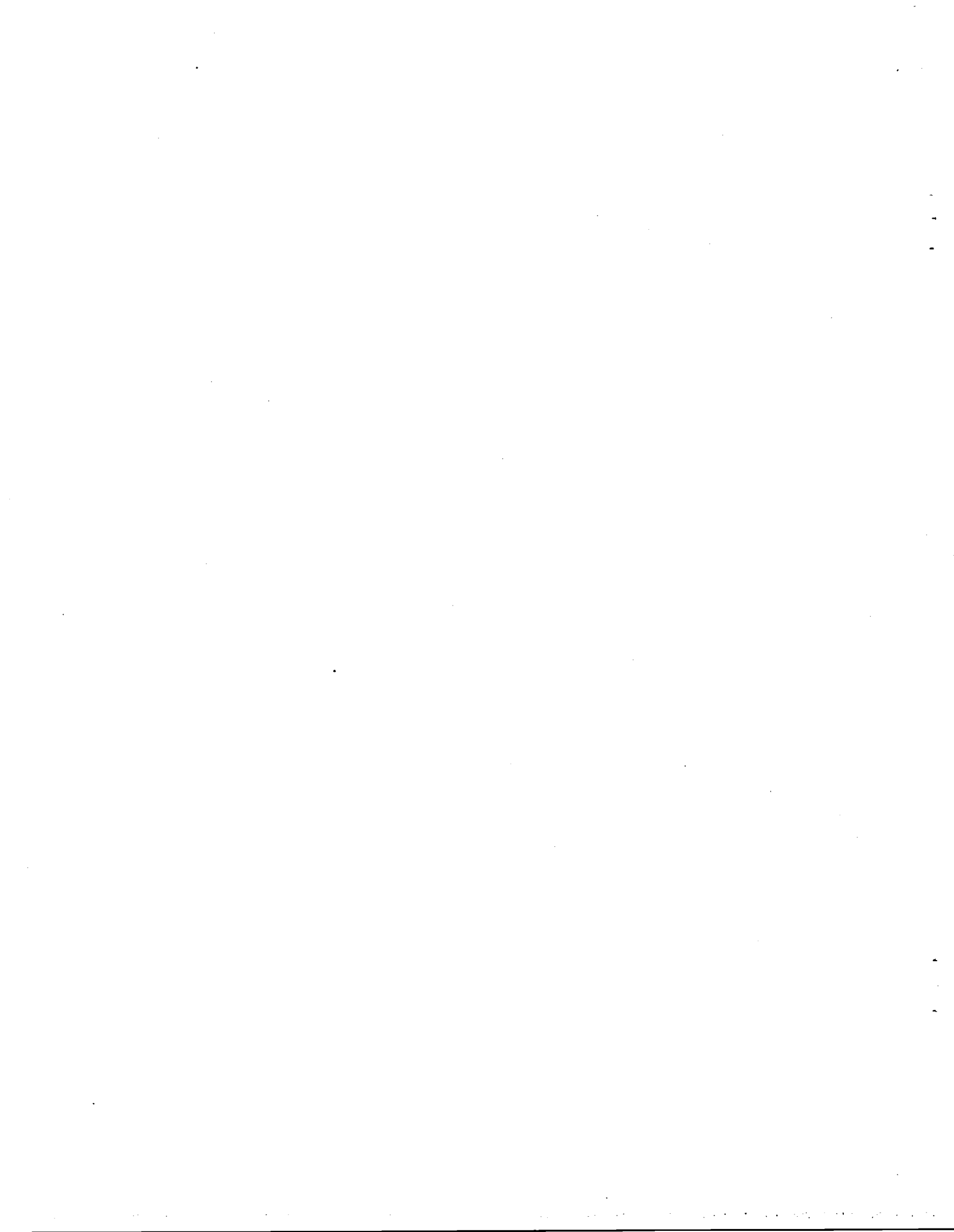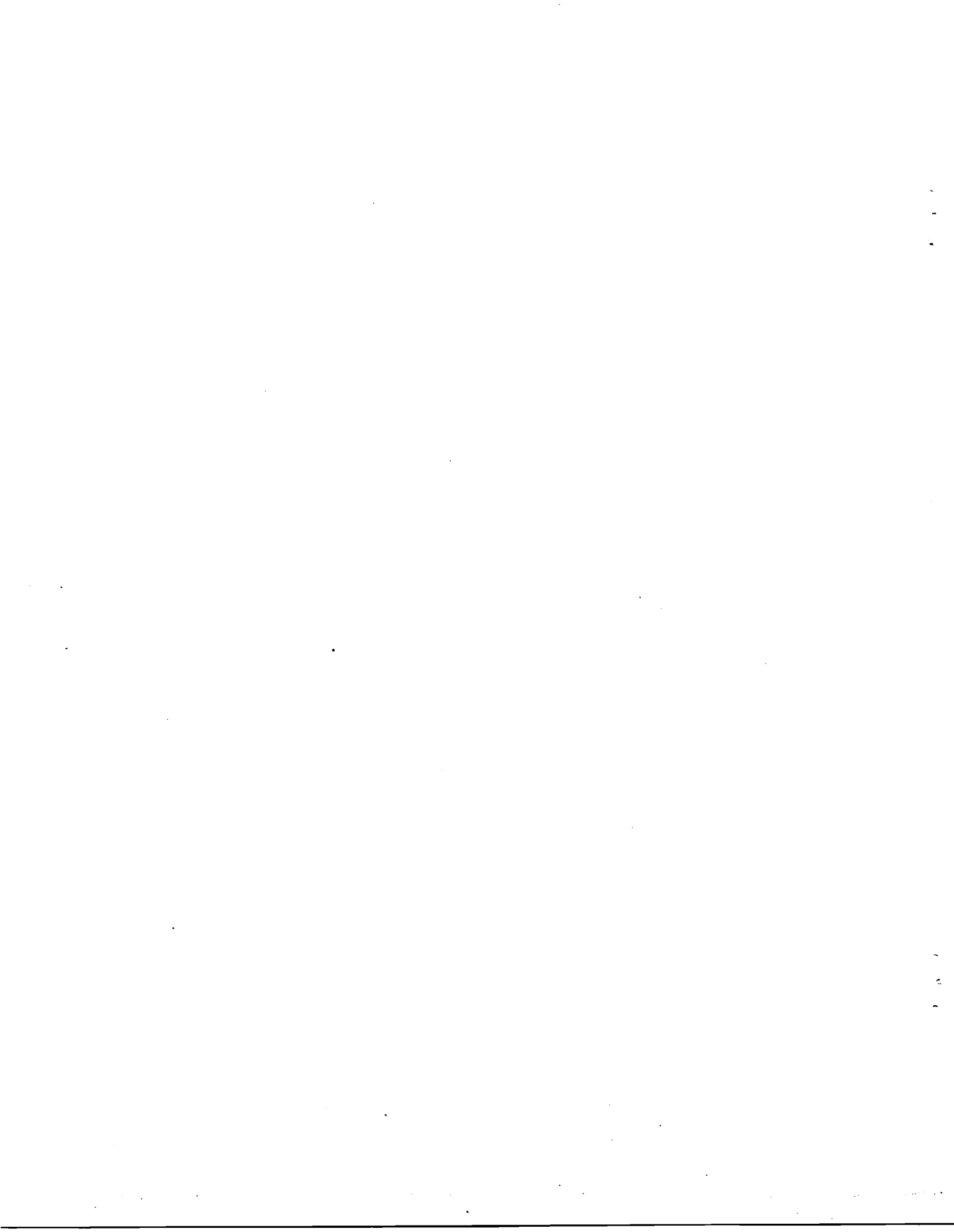FIGURE C.2 TYPICAL INITIAL TIME HISTORY OF SOUND ARRIVING
AT TEST SECTION MIC 22 (CANNON SHOT AT FIRST CORNER)

APPENDIX D

COHERENCE AND PHASE SPECTRA

APPENDIX D
COHERENCE AND PHASE SPECTRA

D.1. Introduction

It has been demonstrated in the NASA Ames 7 x 10-foot wind tunnel [D1, D2] that measurements of the pressure cross-spectral density function by two closely-spaced microphones can provide information regarding the propagating, diffuse and reverberant components of the tunnel acoustic field. The cross-spectral information is presented in terms of the coherence function (which is the square of the magnitude of the cross-spectral density function normalized with respect to the two associated auto-spectra) and the cross-spectrum phase angle.

In principle [D2-D4], the coherence and phase spectra can distinguish between propagating, diffuse and reverberant components in the pressure field and can account for mean flow in the same, or opposite, direction to the acoustic propagation direction. Furthermore, the spectra can be used to distinguish between two propagating components. The terms "diffuse" and "reverberant" are both used in the discussion and have different meanings, although the resulting effects on the measured data may be similar. The term "diffuse" is used to define an acoustic field generated by a multitude of uncorrelated sources, whereas "reverberant" describes the acoustic field generated by, say, a single source in a reverberant chamber.

In practice, the detailed interpretation of measured coherence and phase spectra poses a number of problems. Foremost of these is the effect of reverberation. Under idealized circumstances when the measurement frequency bandwidth is small enough that it contains the resonance frequencies of only one or two modes, and when the integration time is at least as long as the

reverberation time, the coherence function for a reverberant field will be essentially unity (with certain localized losses of coherence at certain frequencies when the transducers are at node points). However, it is often impractical to perform the data reduction in this manner Then, if the analysis bandwidth contains several mode resonance frequencies (i.e., mB<<1 where B is the resolution bandwidth and m the modal density for the acoustic modes in the reverberant space) the coherence function will take on the characteristics of a diffuse field [D4]. Also if the data reduction is performed by means of a fast Fourier transform analyzer in which the integration time is directly related to the upper frequency of interest, the integration time may be very short relative to the reverberation time. For example, the integration time for the Spectral Dynamics SD360 Digital Signal Processor is only 0.1 sec when the upper frequency limit for the data reduction is 5000 Hz. This integration time is only 1%, approximately, of the corresponding reverberation times in the 4 x 7 m tunnel.

Other problems in data interpretation are concerned with the presence of acoustical energy propagating upstream and downstream in the wind tunnel. The general slope of the phase spectrum will indicate the direction of the propagation of the dominant signal, but the detail shape of the spectrum will have to be studied in order to estimate the relative magnitudes of the upstream and downstream components. When the shape of the phase angle spectrum is influenced also by the diffuse and reverberant contributions, an accurate breakdown of the components is difficult.

D.2. Summary of Analysis

A review of the data analysis methods is given in references D1 and D2. Thus, only a brief statement will be provided here. The general approach is to calculate coherence and phase angle

spectra for different combinations of values for the important parameters, and to compare the predicted spectra with measurements. The two main combinations investigated are propagating/diffuse/noise and upstream propagation/downstream propagation/noise where noise represents unwanted components in the two data signals.

The relationships for the coherence (γ^2) and phase (ϕ) functions associated with the combination of propagating, diffuse and noise components is given by

$$\gamma^2 = \{ (\frac{R \sin\phi_o}{\phi_o} + \cos \phi_1)^2 + \sin^2 \phi_1 \}/(1 + R + G_n/G_p)^2 \qquad (1)$$

$$\phi = \tan^{-1} [\sin \phi_1 / (\frac{R \sin\phi_o}{\phi_o} + \cos \phi_1)] \qquad (2)$$

where $\phi_o = k_o d = 2\pi fd/c_o$

$\phi_1 = k_1 d = 2\pi fd/c_1$

$c_1 = \dfrac{c_o}{\cos (\theta-\alpha)} + \dfrac{U}{\cos \alpha}$

G_p = pressure auto-spectrum of propagating component

G_d = pressure auto-spectrum of diffuse component

G_n = auto-spectrum of noise component

$R = G_d/G_p$.

The general arrangement of the microphones with respect to the propagation and flow direction is shown in Figure D.1.

The corresponding equations for the case of signal 1 propagating downstream and signal 2, upstream in the absence of reverberant and diffuse components, are

D-3

$$\gamma^2 = \frac{G_1^2 + G_2^2 + 2\,G_1 G_2 \cos\,(\alpha_1 - \alpha_2)}{(G_1 + G_2 + G_n)^2} \tag{3}$$

$$\phi = \tan^{-1}\left[\frac{G_1\,\sin\phi_1 + G_2\,\sin\phi_2}{G_1\,\cos\phi_1 + G_2\,\cos\phi_2}\right]$$

$$\phi_i = 2\pi F d/c_i \;, \qquad c_i = \frac{c}{\cos\,(\theta_i - \alpha)} + \frac{U}{\cos\,\alpha} \tag{4}$$

Typical shapes of the coherence and phase spectral curves calculated by means of Eqs. (D1) and (D2) are shown in Figures D.2 and D.3, respectively. Representative phase spectra calculated by means of Eq. (D4) are shown in Figure D.4. In Figures D.2 and D.3 it is assumed that the acoustic propagation direction is along the tunnel centerline in the downstream direction; the flow speed is 20.6 m/s (67.6 ft/sec). Curves are drawn for different values of R, assuming that the noise (G_n) is zero. Introduction of noise will have no effect on the predicted phase but will reduce the predicted coherence at a given frequency. The phase spectrum in Figure D.4 shows the straight-line ramp where R = 0; deviations from the straight-line increase with R but at high frequencies the influence of the diffuse field is very small (although R has a large influence on the coherence).

Figure D.4 shows phase spectra computed for two propagating wave systems, one upstream and the other downstream with a flow speed of 41 m/s (135.1 ft/sec). Spectra are plotted for different ratio of G_1 to G_2, where suffix 1 denotes downstream propagation, and suffix 2, upstream. In this case the phase spectrum deviates from the straight-line ramp as G_1/G_2 tends to unity. When G_1/G_2 is greater than unity, the dominant propagation direction is downstream and the slope is negative.

D-4

D.3. Measurement Procedure

Two series of tests were performed. In one series, #6, an electro-acoustic sound source was placed at different locations in the tunnel circuit and noise propagation measurements were made under zero flow conditions. Then, in test series #7, noise propagation measurements were made under two flow conditions specified in terms of the flow speed in the test section; the flow speeds were 20 m/s (40 kts) and 41 m/s (80 kts).

Microphone locations in the tunnel circuit are shown in Figure D.5. Three locations (2, 7 and 14) were in the diffuser upstream of the fan, three (16, 17, and 18) in the settling chamber downstream of the fan, and two (19 and 22) in the test section. All the microphones, except location 19, were in the tunnel flow when the tunnel was operating. Each location shown in Figure D.5 represents a pair of microphones positioned in one of two alternative arrangements identified as Configuration A or Configuration B. The two arrangements are shown in Figure D.6. The microphones were always oriented so that they pointed in the upstream direction, even during Test 6 when there was no flow. B&K nose cones were fitted to the microphones for the flow-on tests. Configurations A and B were utilized for Test 7 but only Configuration A was used for Test 6. Microphone height above the tunnel floor was six feet at all locations except location 18 where the height was twelve feet.

Locations of the noise source for Test 6 were shown in Figure D.7. The locations, identified at Configurations 6-1, 6-2, and 6-3 were used. For Configurations 6-2 and 6-3 the horn of the source was pointing in the downstream direction; for Configuration 6-1 the source was pointing upstream. In addition, Configuration 6-2 was repeated with the source pointing upstream. (This orientation is identified as Configuration 6-2R.)

During the reduction of the data it was found that some of the signals were contaminated by a periodic noise component which affects the coherence and phase data, particularly at high frequencies. This was true particularly at locations 16 and 17 in the settling chamber. However, in only one case was the data sample completely lost. In other cases the noise contamination was restricted to frequencies above about 2500 Hz.

A second problem encountered in the data reduction was associated with the dynamic range of the tape recorder. On-line data reduction performed at the time of the tests showed that at some microphone locations a dynamic range of at least 60 dB was required in the frequency range 0 -5000 Hz. This could not be provided by the tape recorder, as a consequence coherence and phase data at high frequencies has to be disregarded at certain microphone locations. Evidence of this dynamic range problem is given, in part, by a sudden rise in the value of the coherence function and a change in character of the phase spectrum.

D.4 Technique for Application of Analytical Results to Data

The values of R and θ were determined by the trial fit of calculated phase angle curves to the measured data. Using the analysis described above, two families of phase angle curves were computed for a given pair of microphones and known mean flow speeds, one family being associated with upstream noise propagation and the other downstream. The computed spectra were superimposed on the measured spectrum and appropriate values of R and θ selected by visual inspection. For convenience it was assumed that θ remained constant over a frequency regime where φ changed gradually between ±π. Then θ was allowed to change to a different value for the next higher frequency regime, although in some cases it seemed reasonable to assume a constant value for θ. Because of the fluctuations in the data from frequency to

frequency, it is obvious that some subjective assessment had to be made in the data fit.

As will be shown below, and in Sec. 2 of the main body of the report, at frequencies above 2000 Hz, the computed phase angle and coherence spectra were relatively insensitive to assumed values for R. However, the convected pattern may still be well defined and values of θ could be assigned with reasonable precision (see, for example, Figs. 21 through 23). In other cases it was very difficult, if not impossible, to assign a value of θ to the data (e.g., Fig. 17) and in such cases it was sometimes assumed that θ remained constant as frequency increased. Corresponding straight-line curves were plotted on the measured spectra for qualitative comparison purposes.

D.5. Acoustic Source Test Results

The acoustic signal generated by the sound source was essentially broadband noise with a low frequency cut-off at 80 Hz and a high frequency cut-off at 5000 Hz. Representative narrowband spectra measured in the tunnel are shown in Figure D.8. The figure contains three pairs of spectra. However, for each pair the spectra collapse on top of each other since the microphones of each pair are close together.

Coherence and phase measurements were made at locations 2, 7, 14 and 22 for source configurations 6-1 and 6-3; measurements were made at locations 16, 17, 18 and 22 for configurations 6-2 and 6-2R. The resulting coherence and phase spectra are shown in Figure D.9 through D.12 for the frequency range 0 to 5000 Hz. The spectra were obtained from the ensemble average of 2048 overlapping samples, each sample having a length of 0.1 sec. The total length of the signal used in the analysis was 3.75 minutes; the frequency resolution of the spectral analysis was 10 Hz.

(Note that instrumentation noise contaminates high frequency data for locations 16 and 17 in Figure D.11.)

The phase angle spectra are plotted such that the phase angle lies between $+\pi$ and $-\pi$. Consequently, when the phase angle fluctuates around either $+\pi$ or $-\pi$ the plotting pen performs excursions across the entire ordinate direction of the figure causing a series of full-sweep plots which tend to confuse the general trend of the data.

Discussion regarding the interpretation of coherence and phase data has been given in SectionS D.2 AND D.4. The results can now be applied to the test data. The situation is one in which there is essentially a single source in a large reverberant environment, although there is the likelihood of noise propagation around the tunnel into the test section, with subsequent dissipation.

If the environment was truly reverberant, the frequency resolution sufficiently small that only one or two acoustic modes were contained in each frequency band, and the integration time equal to the reverberation time (i.e. an order of magnitude greater than the integration time 0.1 sec actually used), then the coherence should be almost unity. In contrast, Figures D.9 through D.12 contain the coherence spectra which generally show the (sin kd)/kd type of relationship associated with a diffuse field. However, the data are useful in "calibrating" the coherence and phase spectra in terms of the effective value of R introduced by the data reduction process. These "calibration" values of R can then be used for comparison with "flow-on" test data.

The acoustic test data are also valuable in calibrating the phase spectrum slope in terms of propagation direction, since the location of the noise source is well-defined. Inspection of the spectra in Figures D.9 through D.12 shows that a negative slope

is indicative of downstream propagation of the sound and a positive slope indicates upstream propagation. This information will be used in the interpretation of the flow-on results.

There are other properties of the coherence and phase spectra which are worthy of note. The highest coherence throughout the frequency range of interest was measured at location 22 with the source configuration 6-3 (Figure D.12). The high coherence is associated with a strong propagating field - the microphone is close to the noise source and the test chamber is not as highly reverberant as the tunnel circuit. The phase spectra confirm the interpretation of a strong propagating acoustic field.

When the sound source is placed in the tunnel circuit (Configuration 6-1 or 6-2) the phase spectra show some indication of a propagating component in the sound field at the microphone locations closest to the source (location 14 for configuration 6-1 and location 16 for configuration 6-2). As the measurement position moves away from the source the evidence of propagating component in the sound field decreases and the phase spectra take on the random characteristics of a reverberant environment.

D.6 Flow Test Results

The microphone locations used for the coherence and phase tests in the presence of flow are shown in Figure D.5. The measurements were made in two parts. For test 7-1, the microphone pairs were located in the tunnel diffuser at locations 2, 7, and 14, and in the test section at location 22. Then, for test 7-2, the microphones were located in the settling chamber at locations 16, 17 and 18 and in the test section location 19, out of the flow. The microphone pairs were positioned with the microphone axes parallel to the tunnel centerline, as shown in Figure D.6, except for location 14 where the axes were inclined

to the tunnel centerline. The angle between the microphone axes
and the tunnel centerline was determined by NASA personnel on the
basis of their information regarding the mean flow direction at
that location in the tunnel.

Pressure spectra at different locations in the tunnel were
measured for a range of tunnel flow speeds under a separate
test. The measurements indicate that the spectra are essentially
broadband in character but that, at the lower speed (20 m/s)
there is evidence of discrete frequency components at about 300
Hz and multiples thereof. These are generated by the oil pump in
the fan motor housing. Also, the pressure spectra measured in
the test section show some contributions associated with noise
generation due to flow over the microphone support hardware.

In the case of the coherence and phase tests, it is of
particular interest to establish that the pressure signals are
essentially identical at both microphones of a given pair. In
general, the signals are, for all practical purposes, identical,
as shown in Figure D.13. The exception is microphone 22 in the
test section, where the spectra show differences in the frequency
range below about 1500 Hz. The trailing microphone spectra con-
tain certain peaks which are not found in the spectra for the
leading microphone; the discrepancies are greater when the
lateral separation has its smaller value. These results suggest
that, for the high flow speeds encountered at this location, the
trailing microphone measures pressure fluctuations due to flow
disturbances at the leading microphone. These fluctuations may
be aerodynamic or acoustic in nature, but if they are acoustic
the directivity is such that the signals are not observed at the
lead microphone. Furthermore, the coherence data suggest that
the signals are not highly correlated.

The spectra indicate that the measured data at locations in the diffuser contain relatively more low frequency energy than elsewhere. It is believed, as is discussed later, that the low frequency levels are due to aerodynamic self-noise. Whatever the cause, however, these high levels exacerbate the signal-to-noise ratio problems of the recorded data. Thus, for example, data for location 2 is of little value above about 2000 Hz and for location 7 above about 3000 Hz.

Coherence and phase spectra measured during operation of the tunnel are shown in Figure D.14 through D.21 for the eight microphone locations shown in Figure D.5. Data are shown for two flow conditions and two microphone arrangements except for location 17 where data for one run had to be discarded because of instrumentation noise problems.

The coherence spectra show a rapid decay in the value of the coherence function as frequency increases; however, indications of a (sin kd)/kd type of pattern in a similar number of cases such as at location 16 when the flow speed is 41 m/s (80 kts). At locations 16, 17 and 18 in the settling chamber, where the flow speeds are very low (less than 5 m/s) and at location 19 which is in the test section but outside the flow, the coherence approaches unity at low frequencies, as is predicted in the absence of noise contamination of the signals. However, when the microphones are in regions of higher flow speed the maximum value of the coherence function decreases, presumably because of the effect of aerodynamic self-noise which is uncorrelated between the two microphones of a given pair. Thus, at location 7 where the average local flow speeds are approximately 7.3 m/s (24 ft/sec) and 14.6 m/s (48 ft/sec) for the two test conditions, the maximum value of the coherence function is 0.8 to 0.9. At location 2, where the flow speeds are essentailly the same as at location 7, the maximum coherence is about 0.5 at the higher

speed and 0.25 at the lower speed (neglecting the influence of pump noise components). This is further evidence that self-noise induced by flow fluctuations in the first stage diffuser, is significant at microphone location 2, at least for low frequencies. Loss of coherence due to steady-state mean flow self-noise effects would be responsible only to the extent observed at location 7.

In the test section (location 22), where the flow speeds are the highest for a given tunnel condition, the maximum value of the coherence function lies in the range 0.7 to 0.9. The discrepancy between these values and values closer to unity is probably due to uncorrelated aerodynamic self-noise induced by the mean flow (and any baseline turbulence) in the test section - as was discussed earlier with respect to Figures D.13(f) and (g).

The pressure signals measured at microphone location 14 contain intermittent fluctuations which are probably due to flow disturbances. Also the coherence at low frequencies has lower values than at locations 7 and 22, although they are higher than at location 2. Flow fluctuations are probably present here also. It is interesting to note that the lowest coherence occurs at the lower flow speed at location 2 and at the higher flow speed at location 14. This is probably indicative of the flow conditions within the tunnel as flow speed changes.

Inspection of the phase spectral slope indicates the presence of a dominant acoustic propagation path in the downstream direction into the settling chamber and an upstream propagation path through the diffuser. However, at the entry to the contraction between the settling chamber and the test section, the acoustic field appears to be mainly reverberant. At the nozzle exit into the test section (location 22) the dominant propagation path is in the downstream direction for frequencies

below about 750 Hz, and upstream at higher frequencies. As a general trend, the propagating wave pattern in the phase spectra is more clearly defined at the higher speed for both microphone configuration. This is true even in the settling chamber where the flow speeds are very low. A satisfactory explanation for this phenomenon has not yet been found.

The identification of a dominant propagation path should not be construed as an indication that all the propagating acoustic energy travels in one direction. It is possible that there is propagation in both the upstream and downstream directions at any given location. The phase spectra identify only the direction of the net flow of acoustic energy. The ratio of power spectra densities for the downstream and upstream components may be close to unity. This is particularly important for the test section sound levels where it is estimated that there may be only 3 dB to 6 dB difference between the upstream and downstream propagating components.

REFERENCES

D1. Wilby, J.F., et al, "Coherence and Phase Techniques Applied to Noise Source Diagnosis in the NASA Ames 7x10-foot Wind Tunnel No. 1", NASA CR-152039 (1977).

D2. Wilby, J.F., and A.G. Piersol, "Coherence and Phase Techniques Applied to Wind Tunnel Acoustics", AIAA Paper 77-1306 (1977).

D3. Markowitz, A.E., "Cross-spectral properties of some common waveforms in the presence of uncorrelated noise", NUSC Technical Report 4947 (1975).

D4. Piersol, A.G., "Use of Coherence and Phase Data Between Two Receivers in Evaluation of Noise Environments", _Journal of Sound and Vibration_, 56, 2, 215-228 (1978).
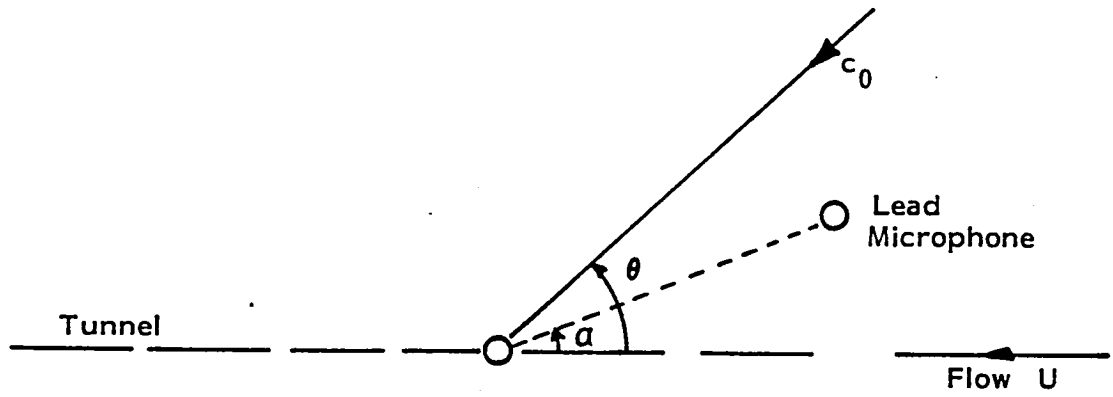
FIGURE D.1   GENERAL ARRANGEMENT OF TRANSDUCERS WITH FLOW AND
             PROPAGATING ACOUSTIC WAVES

D-15

Microphone Configuration A   U = 20 m/s (68 ft/sec) $\theta = \alpha$
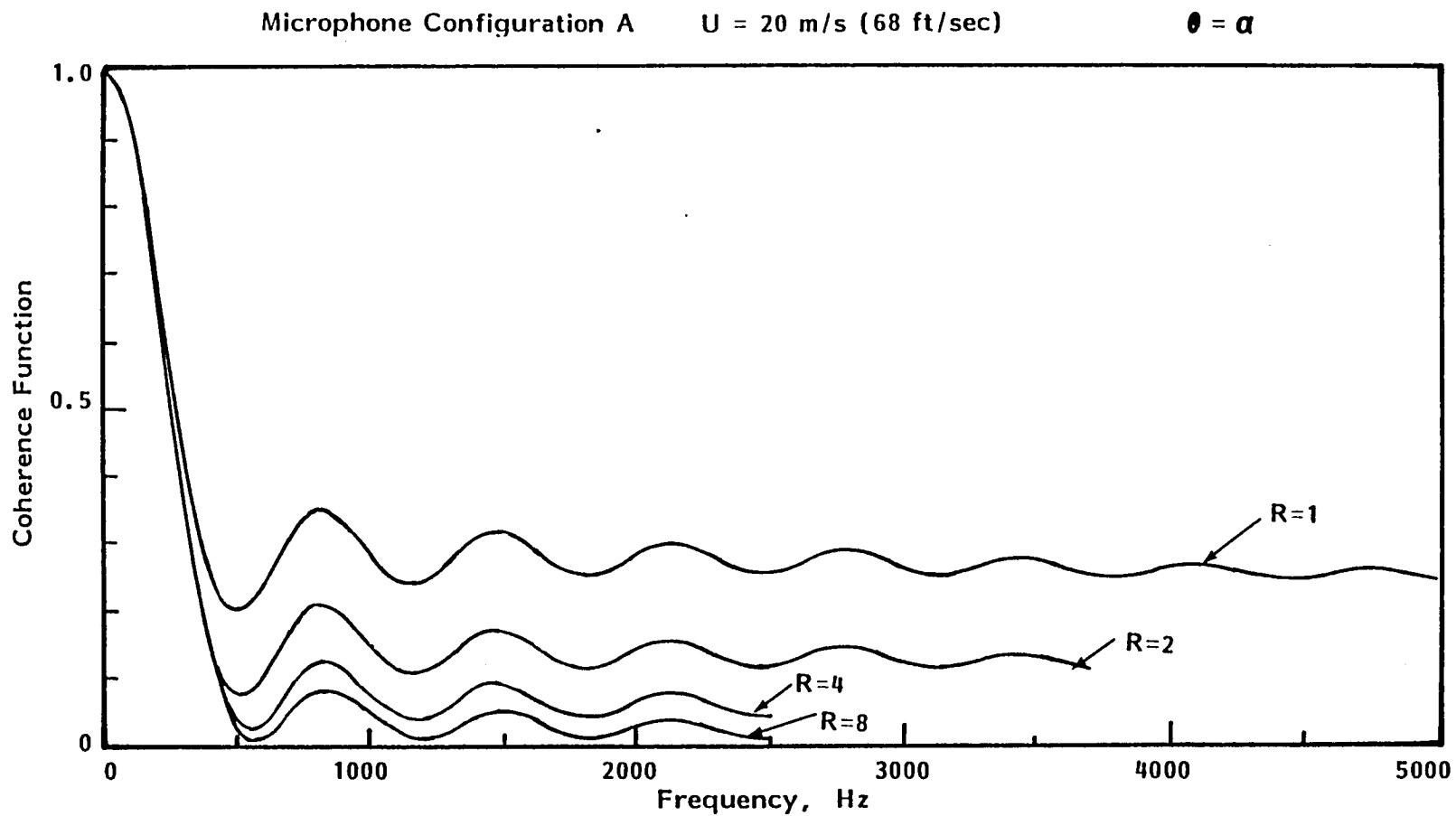
FIGURE D.2 COHERENCE SPECTRA PREDICTED FOR A COMBINATION OF PROPAGATING AND DIFFUSE ACOUSTIC FIELDS IN THE PRESENCE OF MEAN FLOW
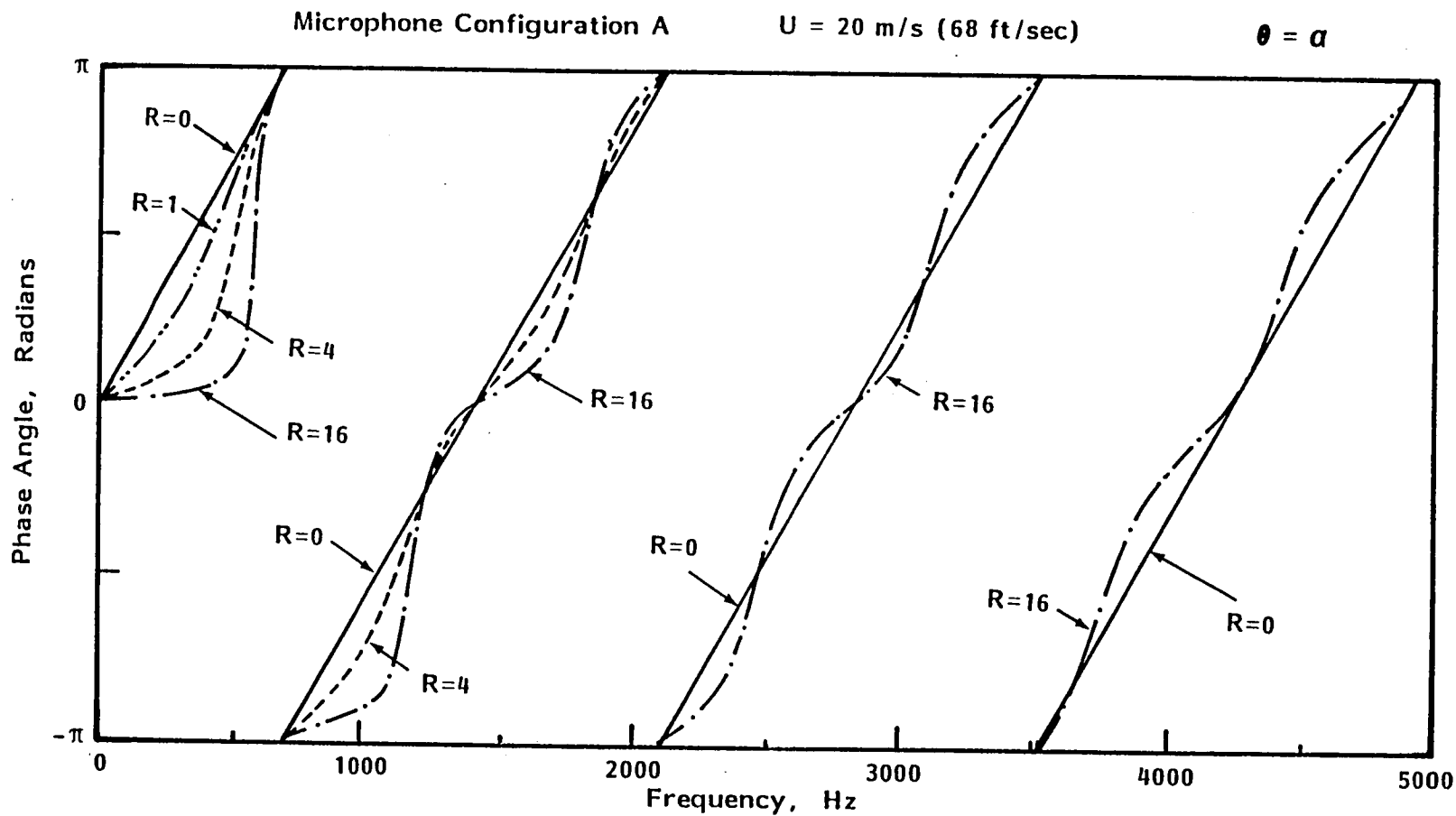
FIGURE D.3 PHASE ANGLE SPECTRA PREDICTED FOR A COMBINATION OF PROPAGATING AND
DIFFUSE ACOUSTIC FIELDS IN THE PRESENCE OF MEAN FLOW

Microphone Configuration A   U = 41 m/s (135 ft/sec)

Phase Angle, Radians

π

$G_1/G_2=0.25$

$G_1/G_2=0.5$

$G_1/G_2=0.9$

$G_1/G_2=0.25$

0

$G_1/G_2=0.9$

$G_1/G_2=0.5$

$G_1/G_2=4.0$

$G_1/G_2=4.0$

$-\pi$

0   1000   2000   3000   4000   5000

Frequency, Hz
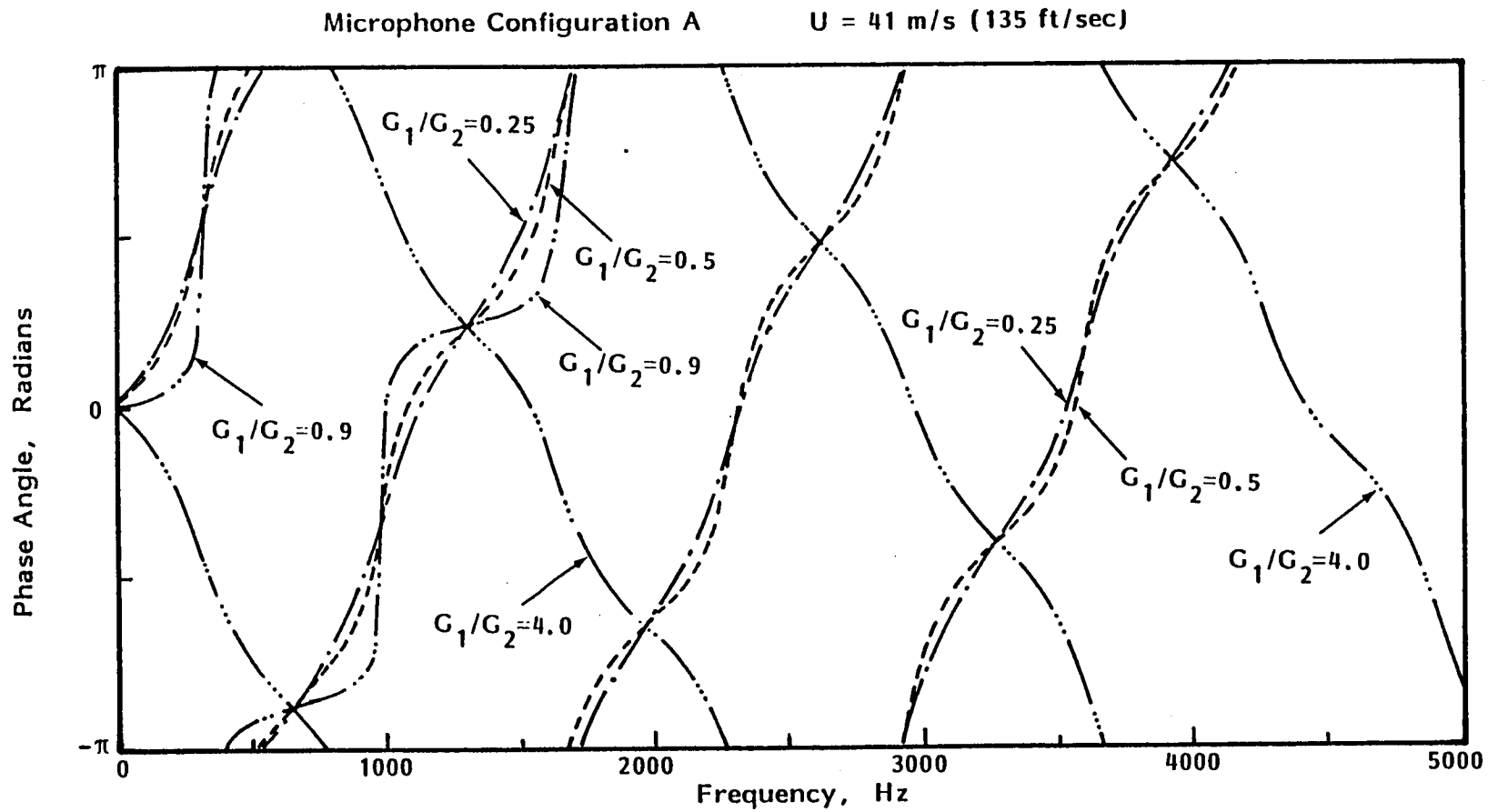
FIGURE D.4 PHASE ANGLE SPECTRA FOR UNCORRELATED ACOUSTIC WAVES PROPAGATING IN OPPOSITE DIRECTIONS IN THE PRESENCE OF MEAN FLOW
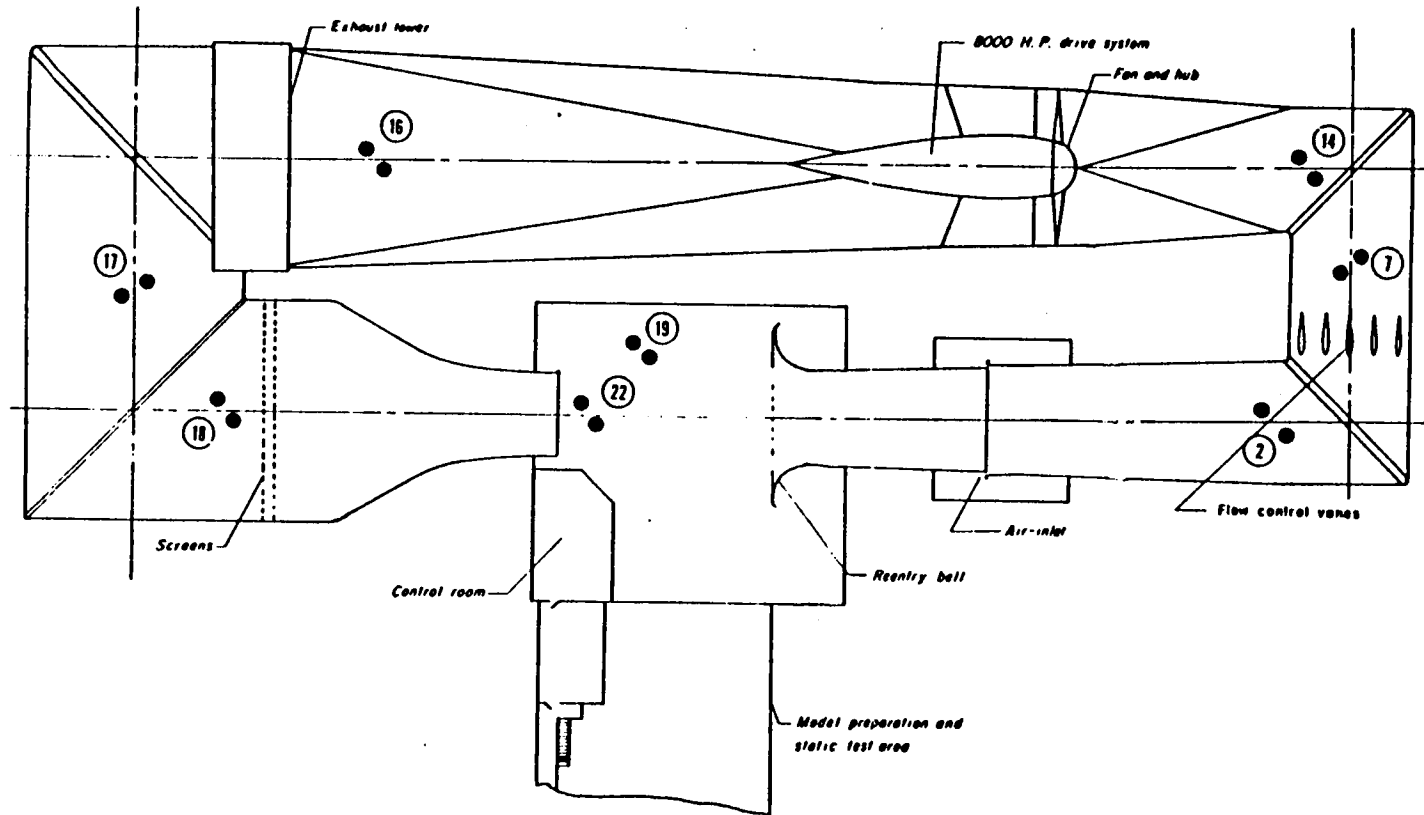
FIGURE D.5 MICROPHONE LOCATIONS FOR COHERENCE AND PHASE MEASUREMENTS
(TESTS 6 AND 7)

Configuration A
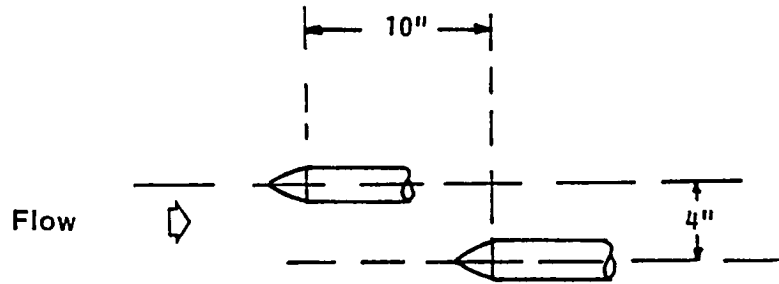
Configuration B
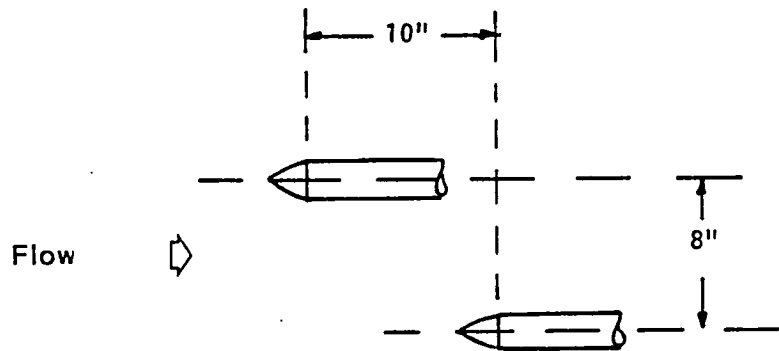
FIGURE D.6   ARRANGEMENTS FOR MICROPHONE PAIRS (TESTS 6 AND 7)

Exhaust tower
8000 H. P. drive system
Fan and hub
6-2
6-2R
6-1
6-3
Screens
Control room
Reentry bell
Air-inlet
Flow control vanes
Model preparation and
static test area
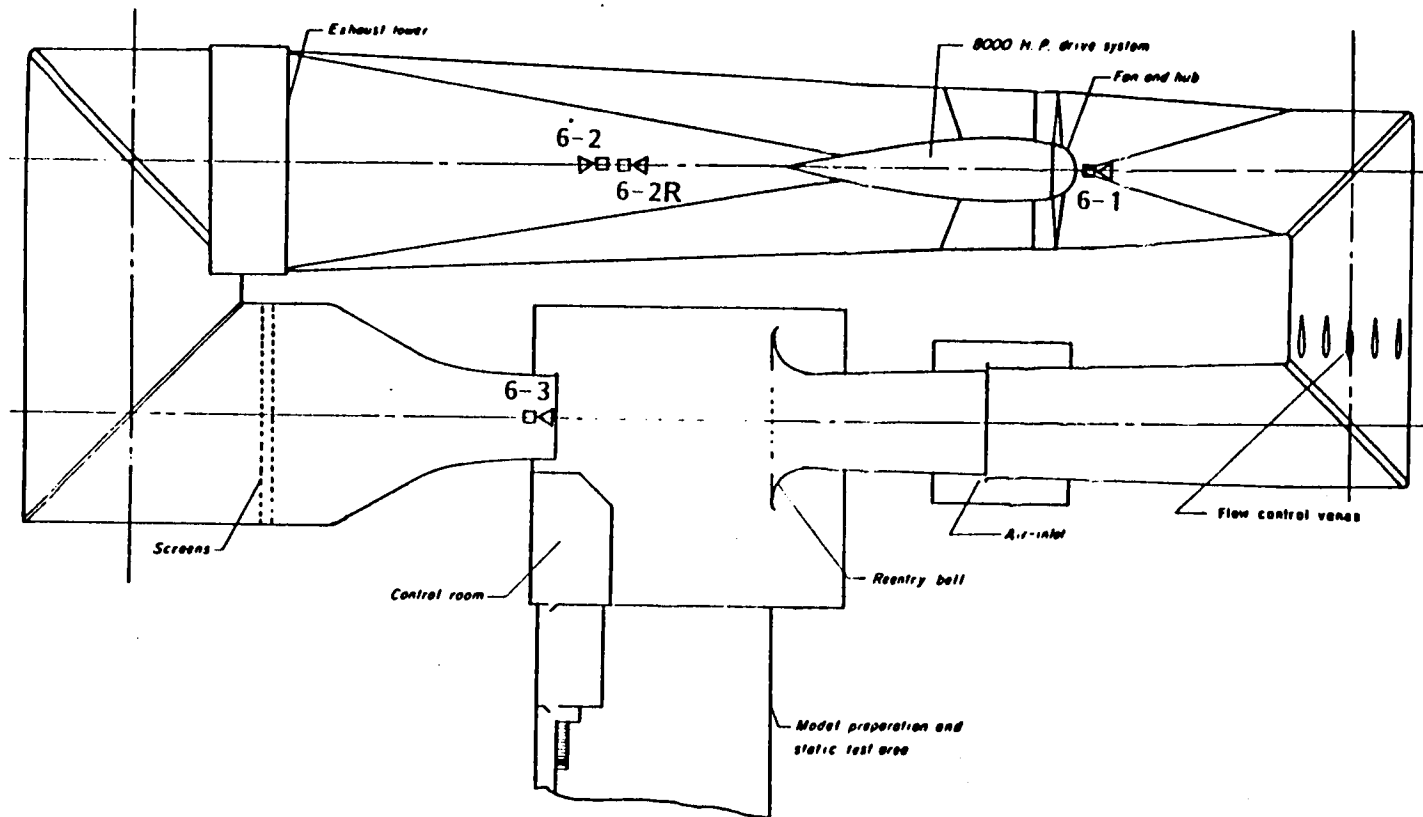
FIGURE D.7 ACOUSTIC SOURCE LOCATIONS FOR COHERENCE AND PHASE MEASUREMENTS
(TEST 6)
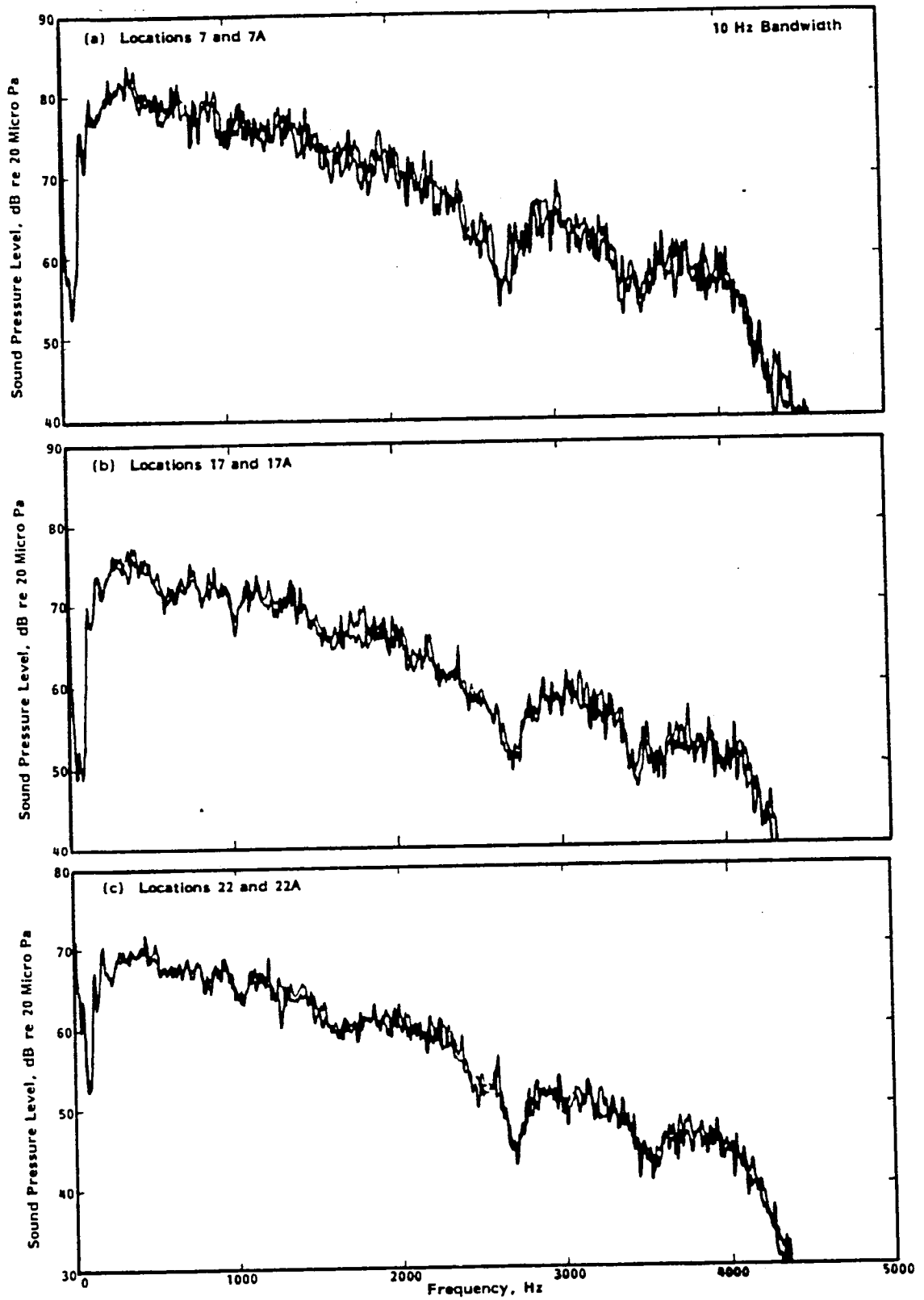
FIGURE D.8   SAMPLE ACOUSTIC SPECTRA FOR MICROPHONE PAIRS (TEST 6)
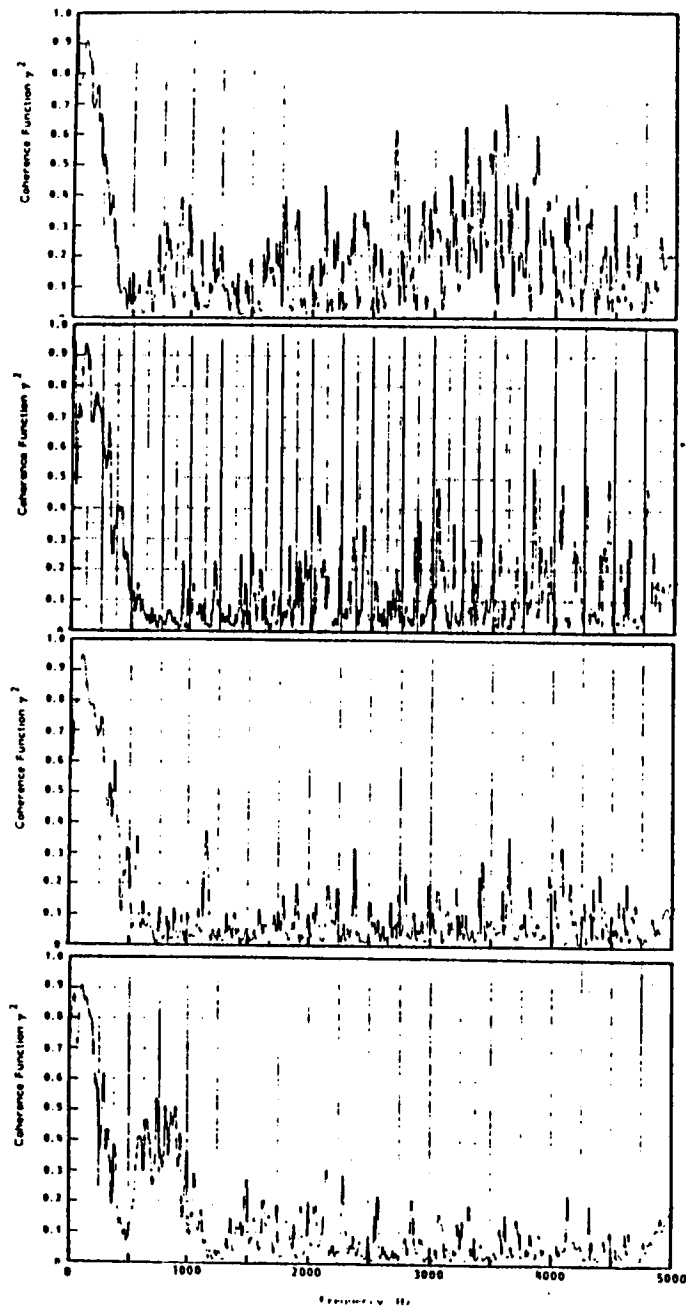
MICROPHONE
LOCATION

14
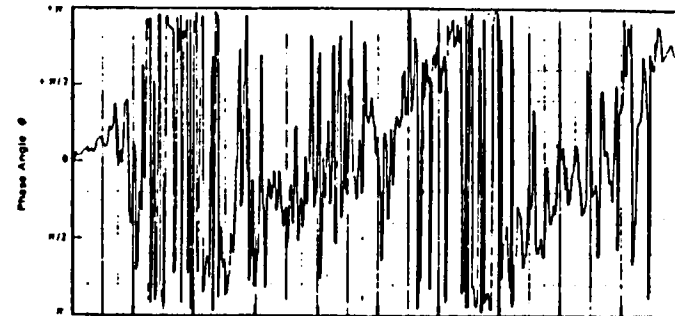
7

2

22
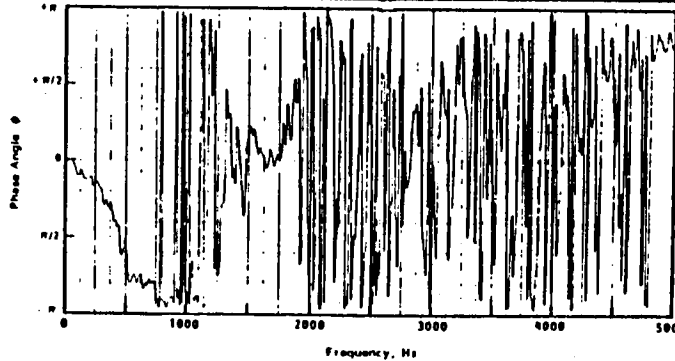
FIGURE D.9 COHERENCE AND PHASE SPECTRA MEASURED IN DIFFUSER AND TEST
SECTION; ACOUSTIC SOURCE CONFIGURATION 6-1
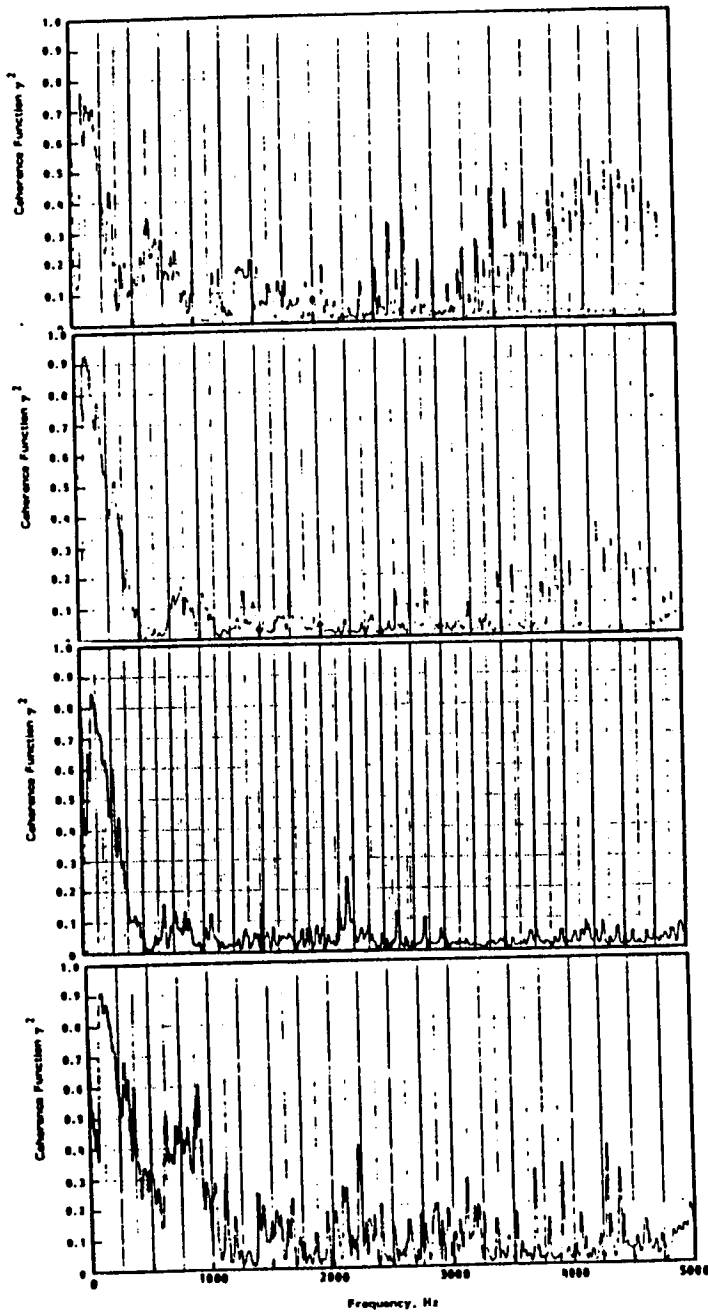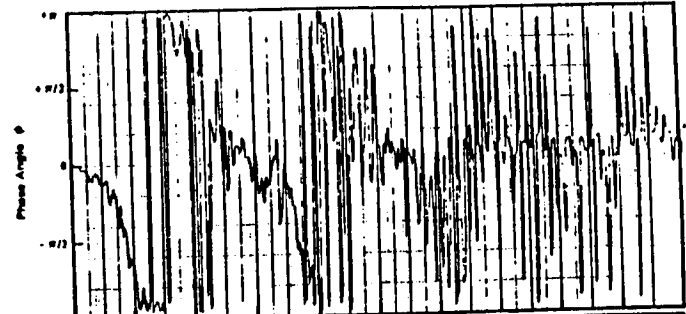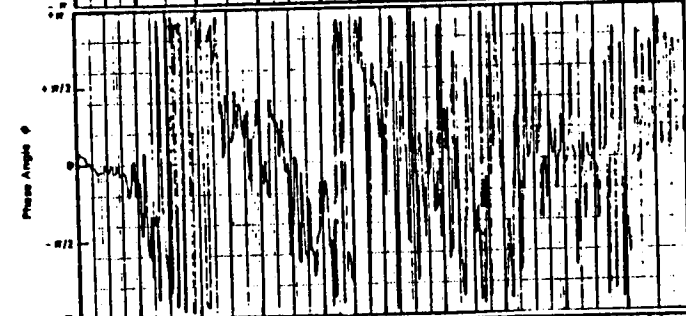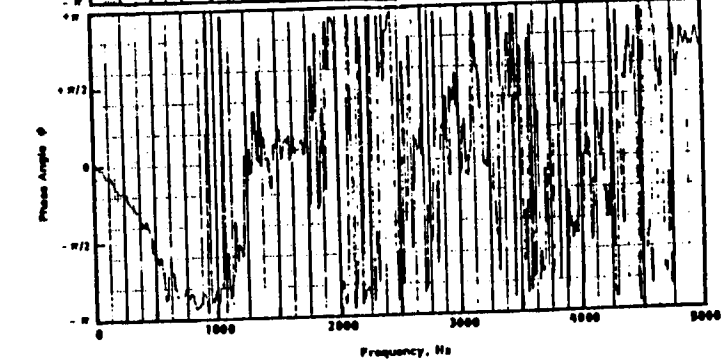
FIGURE D.10 COHERENCE AND PHASE SPECTRA MEASURED IN SETTLING CHAMBER AND TEST SECTION; ACOUSTIC SOURCE CONFIGURATION 6-2R
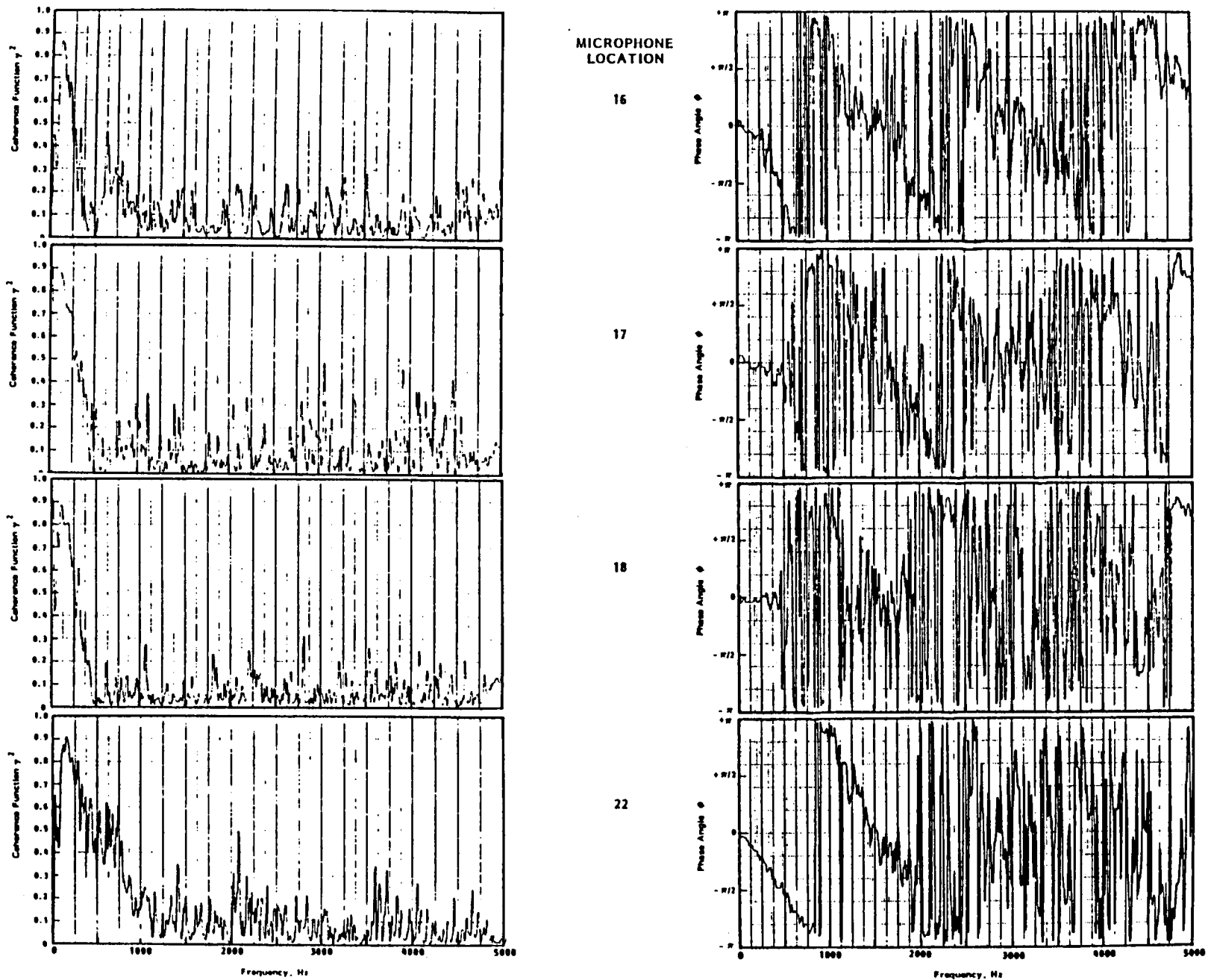
FIGURE D. 11 COHERENCE AND PHASE SPECTRA MEASURED IN SETTLING CHAMBER
AND TEST SECTION; ACOUSTIC SOURCE CONFIGURATION 6-2

MICROPHONE
LOCATION

14

7

2

22
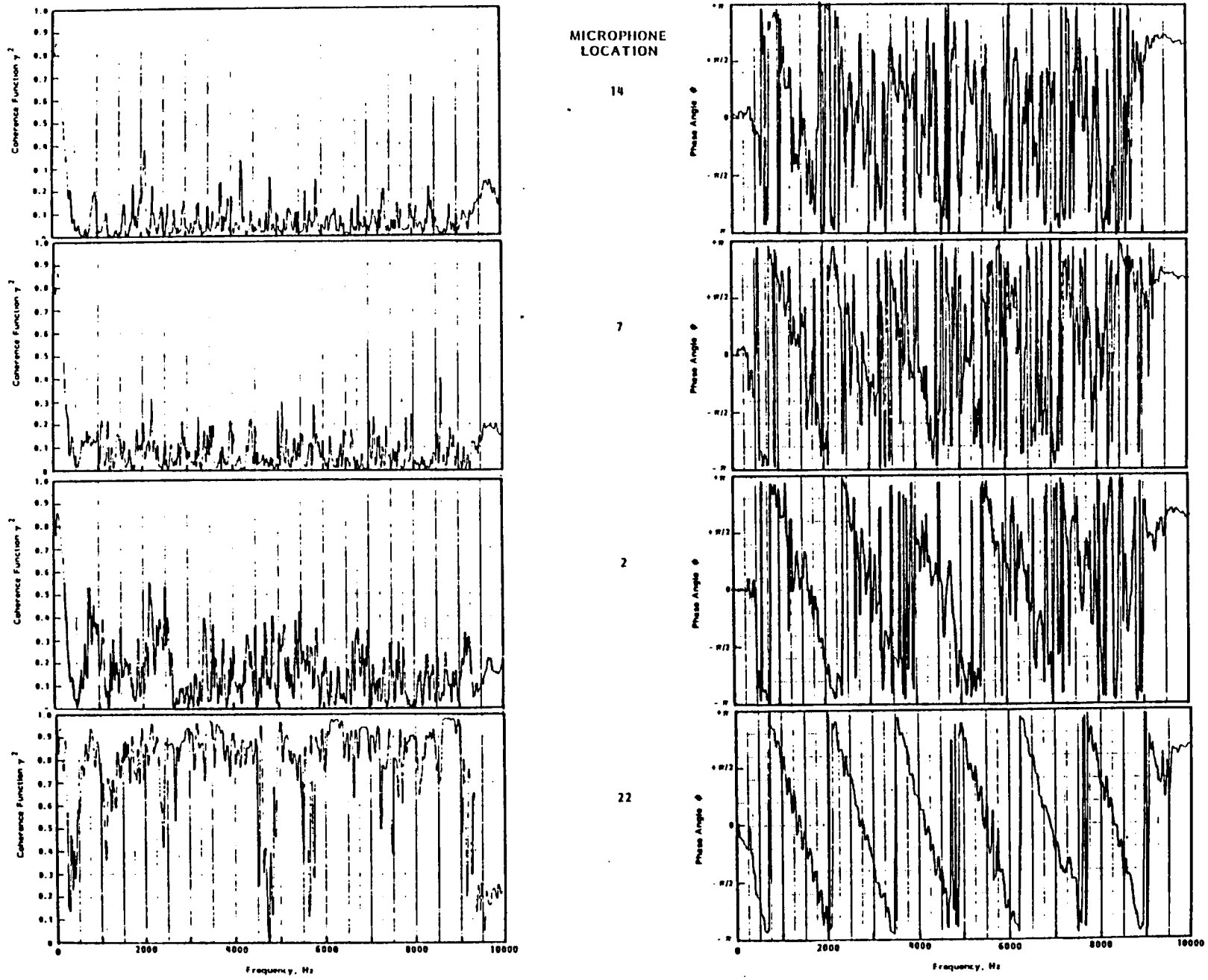
FIGURE D.12 COHERENCE AND PHASE SPECTRA MEASURED IN DIFFUSER AND TEST
SECTION; ACOUSTIC SOURCE CONFIGURATION 6-3
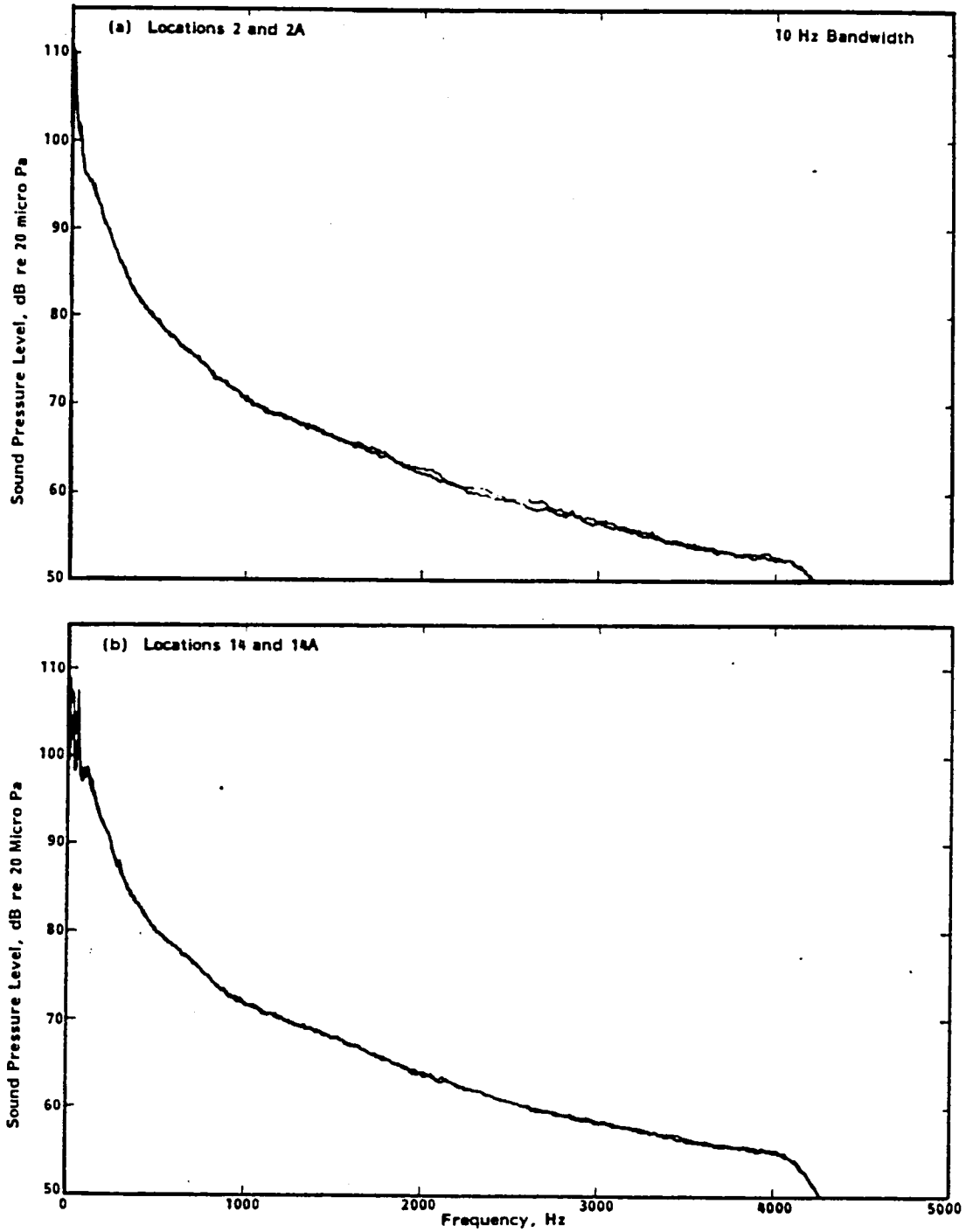
FIGURE D.13 SAMPLE SPECTRA MEASURED BY MICROPHONE PAIRS (TEST 7;
U = 41 m/s = 135 ft/sec)

(c) Locations 16 and 16A

(d) Locations 18 and 18A

FIGURE D.13 (CONTINUED)

(e) Locations 19 and 19A

Y-axis: Sound Pressure Level, dB re 20 micro Pa

X-axis: Frequency, Hz

FIGURE D.13   (CONTINUED)

(f) Locations 22 and 22A

(g) Locations 22 and 22B

FIGURE D.13   (CONTINUED)

CONFIGURATION A

Test Section Flow Speed
20 m/s (40 kts)

41 m/s (80 kts)

CONFIGURATION B

Test Section Flow Speed
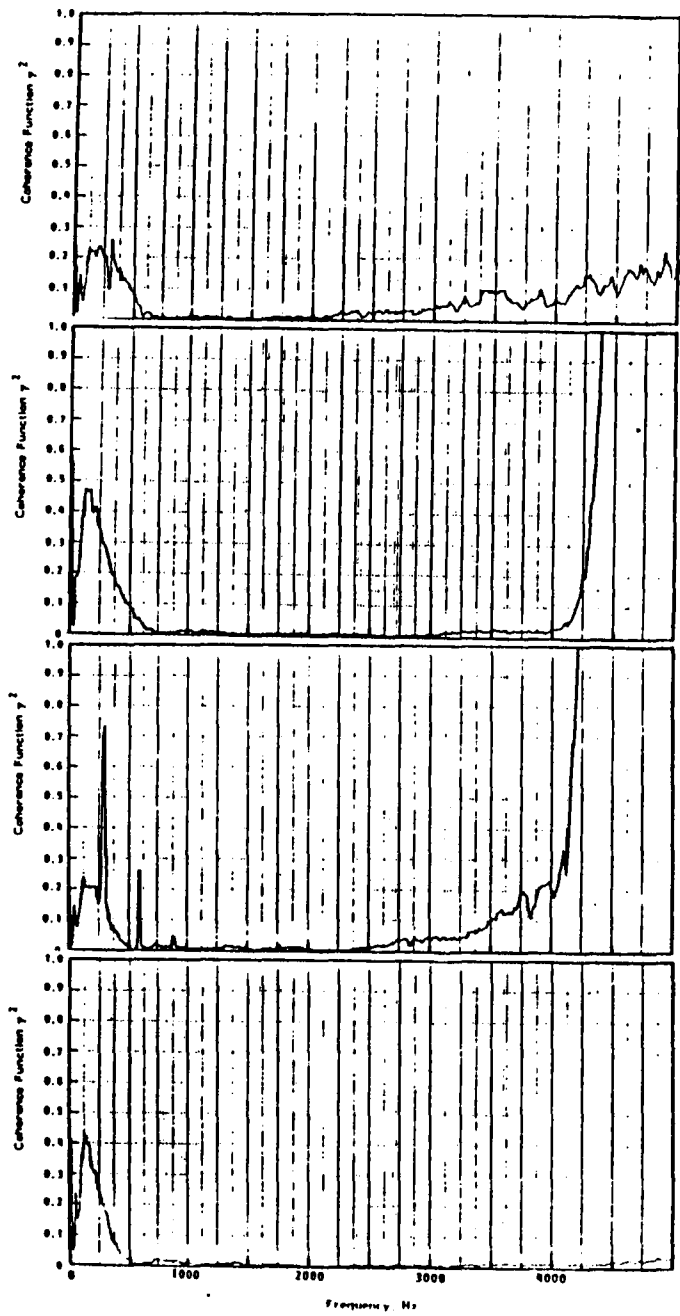20 m/s (40 kts)

41 m/s (80 kts)
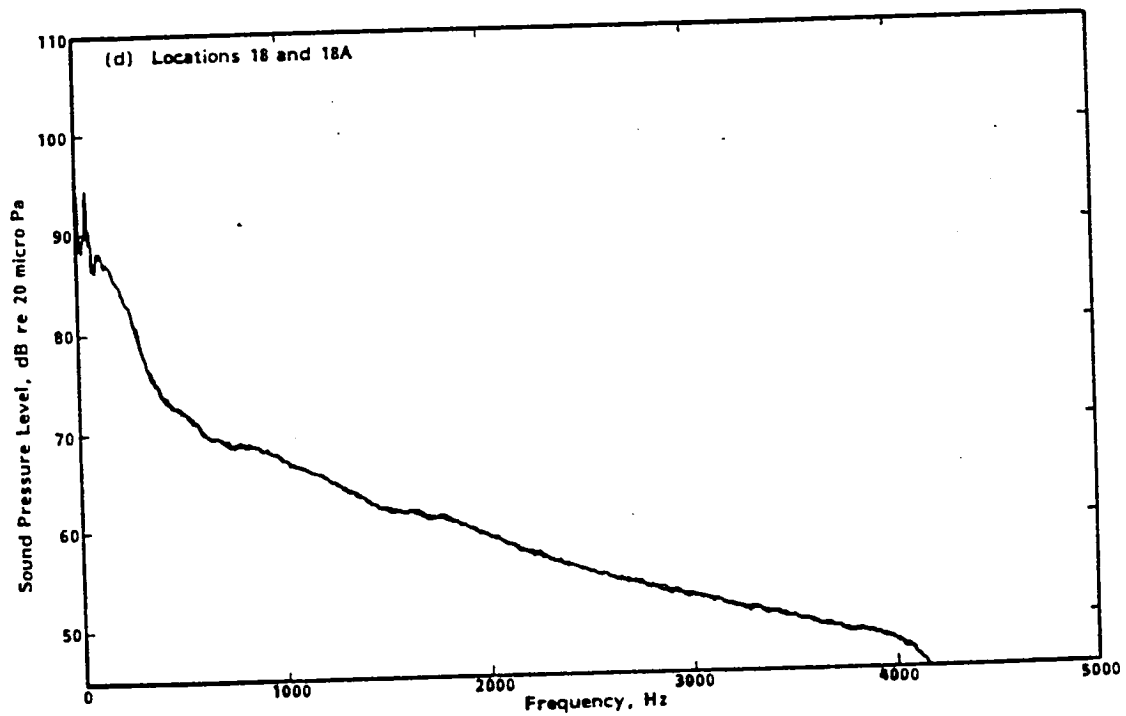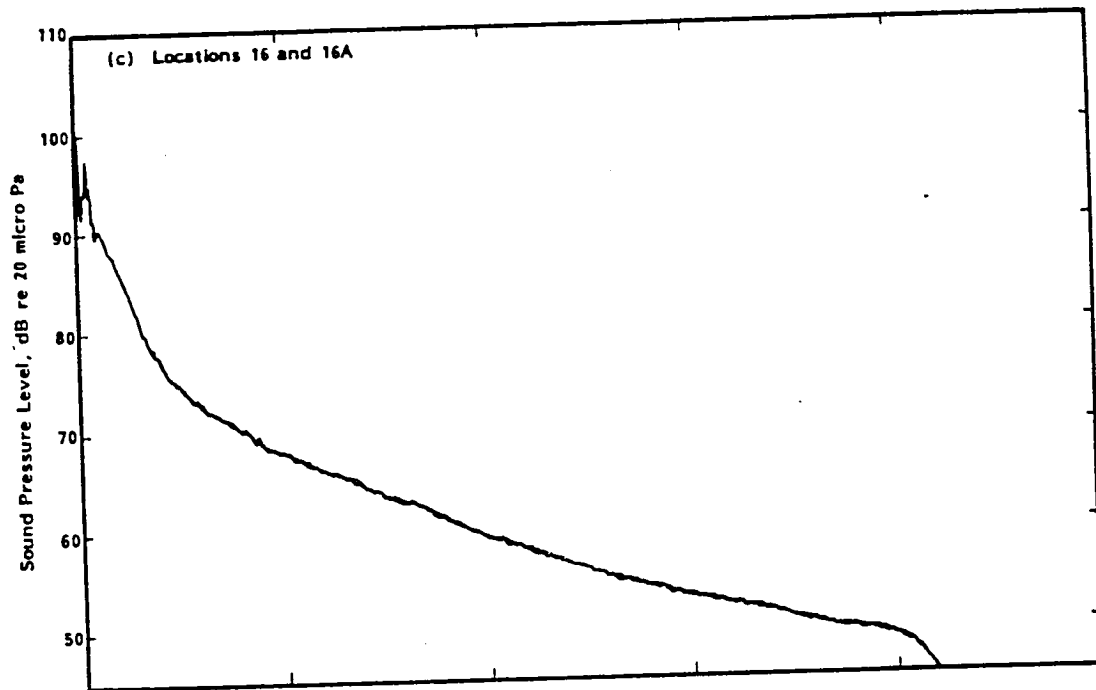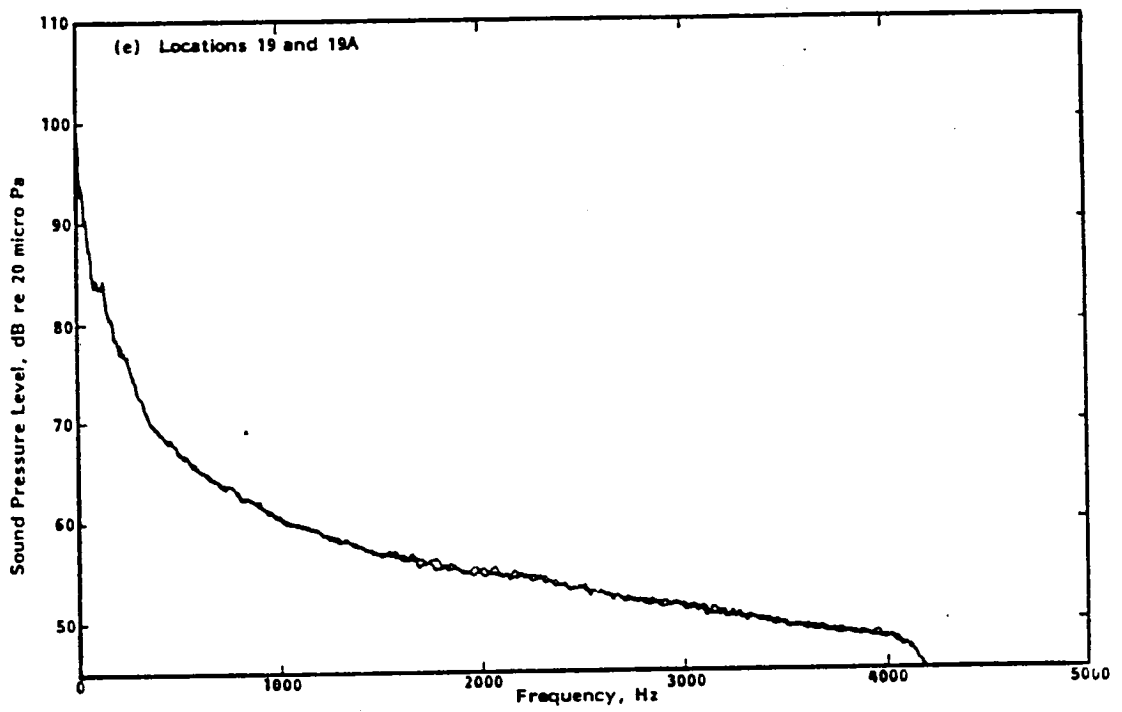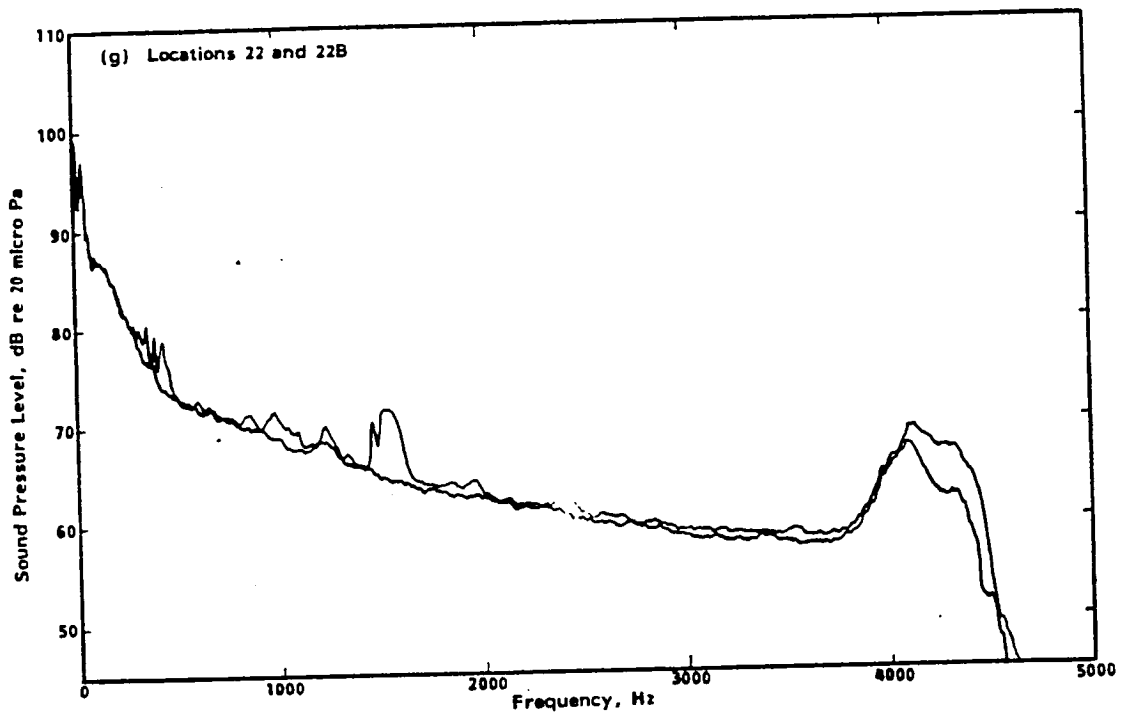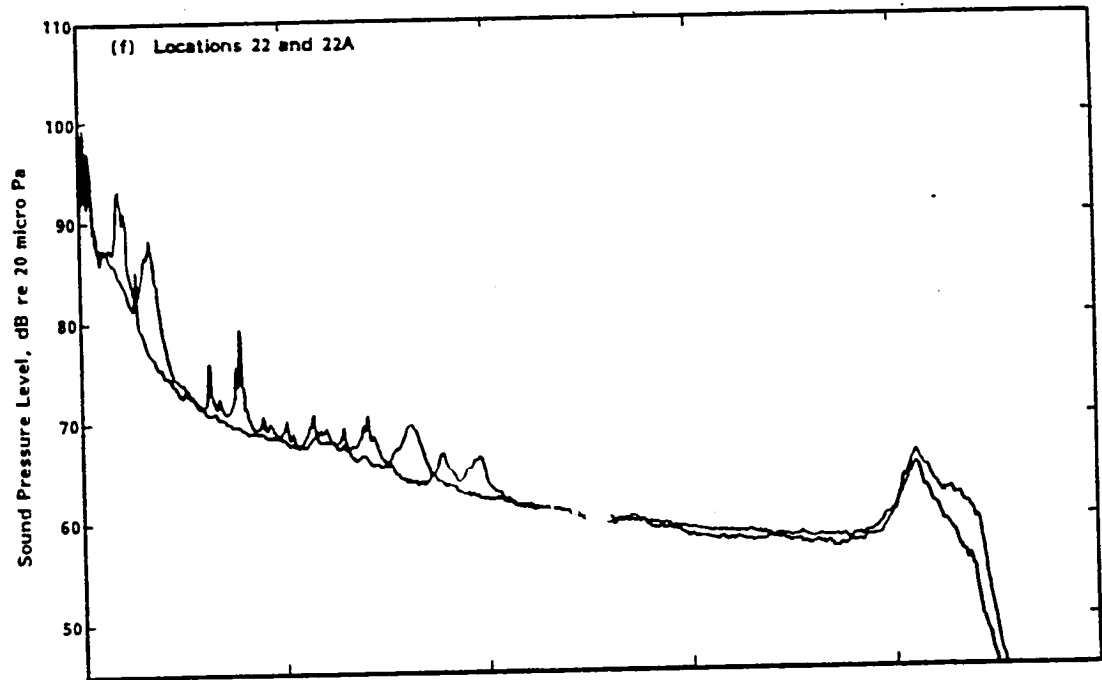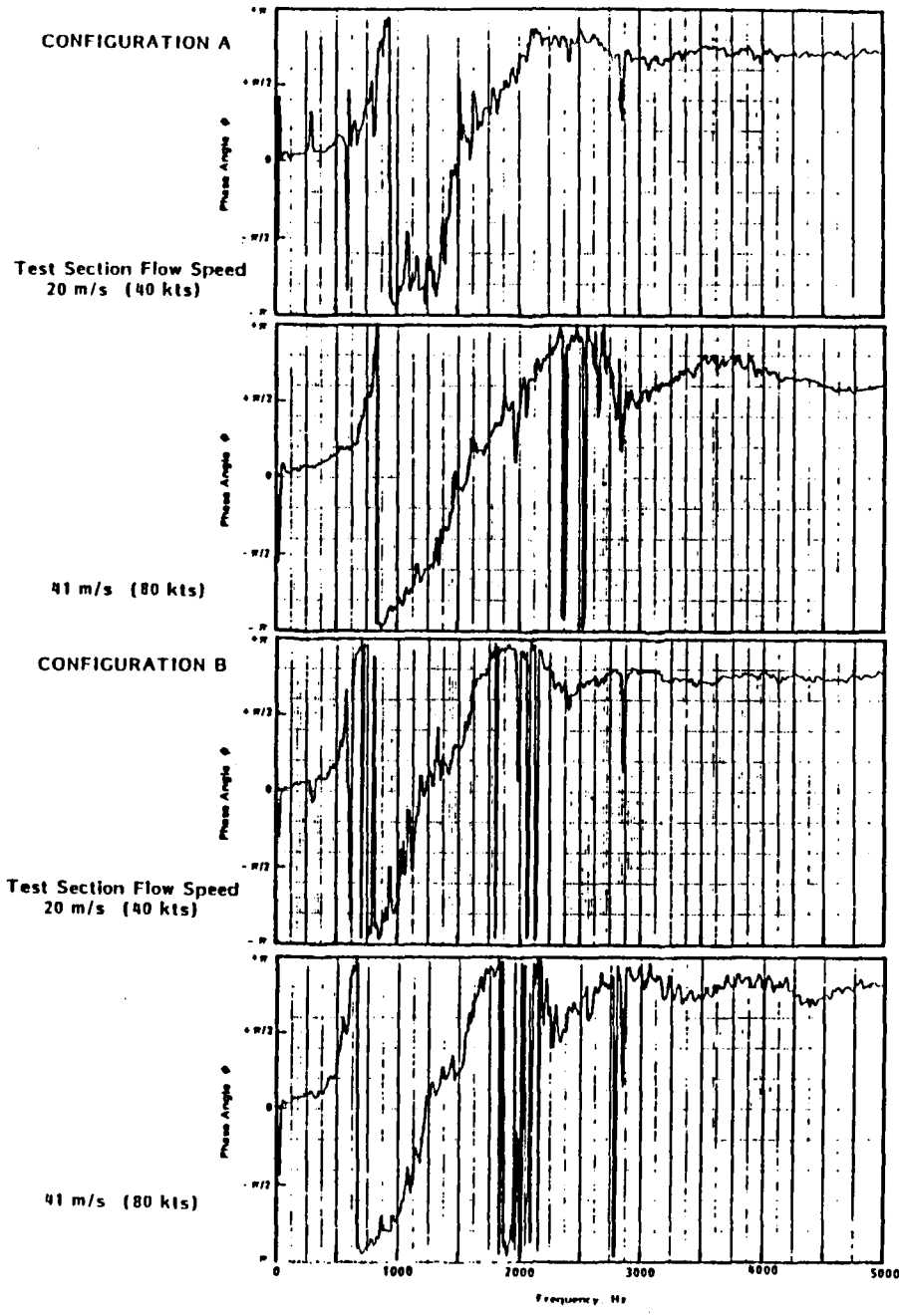
FIGURE D.14 COHERENCE AND PHASE SPECTRA MEASURED AT LOCATION 2 IN
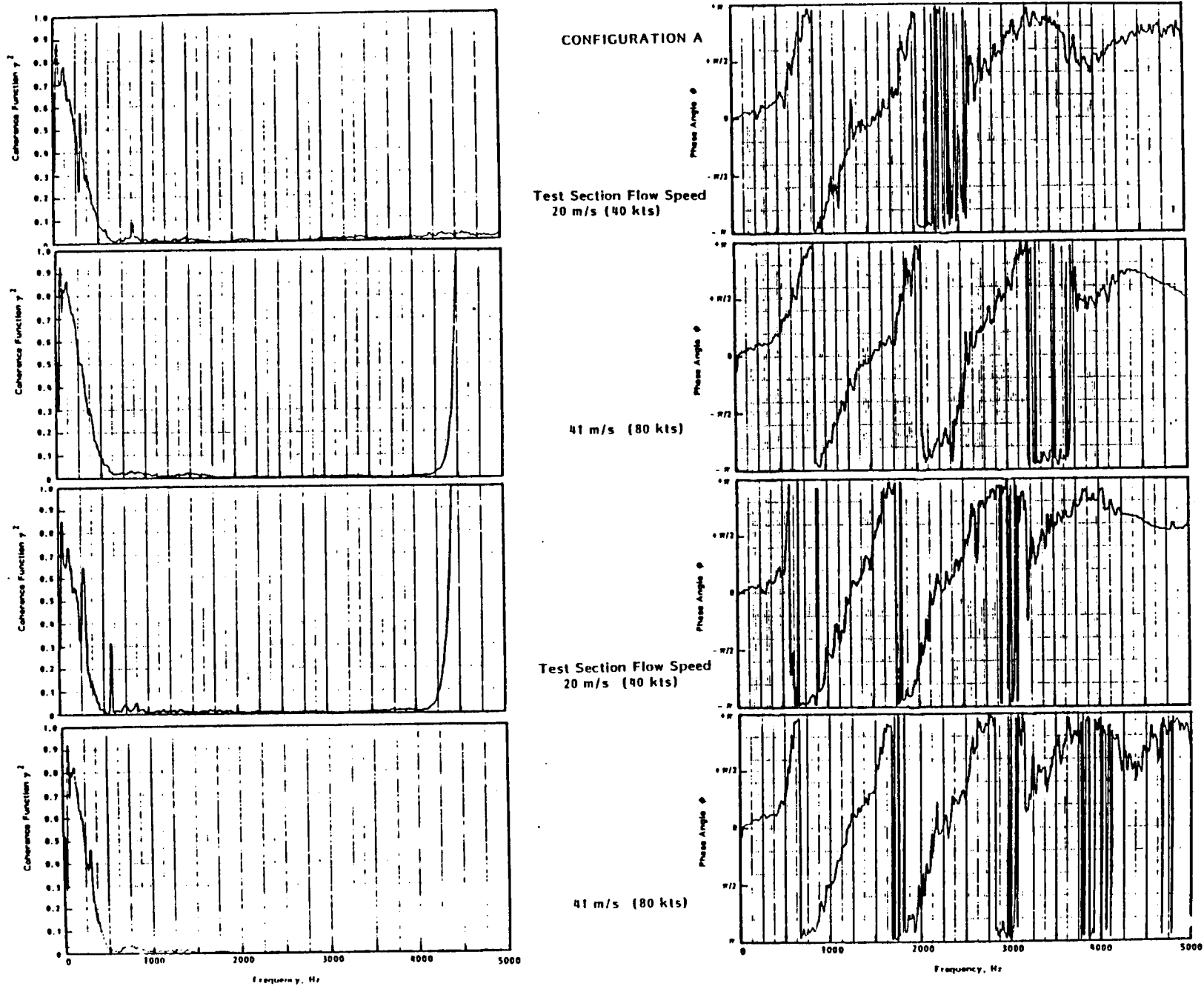DIFFUSER; TUNNEL OPERATING

FIGURE D.15 COHERENCE AND PHASE SPECTRA MEASURED AT LOCATION 7 IN
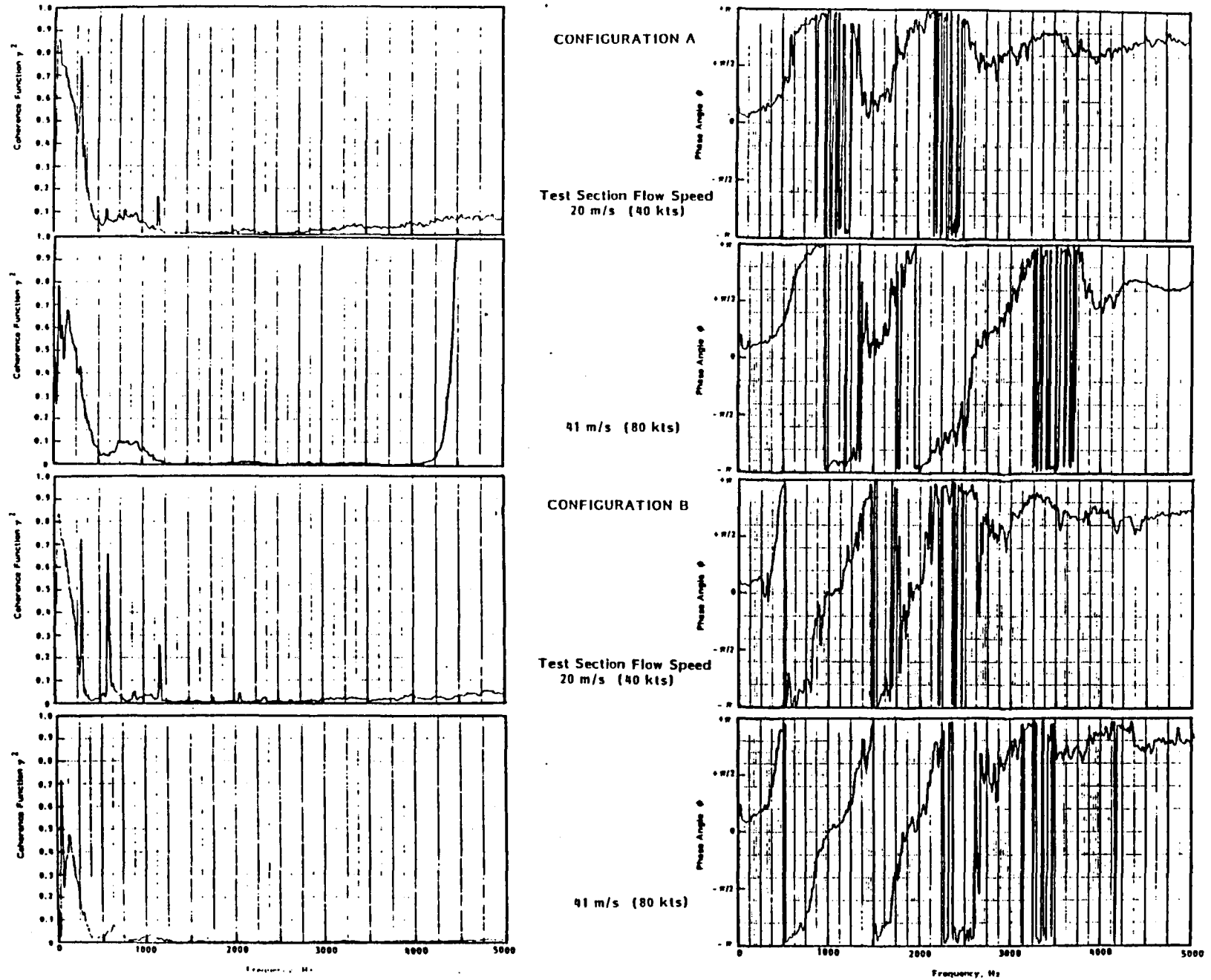DIFFUSER; TUNNEL OPERATING

FIGURE D.16 COHERENCE AND PHASE SPECTRA MEASURED AT LOCATION 14 IN DIFFUSER; TUNNEL OPERATING

CONFIGURATION A

Test Section Flow Speed
20 m/s (40 kts)

41 m/s (80 kts)

CONFIGURATION B

Test Section Flow Speed
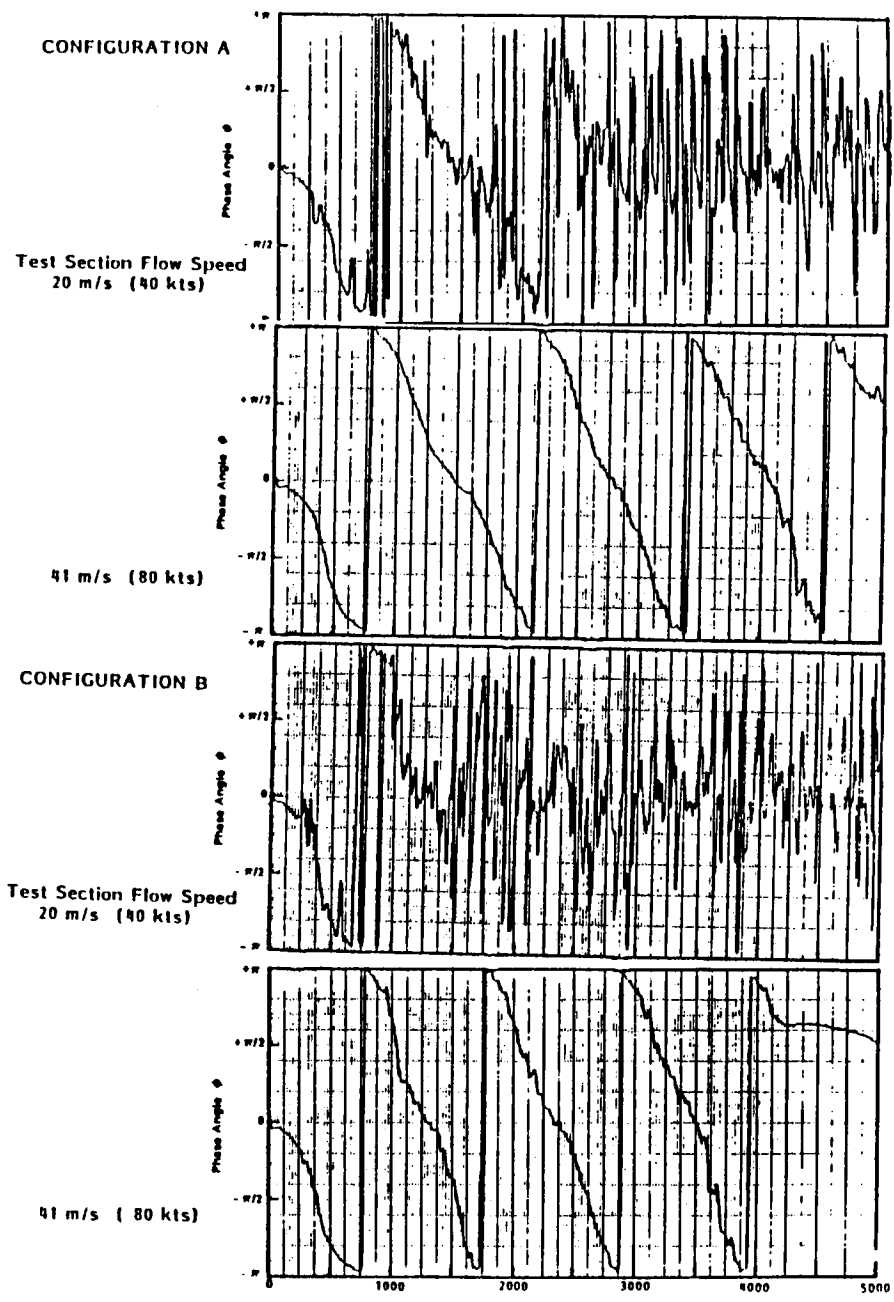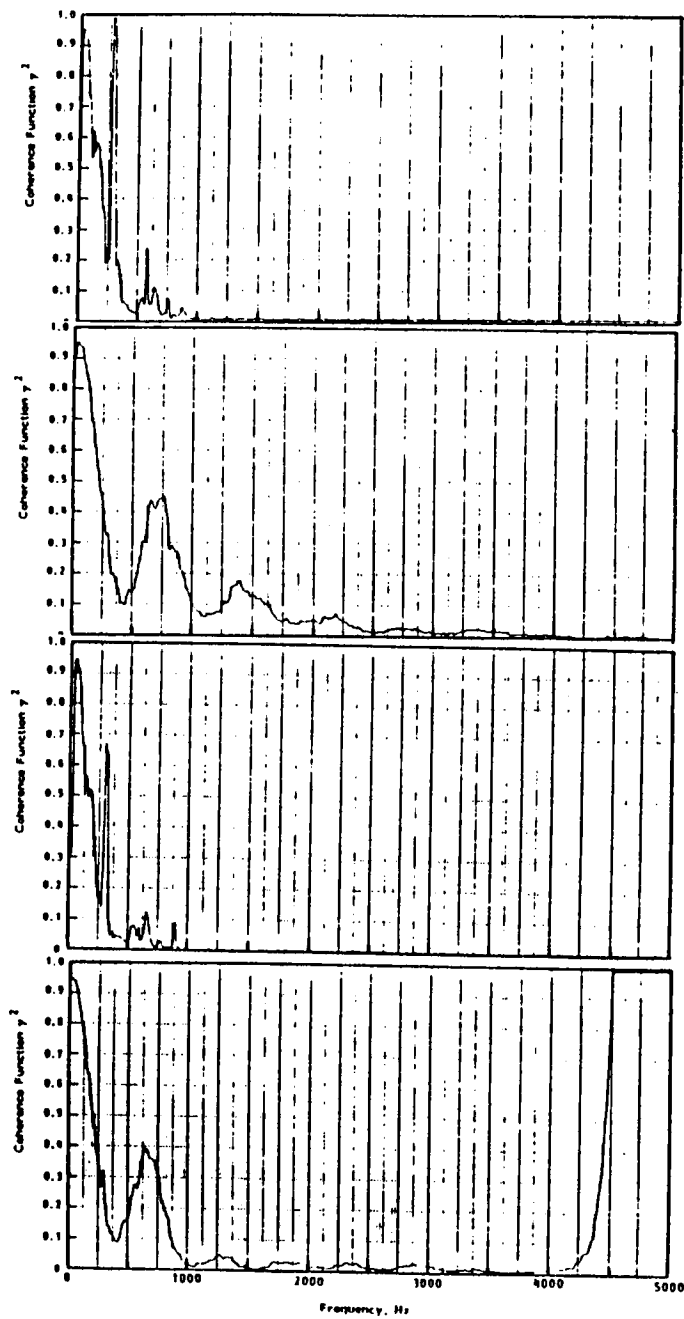20 m/s (40 kts)

41 m/s (80 kts)

FIGURE D.17 COHERENCE AND PHASE SPECTRA MEASURED AT LOCATION 16 IN
SETTLING CHAMBER; TUNNEL OPERATING

CONFIGURATION A
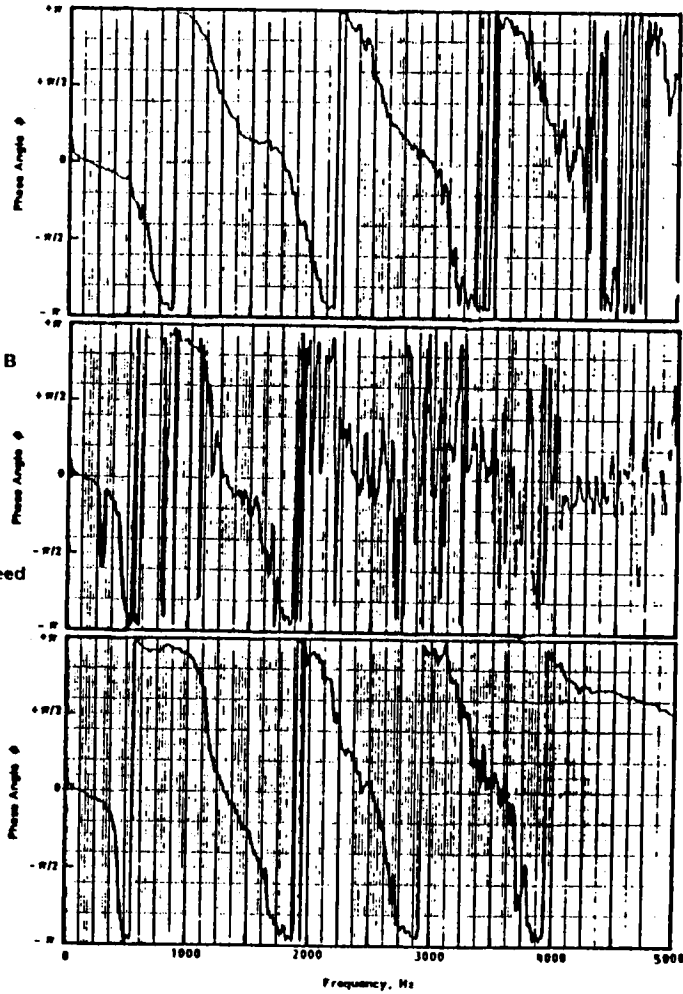
NO DATA
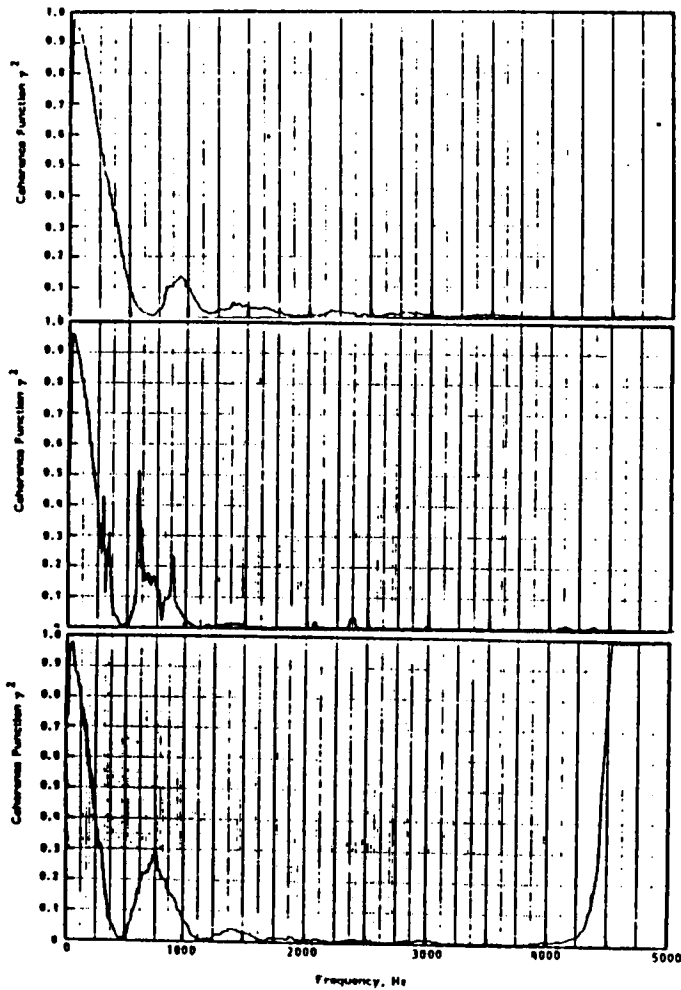
NO DATA

Test Section Flow Speed
20 m/s (40 kts)

41 m/s (80 kts)

CONFIGURATION B

Test Section Flow Speed
20 m/s (40 kts)

41 m/s (80 kts)

FIGURE D.18 COHERENCE AND PHASE SPECTRA MEASURED AT LOCATION 17 IN
SETTLING CHAMBER; TUNNEL OPERATING

CONFIGURATION A

Test Section Flow Speed
20 m/s (40 kts)

41 m/s (80 kts)

CONFIGURATION B

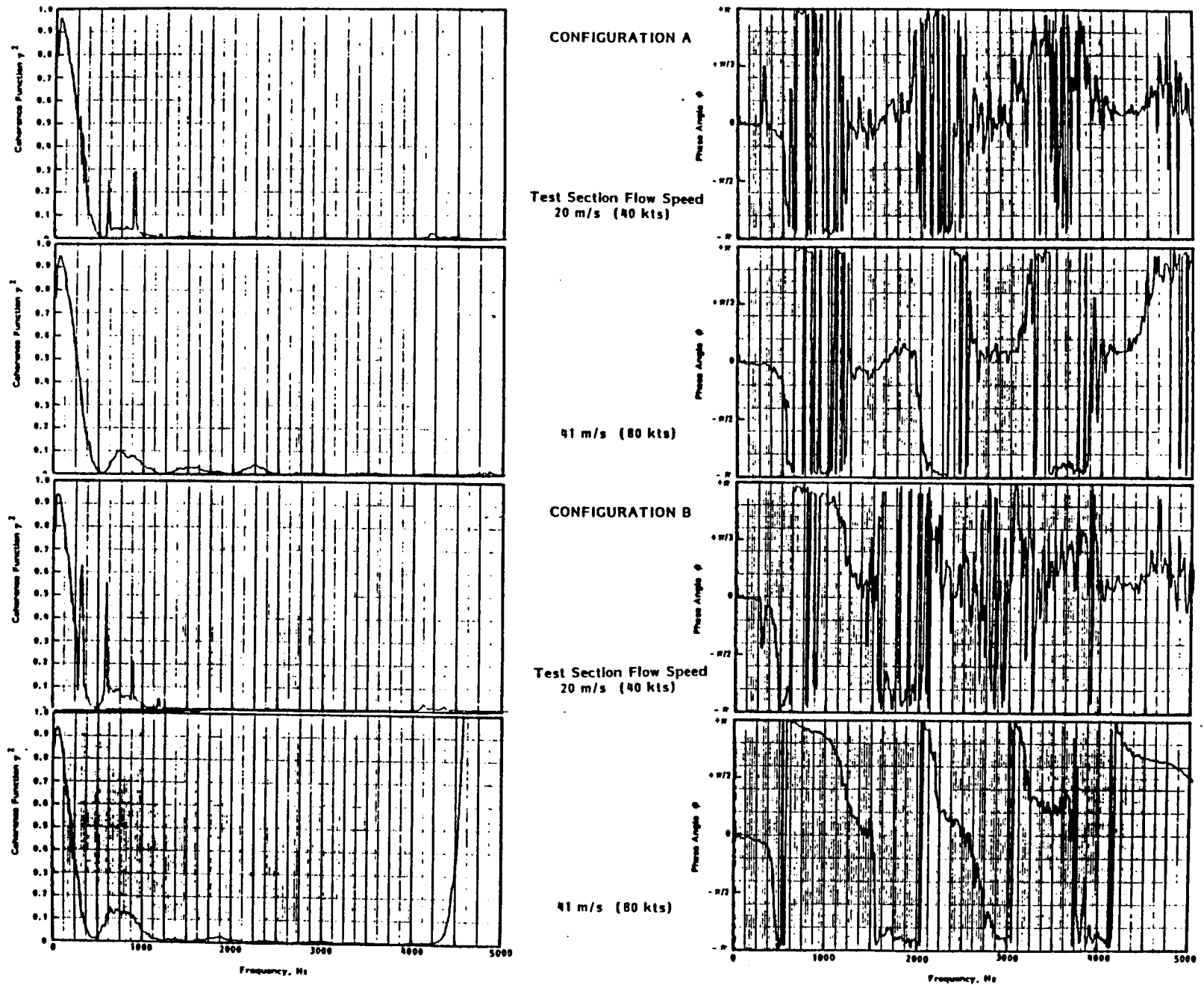Test Section Flow Speed
20 m/s (40 kts)

41 m/s (80 kts)

FIGURE D.19 COHERENCE AND PHASE SPECTRA MEASURED AT LOCATION 18 IN
SETTLING CHAMBER; TUNNEL OPERATING

CONFIGURATION A

Test Section Flow Speed
20 m/s (40 kts)

41 m/s (80 kts)

CONFIGURATION B

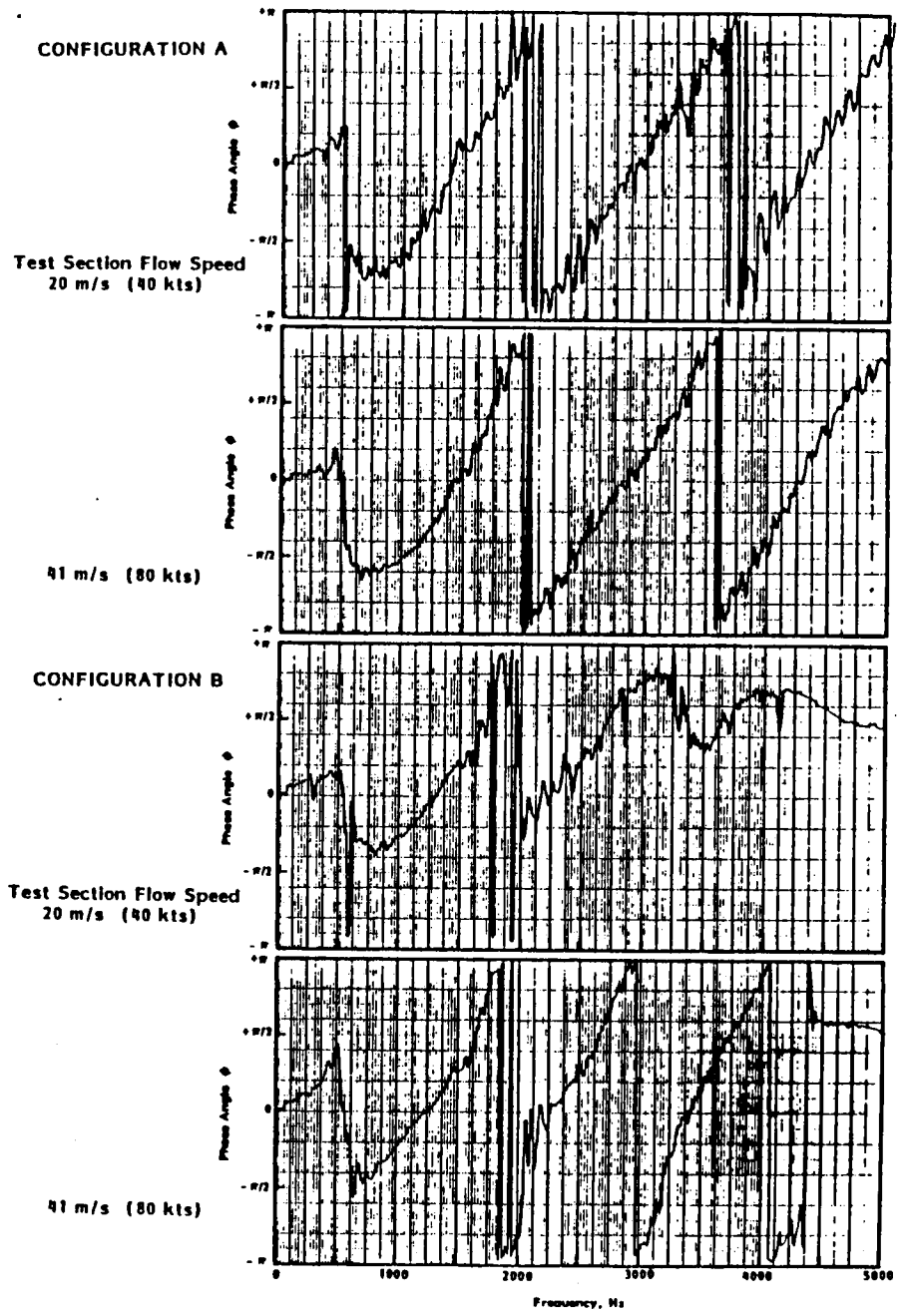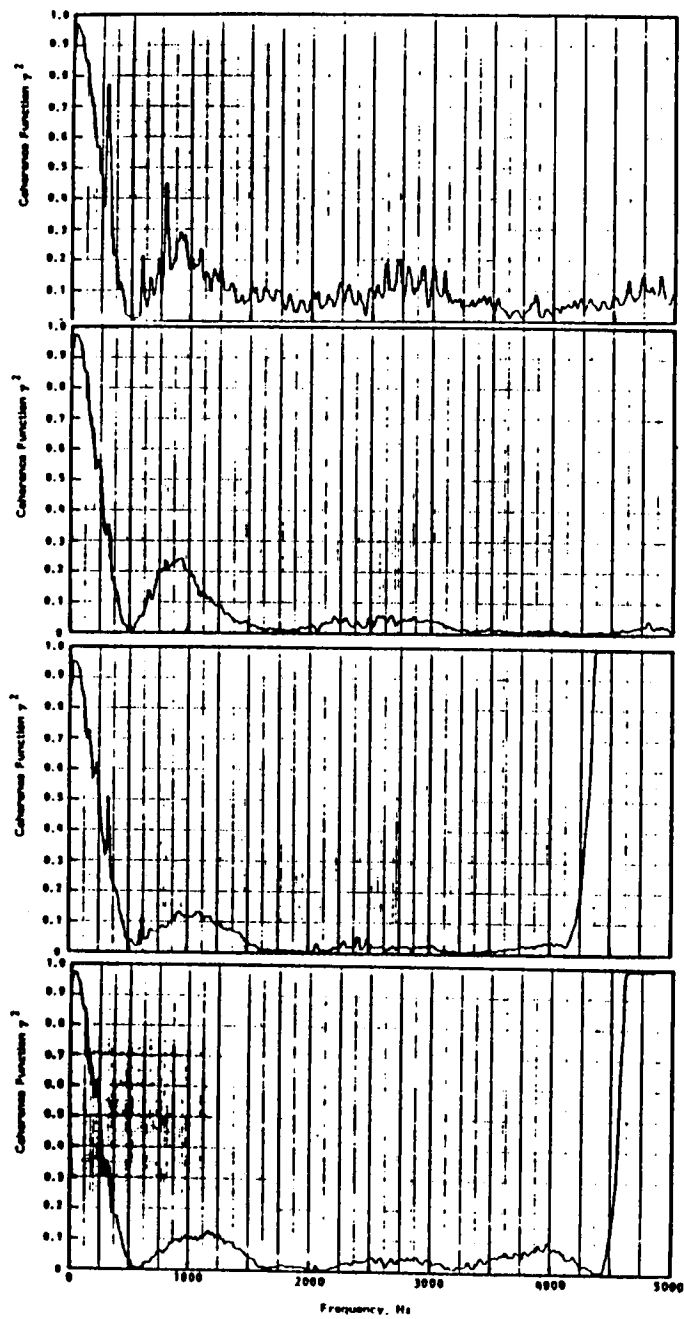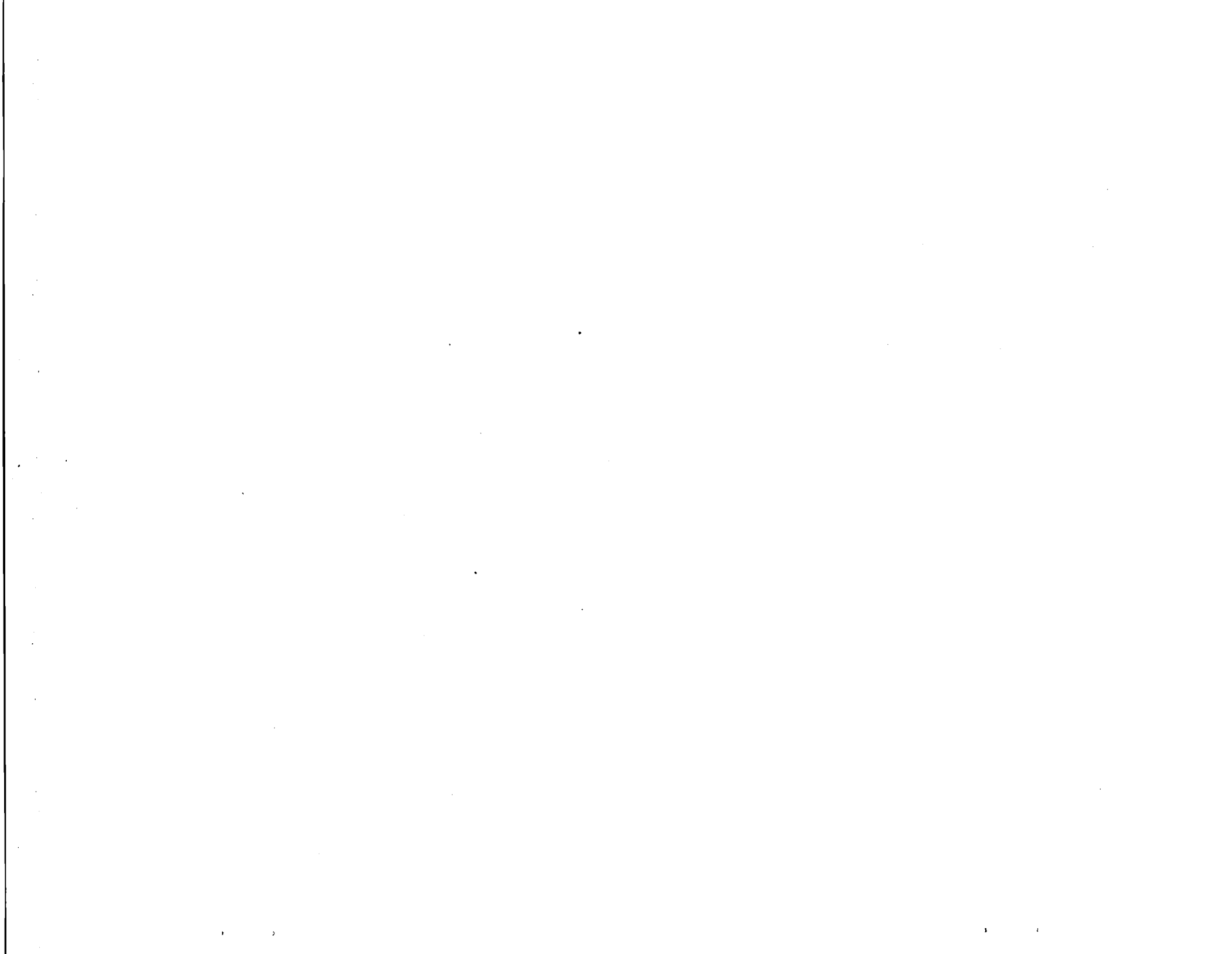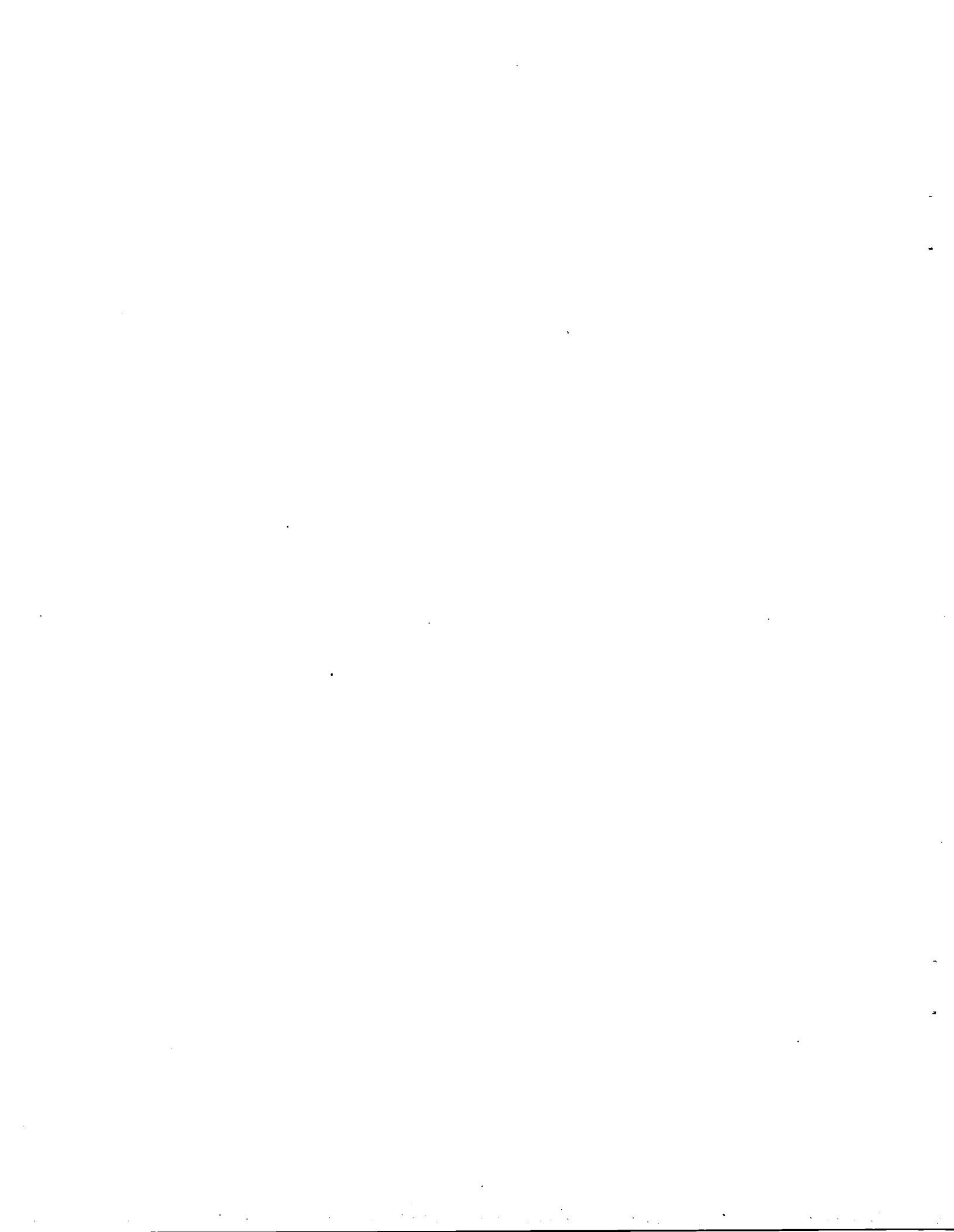Test Section Flow Speed
20 m/s (40 kts)

41 m/s (80 kts)

FIGURE D.20 COHERENCE AND PHASE SPECTRA MEASURED AT LOCATION 19 IN
TEST SECTION; TUNNEL OPERATING

APPENDIX E

TURNING VANE SOUND GENERATION AND TRANSMISSION

APPENDIX E

TURNING VANE SOUND GENERATION AND TRANSMISSION

Turning vanes may be both sources of sound and may also transmit sound generated elsewhere in the tunnel. This section deals with both aspects.

E.1. Transmission

Sound pressure cross-correlation measurements were performed in the diffuser in order to obtain an indication of the role played by the turning vanes in reflecting acoustic waves. Soderman [E1] has used the technique in the diffuser of the NASA Ames 7 x 10-ft wind tunnel when the walls of the diffuser are treated with acoustic treatment. The case of an untreated diffuser, such as that in the 4x7 m tunnel, is more complicated because the reflections from the walls introduce additional propagation paths. In addition, the second stage diffuser in the 4x7 m tunnel contains five flow control vanes with trailing edge flaps; these surfaces add to the potential reflections for sound waves propagating through the diffuser.

E.1.1 Measurement procedure

Two tests, identified as #4 and #5, were performed to measure the sound transmission through the turning vanes. Test 5 was concerned with transmission through the vanes of the first corner; microphone and noise source locations associated with this test are shown in Figure E.1. Transmission through the vanes of the second corner was measured in Test 4; the locations of the microphones and source are shown in Figure E.2.

The source consisted of an electro-acoustic driver with a horn. In both tests the horn was pointing in the upstream direction with the axis of the horn parallel to the tunnel

centerline (and the source on the centerline). Measurements were also performed with the axis of the horn at a non-zero angle to the tunnel centerline but the data from these runs are not presented here as they do not add to the data interpretation. The acoustic signal generated by the horn was essentially pink noise in the frequency range 80 to 5000 Hz; and one-third octave band spectra will be similar to those shown in Appendix B.

Cross-correlation functions were measured for pairs of microphones, with microphone 6 or 7 being the reference microphone for Test 5 and 13 or 14 for Test 4. The correlation functions were obtained by replaying the recorded analog signals through high-pass filters into a Spectral Dynamics SD360 Digital Signal Processor. The cut-off frequency of the high-pass filters was 0, 1000, 2000, or 3000 Hz. The progressive increase in cut-off frequency was used in order to investigate the differences between low and high frequency acoustic paths.

E.1.2 Propagation along tunnel centerline

Before considering noise transmission through the turning vanes it is of interest to investigate the pressure cross-correlation function for the microphone pair 6 and 7 located on the centerline of the tunnel in the second diffuser. Two correlation functions for 0 to 5000 Hz and 1000 to 5000 Hz are shown in Figure E.3. The data are presented for time delays in the range -50 ms to +50 ms.

The correlation curves in Figure E.3 show the main peak at about +22 msec. This is associated with the direct path from microphone 7 to microphone 6. (Microphones 6 and 7 were separated by a distance of about 7.5 m.) There is a second peak at about +24 msec; this is probably associated with a reflected path via one surface of the flow control vanes. Then other peaks occur at greater time delays associated with longer indirect paths.

It is interesting to note that there is no significant peak at -22 msec. This time delay would be associated with a reflected wave traveling parallel to the tunnel centerline - the reflection occuring, say, at the sidewall of the first stage diffuser. It appears from these data that there is no strong reflected wave, unless it is traveling by a much longer path due to multiple reflections.

E.1.3 Transmission through first corner vanes

Cross-correlation functions measured for three microphone pairs at the first corner turning vanes are shown in Figures E.4 through E.6. The reference microphone is #7 in all cases and the secondary microphones are #1 in Figure E.4, #2 in Figure E.5 and #3 in Figure E.6. The figures show correlation functions for time delays from 0 to +100 msec, and for three frequency bandwidths.

Measurements were also made to check the magnitude of the correlation function at negative time delays in the range -50 msec to zero. A typical set of data is shown in Figure E.7 for microphone pair (7-2). It is seen that there are some correlation components in the negative time delay region but that the magnitude of the correlation function is significantly lower than the peaks in the positive time delay region. It should be remembered, however, that the correlation function is plotted linearly rather than logarithmically.

The objective of the analysis is to select regions of significant cross-correlation and to associate the corresponding time delay with possible transmission paths using single ray tracing procedures. Each of the three figures attempts to make this correlation between time delay and transmission path in a schematic manner. The first (i.e., smallest time delay) significant peak in the correlation function can be associated

with the shortest path between the two microphones. However allowance should be made for rays which travel directly from the source to the second microphone without traveling directly past microphone 7. Such rays are shown in the figures.

In the case of the first corner turning vanes, the most direct path does not necessarily follow the straight line from microphone 7 to the second microphone. There are several reasons for this observation. First the turning vanes may not allow direct (no reflection) paths through the corner at the frequency and angle of incidence of interest. Secondly, and this applies only to the first corner, the presence of the flow control vanes prevents direct, straightline propagation except at small angles to the tunnel centerline.

Comparing the data in Figures E.4 through E.6, it is seen that time delays associated with the major peaks in the cross-correlation functions, and, hence, with the main pair of the transmitted acoustic energy, occur at significantly different time delays for the three microphone pairs. For microphone pair (7-1) there is a significant fraction of the acoustic power being transmitted by the (almost) direct path. In contrast, for microphone pair (7-2), much of the acoustic power arrives at the second microphone via quite long paths, some of which involve multiple reflections. Transmission path-time delays for micro-phone pair (7-3) appear to lie somewhere in between these two extremes, although the geometric characteristics of the potential paths seem to be quite similar to those for microphone pair (7-2). In fact, much of the acoustic power for the frequency ranges of interest seems to be transmitted around the first corner via a single reflection on the turning vane surfaces.

At low frequencies the pattern is less distinct. For example, Figure E.8 contains cross-correlation functions which

include all the low frequency acoustic power (filter range 0 to 5000 Hz). It is still possible to discern the correlation peaks shown in Figures E.4 and E.6 for corresponding filtered signals. However, in Figure E.8 the ratio of peak amplitude to general correlation amplitude is much smaller, indicating that the corresponding transmission paths are not as significant as at higher frequencies. This is consistent with the general concept that low frequency sound waves would propagate through the vanes without significant reflection, but would then be reflected by the tunnel walls.

E.1.4 Transmission through second corner vanes

Cross-correlation functions measured for three microphone pairs at the second corner turning vanes are shown in Figures E.9 through E.11. The reference microphone is #14 and the secondary microphones are 8, 9, and 10, respectively. The cross-correlation functions are plotted for time delays from -50 ms to +50 ms and for three frequency bandwidths.

The objective of the analysis, as is the case for the first corner, is to determine acoustic transmission paths through the vanes and to determine whether the sound waves are reflected by the vanes or by the tunnel walls. Thus, peaks in the cross-correlation functions have been associated with possible ray paths - the figures show these potential paths.

The test arrangement for the second corner measurements is shown in Figure E.2 where it is seen that microphone 14 is much closer to the turning vanes than is microphone 7 in the first corner (Figure E.1). Consequently the time delays associated with the first peaks in the cross-correlation function are much smaller than for the first corner. Also, there are no flow control vanes to influence the sound propagation paths at the second corner. Finally, the source is well separated from the

mircophone array, with the result that the intitial peaks in the cross-correlation function are associated with rays to the secondary microphones which do not first pass microphone 14.

Inspection of the cross-correlation functions in Figures E.9 through E.11 shows that the peaks associated with reflections by the turning vanes are usually strongest at the higher frequency ranges. Thus, for microphone pairs (14-8) and (14-9) the correlation function for the frequency range 3000 to 5000 Hz shows the most definite evidence of reflections at the vanes. The evidence is least definite in the frequency range 1000 to 5000 Hz. Furthermore in this frequency range there is much more evidence of sound transmission in both directions (i.e., there are correlation peaks at negative as well as positive time delays) than there is at higher frequencies.

It is concluded, therefore, that the low frequency sound waves pass through the turning vanes without significant reflection, but the waves are then reflected at the sidewall of the second stage diffuser. At high frequencies the sound waves are reflected or "directed" around the corners mainly by the vanes.

E.2 Turning Vane Sound Generation

E.2.1. Introduction

Turning vanes generate sound as a consequence of:

- unsteady inflow, which causes fluctuating turning forces, as well as localized leading edge sources of sound;

- self-generated unsteady flows, including attached turbulent boundary layers, separated flows, and wakes;

- vibration, including aeroelastic effects.

E-6

The sources of unsteady inflow are freestream turbulence, diffuser boundary layers and separated flows, and wakes from upstream obstructions (such as other vanes, flow control devices, fan, models in test section, etc.) In the case of the first corner vanes, the first diffuser is the primary source of flow disturbances - diffuser turbulence - is known to be intense. Second corner vanes would experience flow fluctuations caused by the first corner vanes, the flow deflectors, and the second diffuser (crossleg). In order to calculate turning vane noise from first principles, a great deal of detail about the flow field is required (turbulence intensities in three directions, length scales, and convection speeds). Such detail is neither available for the 4x7 m nor for other tunnels, nor is much data available in the literature for idealized elements, such as simple diffusers. Therefore, we looked first to certain experimental data for evidence of noise generation.

E.2.2 Surface pressure data

Surface pressure spectra can provide an input into several analytical models of noise generation. Surface pressure sensors were located near the trailing edges of the first corner vanes and the flow deflectors in the first crossleg to see if it was possible to obtain such input for empirical or exact source models. The major concern about the feasibility was the high ambient acoustic environment, which could mask localized pressures. The test configurations are shown in Figure E.12. Note that time constraints did not permit measurements at other locations on the vanes, such as near midspan where higher flow speeds would be expected, nor at the leading edge.

Spectral data for runs are shown in Figs E.13 to E.14. If the fluctuating pressure data measured are hydrodynamic in nature - arising from either free-stream turbulence or self-generated

unsteady flow, then the pressure spectra should scale as V^4 in amplitude and in direct proportion to velocity in the frequency domain. If the surface pressures are merely those caused by the tunnel's acoustic environment, then the spectra will scale accordingly (roughly as V^5). In both cases, it is necessary to assume that the turbulence characteristics are Reynolds-number independent, which may not be true in the 4x7 m tunnel. Figures E.15 to E.16 show such comparisons; it appears that the sensors on the "upper" (suction) surface of the turning vanes are indeed measuring hydrodynamic pressure at frequencies above 100 Hz, while the sensors on the "lower" (pressure) surfaces of the vanes and flaps may be measuring acoustic pressures at low and high frequencies.

Converting this data to a ratio of p/q (where q is the local tunnel <u>centerline</u> dynamic pressure), shows values in the range expected for trailing edges of lightly-loaded airfoils or flat plates. (If the local velocity and dynamic pressure were known at the measurement station, the ratio of p/q_{local} would be greater than that indicated.)

Since there were nearby microphones, and the areas around the vanes and flaps are highly reverberant, it is of interest to compare the pressure data measured on the flaps with those measured at the microphones away from the surface. These comparisons are shown in Figs E.17 and E.18, in which it is seen that the surface pressures are only marginally higher than the acoustic pressures nearby. Thus, these data have not provided unambiguous data to use as inputs to calculation procedures for trailing edge source models.

E.2.3 Cross-Correlations

Cross-correlations were made between the surface pressure sensors and the nearby microphones to see if one could identify

either upstream propagating sound from the fan, or causality correlation between the surface pressures and the nearby microphones. In the latter case, correlation coefficients were expected to be small due to the extensive source area associated with the turning vanes, although the microphones were located within what was thought to be the "hall radius" of the instrumented vane to increase its contribution to the acoustic field relative to other vanes.

For the case of the instrumented flow deflectors, correlations (cross-covariance coefficients of up to 0.3) exist at frequencies below 4 kHz. The time delay associated with a trailing edge source propagating downstream toward the microphone would be around +2.4 ms, while a wave propagating upstream along the tunnel axis would have a time delay of approximately -2.4 ms. The data showed correlations peaking at either 0 or negative time delays, thus indicating that the microphone and the surface pressure sensors are both sensing acoustic waves traveling upstream or in some oblique mode (which would produce smaller time delays than a wave propagating along the axis.

The similar comparisons for the instrumented turning vanes showed much weaker correlations and different trends in different frequency ranges. In the 63 Hz octave band, there was evidence of upstream propagating waves, while in the 125 Hz octave band, the envelope of the correlation function seemed to indicate a causality correlation, i.e., a peak at a time delay corresponding to a wave originating at the surface propagating downstream. However, this could also be caused by a downstream propagating wave originating upstream of the corner or reflected from the corner (note that a reflected upstream propagating wave would also produce a peak in the correlation coefficient at negative time delays). Above 125 Hz, the correlation coefficients became small and difficult to interpret; but inasmuch as they are small,

they suggest that the surface pressure data is at least not dominated by <u>propagating</u> acoustic energy.

Surface-to-surface pressure measurements were made to obtain length scale information. However, these data were limited due to experimental artifacts (sensors slipping out of mounts, inadequate isolation of case, etc.)

Due to the location of the first corner vanes - close to the test section, it is important to refine the data base with which to make reliable estimates of the turning vane noise. The relative importance of first corner turning vane noise could define the treatment details for all upstream-propagating noise.
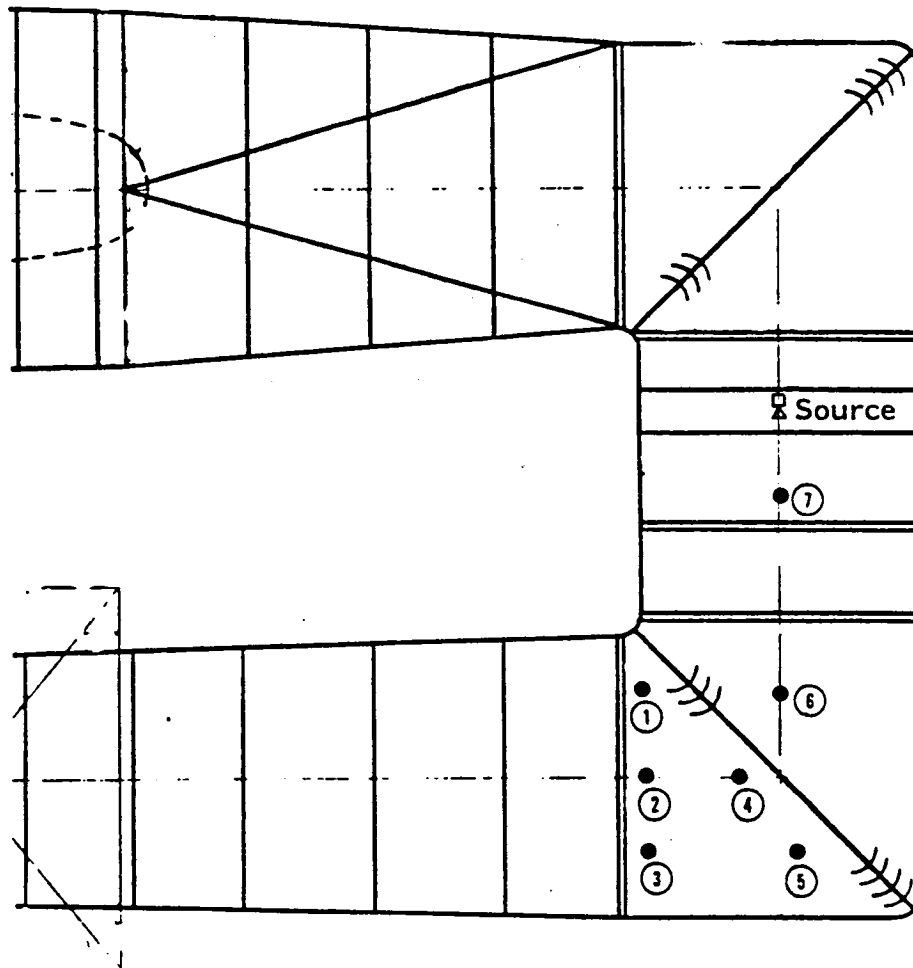
FIG. E.1 MICROPHONE AND SOURCE LOCATIONS FOR NOISE TRANSMISSION MEASUREMENTS THROUGH TURNING VANES OF FIRST CORNER (TEST 5)
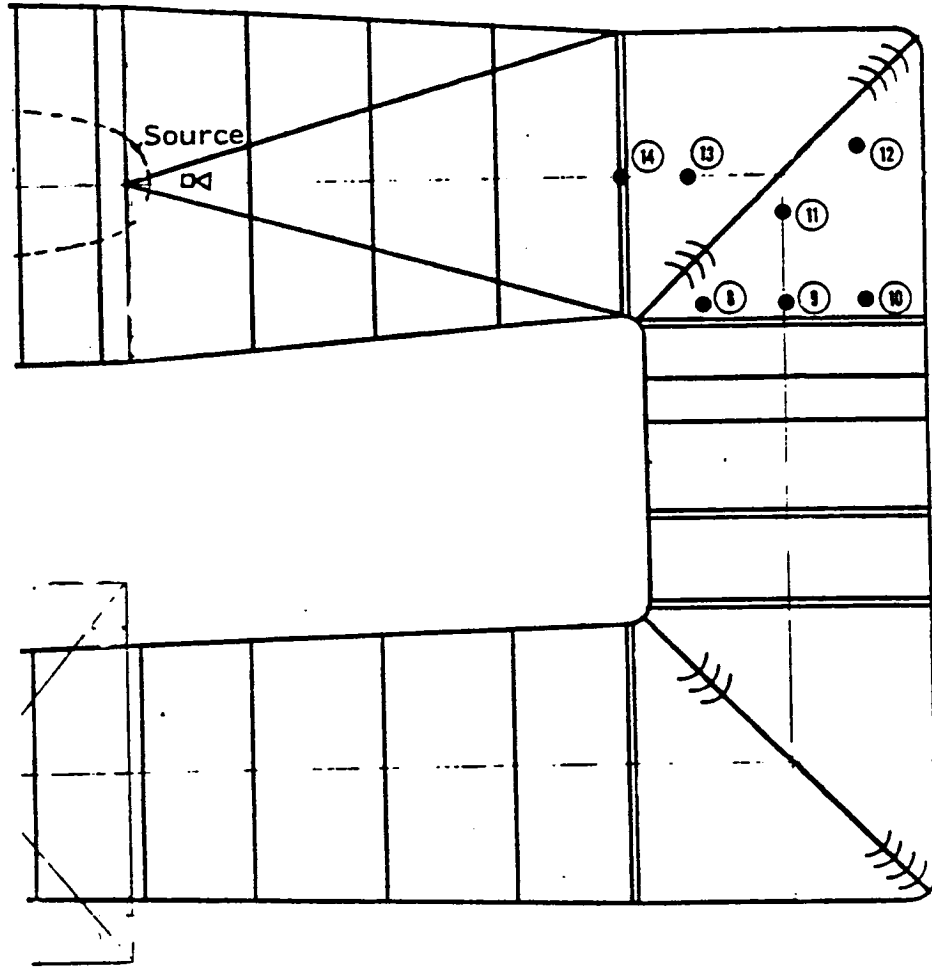
FIG. E.2 MICROPHONE AND SOURCE LOCATIONS FOR NOISE TRANSMISSION
MEASUREMENTS THROUGH TURNING VANES OF SECOND CORNER
(TEST 4)
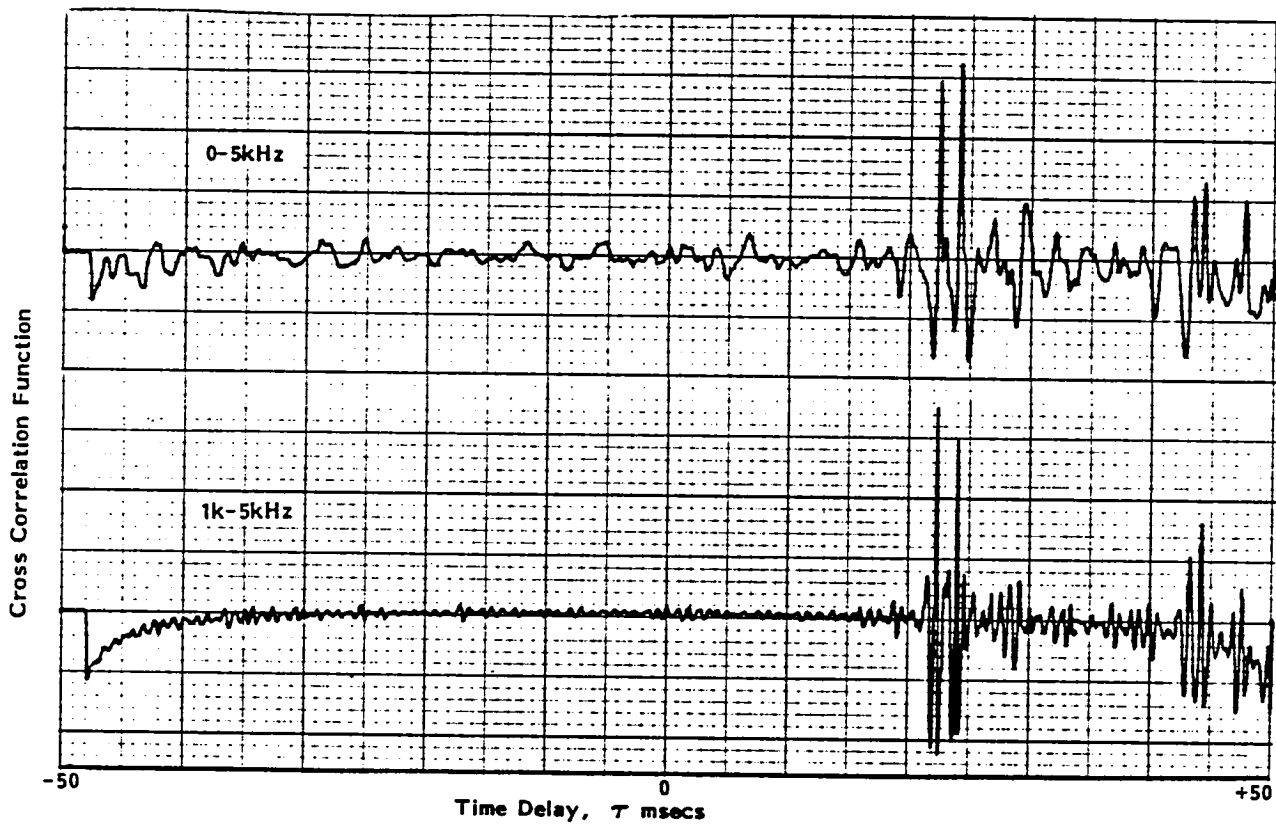
**FIG. E.3 SOUND PRESSURE CROSS CORRELATION BETWEEN MICROPHONES 6
AND 7 IN SECOND STAGE DIFFUSER (TEST 5)**

E-13
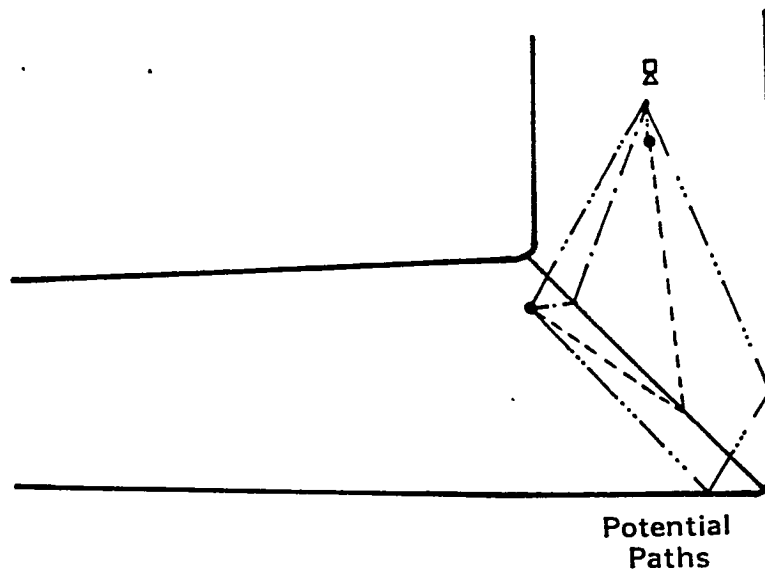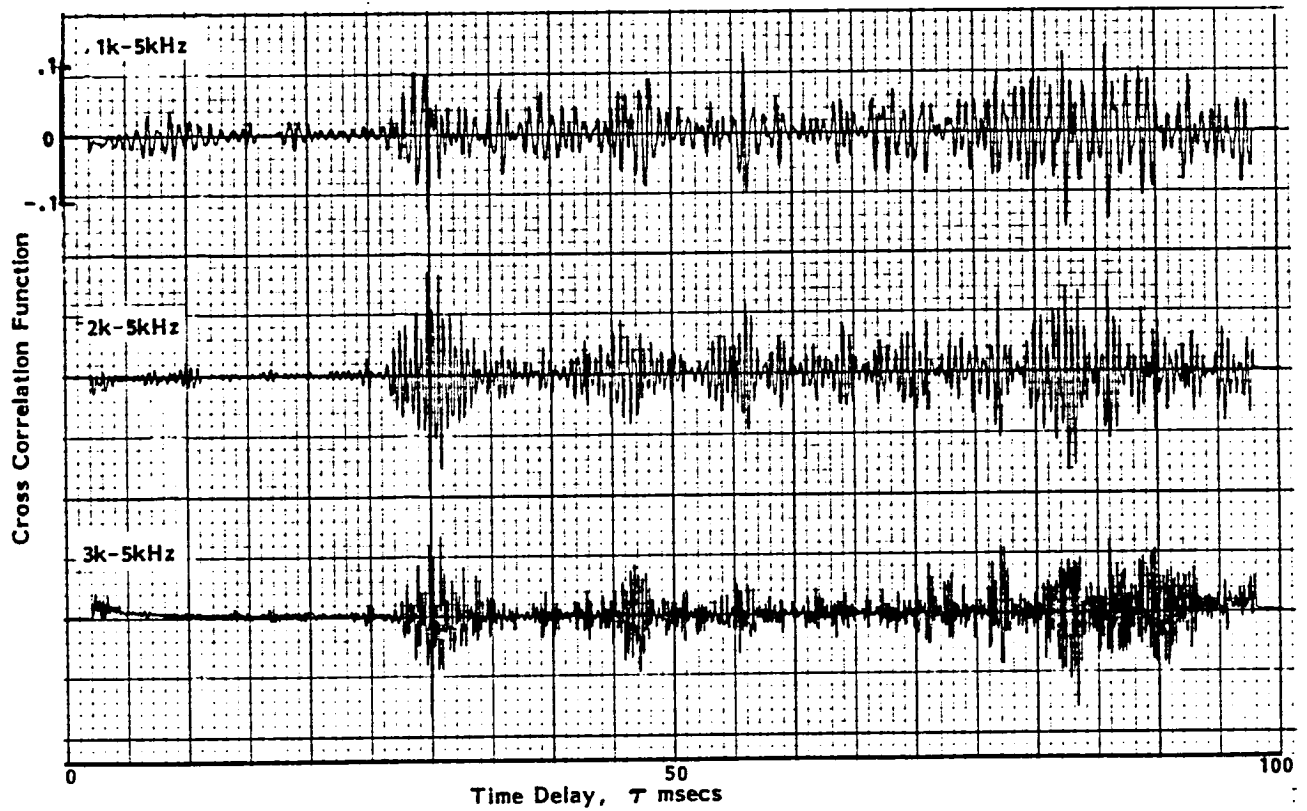
FIG. E.4   SOUND PRESSURE CROSS CORRELATIONS BETWEEN MICROPHONES 1
AND 7 IN FIRST CORNER (TEST 5)

E-14
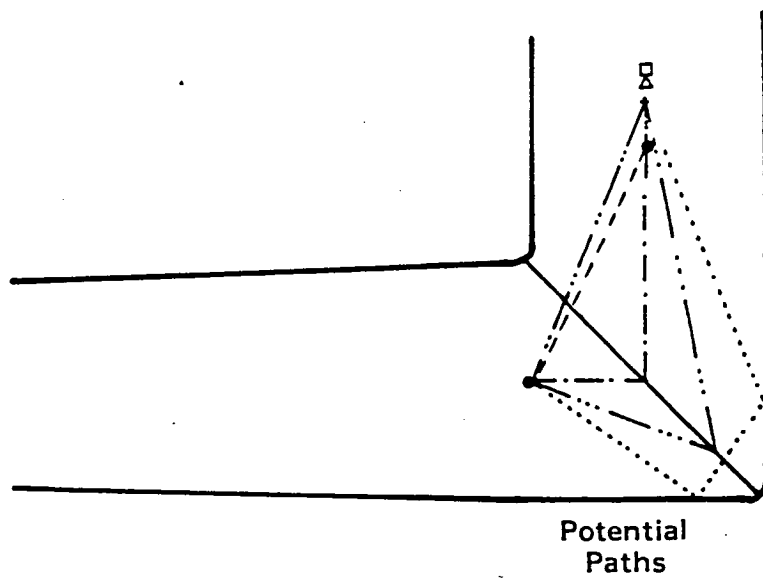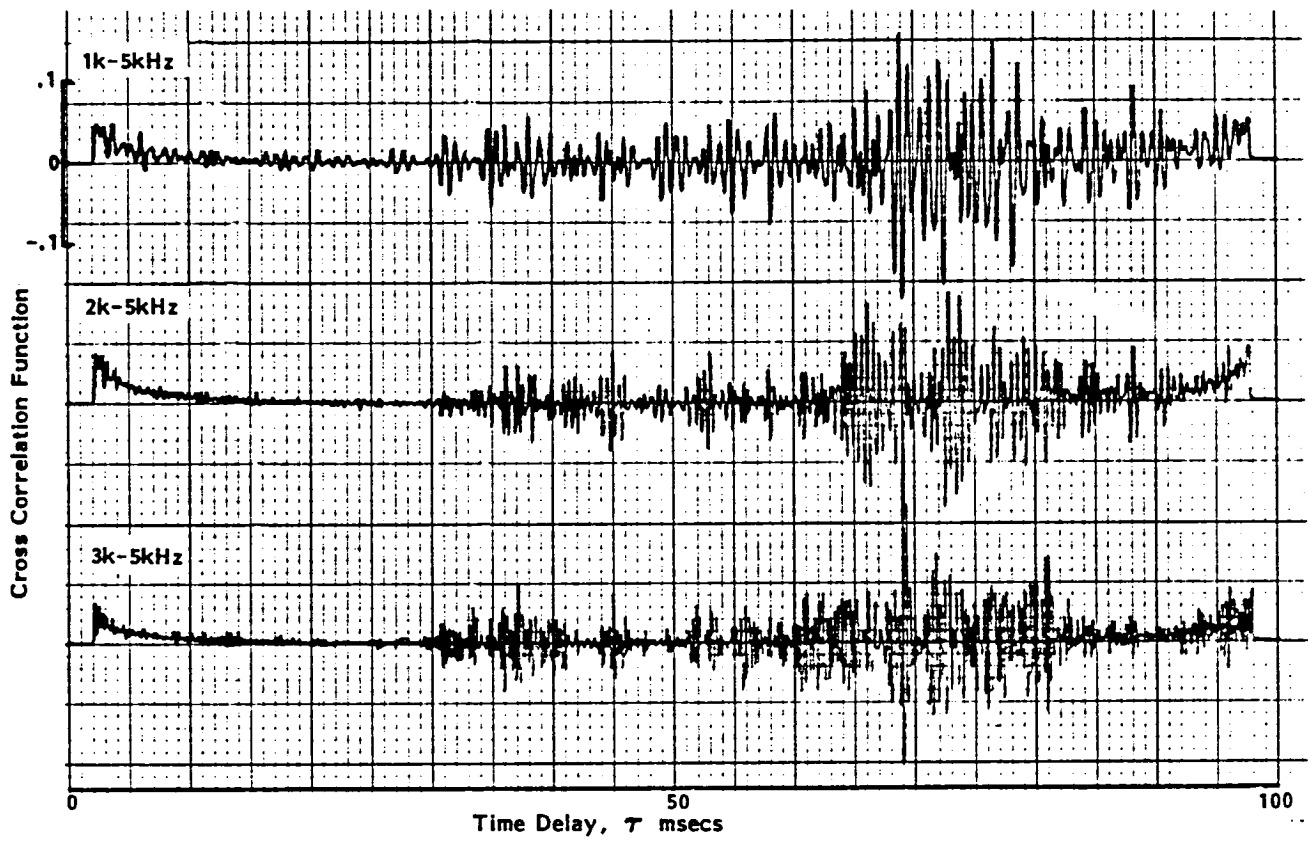
FIG. E.5 SOUND PRESSURE CROSS CORRELATIONS BETWEEN MICROPHONES 2
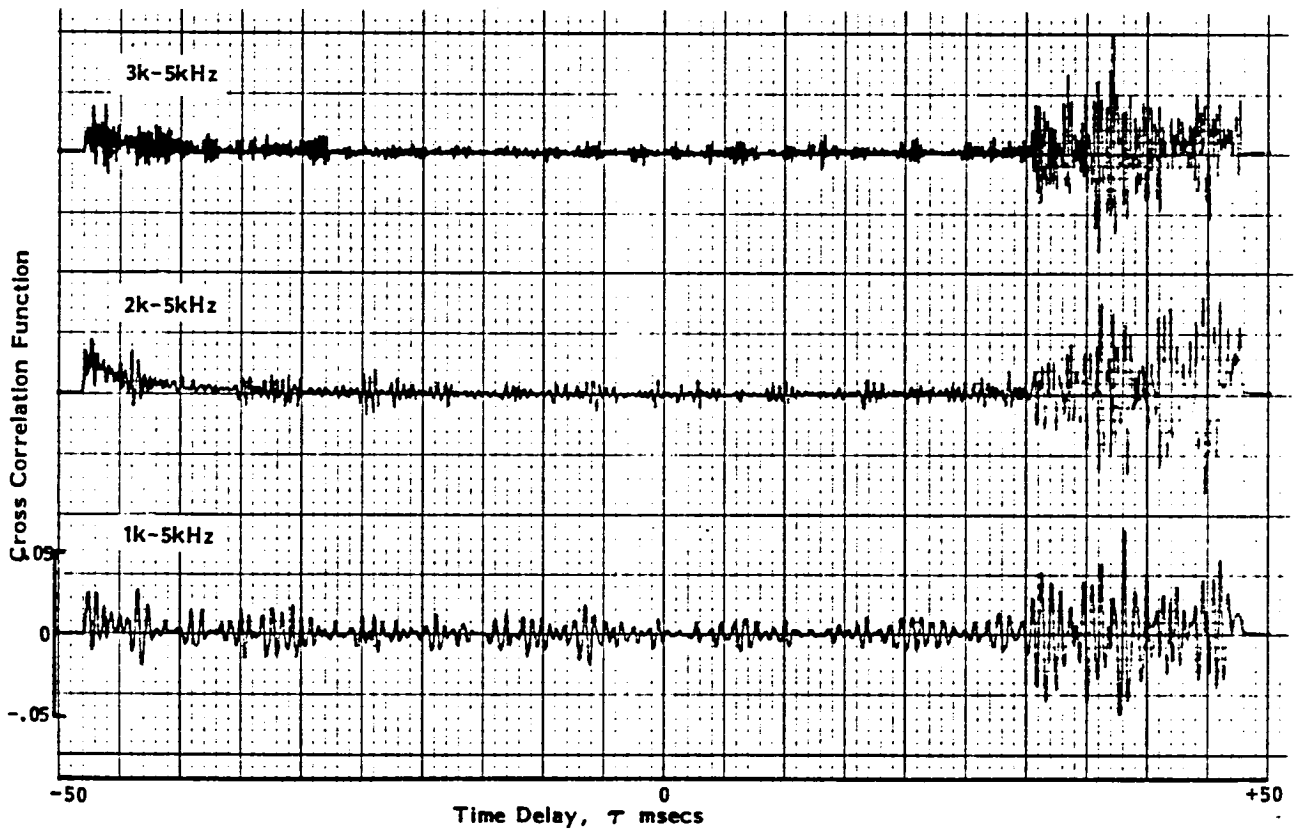   AND 7 IN FIRST CORNER (TEST 5)
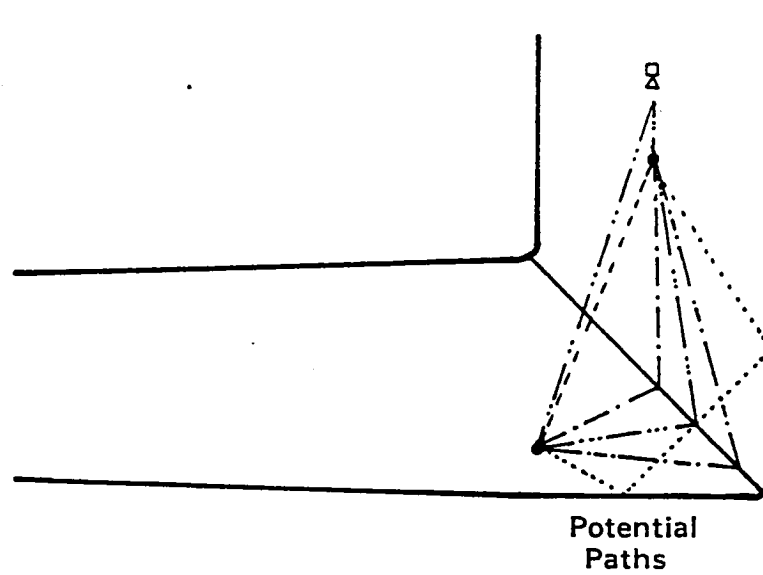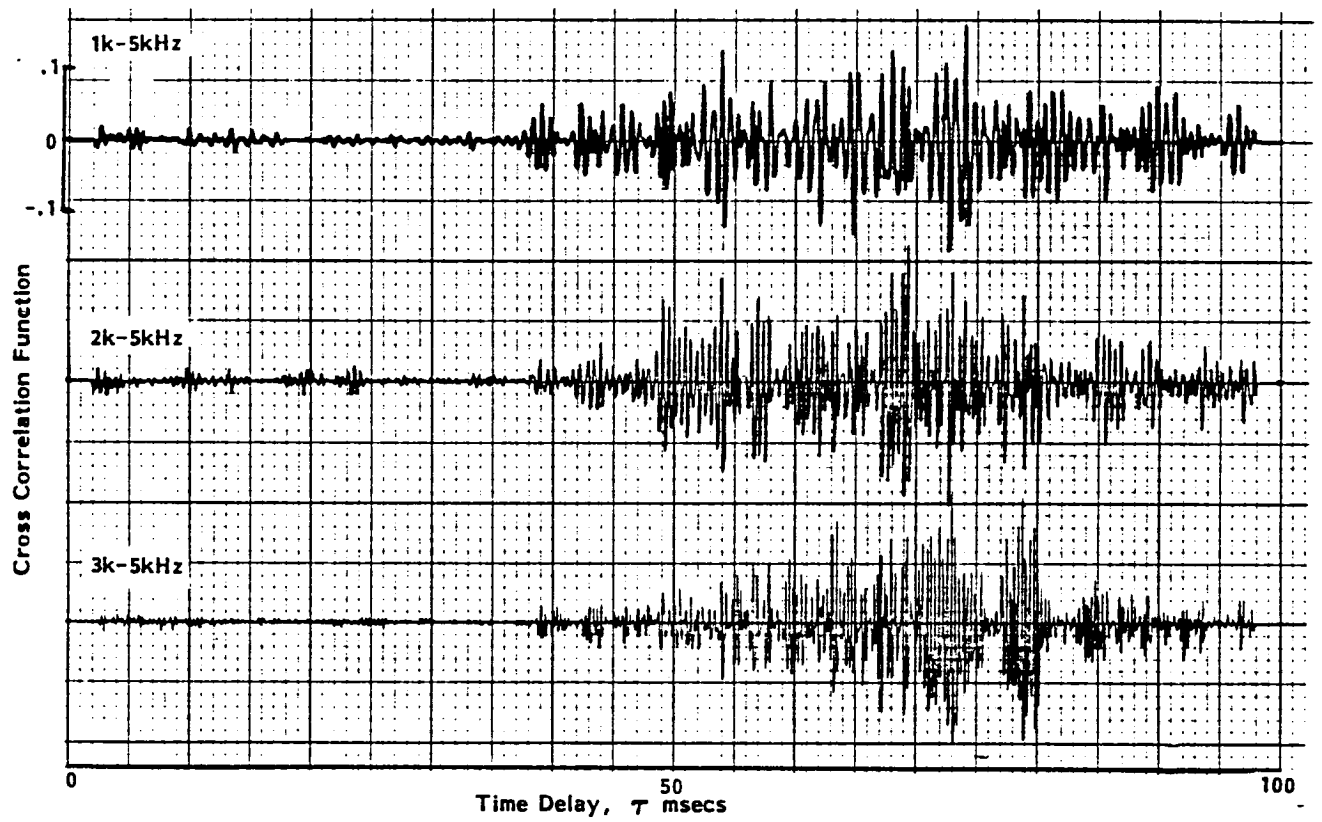
FIG. E.6 SOUND PRESSURE CROSS CORRELATIONS BETWEEN MICROPHONES 3 AND 7 IN FIRST CORNER (TEST 5)

E-16

FIG. E.7 SOUND PRESSURE CROSS CORRELATIONS BETWEEN MICROPHONES 2
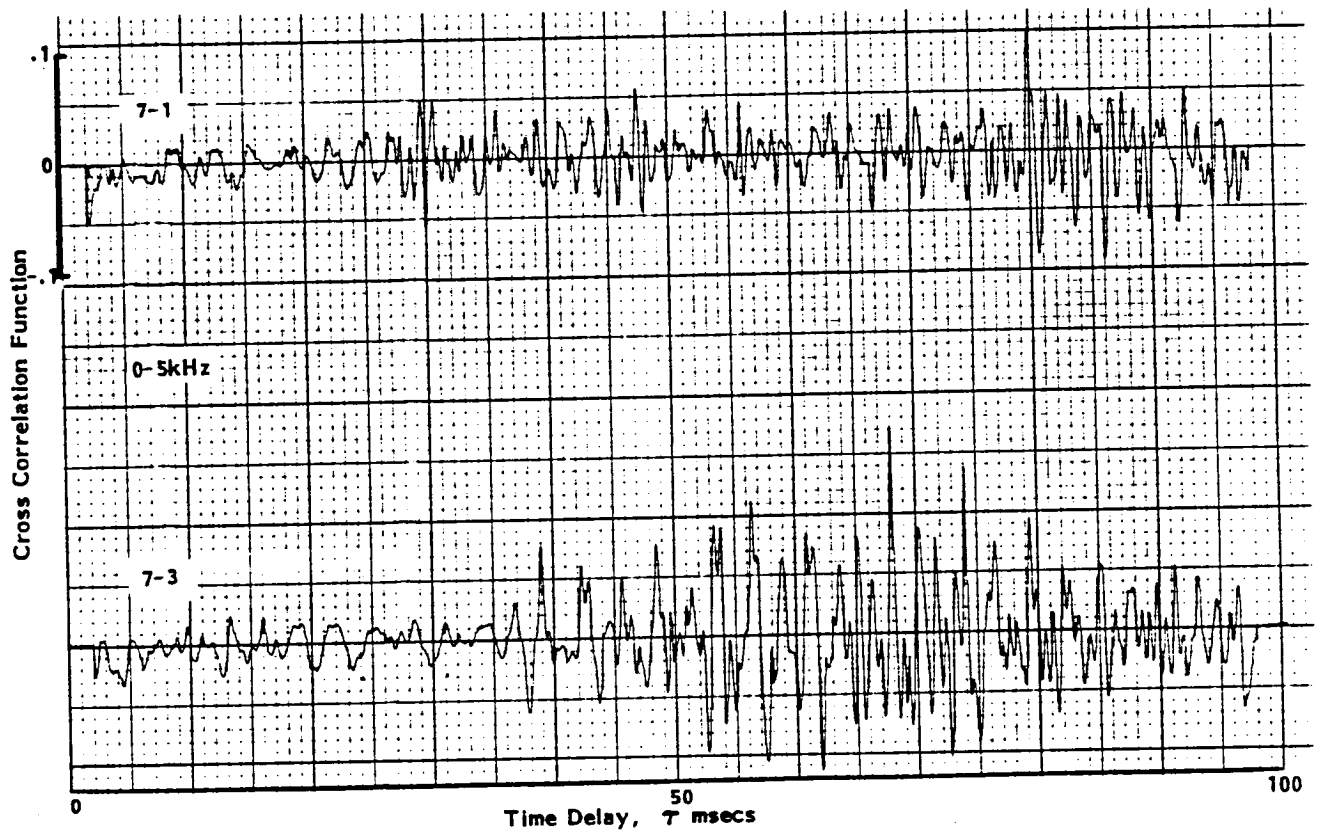AND 7 SHOWING NEGATIVE TIME DELAY REGION

E-17

FIG. E.8   LOW FREQUENCY SOUND PRESSURE CORRELATIONS FOR
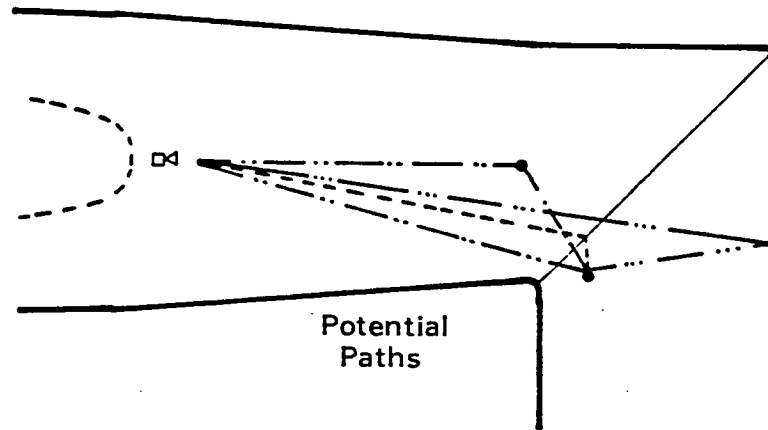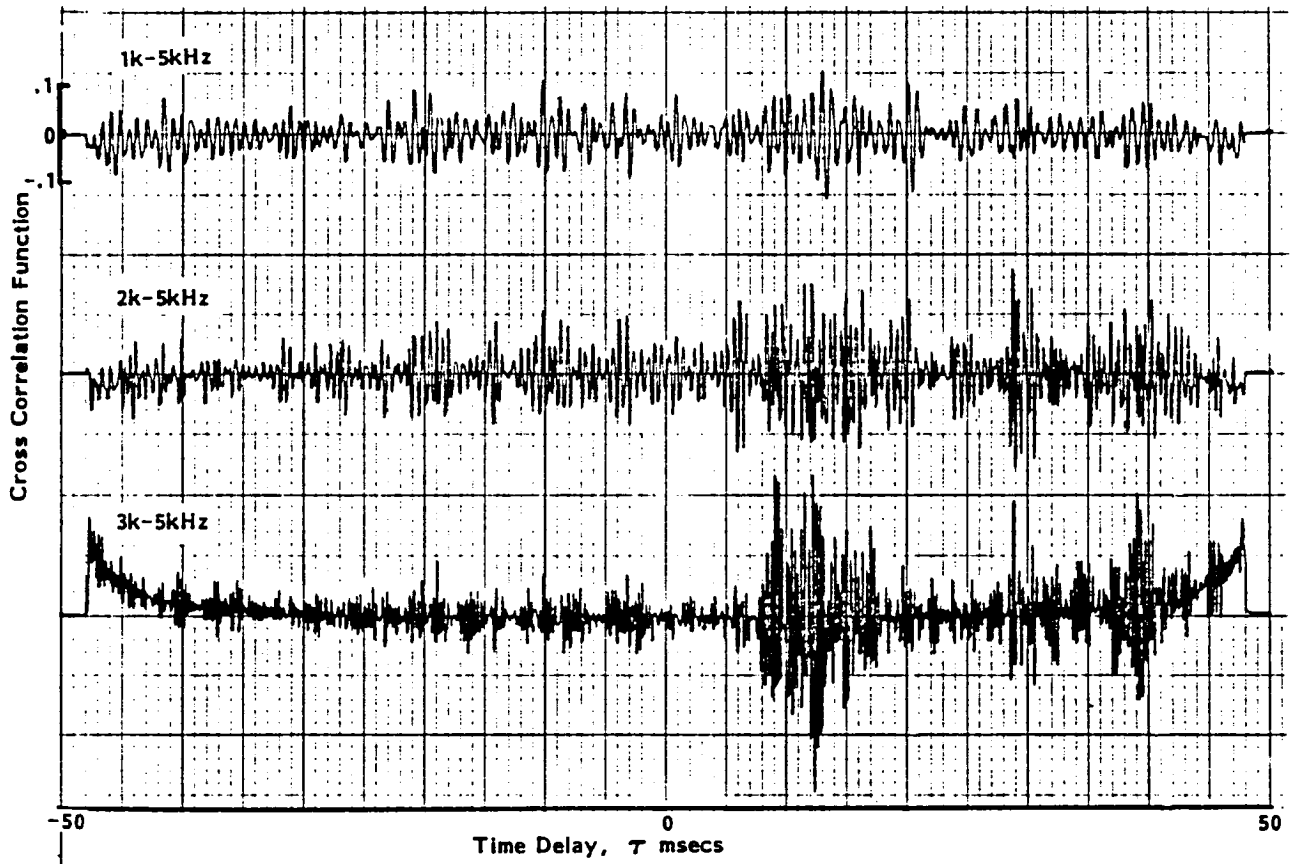   MICROPHONE PAIRS (7-1) AND (7-3)

FIG. E.9   SOUND PRESSURE CROSS CORRELATIONS BETWEEN MICROPHONES 8
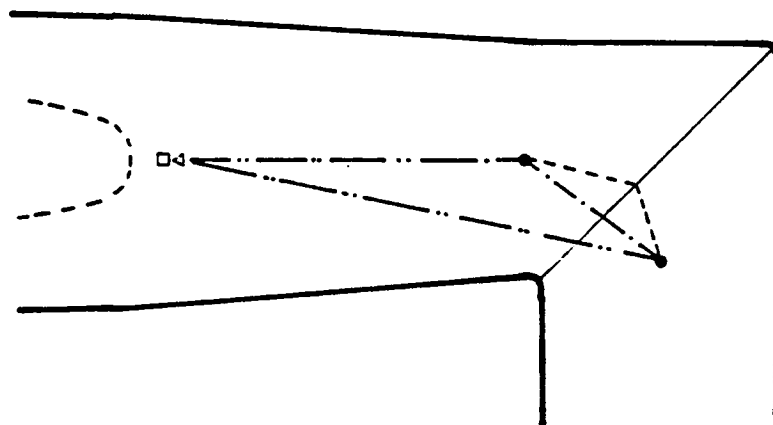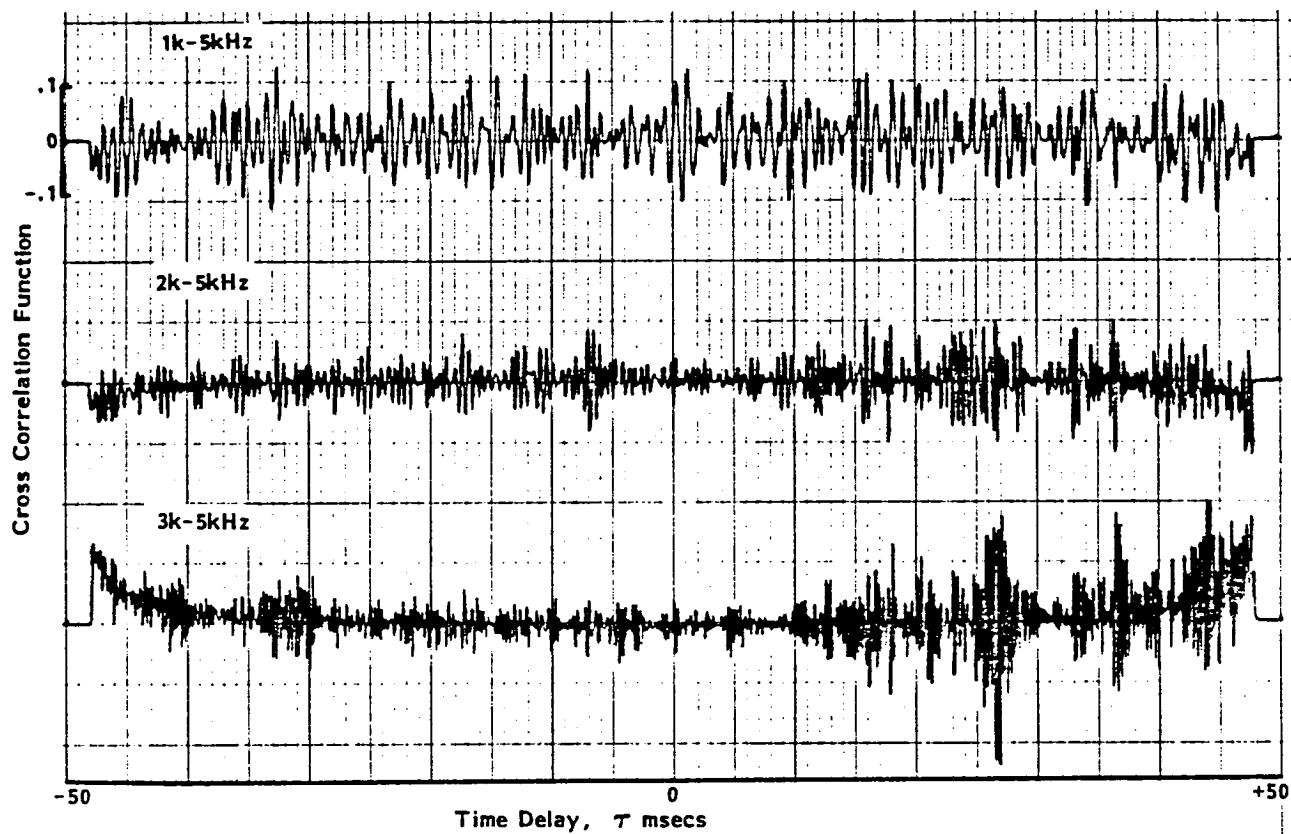   AND 14 IN SECOND CORNER (TEST 4)

FIG. E.10   SOUND PRESSURE CROSS CORRELATIONS BETWEEN MICROPHONES
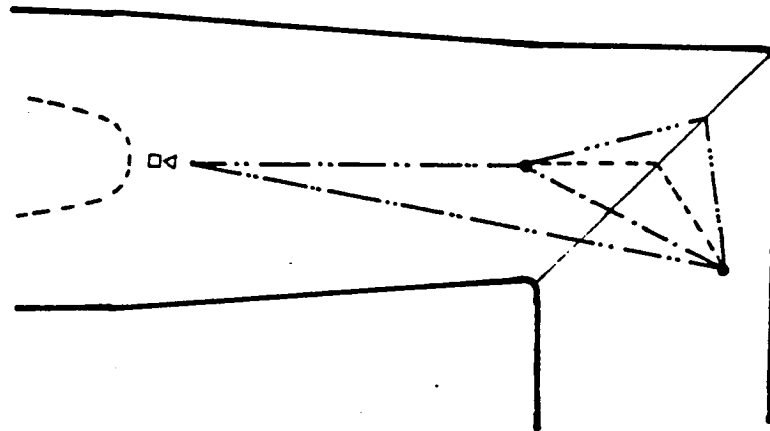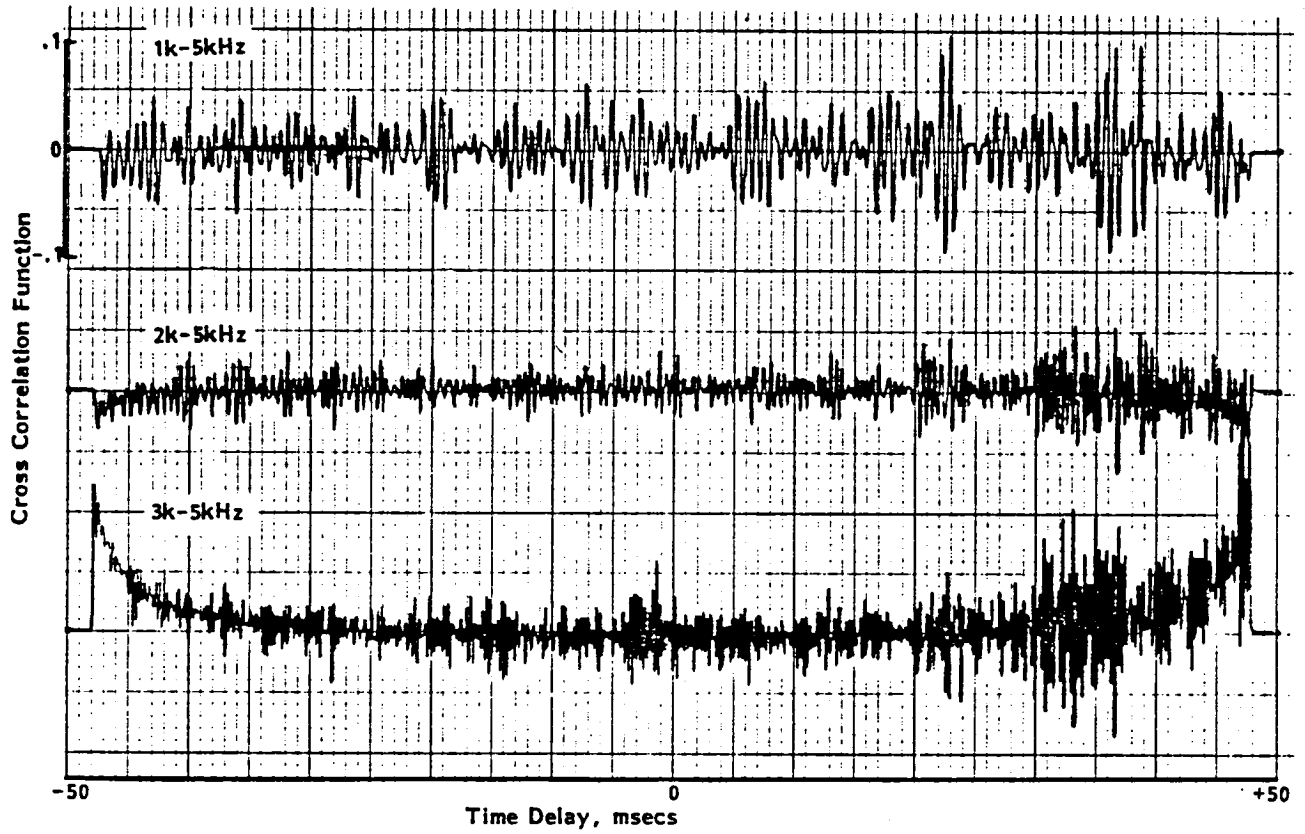9 AND 14 IN SECOND CORNER (TEST 4)

FIG. E.11   SOUND PRESSURE CROSS CORRELATIONS BETWEEN MICROPHONES
10 AND 14 IN SECOND CORNER (TEST 4)

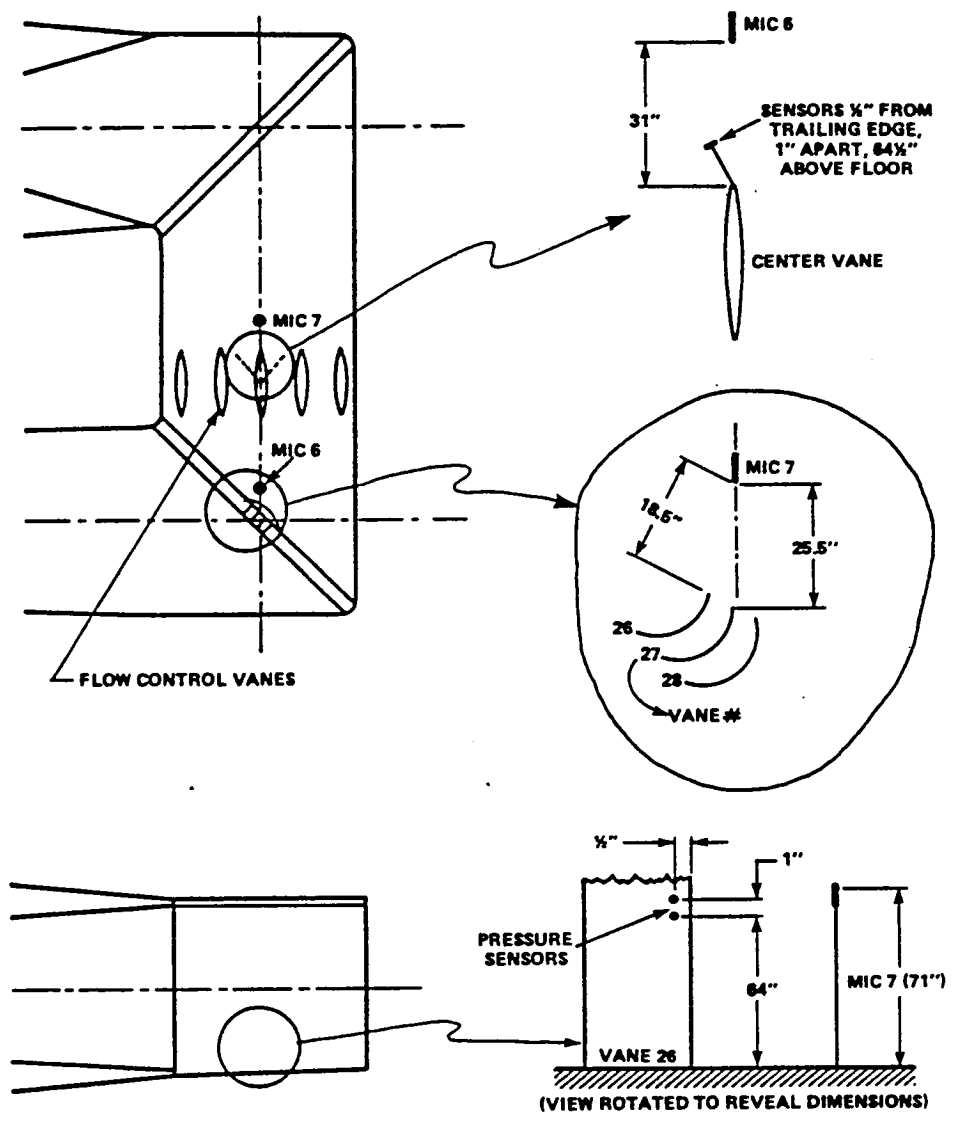FIG. E.12 TURNING VANE AND FLAP TEST CONFIGURATIONS
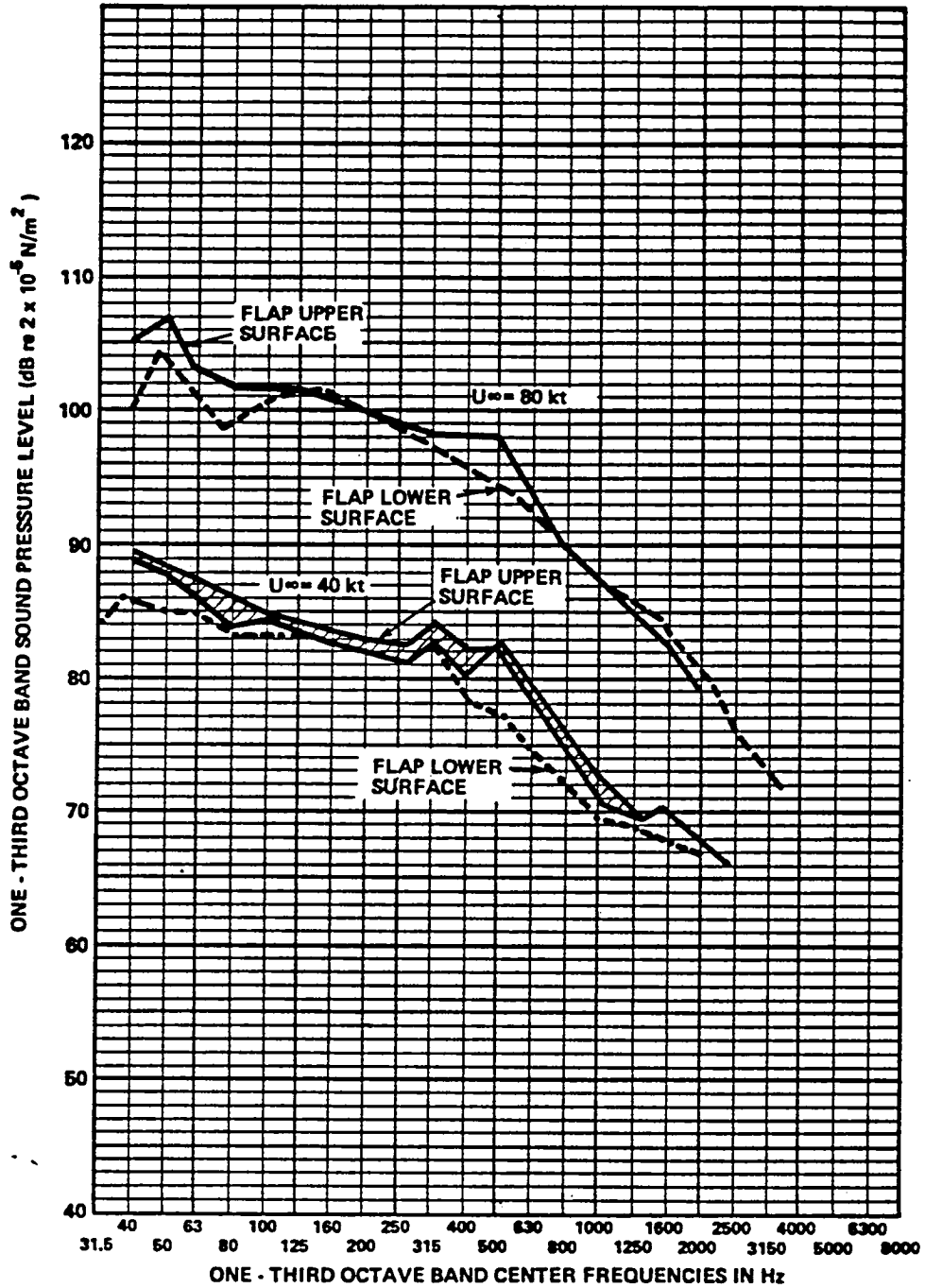
FIG. E.13 SURFACE PRESSURE SPECTRA 1.27 CM (1/2") UPSTREAM OF TRAILING EDGE; CENTER FLOW DEFLECTOR
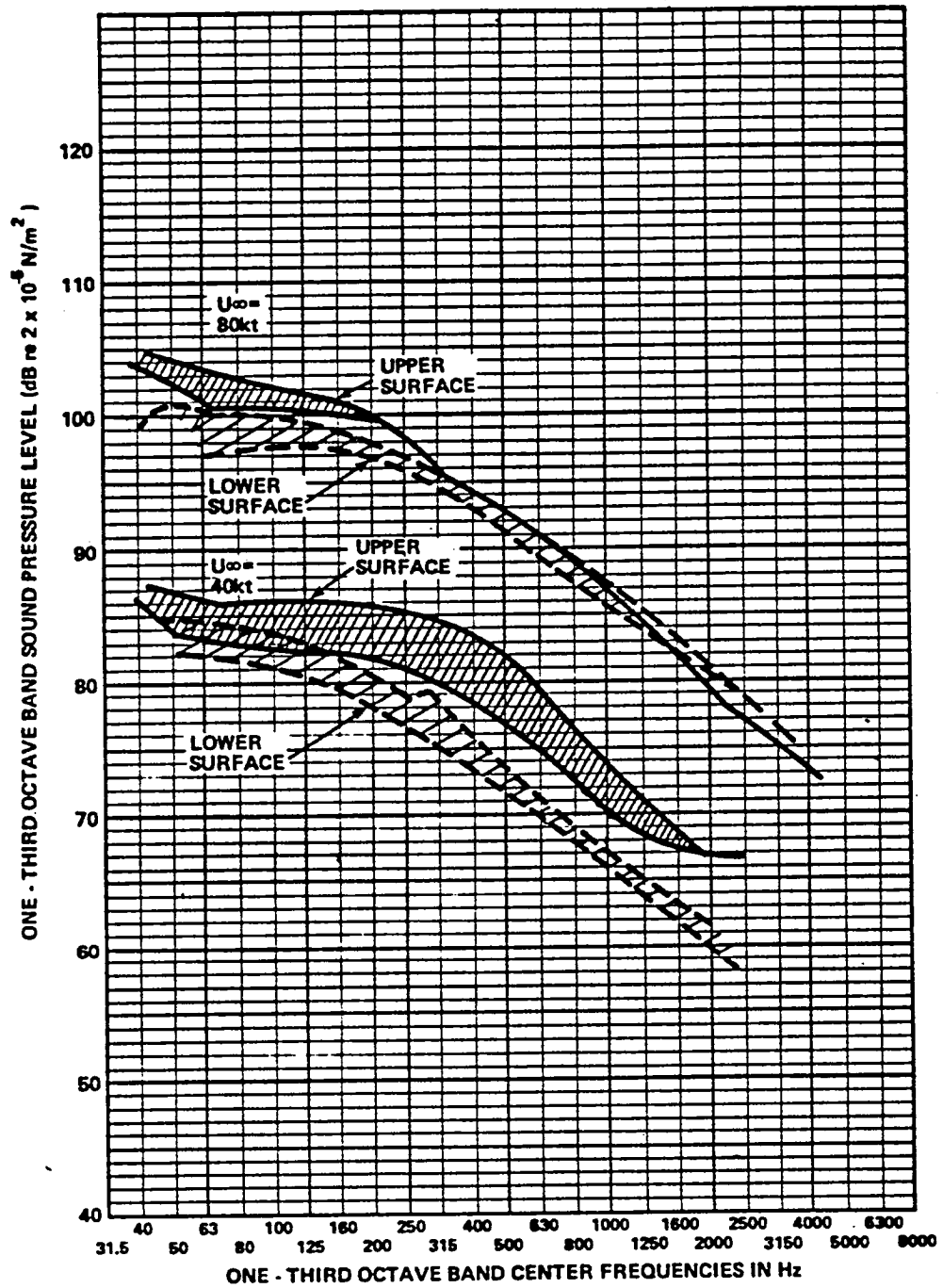
FIG. E.14 SURFACE PRESSURE SPECTRA 1.27 CM (1/2") UPSTREAM OF
TRAILING EDGE; 1ST CORNER VANES
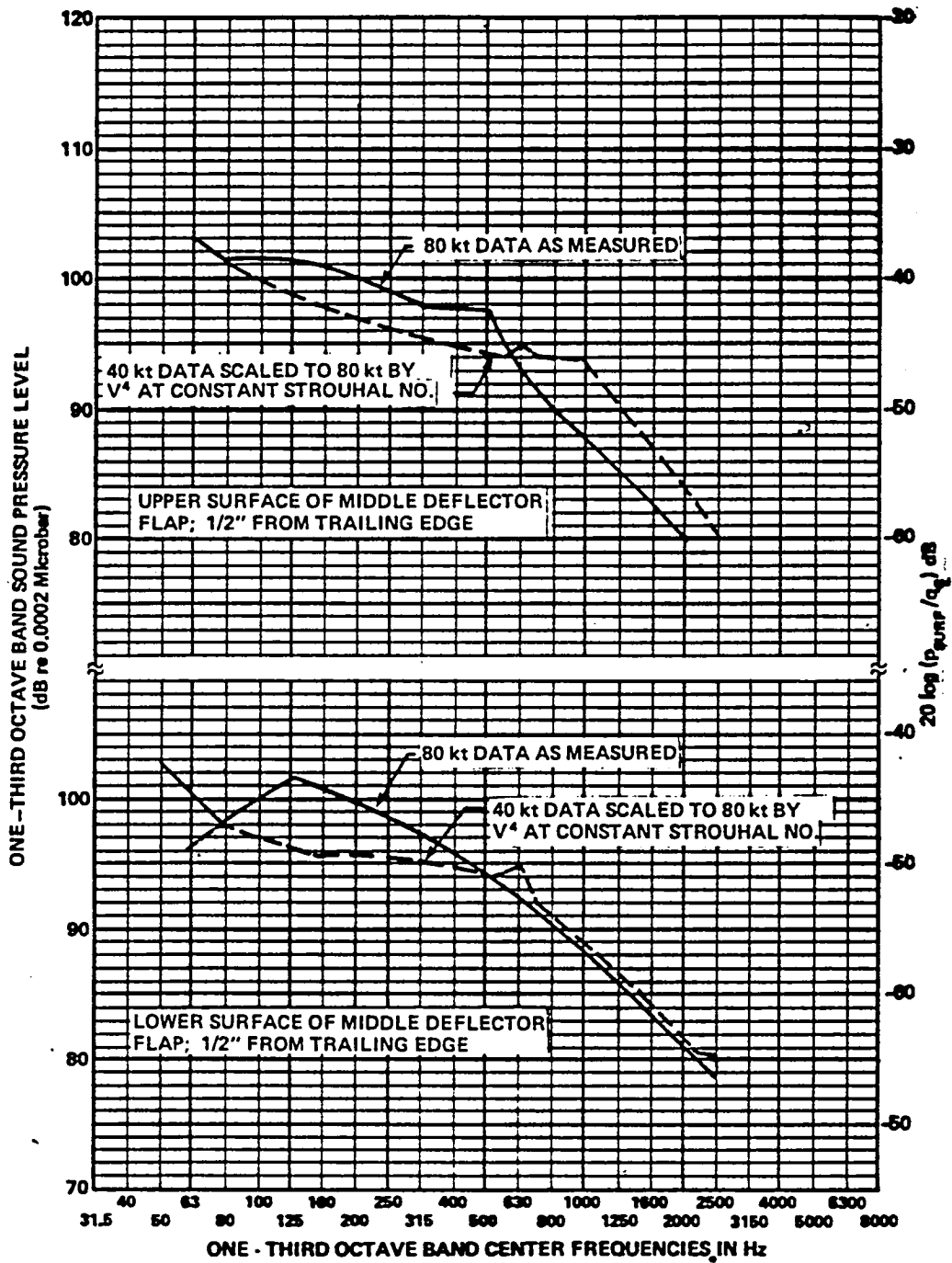
FIG. E.15 SCALING COMPARISON OF DEFLECTOR FLAP TRAILING EDGE
SURFACE PRESSURES

E-25

FIG. E.16 SCALING COMPARISON OF FIRST CORNER VANE SURFACE
PRESSURES

FIG. E.17   COMPARISON OF DEFLECTOR FLAP SURFACE PRESSURES WITH NEARBY MICROPHONE DATA

FIG. E.18   COMPARISON OF FIRST CORNER VANE SURFACE PRESSURES WITH NEARBY MICROPHONE DATA

APPENDIX F

ACOUSTIC CHARACTERISTICS OF TEST SECTION

WHICH AFFECT FREEFIELD NARROWBAND MEASUREMENTS

APPENDIX F
ACOUSTIC CHARACTERISTICS OF TEST SECTION

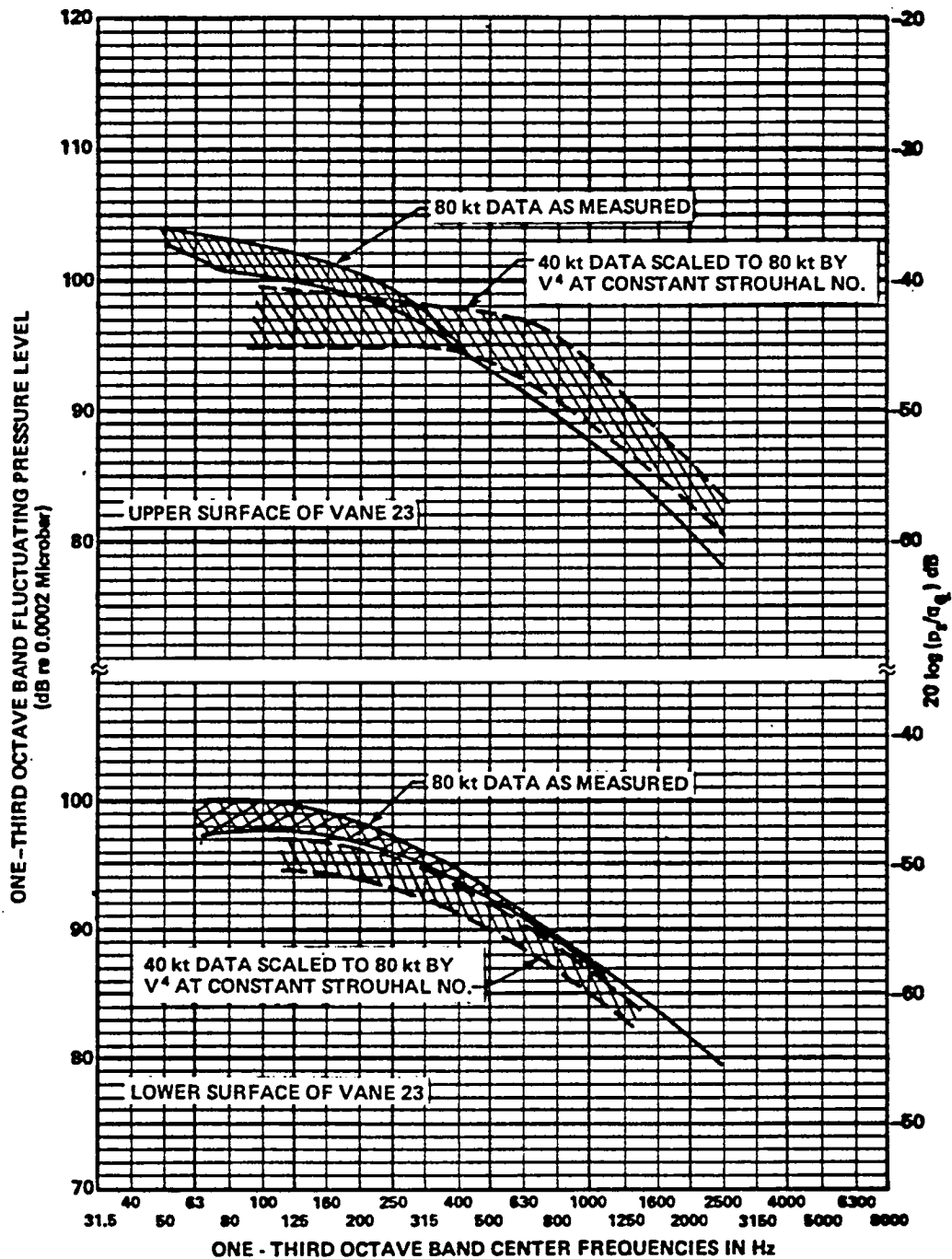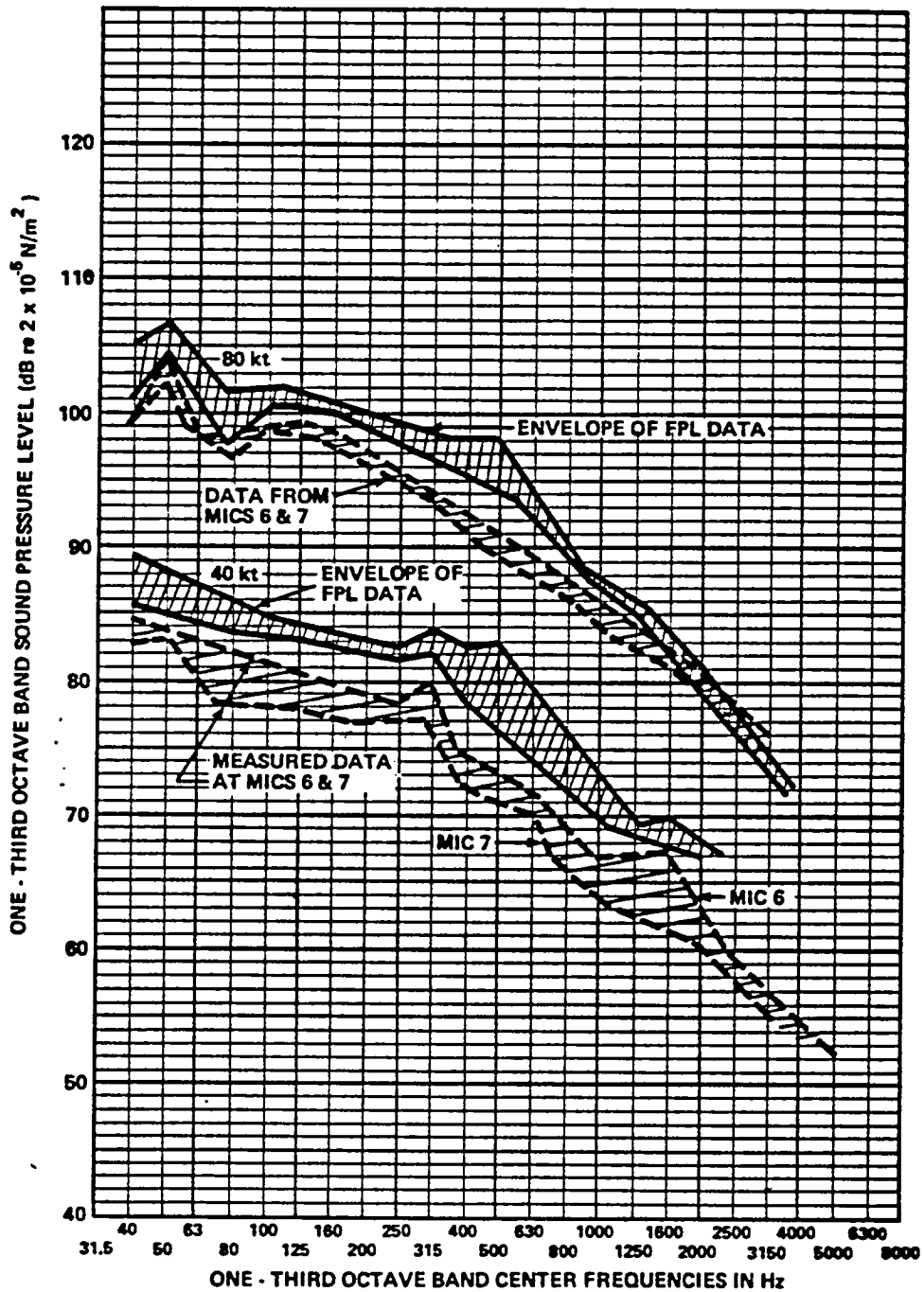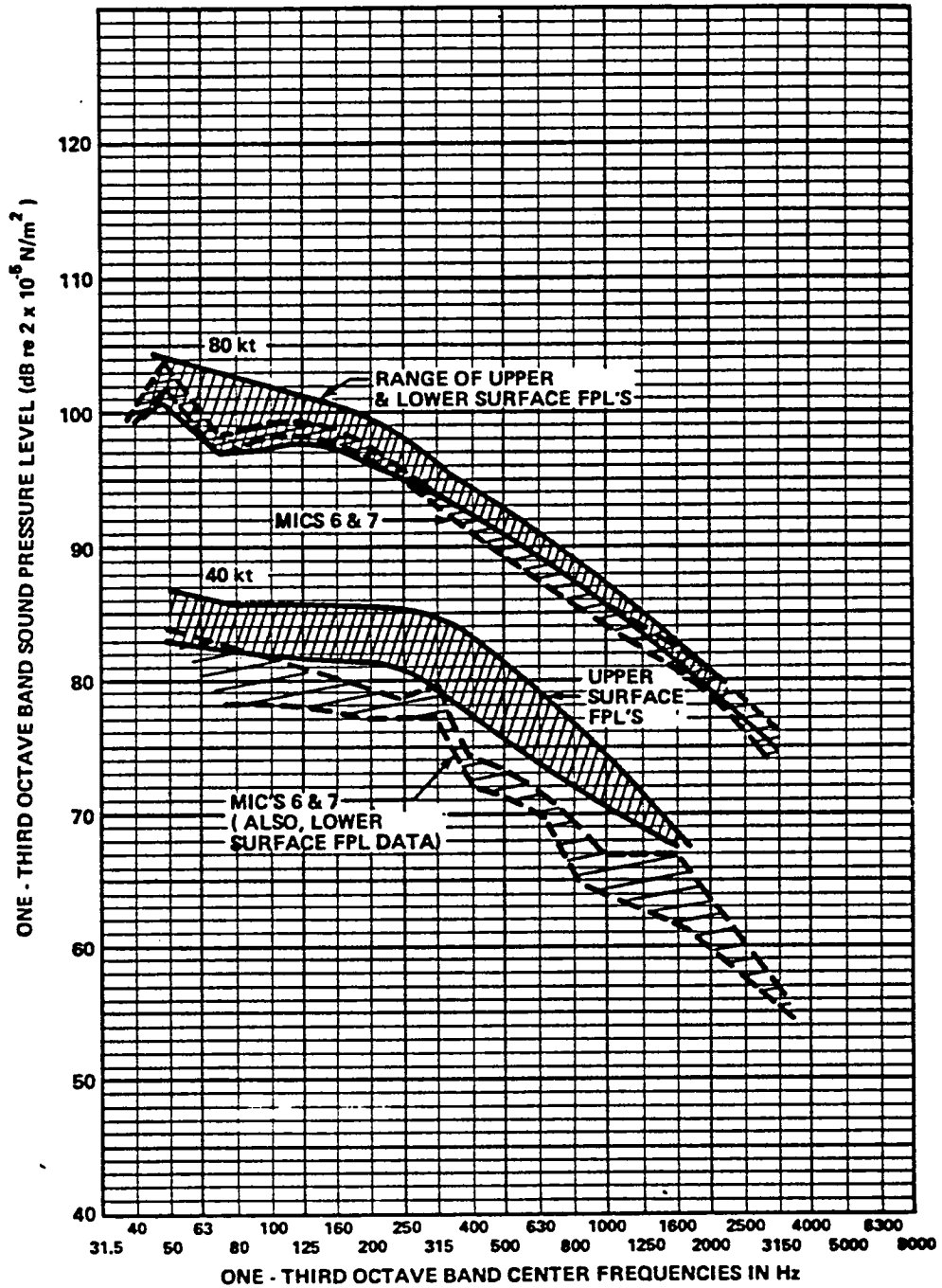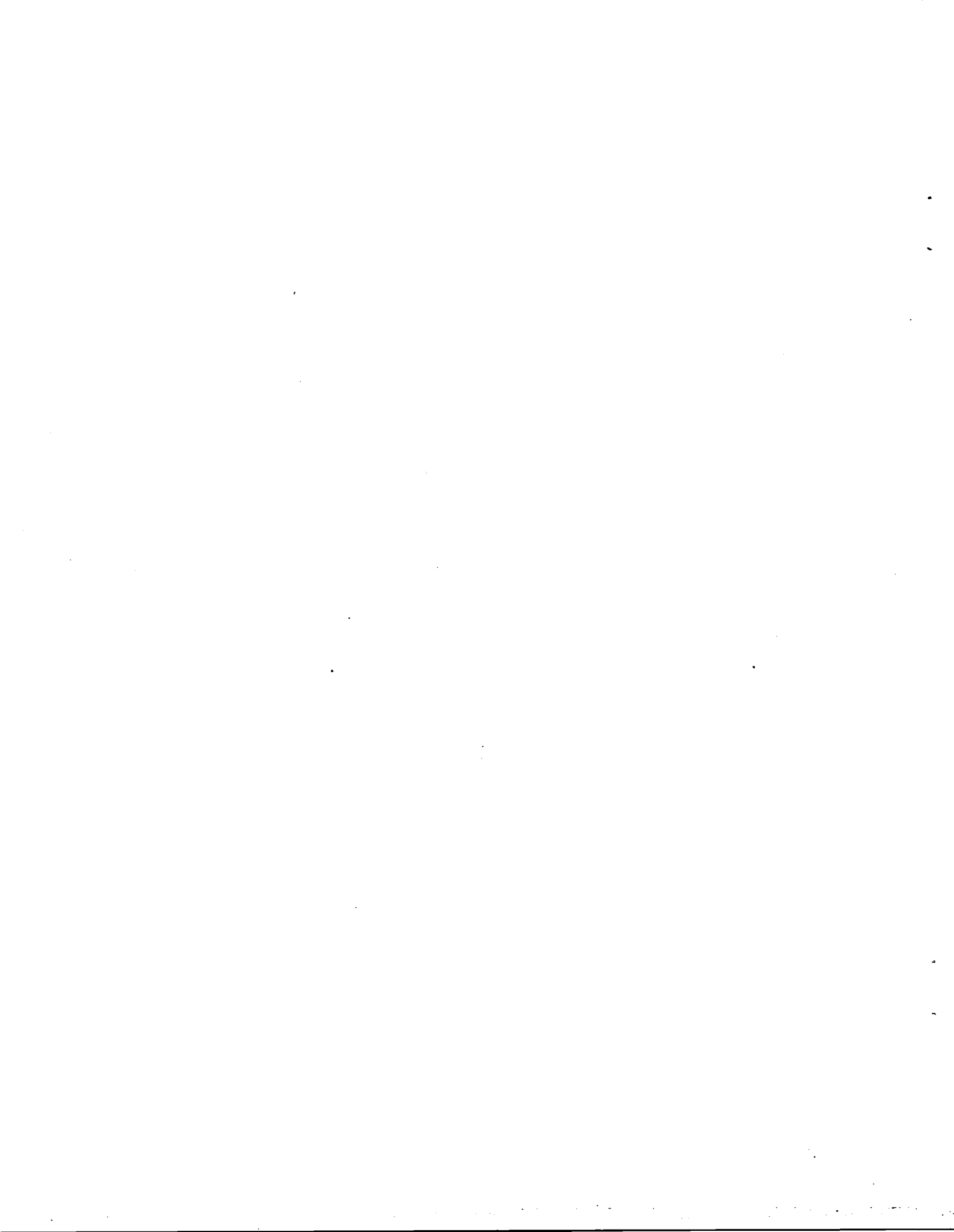The test chamber surrounding the open jet of the V/STOL tunnel has numerous reflecting surfaces, identified in Fig. F.1. These surfaces will reflect sound radiated from models in the test section and may thus create extraneous signals at measurement stations throughout the test section. The broadband acoustic characteristics of the test sections have been previously studied in model scale and full scale [F.1, F.2, F.3]. However, the planned use of the facility for rotor and propeller discrete frequency measurements introduces an additional dimension to the problem of reflections and "standing waves" in the test section. Interference between outgoing and reflected waves can be very pronounced when discrete frequencies are involved, resulting in rapid fluctuations in observed acoustic level observed both in space and in frequency.

In order to evaluate the quality of the 4 x 7 chamber for making accurate discrete frequency noise measurements, a dodecahedron source was located at several points in the test section corresponding to typical model positions. These are shown on Fig. F.2, along with microphone positions used to record the output (note that source location on the floor was chosen to eliminate that reflection which is already well known). Microphones were located close to the source to serve as references and to provide a feedback signal to the driver so that the output could be kept constant.

The output of the control microphone is plotted on Fig. F.3, where it can be seen to vary by less than ± 1 dB from 100 Hz to 1900 Hz, the frequency chosen as the upper limit of these plots to aid in clarity of data presentation. Figures F.4 - F.11 present the measurements of received acoustic level at each of the microphones, T4 through T11, for a typical source location.

The variations are very large and rapid with changing frequency. (Note that we believe that the slowly varying mean level may, in fact, be an artifact of controlling a multi-element source from a single microphone which may receive energy from sidelobes of adjacent speaker elements at some frequencies; however those fluctuations which occur rapidly with changing frequency are related to room acoustic characteristics.)

The extreme fluctuations would obviously render futile any attempt to develop a directivity pattern for a helicopter or propeller.

Other data were recorded for future use in locating the sources of reflections. However, it is obvious that all surfaces will require substantial treatment to reduce the fluctuations observed. The most difficult reflections to eliminate will be those associated with he nozzle and collector, since these elements are essential to the circuit operation, and as such must be kept structurally rigid. However, it is critical to develop some form of absorbing treatment for the collector cowl and highly desirable to treat the nozzle lip.

REFERENCES
(for Appendix F)

1. Ver, I.L., "Acoustical Evaluation of the NASA Langley V/STOL Wind Tunnel", NASA CR-145087, 1976.

2. Ver, I.L., D.W. Andersen, D.B. Bliss, "Acoustical Modeling Study of the Open Test Section of the NASA Langley V/STOL Wind Tunnel", NASA CR-145005, 1976.

3. Theobald, M.A., "Evaluation of the Acoustic Measurement Capability of the NASA Langley V/STOL Wind Tunnel Open Test Section With Acoustically Absorbent Ceiling and Floor Treatments", NASA CR-165796, 1978.
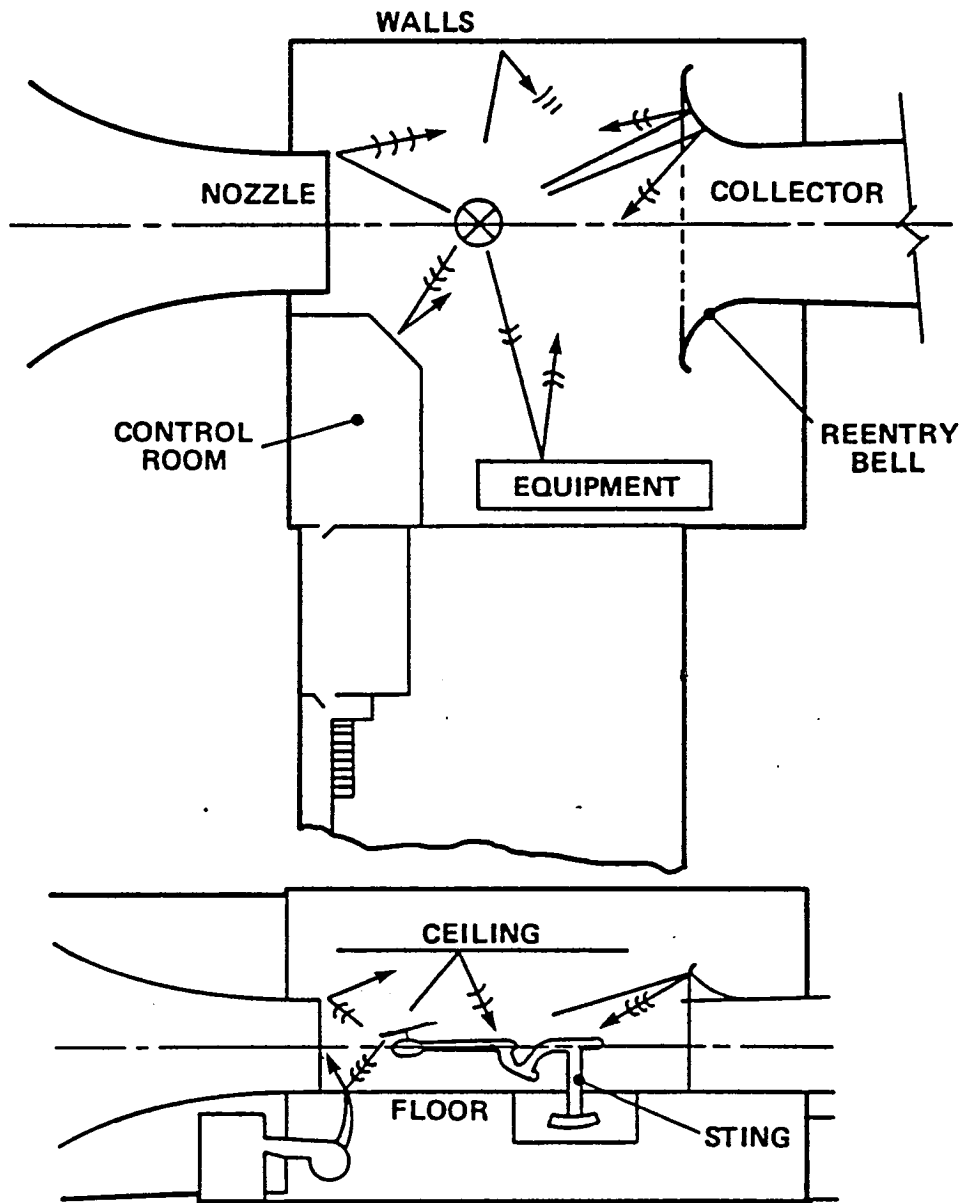
FIGURE F.1.   REFLECTING SURFACES IN TEST SECTION

F-4
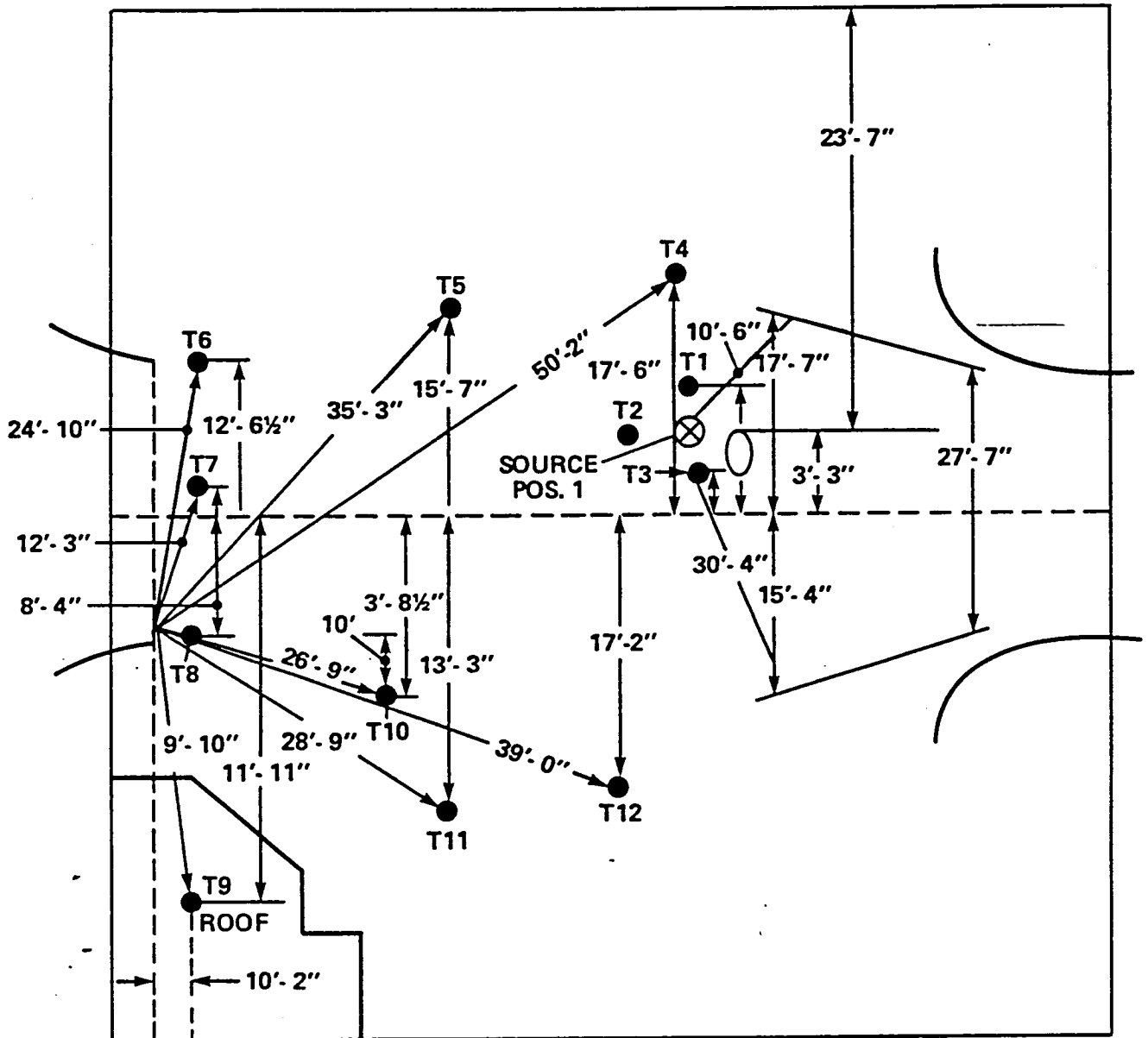
FIG. F.2. MICROPHONE AND SOURCE LOCATIONS FOR REFLECTION TESTS
(Note: Dimensions are projected to floor.)

F-6

10 dB
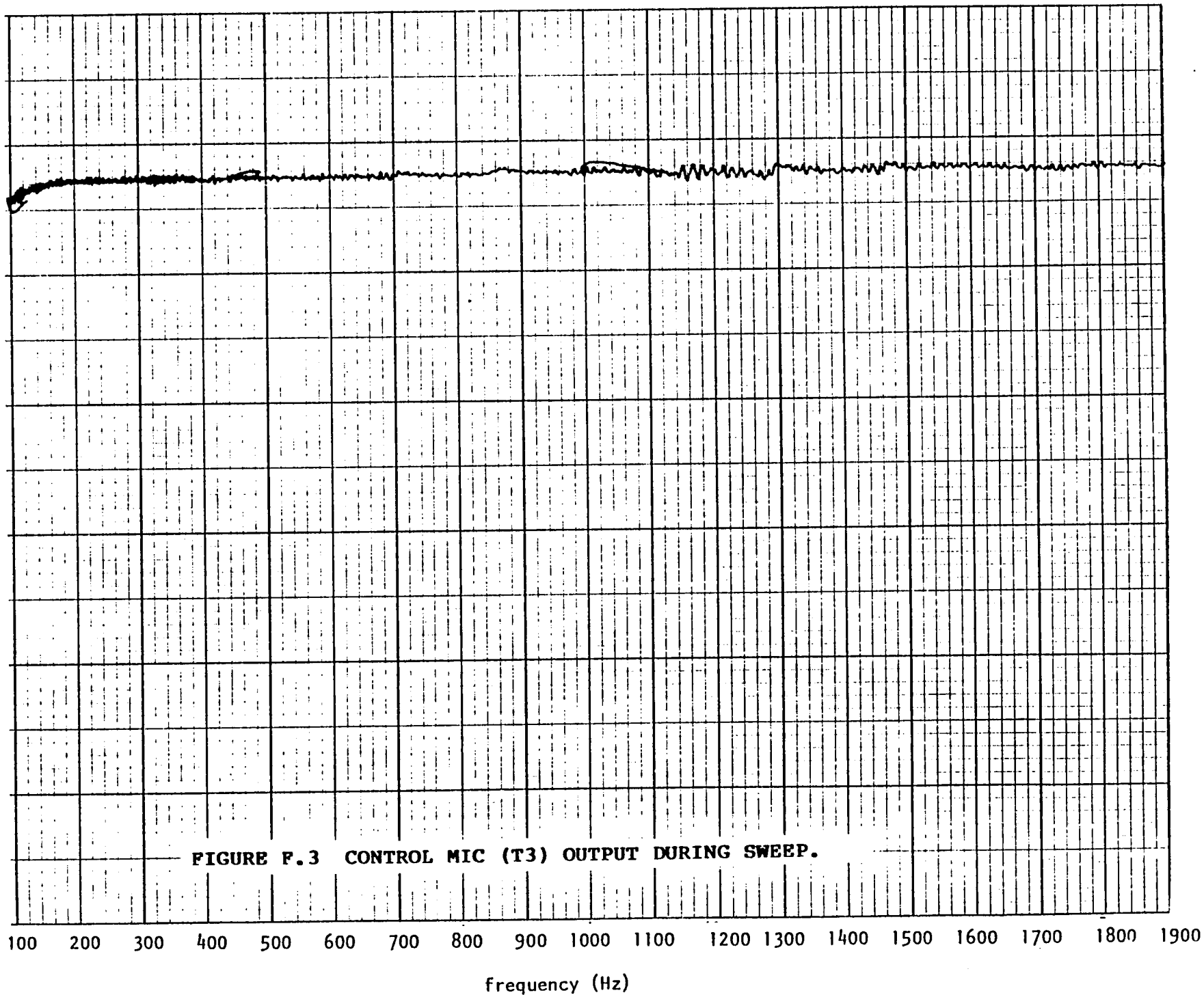
FIGURE F.3 CONTROL MIC (T3) OUTPUT DURING SWEEP.

100   200   300   400   500   600   700   800   900   1000 1100   1200 1300   1400   1500   1600   1700   1800 1900
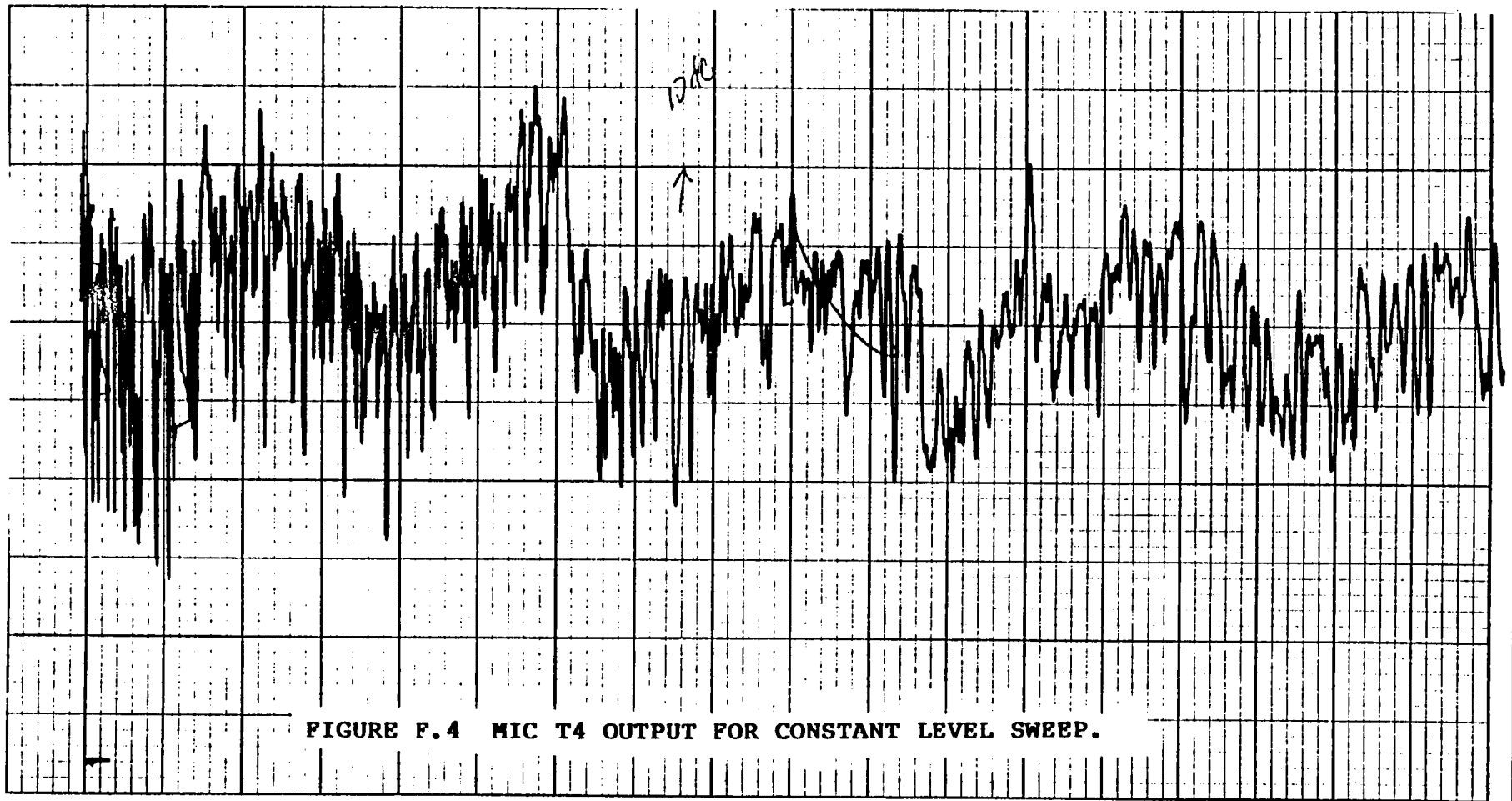
frequency (Hz)

FIGURE F.4 MIC T4 OUTPUT FOR CONSTANT LEVEL SWEEP.

frequency (Hz)

F-7
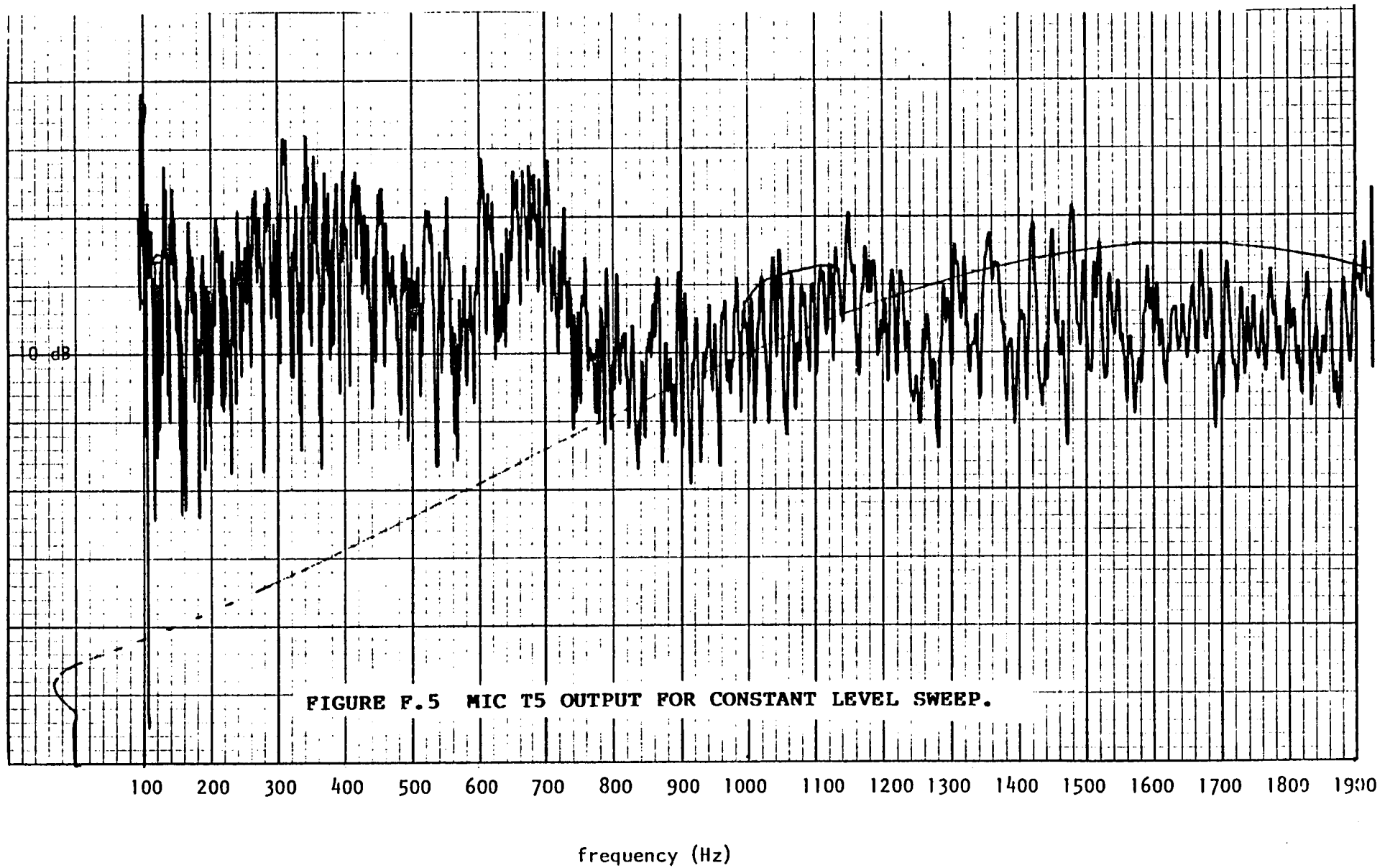
FIGURE F.5 MIC T5 OUTPUT FOR CONSTANT LEVEL SWEEP.

frequency (Hz)

F-8

FIGURE F.6 MIC T6 OUTPUT FOR CONSTANT LEVEL SWEEP.

F-9
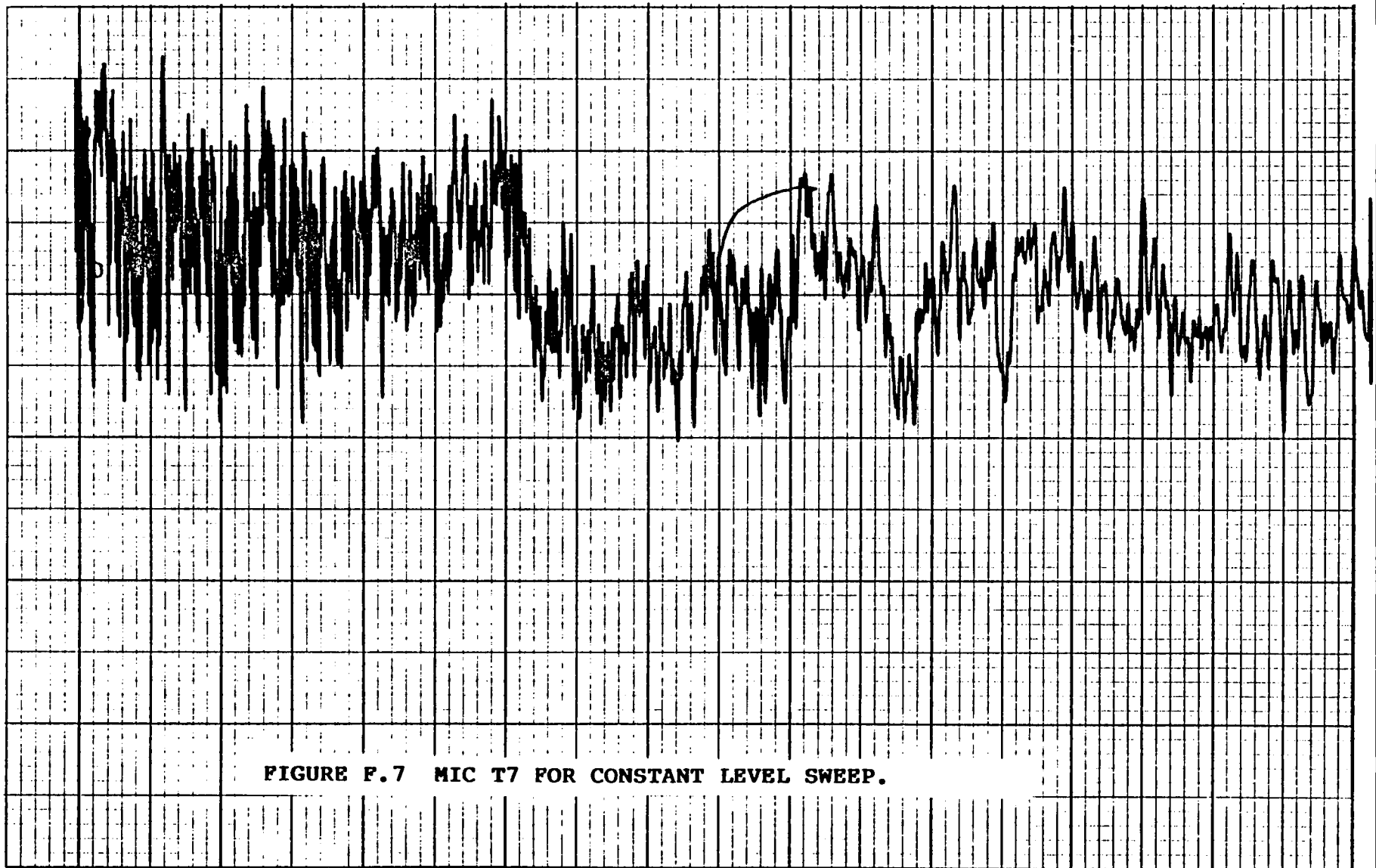
10 dB

frequency (Hz)

FIGURE F.7 MIC T7 FOR CONSTANT LEVEL SWEEP.

10 dB

F-10
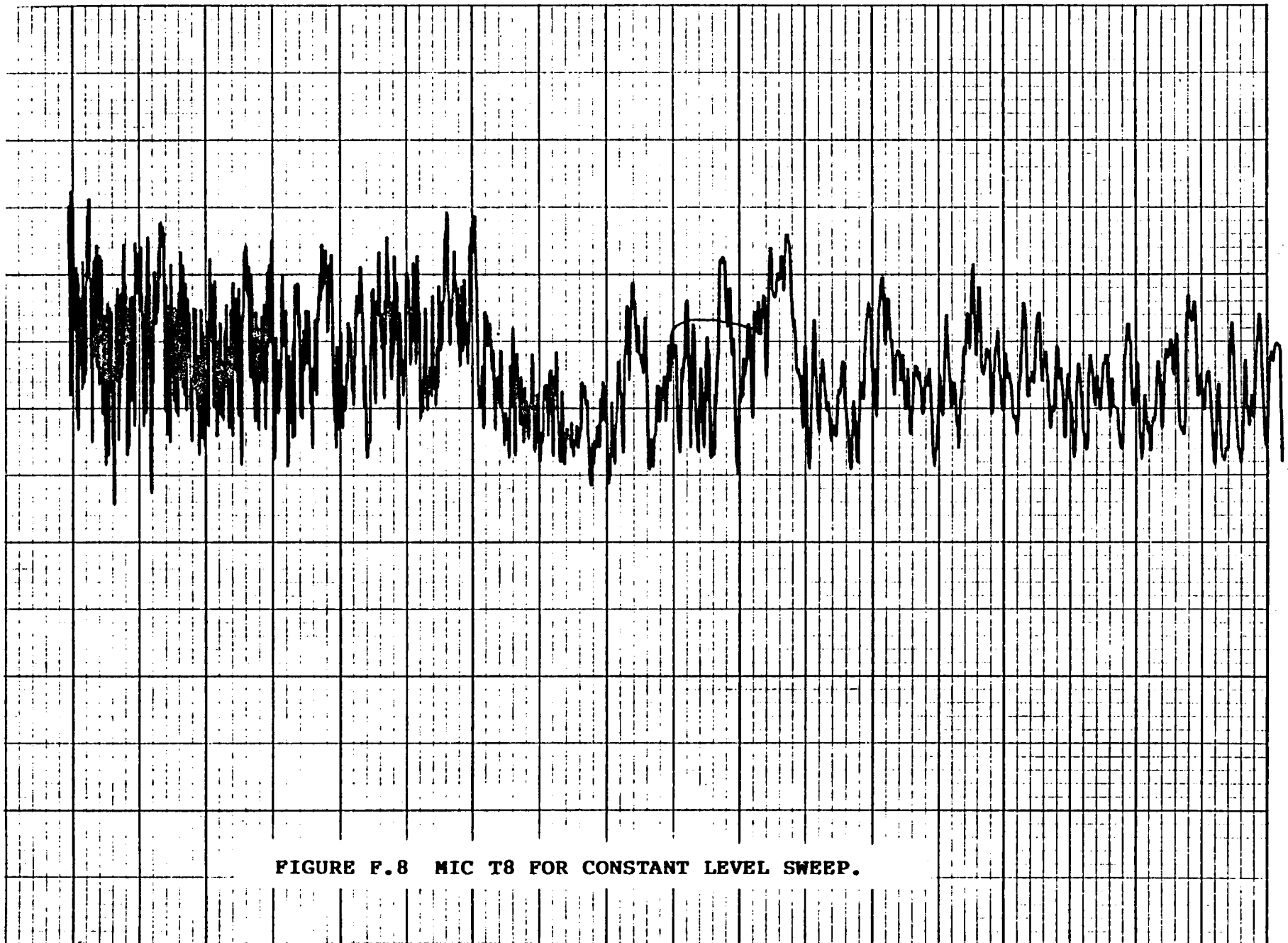
frequency (Hz)

FIGURE F.8 MIC T8 FOR CONSTANT LEVEL SWEEP.
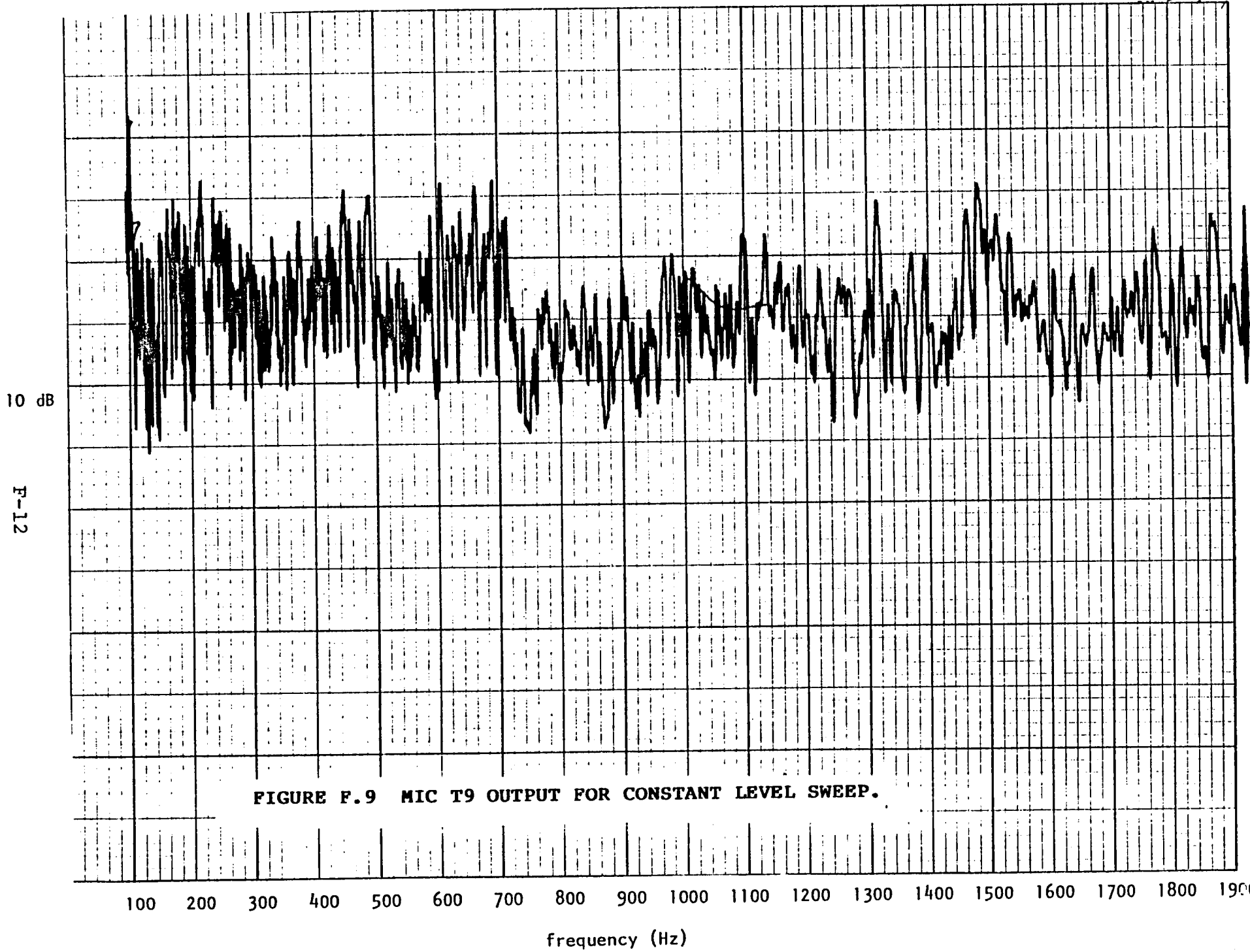
FIGURE F.9   MIC T9 OUTPUT FOR CONSTANT LEVEL SWEEP.

10 dB

F-12

frequency (Hz)

FIGURE F.10   MIC T10 OUTPUT FOR CONSTANT LEVEL SWEEP.

10 dB

F-13

frequency (Hz)

FIGURE F.11   MIC T11 OUTPUT FOR CONSTANT LEVEL SWEEP.

10 dB

Frequency (Hz)

F-14

APPENDIX G

FLOW-INDUCED SIGNALS IN CONDENSER MICROPHONES
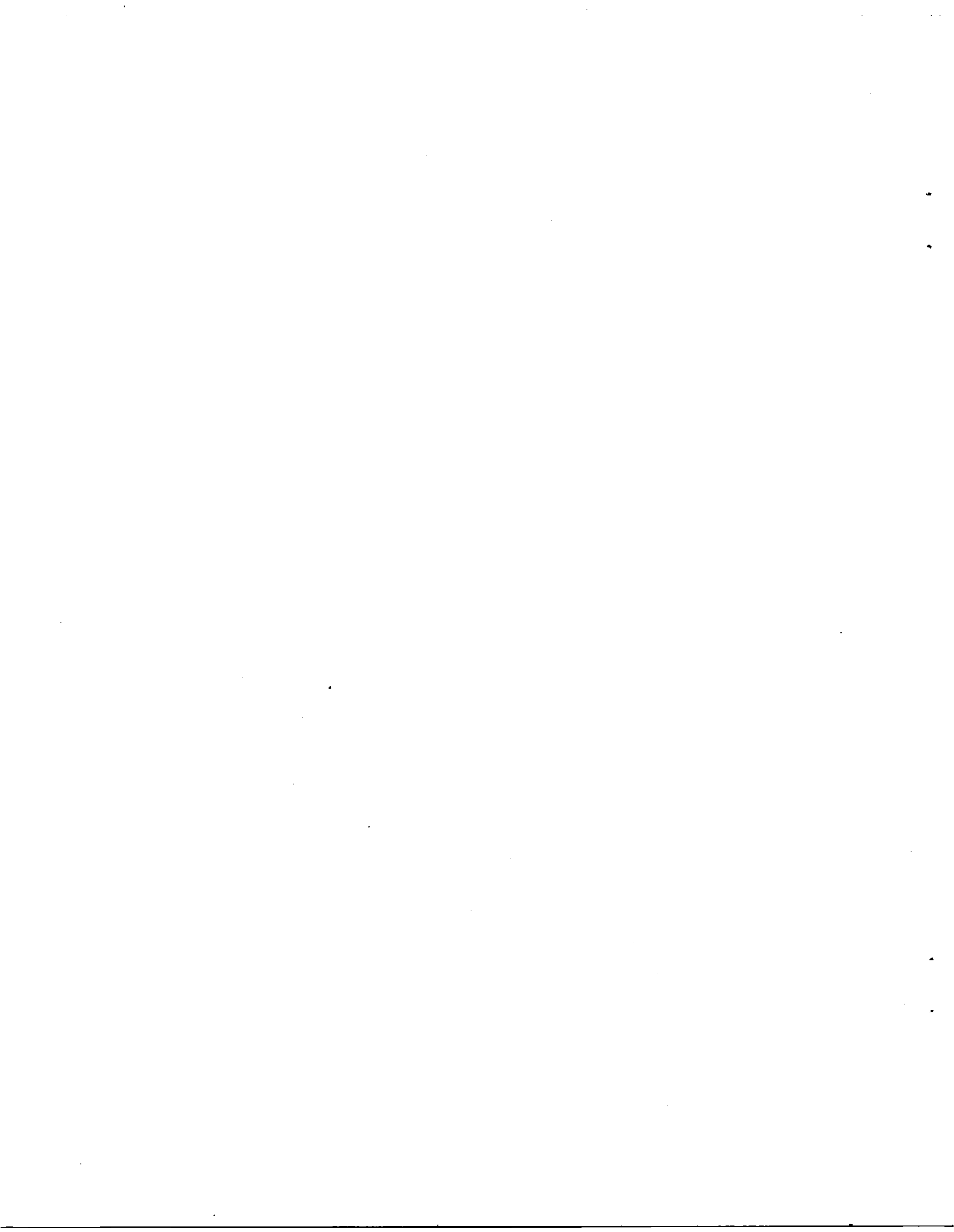
APPENDIX G.

FLOW-INDUCED SIGNALS IN CONDENSER MICROPHONES

G.1 Introduction

Microphones placed in moving airstreams are sensitive to non-acoustic pressures as well as acoustic pressures. If the flow is highly turbulent, such as is the case in diffusers of a wind tunnel, the flow-induced pressures can easily dominate the acoustic pressures. A microphone placed in a low-turbulence airstream will also be subject to non-acoustic pressures generated by its own boundary layer interacting with the acoustically "transparent" openings to the sensing area and other surface discontinuities. These non-acoustic pressures must be accounted for when attempting to interpret in-flow measurements.

Other effects of placing microphones in airstreams include the generation of acoustic energy by flow interaction with the microphone body, fairings, clamps, support stands, guy wires, tape and even small screws. Since the source of this acoustic energy is very close to the sensing area of the microphone, it can also mask the sound which one is trying to measure. A final effect which may be encountered when carrying out measurements in flow is spurious output of a microphone caused by vibration. Such signals may be generated by the vibration-induced motion of the diaphragm or motion of internal conductors. Buffeting of microphone stands caused by turbulent inflow or vortex shedding may lead to such effects in wind tunnel applications.

G.2 Prediction of Microphone Output Caused by Non-Acoustic Pressures

The non-acoustic effects of flow on microphone output consist of "embedded" pressure fluctuations i.e., those caused by vorticity in the flow, and "induced" pressure fluctuations caused by interactions between turbulence and the microphone. There is

no way for a single microphone to be made insensitive to "embedded" pressure fluctuations which have a length scale much larger than the sensing area; indeed ported or specially-adapted microphones are often used to quantify the unsteady non-acoustic pressures in jets and engine exhausts. Induced pressures are a function of the details of unsteady inflow and the particular microphone geometry. No completely definitive study has been made to model the response of typical condenser microphones to self-induced as well as externally-induced pressures. However, some studies are available which can be used for guidance.

The often-used Bruel and Kjaer (B&K) condenser microphone family is also the most-studied. Unfortunately, the B&K literature (Refs. G.1, G.2, and operation manuals for each type of microphone) quotes induced noise levels derived from a spinning rig in which the microphones operated in their own wake. Therefore, these data show excessive induced noise levels, and to date have not been supplemented or replaced with data taken from microphones immersed in more representative and better-documented flow environments.

A more definitive set of data was derived by Noiseux et al (Refs. G.3 - G.5) using both a low turbulence flow in a quiet semi-anechoic wind tunnel, and a controlled source of high turbulence, also in a quiet free jet wind tunnel environment. For the case of a low turbulence flow, Noiseux (Ref. G.4 and G.5) produced a set of "self-noise" curves (1/3 octave band spectra) and corresponding turbulence spectra. These data covered a speed range of 25-71.2 m/s (82-235 fps); the overall rms turbulence intensity $\frac{\sqrt{u^2}}{U}$ was less than .003 for all speed ranges. A very low noise microphone support and fairing of the preamplifier body were used. Noiseux postulated a simple model that predicted the pressures induced by the turbulent inflow to be proportional to the mean dynamic pressure of the flow at the microphone and the local turbulence intensity. However, to achieve a good normal-

ization of the data, he required an empirical correction of the amplitude by a factor of $\sqrt{U}$, where U is the local velocity. Thus, at constant Strouhal number, his normalization suggests a U^5 dependence rather than the expected U^4 dependence. It is possible that his data for low turbulence flows included some contribution of the tunnel background or microphone support acoustic pressures. His data are presented in normalized form in Fig. G.1. It can be safely stated that these data represent a probable practical <u>lower</u> bound on self-noise of B&K microphones with conventional bullet-shaped nose cones in low turbulence flow. The data in Figure G.1 are for microphones aligned with the flow direction (0° incidence). For non-aligned flows, the induced levels increase as a function of incidence angle.

Turning to data from a separate study by Noiseux (G.3) we find that for high turbulence levels, the data collapse was reasonably good using the same model, although a different normalized value is found, presumably because a different mechanism is dominant in each case. From this data, we can derive a separate curve for use in high turbulence flows (Fig. G.2). Note again that this data is for mean flow directions which are aligned with the microphone axis; for flows at other angles, the induced pressures increase with increasing "angle of attack".

It should again be noted that neither of the above curves provides a complete general description of the relationship between flow field parameters, microphone geometry and "induced" noise. However, since the data were acquired at flow speeds comparable to those experienced in the 4x7m tunnel test program, the lack of generality in their application does not significantly affect the levels predicted using these curves. It should also be noted that in other tests using the same facility in which Noiseux's data was derived, higher self-noise levels ere measured when careful fairing of the microphone stands was not carried out.

G.3 Predicted Induced Noise for Microphones Used in 4X7m Noise Survey Test Section Mics

Test Section Microphones

The curves from Figure G.1 were applied to the in-flow test section microphones using an overall turbulence level of 0.2% as reported in NASA measurements. Figure G.3 shows the predicted self-noise for microphones 22 and 23 for a test section velocity of 80 kt. The comparison shows that the test section microphones were apparently free of flow-induced pressure fluctuations, although high frequency acoustic noise from the microphone stands was evident. As shown in Appendix A, the high frequency noise from the microphone supports, guy wires, etc., can be removed by comparison of out-of-flow acoustic spectra with and without the stands present in the flow.

First Corner Microphone (Mic 2): Figure G.4 shows the comparison of flow-induced pressures at the first corner microphone for the 80 kt test section velocity. An rms turbulence level of 8% was used and the spectrum was derived from an in-duct spectrum taken by Hayden (see Sec. 3) suitably adjusted for overall level. Comparison of the predicted induced noise curves with the measured curve leads to the conclusion that first corner measurements are probably not dominated by flow-induced pressures, except possibly at very low frequencies. This conclusion is supported by the consistency of the first corner levels with other data from around the circuit, and the identifiable propagating waves from the phase measurements. However, the levels of the induced pressures are close enough to the "acoustic" pressures to cause the low coherence between adjacent pairs of microphones which was observed in the phase and coherence measurements.

Second Corner Microphones (Mics 9 & 14): The only other
microphones immersed in relatively high speed flow were located
near the second corner. As previously discussed, microphone 14
produced excessively high output at high tunnel speeds as the
support apparatus was apparently vibrating excessively. At 20
and 40 kt speeds, the levels from mic 14 were consistent with
those at microphone location 9. Figure G.5 shows the predicted
induced pressure levels for mics 9 and 14 as compared with
measured data, that using an overall turbulence level of 5%. It
appears that the data at these microphones is not contaminated by
flow induced pressures.

G.4 Conclusions

Microphone signals measured in the 4x7m tunnel acoustic
diagnosis are generally free from spurious signals induced by
turbulence. This conclusion is derived using available semi-
empirical data but without use of actual turbulence spectra from
the 4x7m facility; therefore, if the turbulence spectra are
dramatically different than what were assumed, the relative
contribution of acoustic pressures and flow-induced pressures may
change.

Test section microphones showed evidence of acoustic
contamination caused by sound generation of flow over the stand,
guy wires, etc.. However, this acoustic contamination was
accounted for by use of out-of-flow microphones (see App. A).

Although the flow-induced contamination problem did not
affect the noise measurements in the present test program, flow-
induced signals would mask acoustic signals in a much quieter
tunnel, and will probably dictate that future in-flow acoustic
measurements in a quieted 4x7 tunnel be made with special low-
self-noise sensors, which may not even exist at present.

REFERENCES
(for Appendix G)

1. Bruel, P.V., "Aerodynamically INduced Noise of Microphones and Windscreens," Bruel and Kjaer Technical Review No. 2, 1960.

2. Rasmussen, G., "Windscreening of Microphones", Internal B&K Technical Memorandum, 1973.

3. Noiseux, D.U., "Study of Porous Surface Microphones for Acoustic Measurements in Wind Tunnels," NASA CR-114593 (also BBN Report 2539), April 1973.

4. Noiseux, D.U., and N.B. Noiseux, "Noise and Acoustic Response of Bruel and Kjaer and Porous Surface Microphones in Flow", NASA CR-145038, (also BBN Report 3323), 1976.

5. Noiseux, D.U., N.B. Noiseux and Y. Kadman, "Development, Fabrication, and Calibration of A Porous Surface Microphone in an Airfoil," NASA CR-132636, 1975.
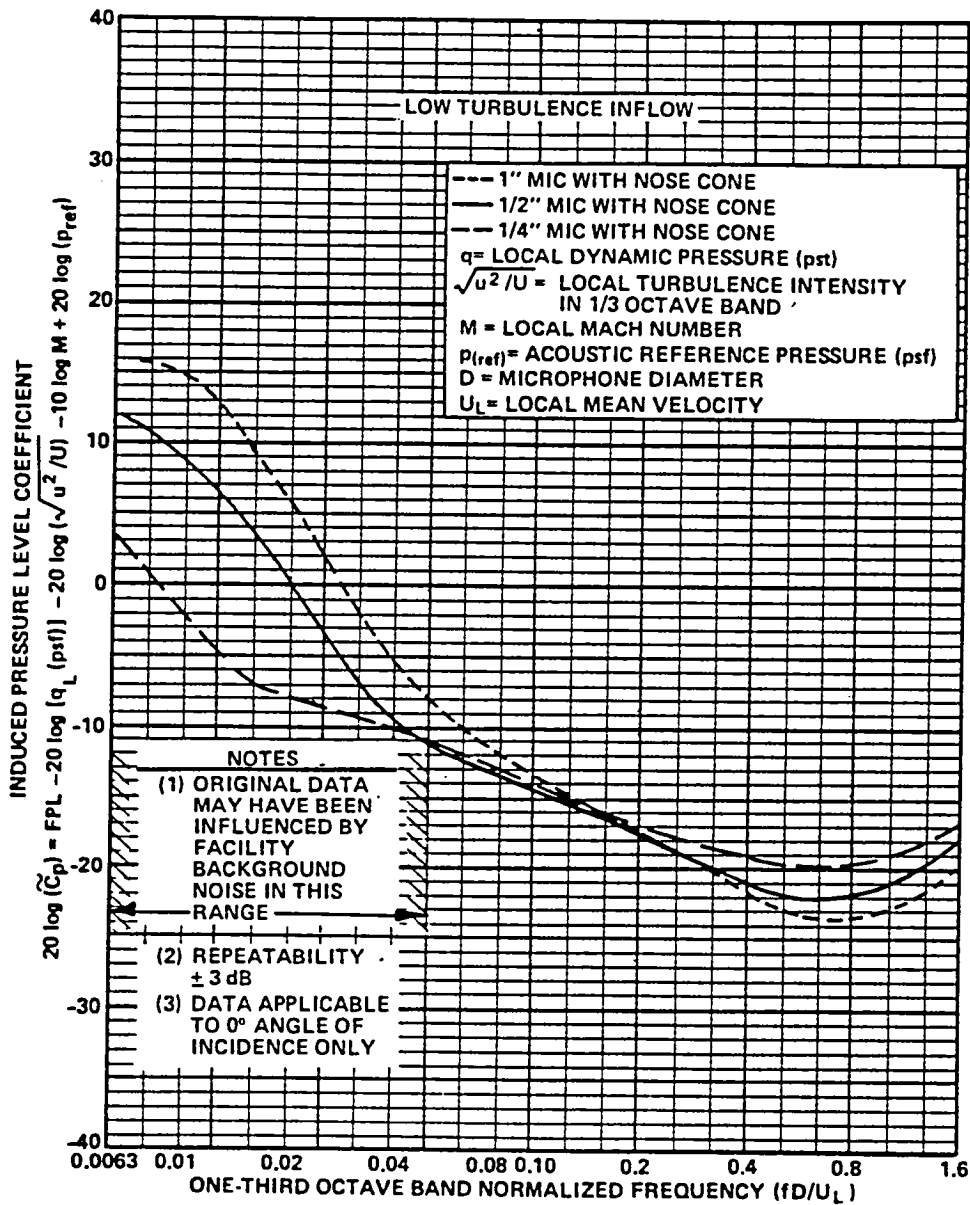
FIG. G.1 NORMALIZED SPECTRUM OF FLOW-INDUCED PRESSURES ON CONDENSER MICROPHONES IN LOW TURBULENCE FLOW.

G-7
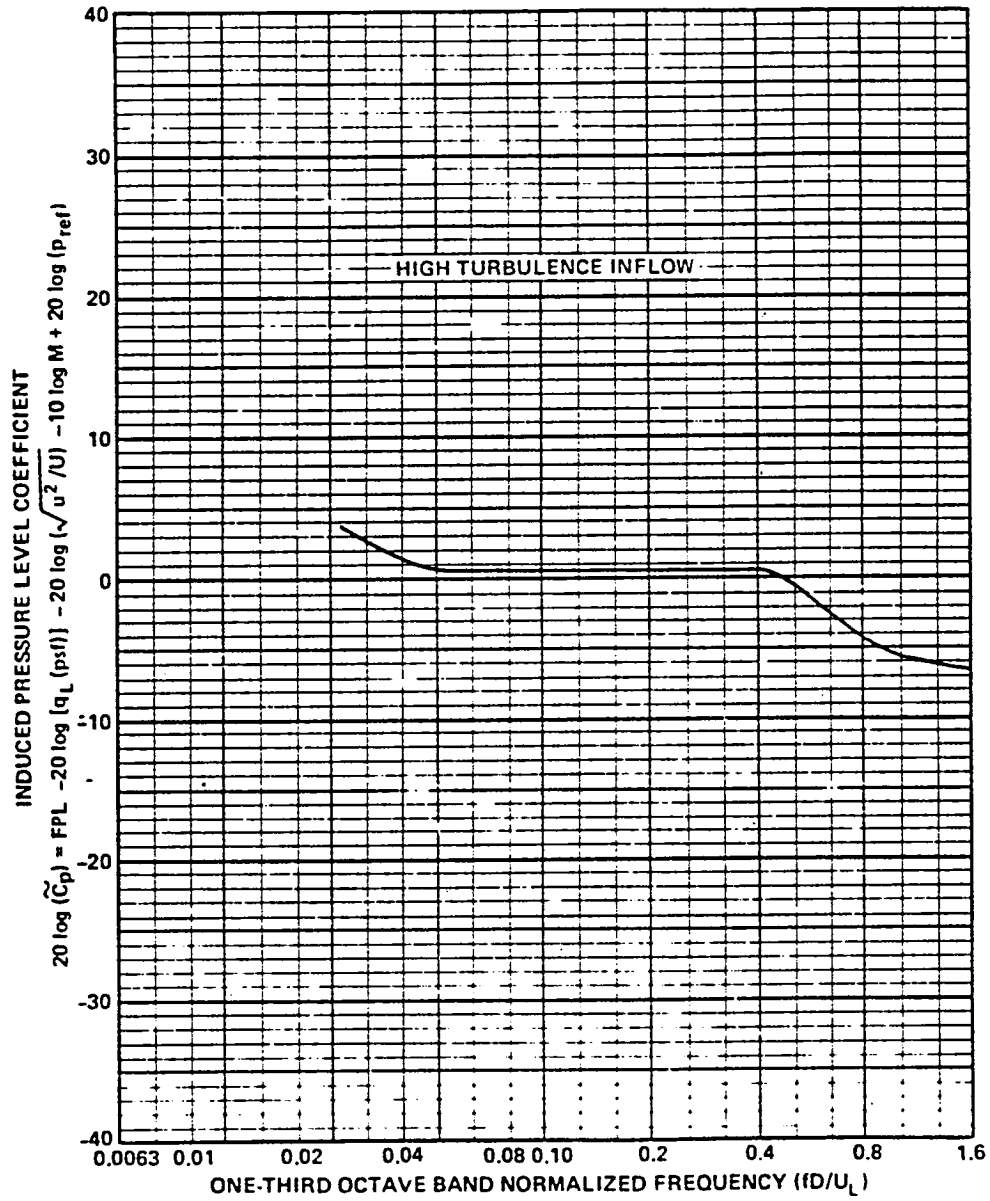
FIG. G.2 NORMALIZED SPECTRUM OF FLOW-INDUCED PRESSURES ON CONDENSER MICROPHONE IN HIGHLY TURBULENT FLOWS.

G-8

Y-axis: ONE-THIRD OCTAVE BAND PRESSURE LEVEL dB (re 2 x 10^{-5} N/m^2)

Legend:
- 80 kt DATA AT MICS 22 AND 23
- 80 kt DATA CORRECTED TO REMOVE ACOUSTIC CONTAMINATION CAUSED BY MIC STANDS
- PREDICTED OUTPUT INDUCED BY FLOW

USING OTHER DATA FROM SAME FACILITY BUT DIFFERENT MICROPHONE SUPPORT

USING NOISEUX DATA

X-axis labels: 31.5 40 50 63 80 100 125 160 200 250 315 400 500 630 800 1000 1250 1600 2000 2500 3150 4000 5000 6300 8000

ONE - THIRD OCTAVE BAND CENTER FREQUENCIES IN Hz

FIG. G.3 PREDICTED PRESSURES AT TEST SECTION MICROPHONES 22 & 23

FIG. G.4   PREDICTED INDUCED PRESSURES AT MICROPHONE LOCATION 2.

FIG. G.5 PREDICTED INDUCED PRESSURES AT MICROPHONE LOCATIONS 9 & 14.

G-11

REFERENCES

1. Raney, J.P., "Status Report; 4x7-meter Wind Tunnel
    Treatment/Feasibility Study," presented at First Annual
    NASA/AHS Meeting, Hampton, VA, November 29-December 1, 1983.
    NASA CP-2308, 1984, pp. 195-208.

2. Ditshuizen, J.C.A. van, et al., "Acoustic Capabilities of
    the German-Dutch Wind Tunnel DNW," AIAA Paper 83-0146,
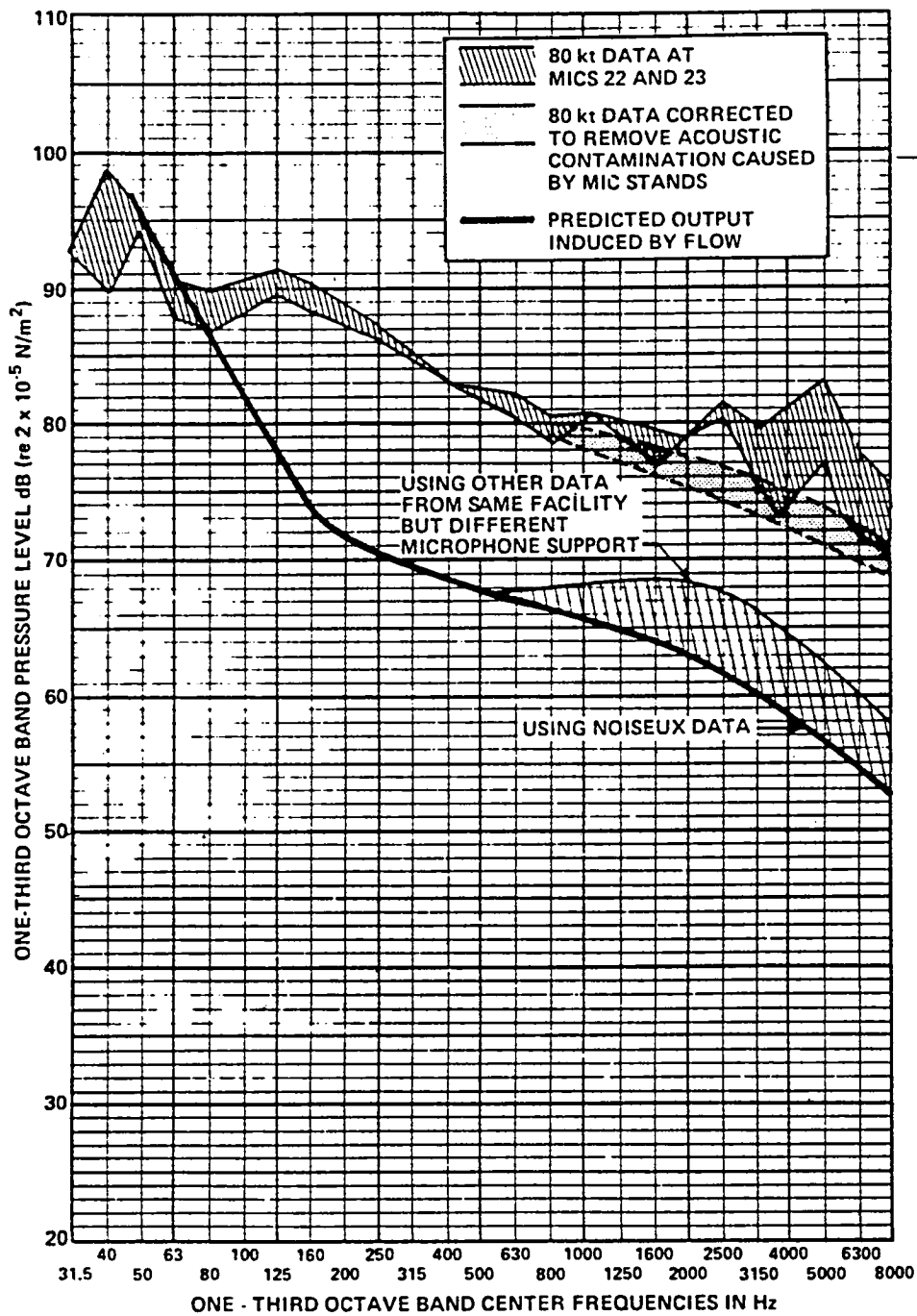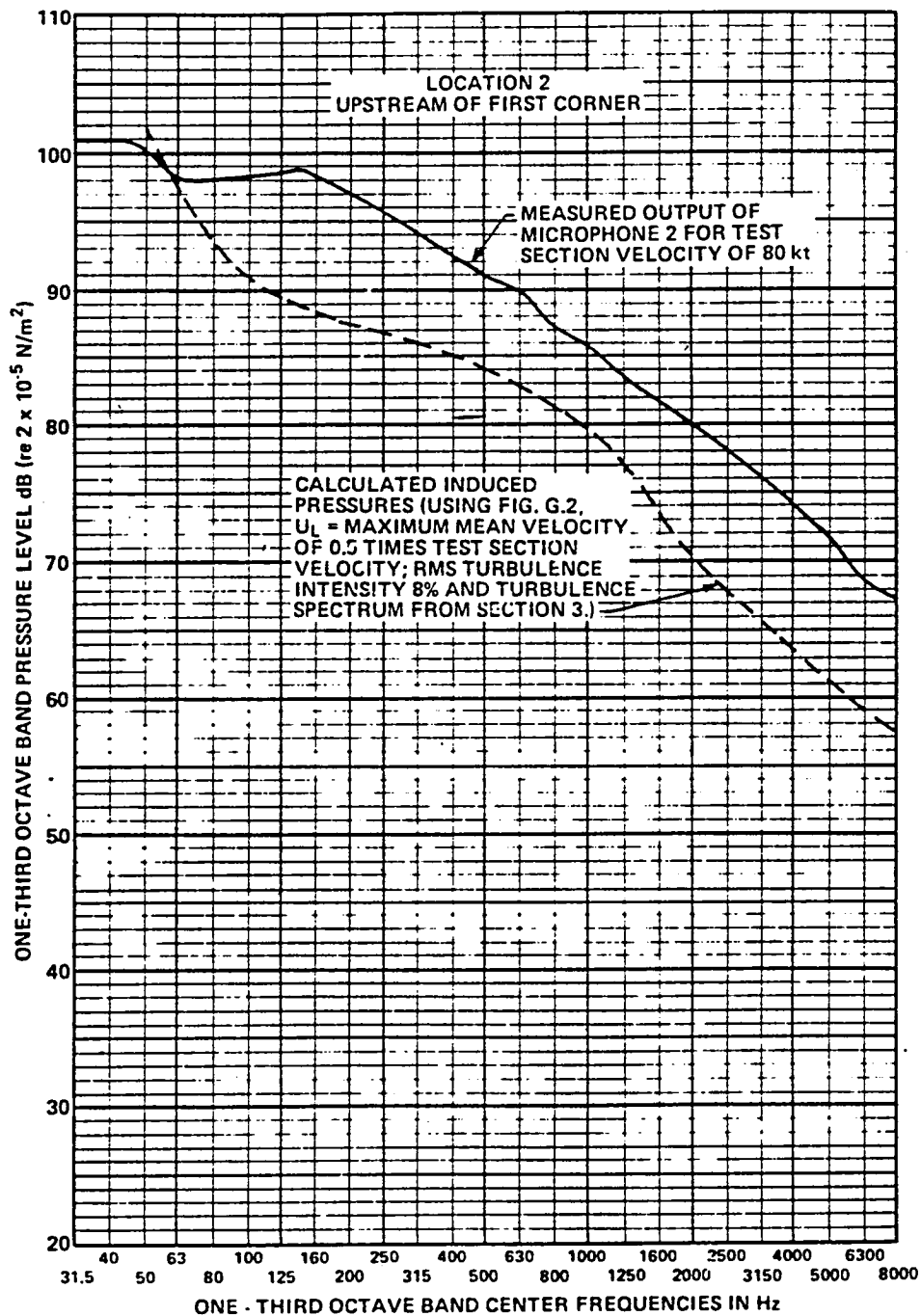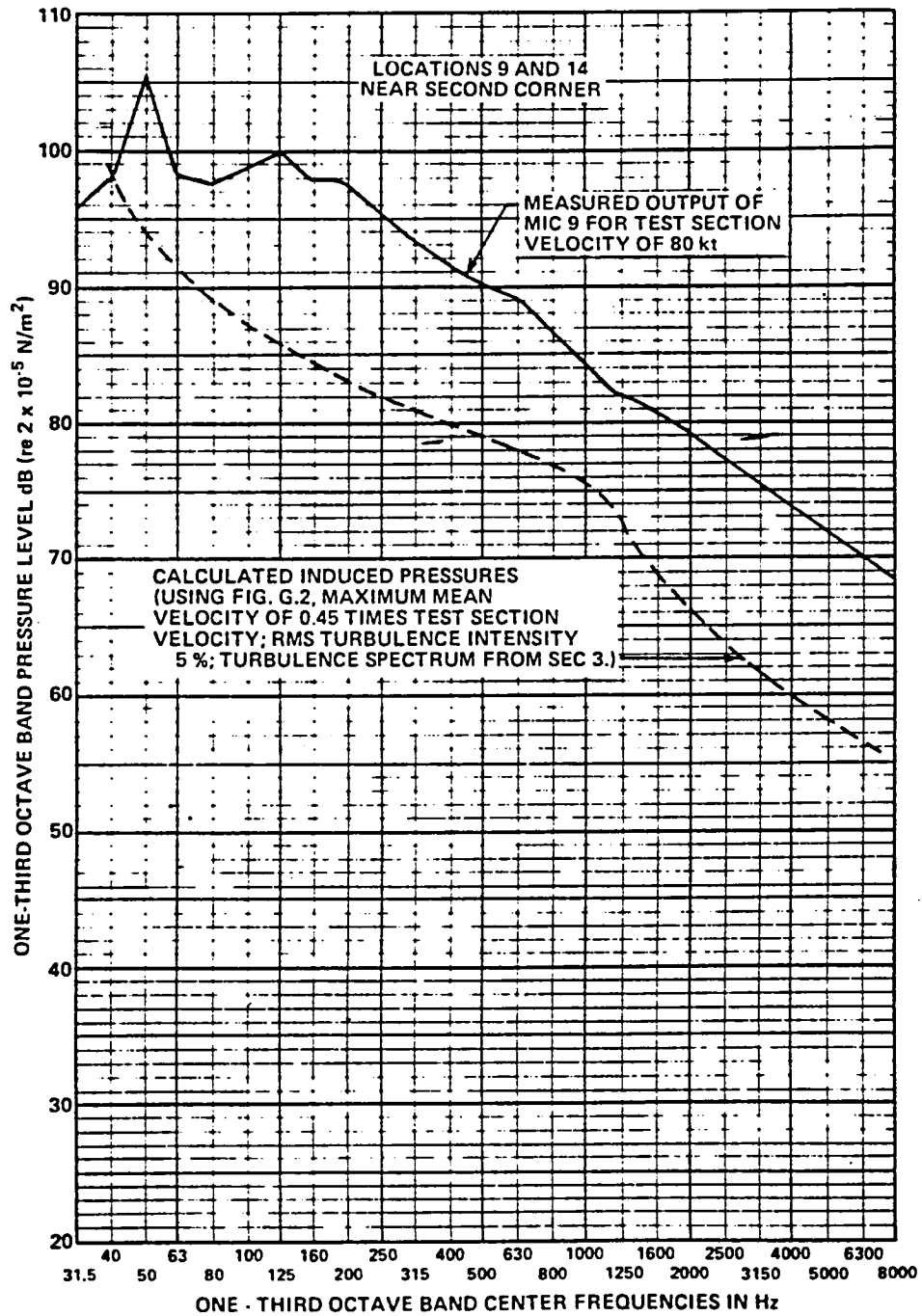   presented at the 21st Aerospace Sciences Meeting, Reno, NV,
    January 1983.

3. Soderman, P.T., and L.E. Hoaglund, "Wind Tunnel Fan Noise
    Reduction Including Effects of Turning Vanes on Noise
    Propagation," AIAA Paper 79-0642, presented at the AIAA 5th
    Aeroacoustics Conference, Seattle, WA, March 1979.

4. Rennison, D.C., J.F. Wilby, and C.G. Gordon, "Design
    Concepts for Sound Absorbing Linings in the Test Section of
    the NASA Ames 80' x 120' Wind Tunnel," NASA CR-152155, May
    1978.

5. Wilby, J.F. and T.D. Scharton, "Evaluation of the NASA Ames
    No. 1 7x10 Wind Tunnel as an Acoustic Facility," NASA CR-
    137712, June 1975.

6. Howe, M.S., "A Review of the Theory of Trailing Edge Noise,
    "NASA CR-3021, also J. Sound Vib., 61, 437-466, 1978.

7. Brooks, T.F. and T.H. Hodgson, "Prediction and Comparison of
    Trailing Edge Noise Using Measured Surface Pressures," AIAA
    Paper 80-0977, presented at AIAA 6th Aeroacoustics
    Conference, Hartford, CT, June 1980. (Also published in J.
    Sound Vib., (1981) 78 (1) 69-117.

8. Hayden, R.E., "Noise Generation by Duct Elements in Low
    Speed Airflows." Paper presented at Purdue University
    Proc. Conf. on Noise Control (1971)

9. Heller, H.H., D.B. Bliss, E.E. Ungar and S.E. Widnall,
    "Feasibility of Aircraft Stall Detection by Means of
    Pressure Fluctuation Measurements," AFFDL-TR-70-147, 1970.

10. Barna, P.S., "Experimental Investigations on the V/STOL
    Tunnel at NASA Langley Research Center," NASA CR-165655,
    February 1981.

11. Hayden, R.E., Y. Kadman, D.B. Bliss and S.A. Africk,
    "Diagnostic Calculations of Airframe-Radiated Noise," AIAA
    Paper 75-485. Also appears in AIAA Progress Series on
    Aeronautics.

12. Hayden, R.E., H.L. Fox and R.C. Chanaud, "Some Factors Influencing Radiation of Sound from Flow Interaction with Edges of Finite Surfaces," NAS1-9559-25, 1974.

13. Ver, I.L., D.W. Anderson, and D.B. Bliss, "Acoustical Modeling Study of the Open Test Section of the NASA V/STOL Wind Tunnel," BBN Report No. 3179, December 1975.

14. Cicci, F., and A.F. Toplis, "Noise Level Measurements on a Quiet Short Haul Turboprop Transport," SAE Paper 760455, presented at SAE Business Aircraft Meeting, Wichita, KS (April 1976).

15. Brown, N.A., "Use of Skewed Blades for Ship Propellers and Truck Fans," proceedings of ASME Symposium on Fluid Machinery, pp. 201-207, 1977.

16. Longhouse, R.E., "Noise Mechanisms in Automotive Cooling Fans," proceedings of ASME Symposium on Fluid Machinery, 1977.

17. Longhouse, R.E., "Noise Mechanism Separation and Design Considerations for Low Tip Speed Axial Flow Fans," _Journal of Sound and Vibration_, 48, 1976.

18. Mellin, R.C., "Selection of Minimum Noise Fans for a Given Pumping Requirement," _Noise Control Engineering_, Jan.-Feb. 1975.

19. Beranek, L.L. (ed.), _Noise and Vibration Control_, McGraw-Hill Book Co., 1971.

20. Powell, A., "Theory of Sound Propagation Through Ducts Carrying High-Speed Flows," _J. Acoust. Soc. Amer._, 32 (1960), 1640-1646.

21. Kurze, U., "Schallabstrahlung an der Austrittsoffnung von Kanalen," _Acustica_, 20 (1968), 253-263.

22. Ronneberger, D., "Experimentalle Untersuchungen zum akustischen Reflexionsfaktor von unstetigen Querschnittsanderungen in einem luftdurchstromten Rohr," _Acustica_, 19 (1967/68).

23. Alfredson, R.J. and P.O.A.L. Davies, "Performance of Exhaust Silencer Components," _J. Sound Vib._, 15 (1971), 175-196.

24. Munger, P. and H.E. Plumblee, "Propagation and Attneuation of Sound in a Soft-Walled Annular Duct Containing A Sheared Flow," NASA SP 207, 305-327 (1969).

25. Kurze, U.J. and C.H. Allen, "Influence of Flow and High Sound Level on the Attenuation in a Lined Duct," _J. Acoust. Soc. Amer._, 49 (1971), 1643-54.

26. Soderman, P.T., "A Study of Resonant Cavity and Fiberglass-Filled Parallel Baffles as Duct Silencers," NASA Technical Paper 1070, AVARADCOM Technical Report 81-A-2, April 1982.

27. Mechel, F.P., "Design Criteria for Industrial Mufflers," Inter-Noise 75 Proceedings, Sendai, Japan, 1975.

1. Report No. NASA CR-172446-1	2. Government Accession No.	3. Recipient's Catalog No.
4. Title and Subtitle Sources, Paths, and Concepts for Reduction of Noise in the Test Section of the NASA Langley 4x7m Wind Tunnel		5. Report Date September 1984
		6. Performing Organization Code
7. Author(s) Richard E. Hayden, John F. Wilby		8. Performing Organization Report No. BBN Report No. 5416
9. Performing Organization Name and Address Bolt Beranek and Newman Inc. 10 Moulton Street Cambridge, MA 02238		10. Work Unit No. (TRAIS)
		11. Contract or Grant No. NAS1-16521-14
12. Sponsoring Agency Name and Address National Aeronautics and Space Administration Washington, DC 20546		13. Type of Report and Period Covered Contractor Report July 1983 – March 1984
		14. Sponsoring Agency Code 532-06-13-03

15. Supplementary Notes
NASA Langley Technical Monitor: Dr. John P. Raney Final Report

16. Abstract

NASA is investigating the feasibility of modifying the 4x7m Wind Tunnel at the Langley Research Center to make it suitable for a variety of aeroacoustic testing applications, most notably model helicopter rotors. This study was aimed at determining the amount of noise reduction required to meet NASA's goal for test section background noise, quantifying the predominant sources and paths causing the background noise, and carrying out trade-off studies between schemes to reduce fan noise at the source and those to attenuate the sound generated in the circuit between the sources and the test section. An extensive data base is also presented on circuit sources and paths.

17. Key Words Wind Tunnel Aeroacoustic Testing Noise Control Diagnostic Methods	18. Distribution Statement Unclassified – Unlimited Subject Category 71		
19. Security Classif. (of this report) Unclassified	20. Security Classif. (of this page) Unclassified	21. No. of Pages 325	22. Price A14